UNIVERSITY OF SOUTHAMPTON

FACULTY OF ENGINEERING AND THE ENVIROMENT

INSTITUTE OF SOUND AND VIBRATION RESEARCH

SUBJECTIVE AND BIODYNAMIC RESPONSES OF SEATED SUBJECTS EXPOSED TO WHOLE-BODY VERTICAL VIBRATION AT LOW FREQUENCY

by

ZHEN ZHOU

Thesis for the degree of Doctor of Philosophy

July 2014

UNIVERSITY OF SOUTHAMPTON

ABSTRACT

FACULTY OF ENINGEERING AND THE ENVIORNMENT
INSTITUTE OF SOUND AND VIBRATION RESEARCH

Doctor of Philosophy

SUBJECTIVE AND BIODYNAMIC RESPONSES OF SEATED SUBJECTS EXPOSED TO WHOLE-BODY VERTICAL VIBRATION AT LOW FREQUENCY

by ZHEN ZHOU

As the magnitude of vertical whole-body vibration increases, the resonance frequency in the apparent mass of the human body reduces and there are changes in the frequency-dependence of acceleration equivalent comfort contours. It is unclear to what extent these two 'nonlinearities' are related. This thesis seeks to advance understanding of the combined influence of the magnitude and the frequency of whole-body vertical vibration on the subjective and biodynamic responses of the seated human. Specifically, the research was designed to identify whether the nonlinearity in the subjective responses reflects the nonlinearity in the biodynamic responses, and whether comfort would be better predicted from the force applied to the body.

The first experiment was designed to investigate how the biodynamic and subjective responses of seated subjects (20 males and 20 females) depend on the frequency, magnitude, and waveform of vertical vibration when they were exposed to sinusoidal and random vibration. The vertical apparent mass and fore-and-aft cross-axis apparent mass obtained with random and sinusoidal vibration were both nonlinear but similar at the same overall magnitude (0.1, 0.2, 0.4, 0.8, and 1.6 ms^{-2} r.m.s.). With both increasing acceleration and increasing force, the rate of growth of discomfort depended on the frequency of vibration. Both acceleration and force equivalent comfort contours (the magnitude of vibration expressed as a function of frequency which produces similar degrees of discomfort) varied with the magnitude of vibration. The equivalent comfort contours were less dependent on the magnitude of vibration when expressed by force than by acceleration. There were statistically significant positive correlations between the biodynamic responses and subjective responses at all frequencies in the range 1 to 16 Hz.

The second experiment investigated subjective and biodynamic responses to a series of upward and downward vertical mechanical shocks at 13 fundamental frequencies (1 to 16 Hz) and 18 magnitudes (unweighted peak accelerations in the range 0.12 to 8.0 ms^{-2}). The optimum stiffness and optimum damping of two lumped parameter models fitted to the measured acceleration time history decreased as the shock magnitudes increased. With both models, and with both downward and upward shocks, the median principal resonance frequency of the apparent mass of the body decreased from 6.3 to 4 Hz as the magnitude of the shocks increased from 0.05 $ms^{-1.75}$ to 2.0 $ms^{-1.75}$ VDV. There was no consistent difference in the rate of growth of discomfort between acceleration and force, or between upward and downward shocks, or between lower magnitude and higher magnitude shocks.

The final experiment compared subjective responses of the human body with a rigid seat and a soft seat. With increasing magnitude of vibration (both acceleration and force), the rate of growth of discomfort was dependent on the frequency of vibration, but did not differ between the rigid seat and the soft seat. There were no significant differences in either the force or acceleration equivalent comfort contours on the rigid seat compared with those on the soft seat. The frequency-dependence of the force equivalent comfort contours showed less nonlinearity than the acceleration equivalent comfort contours with both the rigid and soft seat conditions.

In conclusion, this study indicates some similarities in the nonlinearity of subjective responses and biodynamic responses of the seated body exposed to vertical vibration. Although force equivalent comfort contours are also nonlinear, they showed less dependence on the magnitude of the excitation than acceleration equivalent comfort contours.

Contents

List of tables

List of figures

DECLARATION OF AUTHORSHIP

I, ZHEN ZHOU

declare that the thesis entitled

Subjective and biodynamic responses of seated subjects exposed to whole-body vertical vibration at low frequency

and the work presented in the thesis are both my own, and have been generated by me as the result of my own original research. I confirm that:

- this work was done wholly or mainly while in candidature for a research degree at this University;
- where any part of this thesis has previously been submitted for a degree or any other qualification at this University or any other institution, this has been clearly stated;
- where I have consulted the published work of others, this is always clearly attributed;
- where I have quoted from the work of others, the source is always given. With the exception of such quotations, this thesis is entirely my own work;
- I have acknowledged all main sources of help;
- where the thesis is based on work done by myself jointly with others, I have made clear exactly what was done by others and what I have contributed myself;
- parts of this work have been published as:

  Zhou, Z and Griffin, M.J. (2014). Response of the seated human body to whole-body vertical vibration: biodynamic responses to sinusoidal and random vibration. Ergonomics, 57(5), 693-713

  Zhou, Z and Griffin, M.J. (2014). Response of the seated human body to whole-body vertical vibration: discomfort caused by sinusoidal vibration. Ergonomics, 57(5), 714-732

  Zhou, Z and Griffin, M.J. (2012). Time-domain modelling of biodynamic responses to vertical whole-body mechanical shocks. *47th UK Conference on Human Response to Vibration*, Southampton.

Zhou, Z and Griffin, M.J. (2011). Nonlinearity in the vertical apparent mass of the seated human body with random and sinusoidal vibration. *46th UK Conference on Human Response to Vibration*, Buxton.

Zhou, Z and Griffin, M.J. (2010). Equivalent comfort contours for vertical whole-body vibration at frequencies between 1 and 16 Hz. *45th UK Conference on Human Response to Vibration*, Institute of Naval Medicine, Gosport.

,

Signed: ……..

Date:…….

Acknowledgements

It is a long journey to complete this PhD thesis. Although this thesis is solely my work, it is these countless number of individuals who have kept me on the path through and without whom this thesis would not have come to fruition.

First I would like to sincerely thank my supervisor Mike Griffin who has played a pivotal role in guiding me through this period. Without his valuable time and patient guidance, it is impossible to complete this thesis.

I would also like to thank all the members of the Human Factors Research Unit. Without their kindly help, it is also difficult for me to complete the thesis.

Last but not the least, I would like to take this opportunity to thank my parents and all the friends around me. Their steady and warm support encourage me to face any difficult in the study and also in the life.

Definitions and Abbreviations

φ	Objective magnitude
Ψ	Subjective magnitude
k	Constant in Steven's power law
n	Exponent in Steven's power law
r.m.s.	Root-mean-square value
VDV	Vibration dose value
AME	Absolute magnitude estimation
RME	Relative magnitude estimation

Chapter 1 Introduction

People in sitting postures may be exposed to vertical vibration while in transport and in working environments. Increases in vibration magnitude result in increasing vibration discomfort and can be assumed to increase the risks to health, so a reduction in vibration can be expected to improve the quality of environments. Understanding the subjective and biodynamic responses of the seated human body exposed to vibration will help to define methods for evaluating vibration with respect to discomfort.

The subjective responses to whole-body vibration are dependent on the magnitude and the frequency of the vibration as well as seating conditions. Previous experimental studies have determined the acceleration required to produce similar discomfort at different frequencies of vibration (i.e., equivalent comfort contours). These contours have been used to define frequency weightings for acceleration at the subject-seat interface. The frequency weightings are standardised and widely used to predict vibration discomfort. However, because of nonlinearity in the subjective responses to vibration, the equivalent comfort contours have a different frequency-dependence at different magnitudes. This suggests the ideal frequency weighting should be different for low and high vibration magnitudes but this is not reflected in current frequency weightings.

Nonlinearity is also evident in the biodynamic responses of the human body exposed to vertical whole-body vibration: the resonance frequency in the apparent mass reduces as the vibration magnitude increases. It is reasonable to expect that the nonlinearity in the biodynamic response might be related to the nonlinearity in the subjective response of the human body exposed to vertical whole-body vibration.

This research was designed to advance understanding of the subjective and biodynamic responses to vertical whole-body vibration and how they depend on the physical characteristics of the vibration (i.e., magnitude, frequency, waveform, shock directions). It was also designed to investigate dynamic force as a predictor of vibration discomfort.

The thesis consists of the following ten chapters:

Chapter 1 introduces the research.

Chapter 2 reviews previous studies of the biodynamic and subjective responses of the seated human body exposed to vertical whole-body vibration. It clarifies the gaps in knowledge in the area and shows the main questions to be answered in the study.

Chapter 3 describes the main experimental equipment and the methods used for data analysis.

Chapter 4 investigates the nonlinearity in the biodynamic response of the human body seated on a rigid seat exposed to sinusoidal and random vertical whole-body vibration.

Chapter 5 studies the nonlinearity in the subjective responses of the human body seated on a rigid seat exposed to sinusoidal vertical whole-body vibration.

Chapter 6 investigates the nonlinearity in the biodynamic response of the human body seated on a rigid seat exposed to vertical mechanical shocks.

Chapter 7 studies the nonlinearity in the subjective responses of the human body seated on a rigid seat exposed to vertical mechanical shocks.

Chapter 8 investigates the nonlinearity in the subjective and biodynamic responses of the human body seated on both rigid and soft seats and exposed to sinusoidal vertical whole-body vibration.

Chapter 9 presents a general discussion of the findings reported in the thesis.

Chapter 10 presents the main conclusions of the thesis and provides recommendation for future work.

Chapter 2 Literature Review

2.1 Introduction

Since the 1960s, the subjective and biodynamic responses of the seated human body exposed to whole-body vibration and shock have been systematically studied and found to depend on a variety of variables: vibration magnitude, vibration frequency, vibration direction, body posture, body position, muscle activity, seating condition, age and gender etc.

The biodynamic responses of the human body are found to be nonlinear: the resonance frequencies in frequency response functions (e.g. apparent mass and transmissibility) decrease with increasing vibration magnitude (e.g. Hinz and Seidel, 1987; Fairley and Griffin, 1989; Mansfield and Griffin, 2000; Mansfield and Griffin, 2002; Nawayseh and Griffin, 2003). The subjective responses of the human body exposed to vertical whole-body vibration were also found to be nonlinear: the rates of growth of sensation vary with the vibration frequency (e.g. Miwa, 1967; Miwa, 1968; Shoenberger and Harris, 1971; Dupuis *et al.* 1972; Jones and Saunders, 1974; Shoenberger, 1975; Howarth and Griffin, 1988; Morioka and Griffin, 2006 etc.). A correlation between subjective and biodynamic responses to whole-body vibration has been found (e.g. Matsumoto and Griffin, 2005; Subashi, *et al.* 2009).

This chapter reviews previous studies of the subjective and biodynamic responses to whole-body vertical vibration and shocks, and also the relation between subjective and biodynamic responses.

2.2 Subjective responses to vibration and mechanical shock

Vibrations or mechanical shocks usually cause unwanted or unpleasant sensations of the human body (e.g., motion sickness, vibration discomfort), although they are also often used to please humans (e.g., musical instruments, massage chairs etc.). This section focuses on the discomfort caused by vibrations or mechanical shocks, and how the variables (e.g., magnitude, frequency, directions of excitation) affect the vibration discomfort.

2.2.1 Vibration discomfort

2.2.1.1 Steven’s Power Law

The relation between a physical input and the sensation caused by the physical input has been investigated in many psychophysical studies. Stevens (1957) concluded that for any given simple stimulus, the sensation magnitude, ψ, can be related to the magnitude of physical stimulus, φ, by the following power law:

$$\Psi = k\,\varphi^{n}$$

where the exponent (also called the rate of growth of sensation), n, and the constant, k, are assumed to be constant for a given stimulus (for example, vibration with a given direction and a given frequency).

An alternative version of this law includes the perception threshold φ_0, which is the lowest magnitude of stimulus that can be perceived by a subject:

$$\Psi = k\,(\varphi - \varphi_0)^{n}$$

Steven's power law has been widely used to study vibration discomfort.

2.2.1.2 Psychophysical measurement methods

Many different methods are applied to relate subjective response to the physical characteristics of stimuli. Both semantic scales and numerical scales have been conducted to determine the subjective response to changes in vibration frequency, magnitude, duration, axis, etc.

Equivalent comfort contours define the manner in which vibration discomfort changes with vibration frequency and axis (Griffin, 1990). They show the vibration magnitudes necessary to produce similar discomfort at each vibration frequency, axis and input position. Equivalent comfort contours obtained by early experimental studies (e.g., Griffin *et al.*, 1982 and Corbridge and Griffin, 1986) have been constructed to standardize frequency weightings (e.g., BS 6841 (1987), ISO 2631-1 (1997)) which will be discussed in detail later. The two principal approaches to determine equivalent comfort contours are the 'absolute' method and the 'relative' method.

The 'absolute' method was widely used in early research. A semantic scale was used to describe subjects' sensations caused by vibration. Different studies have employed different phrases to describe the vibration sensations and wildly different results were obtained (Hanes, 1970). Fothergill and Griffin (1977) compared results of four different category scaling methods and found some agreement between mean values (Table 2.1).

The advantages of the 'absolute' method are: it is easy to use in real environments and many subjects can make their responses at the same time. It also has some critics, for

example, the same phrases used in one experiment may have different meanings for subjects from different backgrounds, cultures and experience. Different semantic phases were used in the different studies and little agreement was found between studies (Oborne, 1978).

Table 2.1 Comparison of results from four experiments using semantic scales (Fothergill and Griffin, 1977)

Study	Scale	Mean Magnitude (ms^{-2} r.m.s.)	Situation
Fothergill (1972)	Very unpleasant – Unpleasant – Mildly unpleasant – Not unpleasant – Noticeable –	2.5 1.7 1.1 0.7 0.3	Seated subjects; magnitudes of 8 Hz sinusoidal vibration
Jone and Saunders (1974)	Very unpleasant – Very uncomfortable – Uncomfortable – Mean threshold of discomfort – Not uncomfortable –	3.7 2.2 1.2 0.7 0.33	Seated subjects; magnitudes of 10 Hz sinusoidal vibration
Oborne and Clarke (1974)	Very uncomfortable – Uncomfortable – Fairly uncomfortable/ Fairly comfortable – Comfortable – Very comfortable –	>2.3 1.2-2.3 0.5-1.2 0.23-0.5 <0.23	Seated subjects; magnitudes of 10 Hz sinusoidal vibration
Fothergill and Griffin (1977)	Very uncomfortable – Uncomfortable – Mildly uncomfortable – Noticeable, but not uncomfortable –	2.7 1.8 1.1 0.4	Seated subjects; magnitudes of 10 Hz sinusoidal vibration

The ‘relative’ method is preferred in later studies, especially in laboratory studies. With this method a subject usually judges a succession of pairs of stimuli (e.g., method of paired comparisons, method of constant stimuli, method of adjustment etc., Griffin 1990).

The method of paired comparisons is a procedure in which subjects compare each stimulus with every other stimulus in a set of stimuli and indicate which of each pair produces sensations which are, in some respect, ‘greatest’. The disadvantage of this method is that it takes a lot of time compared with other methods.

The method of constant stimuli is a procedure in which subjects compare the sensations produced by each stimulus in a set of ‘test’ stimuli with the sensations produced by a fixed ‘reference’ stimulus. The test stimuli may often vary in magnitude and frequency and will be presented in random order. The test stimulus which produces a sensation equivalent to that caused by the reference stimulus may be ascertained from the results.

There are many useful derivative methods based on the above psychophysical methods (e.g. method of cross-modality matching, method of magnitude estimation). The method of cross-modality matching is a procedure in which subjects compare the sensations produced by one stimulus with those produced by a stimulus in another dimension (i.e., compare the discomfort produced by vibration with the discomfort produced by the loudness of sound). The method of magnitude estimation is a procedure which subjects are required to assign numbers to stimuli so that the numbers bear the same ratio to a number given to a reference condition as the sensations bear to the sensation caused by the reference condition (i.e., if the discomfort of a reference stimuli is assigned the value of 100, a stimuli twice as uncomfortable should be given the value of 200, etc.).

2.2.2 Factors influencing vibration discomfort

Griffin (1990) summarises the variables that could affect vibration discomfort (Table 2.2).

Table 2.2 Some variables associated with vibration discomfort

Extrinsic variables
Vibration variables
Vibration magnitude and combinations of magnitudes

Vibration frequency and combinations of frequencies
Vibration direction and combinations of directions
Vibration inputs position and combination of positions
Vibration duration and combination of durations
Other variables
Other stresses (noise, temperature, etc.)
Seat dynamics
Intrinsic Variables
Intra-subject variability
Body posture
Body position
Body orientation (sitting, standing, recumbent)
Inter-subject variability
Body size and weight
Body dynamic response
Age
Gender
Experience, expectation and attitude, personality
Fitness

This thesis mainly studies the subjective and biodynamic responses to vertical vibration and shock influenced by the vibration magnitude, frequency, waveform and seating conditions. The relevant previous studies which mainly focus on these factors are considered in the following sections.

2.2.2.1 Magnitude

There are many parameters which can be used to define the magnitude of vibration (e.g., r.m.s., VDV, peak acceleration and peak-to-peak acceleration). For human vibration, the most frequently used values are r.m.s. and VDV.

The root-mean-square (r.m.s.) value is the square root of the average values of the square of the acceleration record. The r.m.s. value will only be useful for periodic vibration and stationary random vibration, it is not suitable for defining the magnitude of shocks, intermittent vibration or other time-varying conditions.

The vibration dose value (VDV) is given by the fourth root of the integral of the fourth power of the acceleration (Griffin, 1990),

$$VDV = \left[\int_{t=0}^{t=T} a^4\,(t)dt\right]^{1/4}$$

It is a cumulative measure of the vibration and shock received by a person during the measurement period. The time-dependence of the VDV means that a single simple averaging procedure might be applicable over the full range of conditions from individual shocks and repeated impacts to intermittent vibration and long-duration continuous vibration. For the assessment of some effects of transient, shock and non-stationary motions, the root-mean-quad (r.m.q.) and VDV appear more appropriate than either r.m.s or peak values.

The magnitudes generally of interest with whole-body vibration are from about 0.01 to 10 ms^{-2} (peak). Whole-body vibration with a peak magnitude below about 0.01 ms^{-2} will rarely be felt. Whole-body vibration with a magnitude of 10 ms^{-2} r.m.s. may reasonably be assumed to be hazardous. Depending on the frequency, direction and duration of the vibration there may be some hazard associated with vibration magnitudes of about 1 ms^{-2} r.m.s. (Griffin 1990).

2.2.2.2 Frequency

The vibration frequencies of interest vary according to the environment and the effect. The frequency range mostly likely to elicit whole-body vibration discomfort and health responses is from approximately 0.5 to 100 Hz. At lower frequencies (less than 0.5 Hz) the principal effect of oscillation is a type of motion sickness (Griffin 1990).

The dominant vibration transmitted through the seats of vehicles is often at frequencies below 20 Hz. The degree to which vibration is transmitted to the human body depends on vibration frequency. The effects caused by vibration in the body at any location also depend on vibration frequency. Equivalent comfort contours are usually used to represent how vibration discomfort varies with the frequency of vibration. A body map is often used experimentally to investigate how the location of discomfort changes with the magnitude and frequency of vibration.

2.2.2.3 Waveform

The majority of laboratory research concerned with subjective response to whole-body vibration has involved single frequency sinusoidal vibration. However, motions experienced in real situations are never pure sinusoidal, and contain a wider range of frequencies. It is therefore important to know how results obtained for single frequency

vibration can be applied to different types of vibration, more similar to vibration experienced in real transport environment.

When a vibration stimulus contains several frequency components, they are likely to interact with each other in the creation of discomfort. Miwa (1968a) applied to vibration stimuli a model developed by Stevens (1956) for predicting the subjective loudness of acoustic stimuli containing several frequency components. The model is based on the concept of inhibition: due to some frequency components masking other components, the increase of the total discomfort due to the addition of a new component is only a fraction (notated *F*) of the discomfort caused by the additional component when presented alone. Based on this idea, Miwa suggested that the 'Vibration Greatness', VG of a complex vibration can be estimated by:

$$VG_t = (1 - F)VG_m + F\sum_i V\,G_i$$

Where:

VG_t is the vibration greatness of the complex motion

VG_m is the vibration greatness of the worst frequency component

$\sum_i V\,G_i$ is the sum of the VG of all components

F is an inhibition parameter.

Miwa (1968b) found that *F* was equal to 0.3. However, the value of the parameter *F* depended on the separation between the frequencies of the components, and was close to 1.0 when the frequency difference was sufficient.

Fothergill and Griffin (1977) compared the above model with other methods of evaluation. With the method of magnitude production, each stimulus was presented alternately with a reference sinusoidal motion. The magnitude of the reference was then adjusted until both stimuli felt equally uncomfortable, at which point the magnitude of the reference was retained as the 'equivalent magnitude', which is a measure of discomfort. Three prediction methods were compared to predict the equivalent magnitude of complex motions consisting of two frequency components:

Method 1: linear sum $E_t = E_1 + E_2$

Method 2: inhibition $E_t = E_1 + bE_2$

Method 3: root-sum-of-squares $E_t = \sqrt{E_1^2 + E_2^2}$

The inhibition method provided satisfying results with dual-frequency vibration, but was too complicated to predict the 'equivalent magnitude' of the vibration with a greater

number of frequency components. The authors concluded that the root-sum-of-square method was the best of the three methods to predict the equivalent magnitude of complex motions.

In real vibration exposure conditions, the vibration usually has a broad continuous frequency spectrum instead of consisting of discrete frequency components, so it is necessary to compare the effect of sinusoidal and random vibrations on discomfort.

Comparing the equivalent comfort contours for seated subjects exposed to either one-third octave random or sinusoidal vibration at frequencies in the range 3.15 to 20 Hz, Griffin (1976) found subjects were generally more sensitive to random vibration than sinusoidal vibration, although this difference was only statistically significant at 10 Hz and 12.5 Hz and was small compared to inter-subject differences.

A similar study was conducted by Donati *et al.* (1983) who compared the equivalent comfort contours obtained by sinusoidal and 'narrowband' random vibration in the range 2 to 10 Hz. The results showed that random vibration caused more discomfort than sinusoidal vibration when the r.m.s. value was the same.

It can be concluded that subjects are more sensitive to random vibration than to sinusoidal vibration when they are presented at equal r.m.s. magnitudes.

2.2.2.4 Seating conditions

Because different seats have different dynamic properties, it has generally been preferred to determine comfort contours with non-compliant seating (Griffin, 1990). The contours obtained on 'rigid' seats are then applied to vibration measurements obtained on the surface of compliant seat at a position directly beneath the ischial tuberosities of a person. However, the vibration at the ischial tuberosities arises from the dynamic interaction of the response of the body and the response of the seat. If the seat is not rigid the vibration of the body will influence the vibration of the seat and, in the extreme, it is possible for there to be near-zero vibration at the seat but significant vibration in the body. The extent to which this happens with real seats has not been thoroughly explored but, because the vibration in the body can influence vibration at the seat when the seat is not rigid, it appears that equivalent comfort contours will at least be more repeatable if they are obtained with rigid seats.

2.2.3 Subjective responses to vibration

2.2.3.1 Effect of vibration magnitude

When the magnitude of vibration is increased, vibration discomfort (and possibly pain) is increased and it can be assumed that increased magnitude increases the risks to health.

Many researches have studied the values of the exponent in Stevens' power law for whole-body vertical vibration, as shown in Figure 2.1. Miwa (1968) determined exponents for 5, 20 and 60 Hz and found a reduction in the exponent with an increase in vibration magnitude, suggesting an exponent of 0.6 for vibration greater than 1.0 ms^{-2} r.m.s. and 0.46 for vibration less than 1.0 ms^{-2} r.m.s. Shoenberger and Harris (1971) determined exponents for frequencies from 3.5 to 20 Hz and found that the exponent at 5 Hz was significantly greater than at 7, 15 and 20 Hz. Jones and Saunders (1974) found a mean exponent ranging from 0.88 to 0.99, and suggested that an exponent of 0.93 may be used to describe the response to whole-body vertical vibration from 5 to 80 Hz. Howarth and Griffin (1988) investigated exponents for low magnitudes (i.e., 0.04 to 0.4 ms^{-2} r.m.s.) vertical whole-body vibration and found no frequency dependence in the exponent with vertical vibration. Morioka and Griffin (2006) found the greatest exponent was obtained around the principal resonance frequency of the body (0.897 at 4 Hz).

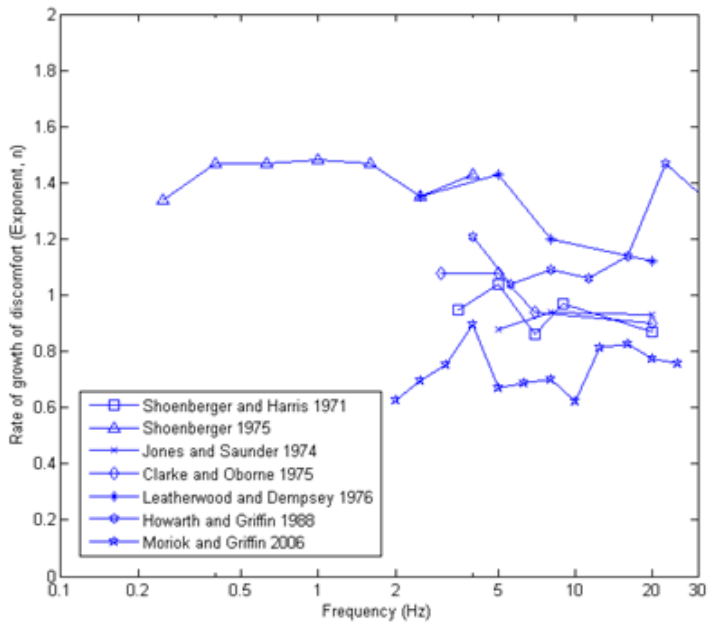

Figure 2.1 Rates of growth of sensation as a function of vibration frequency in previous researches

2.2.3.2 Effect of vibration frequency

The vibration discomfort is also dependent on the frequency of vibration. A constant vibration magnitude does not produce the same discomfort over all vibration frequencies.

The threshold contours and comfort contours have been found to vary with the vibration frequency (e.g., Miwa 1967; Griffin, Whitham *et al.* 1982; Corbridge and Griffin 1986; Howarth and Griffin 1988; Matsumoto and Griffin 2005; Morioka and Griffin 2006a; Morioka and Griffin 2006b; Subashi, Nawayseh *et al.* 2009). The nonlinearity in subjective response to vibration is also evident in the equivalent comfort contours: the comfort contours equivalent to a reference vibration at different magnitudes are not parallel (e.g., Shoenberger and Harris, 1971; Jones and Saunders, 1972; Griffin *et al.*, 1982; Morioka and Griffin, 2006).

Miwa (1967) obtained equivalent comfort contours for vertical vibration of seated persons by the method of paired comparison in which a reference vibration was compared with a variable frequency (Figure 2.2). The frequency of the reference vibration was 20 Hz at five different magnitudes (0.01 g, 0.0316 g, 0.1 g and 0.316 g, where g = 9.8 ms^{-2}). For each magnitude of the reference vibration, the magnitudes and frequencies of the test vibration varied so that the subjects can get the same strength of sensation as the reference vibration. The equivalent comfort contours show that subjects were most sensitive to vertical vibration around 5 or 6 Hz.

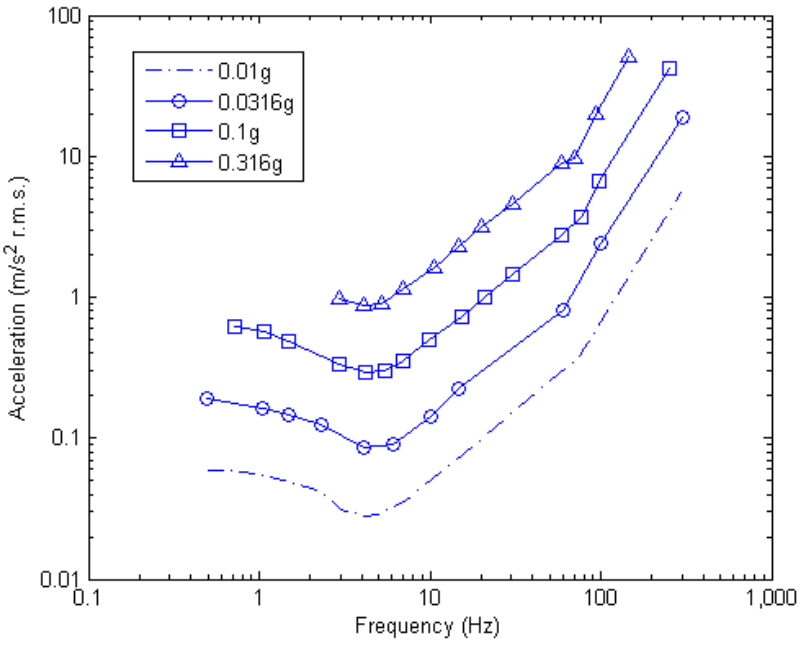

Figure 2.2 Equivalent comfort contours for vertical vibration of seated persons (Miwa 1967).

Dupuis *et al.* (1972a and 1972b) obtained the 'equal-intensity vibration perception' (now called equivalent comfort contours) of nine seated subjects (Figure 2.3). During their experiments, the subjects were asked to adjust the amplitude of the vibration for a given frequency so that it produced the same discomfort as the reference vibration. The equivalent comfort contour had a local minimum in the region of 5 Hz, which is the approximate resonance frequency of the human body. It is suggested that 'this fall is also particularly clear in the curve for readily detectable vibration down to 0.5 Hz, which presumably cannot be explained on the basis of kinetosis, it would appear that in this frequency range below 2 Hz human beings have a second region of special sensitivity.'

Shoenberger and Harris (1971) obtained equivalent comfort contours over the frequency range 3.5 to 20 Hz (3.5, 5, 7, 9, 11, 15 and 20 Hz) with sinusoidal vibration, as shown in Figure 2.4, and the reference frequency was 9 Hz. Six magnitudes were chosen for the reference vibration corresponding to subjective magnitudes magnitude levels of 10, 20, 30, 40, 50, and 60. The corresponding accelerations were 0.08 g, 0.16 g, 0.26 g, 0.36 g 0.46 g and 0.56 g. The experimental technique, intensity matching, was employed which required the subjects to match the subjective intensity of vibration at a reference frequency by adjusting the magnitude of vibration at another frequency until it seemed subjectively as intense as the reference vibration. It was found that subjects were most sensitive in the frequency range 5 to 10 Hz. As the magnitude of the reference vibration increased, the frequency corresponding to the minimum of each contour decreased. This shows nonlinearity in the equivalent comfort contours.

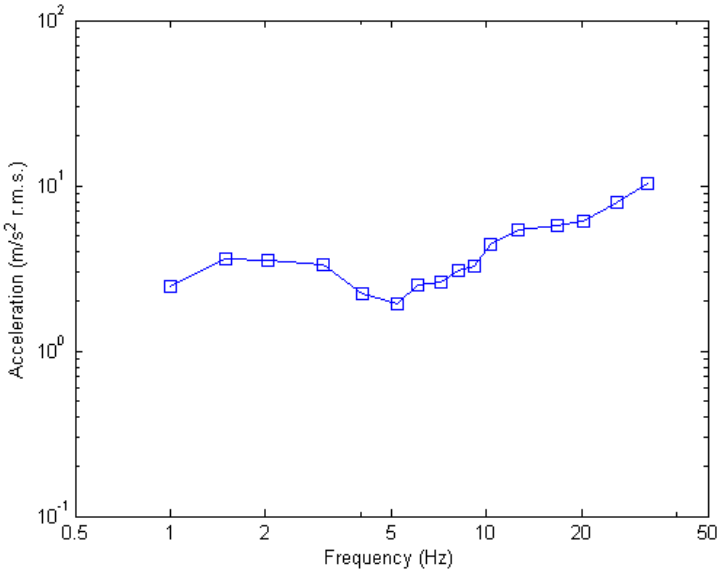

Figure 2.3 Equivalent comfort contours for vertical vibration of seated persons (Dupuis *et al.*, 1972)

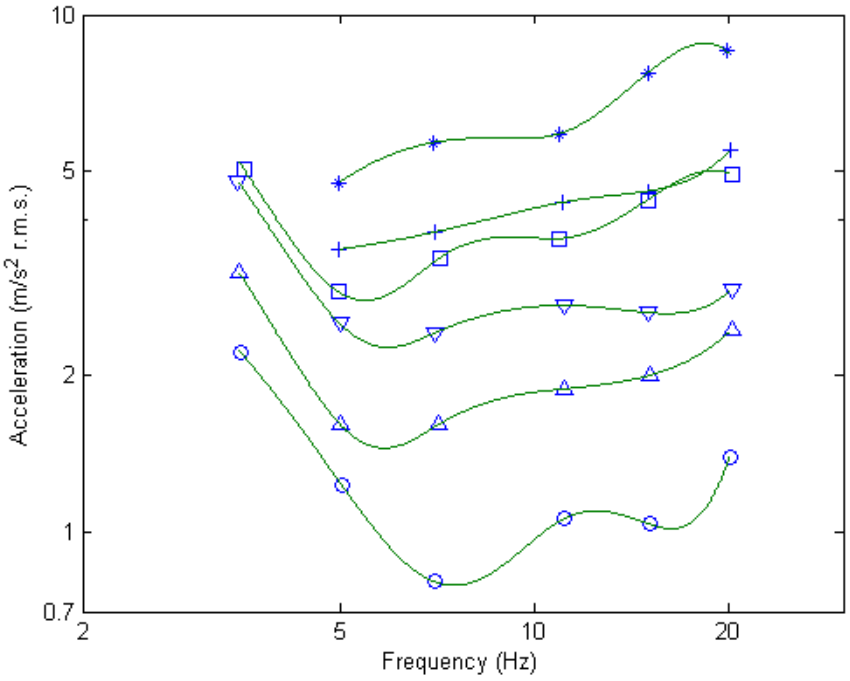

Figure 2.4 Intensity matching curves (Equivalent comfort contours) across frequencies for 9 Hz reference vibration at subjective magnitudes of 10, 20, 30, 40, 50 and 60: —○10, —△20, —▽30, —□40, —+ 50, —* 60 (Shoenberger and Harris, 1971)

Yonekawa and Miwa (1972) obtained equivalent comfort contours of seated subjects with ultra-low frequency oscillations from 0.05 to 1 Hz (0.05, 0.1, 0.2, 0.4, 0.6, 0.8 and 1 Hz), as shown in Figure 2.5. The frequency of the reference vibration was 0.5 Hz. The curve nearly has a slope of 3 dB/oct. It shows the subjects were more sensitive to acceleration at the lower frequencies than the higher frequencies in the frequency range of 0.05 to 1 Hz.

Jones and Saunders (1972) obtained equivalent comfort contours for both men and women in an unrestrained sitting position, over the frequency range 4 to 80 Hz with sinusoidal vibration (Figure 2.6). The method of adjustment was used to obtain subjective responses to vertical vibration. The subjects were asked to vary the test vibration until they considered the test and reference vibrations to be of the same discomfort. The subjects repeated the same procedure for 20-Hz reference vibration at six different magnitudes (0.69, 1.39, 2.08, 2.77, 3.46 and 4.16 ms^{-2} r.m.s.). The figure also shows that the subjects were most sensitive to vertical acceleration around 5 Hz. When the frequency was greater than 5 Hz, sensitivity to the vibration decreased as the frequency increased. It was found that the equivalent comfort contours for men and women were similar.

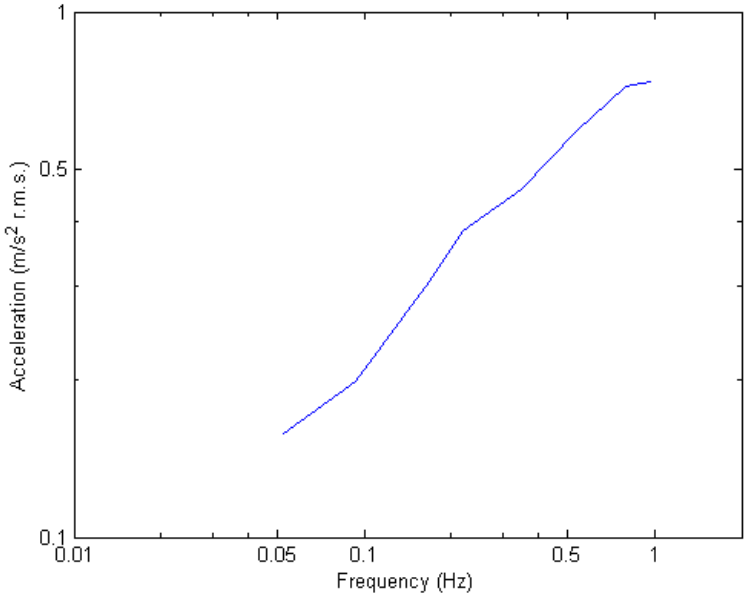

Figure 2.5 Equivalent comfort contours for vertical vibration of seated persons (Yonekawa and Miwa, 1972).

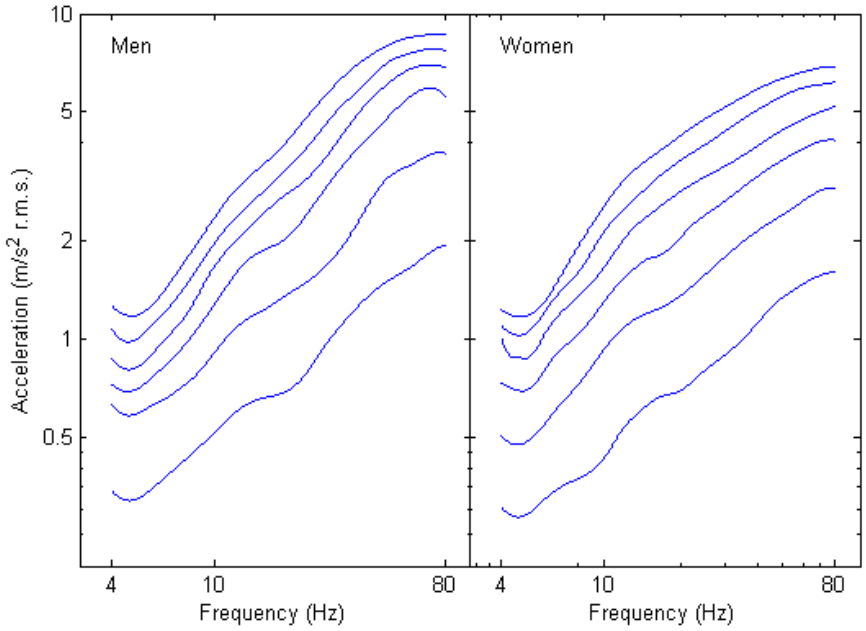

Figure 2.6 The equivalent comfort contours for both men and women (Jones and Saunders, 1972).

Shoenberger (1975) used the method of intensity matching to obtain equivalent comfort contours over the frequency range 0.16 Hz to 4 Hz, as shown in Figure 2.7. The frequency of the reference stimulus was 1 Hz and it had two magnitudes 0.4 g and 0.8 g. It was found that the acceleration level of the matching response was greatest at 0.63 and 1.0 Hz when the magnitude of the reference vibration was 0.4 g, and at 1 Hz

when the magnitude was 0.8 g. In order to avoid the effect of the reference vibration, another reference vibration was used, which was 2.5 Hz and had the same magnitudes as the previous reference vibration. However, the results were similar to the previous results.

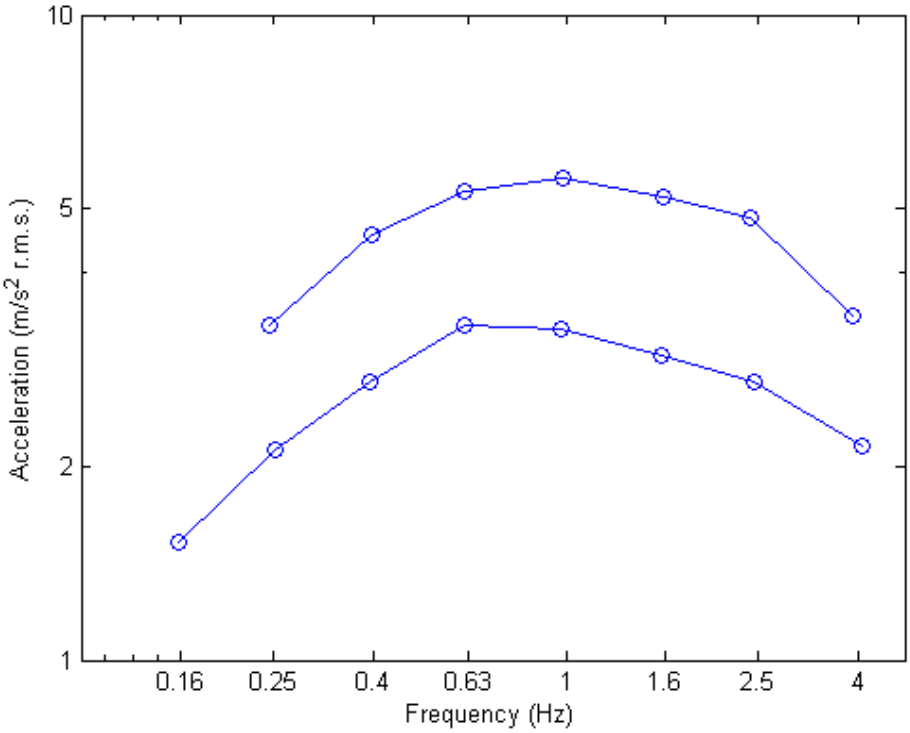

Figure 2.7 The equivalent comfort contours at the frequency range of 0.16 Hz to 4 Hz (Shoenberger, 1975).

Griffin (1976) compared the discomfort produced by whole-body sinusoidal vibration with that produced by one-third octave, one octave, and three-octave bands of vibration. Seated subjects were required to adjust the level of a variable test vibration such that it produced a degree of discomfort similar to that caused by a 10-Hz sinusoidal vertical vibration at 0.75 ms^{-2} r.m.s. The test stimuli were nine sinusoidal vibrations (at 3.15, 4, 5, 6.3, 8, 10, 12.5, 16 and 20 Hz); nine one-third-octave bands of random vibration centred at the above frequencies, three single-octave bands (centred at 4, 8 and 16 Hz) and a three-octave band (centred at 8 Hz). Figure 2.8 shows the mean levels of sinusoidal and third-octave random vibration required to produce similar discomfort to 0.75 ms^{-2} r.m.s. 10 Hz sinusoidal vibration.

Griffin *et al.* (1982) obtained the comfort contours equivalent to 0.8 ms^{-2} r.m.s. 10 Hz vertical sinusoidal vibration which were determined from 18 males and 18 females at preferred third-octave centre frequencies from 1 to 100 Hz (Figure 2.9). It was found that the subjects were more sensitive to the vibration at frequencies around 5 Hz. It

was concluded that the shapes of equivalent comfort contours “need not normally depend on vibration level”, and that males and females produced similar equivalent comfort contours.

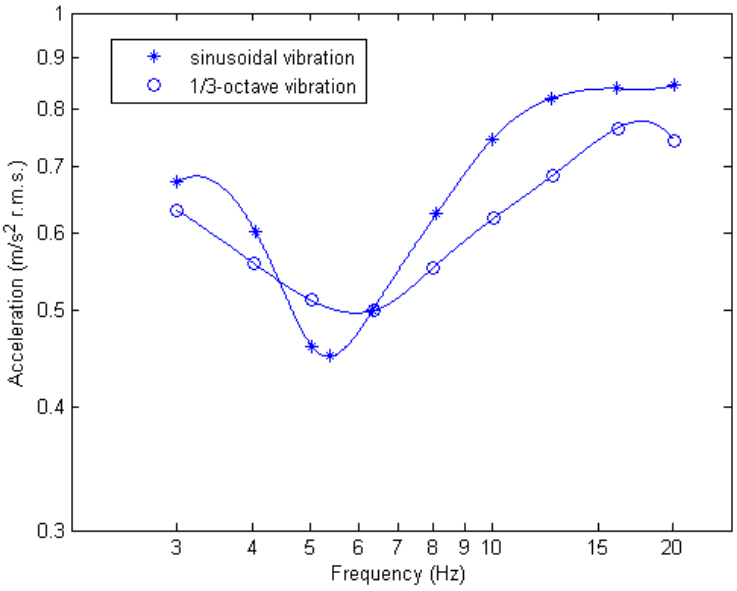

Figure 2. 8 Equivalent comfort contours for sinusoidal and third-octave random vibration (Griffin, 1976).

Corbridge and Griffin (1986) determined the effects of the frequency of whole-body vibration on comfort in the range 0.5 to 5.0 Hz. The first experiment determined the equivalent comfort contours of 40 subjects (20 males and 20 females) with vertical sinusoidal vibration by two references (0.75 and 0.25 ms^{-2} r.m.s., 2 Hz) for each of the 11 preferred third-octave centre frequencies from 0.5 to 5.0 Hz, as shown in Figure 2.10 (left). This shows subjects were more sensitive to acceleration at 5 Hz than at lower frequencies. It also shows a comparison of the median equivalent comfort contours for males and females. With the 0.75 ms^{-2} r.m.s. reference motion, the female subjects were significantly more sensitive to vibration at 3.15 Hz, 4.0 Hz and 5.0 Hz. With the 0.25 ms^{-2} r.m.s. reference motion, the female subjects were significantly more sensitive to vibration at 5.0 Hz. The results indicate that the shapes of the equivalent comfort contours were not greatly influenced by the magnitude of the reference motion (0.75 and 0.25 ms^{-2} r.m.s.). The second experiment determined equivalent comfort contours for 10 male subjects with octave bands of vertical random vibration centred on 0.5, 1.0, 2.0 and 4.0 Hz. The reference motion was 2 Hz 0.5 ms^{-2} r.m.s. sinusoidal vibration. The principal finding is that the shapes of the contours obtained using sinusoidal and random stimuli are similar.

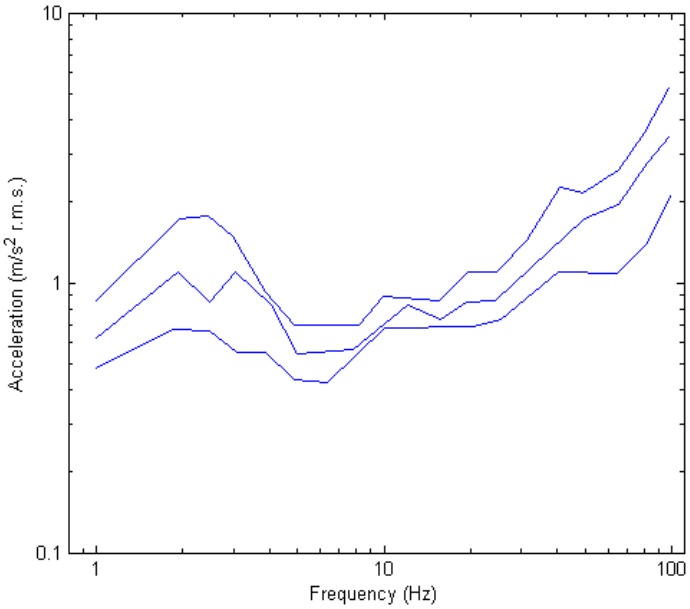

Figure 2.9 Median, 25th and 75th percentile equivalent comfort contours derived from 36 subjects for vertical vibration (Griffin *et al*., 1982).

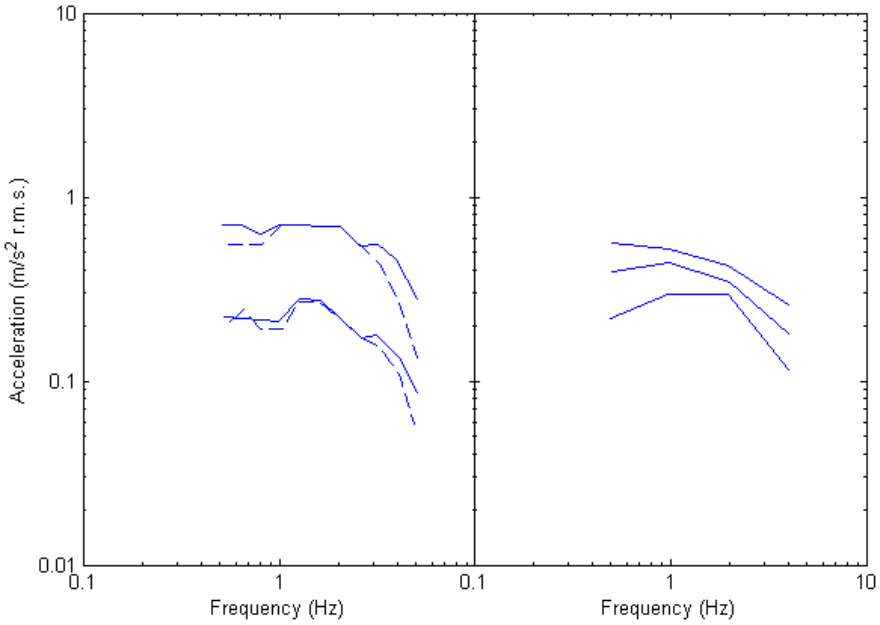

Figure 2.10(Left) Median equivalent comfort contours for 20 male (——) and 20 female (----) subjects using sinusoidal vibration (2 Hz reference stimuli: 0.75 and 0.25 ms^{-2} r.m.s.). (Right) Median, 25th and 75th percentile equivalent comfort contours for 10 male subjects using vertical octave band random vibration (2 Hz reference stimuli: 0.5 ms^{-2} r.m.s.) (Corbridge and Griffin, 1986)

Howarth and Griffin (1988) determined equivalent comfort contours for vertical vibration at magnitudes between 0.04 and 0.4 ms^{-2} r.m.s. within the frequency range 4 to 63 Hz.

The method of magnitude estimation was employed with a sound reference stimulus ($^1/_3$-octave band centred at 1 kHz). The contours corresponding to three magnitude estimates: 50, 100, and 200 are shown in Figure 2.11. It was found the subjects were most sensitive to frequencies around 5 Hz, but suggested slightly greater relative sensitivity at high frequencies than previous studies (e.g., Griffin *et al.*, 1982; Corbridge and Griffin, 1986).

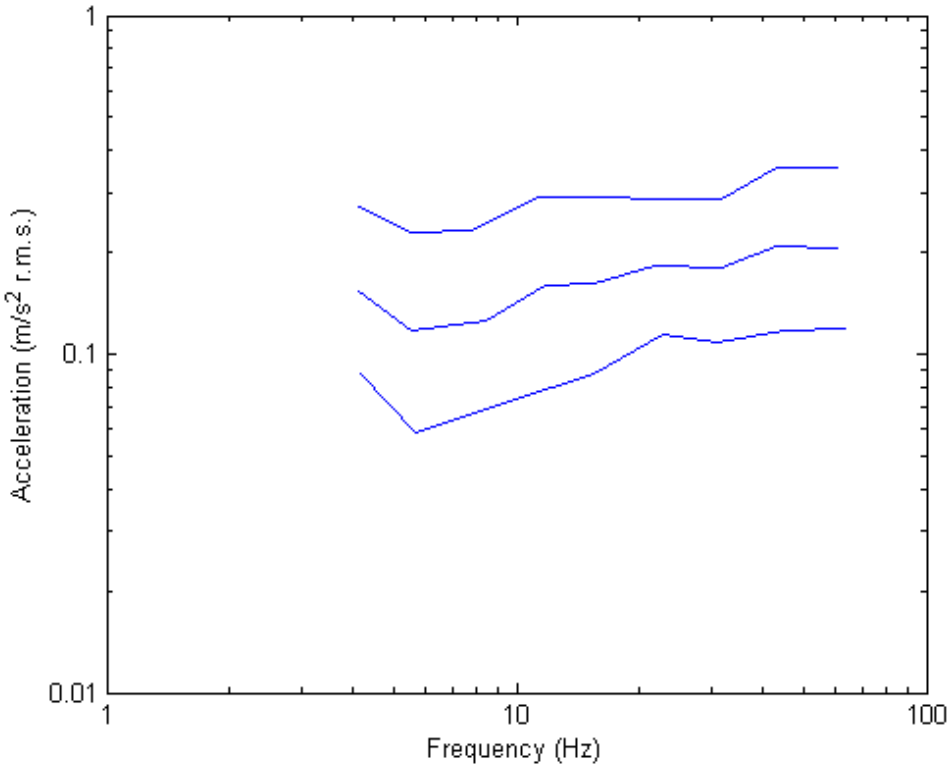

Figure 2.11 Equivalent comfort contours for magnitude estimates of 50, 100, and 200 (100 corresponds to the sound reference stimuli $^1/_3$-octave band centred at 1 kHz, Howarth and Griffin, 1988)

For sinusoidal vibration, Matsumoto and Griffin (2005) found the median magnitude estimate was greatest at 5.0, 6.3 and 4 Hz at 0.5, 1.0 and 2.0 ms^{-2} r.m.s. respectively. The median magnitude estimate at 3.15 Hz was lower than at other frequencies. The effect of frequency on the magnitude estimates was statistically significant for all magnitudes ($p<0.01$ for 0.5 and 1.0 ms^{-2} r.m.s. and $p<0.05$ for 2.0 ms^{-2} r.m.s; Friedman).

Mansfield and Maeda (2005) defined equal comfort contour for whole-body vertical sinusoidal vibration expressed in terms of force and acceleration. The frequencies of sinusoidal vibration were 1, 2, 4, 8, 16 and 32 Hz and the frequency of the reference vibration was 8 Hz. For the 1 Hz trial, the magnitude of the reference is 0.25 ms^{-2}

r.m.s.; for all other trials, the magnitude of the reference was 0.5 ms^{-2} r.m.s. The subjective intensity-matching protocol was used in the experiment. After the pair of stimuli, subjects judged whether the first (reference) or the second (test) stimulus had the greater intensity, or whether they felt the same. If the reference was more intense, the magnitude of the test vibration was increased by 20%. If the reference was less intensity, the magnitude of the test vibration was reduced by 20%. As ratings at 1 Hz were obtained relative to a reference with a magnitude of 50% of that used for all other conditions, measured values for acceleration and force were scaled by a factor of 2 to enable direct comparisons to be made. For the acceleration data, most subjects showed that they were relatively less sensitive to the vibration at frequencies greater than the reference. At frequencies lower than the reference, most subjects also showed a slight reduction in sensitivity, but this was not observed for all individuals (Figure 2.12). For the force data, all subjects showed that they were more sensitive to higher frequency forces than lower frequency forces. At frequencies above the reference (8 Hz), all subjects showed an increase in sensitivity (Figure 2.13).

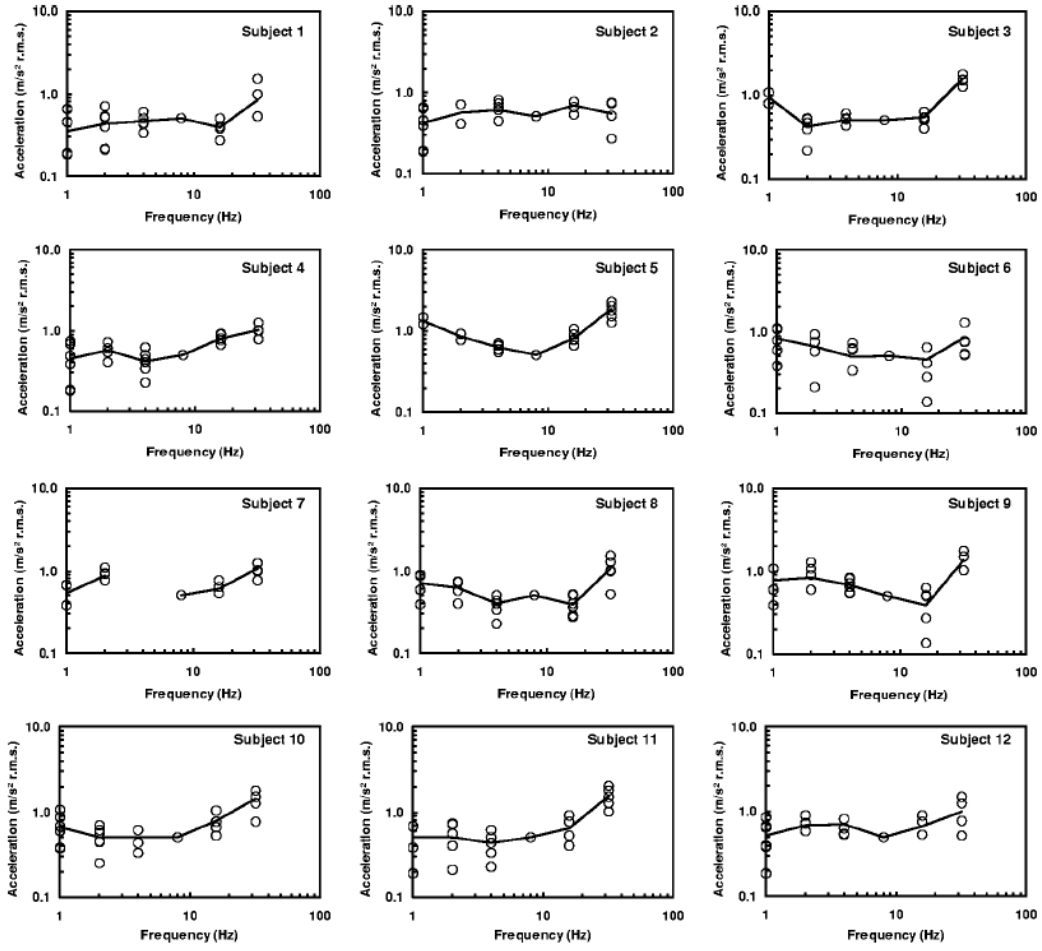

Figure 2.12 Acceleration equal sensation curves for 12 subjects exposed to whole-body vertical sinusoidal vibration (Mansfield and Maeda, 2005)

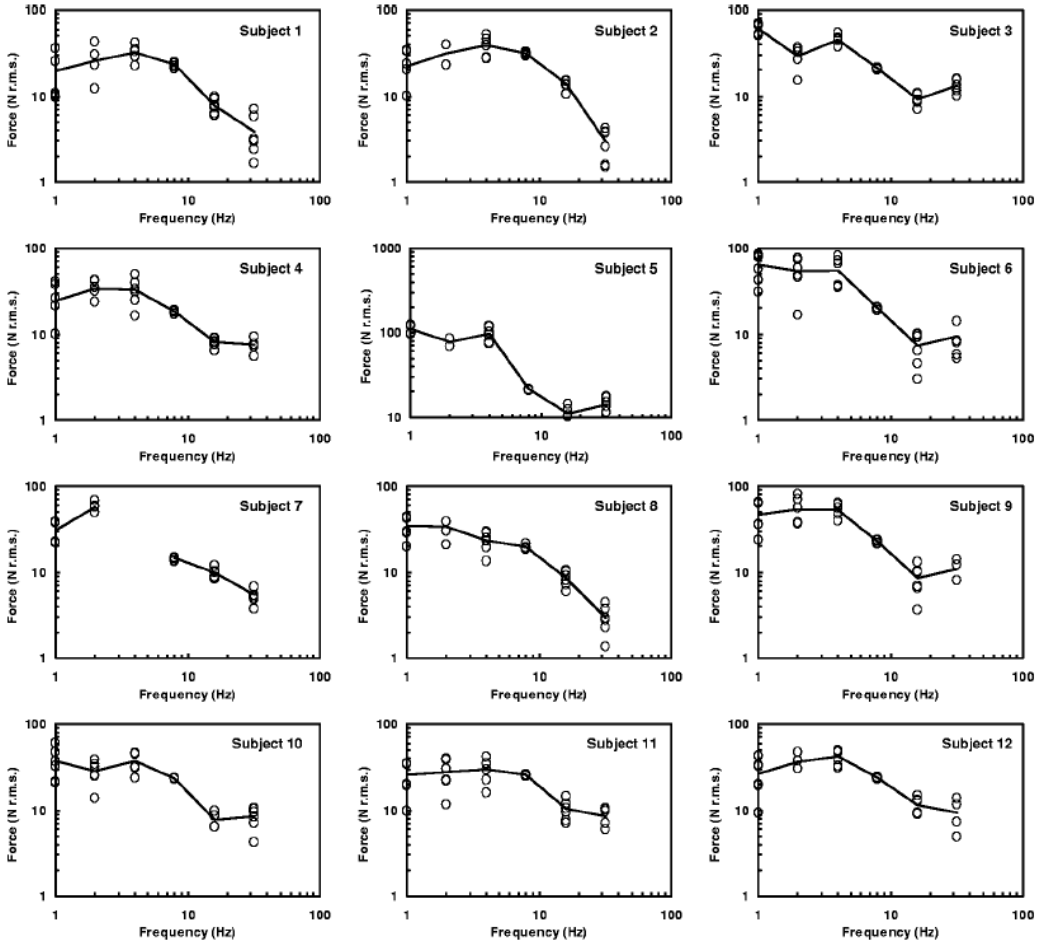

Figure 2.13 Force equal sensation curves for 12 subjects exposed to whole-body vertical sinusoidal vibration (Mansfield and Maeda, 2005)

Morioka and Griffin (2006) determined equivalent comfort contours for the whole-body vibration of seated subjects over the frequency range 2 to 315 Hz in the vertical direction. Twelve male subjects were involved in the experiment. They judged the discomfort caused by vertical sinusoidal vibration at 23 preferred one-third octave centre frequencies between 2 and 315 Hz relative to the reference vibration with a frequency of 20 Hz and a magnitude of 0.5 ms^{-2} r.m.s. The equivalent comfort contours showed subjects were most sensitivity to acceleration between 5 and 10 Hz, as shown in Figure 2.14.

2.2.4 Subjective response to shock

As with whole-body vibration, the prediction of discomfort caused by the whole-body mechanical shock that people experience in their daily lives has been of interest in mechanical, aeronautical and civil engineering. Exposure to such motion may result in discomfort or some risk to human health. Some experiments have designed to

investigate human response to impulsive motion (e.g., Miwa, 1968; Griffin and Whitham, 1980; Hoddinott, 1986; Howarth and Griffin, 1991; Matsumoto and Griffin, 2002a and 2002b; Matsumoto and Griffin, 2005; Ahn and Griffin 2008).

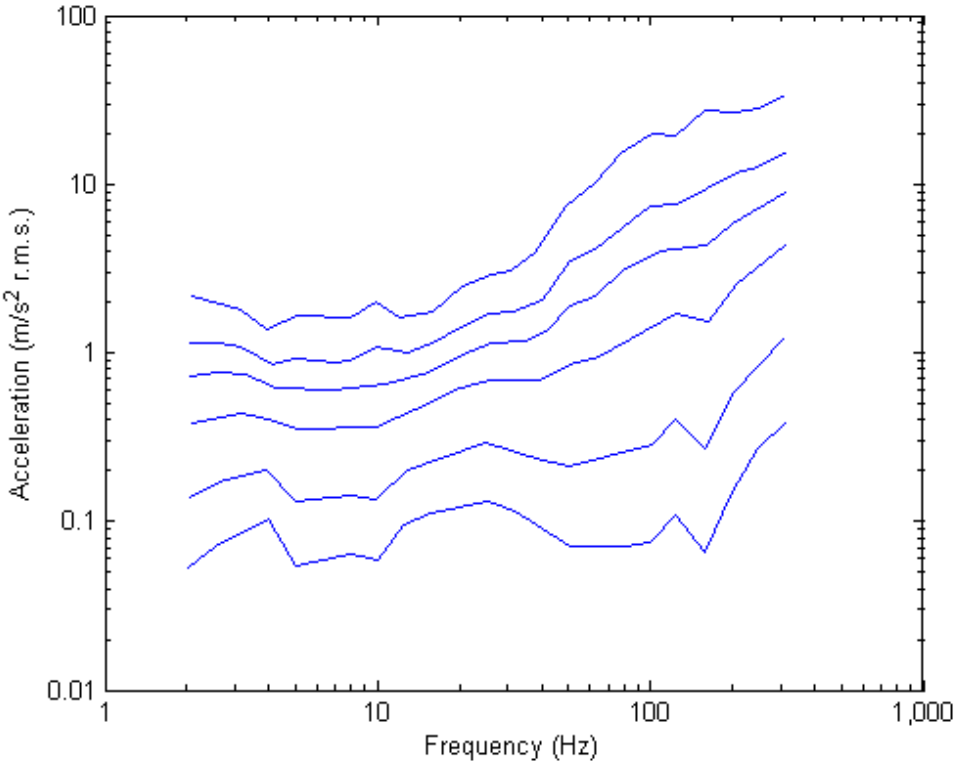

Figure 2. 14 Equivalent comfort contours for sensation magnitudes from 25 to 300 relative to a vertical vibration magnitude of 0.5 ms^{-2} r.m.s. at 20 Hz (Morioka and Griffin, 2006)

Miwa (1968) investigated the effect of duration of pulsed sinusoidal, “damped” and “built-up” vibration and concluded that the sensation increased with vibration duration up to a critical duration (i.e. up to 2.0s for 2-60 Hz stimuli, and up to 0.8s for 60-200 Hz stimuli). Griffin and Whitham (1980) investigated the discomfort produced by impulsive whole-body vibration and found that discomfort increased with increasing duration up to at least 32s, with some variations in the rate of increase between stimuli at 4, 8, 16 and 32 Hz. Ahn and Griffin (2008) investigated the effect of duration of shocks by adjusting the damping ratios, such that shocks with greater damping ratio had shorter durations. They found for most stimuli the discomfort was unaffected by damping when the VDV was constant, but there were significant differences in the range 4.0-10.0 Hz where stimuli of longer duration tended to be judged slightly more uncomfortable than those of shorter duration.

Methods for assessing the discomfort caused by mechanical shock of different durations have been studied by many previous experiments. Hoddinott (1986) suggested that the peak acceleration and root-mean-square procedure did not allow for the effect of duration and the vibration dose value (VDV) predicted the relative discomfort from stimuli of all durations. Spang *et al.* (1984) compared six methods of evaluating impulsive motion in off-road vehicles. They found the shock response spectrum and vibration dose value generally gave the highest correlation coefficients while peak measures and a dose based on r.m.s. measures gave the lowest correlation coefficients.

The following section reviews the effect of magnitude, frequency, and direction on the discomfort caused by mechanical shocks studied in previous research.

2.2.4.1 Effect of magnitude

Howarth and Griffin (1991) investigated subjective reactions to vertical mechanical shocks of various waveforms. The stimuli simulated the transient response of a single-degree-of-freedom damped oscillator to a unit displacement step input. The shocks were presented at three nominal frequencies (1, 4 and 16 Hz), three damping ratios (ζ = 0.125, 0.250 and 0.707) and for upward and downward (vertical direction) displacement step inputs. The stimuli consisted of four magnitudes (VDV = 0.6, 1.0, 1.6 and 2.5 $ms^{-1.75}$) of 1 Hz motion for each damping ratio and both directions, and five magnitudes (VDV = 0.6, 1.0, 1.6, 2.5 and 4 $ms^{-1.75}$) of 4 and 16 Hz motion for each damping ratio and both directions. The method of magnitude estimation was employed in the experiment. The relation between median magnitude estimate and vibration dose value was determined by Steven's power law for each frequency, damping ratio and direction by linear regression. Statistical analysis showed that there was no significant effect of frequency, duration, or direction on the value of the exponent *n*, except between conditions involving 16 Hz 'upward' motion with a damping ratio of 0.125. The results showed that the value of exponent was approximately unity for most conditions. This indicated that when the objective magnitude is presented by the vibration dose value it may be related to the subjective magnitude by a power function for which the exponent remains constant at different frequencies and durations of motion. It indicated that the frequency weighting for the assessment of the reaction to mechanical shock and the rate of growth of discomfort with duration are independent of shock magnitude. It suggested that the evaluation the discomfort of this type of shock may be simplified by a single frequency weighting, and a single method of allowing for the effect of duration. For constant VDV, decreasing the damping ratio was shown to increase discomfort. The results suggested that the VDV may underestimate the time-

dependency of discomfort for some low frequency shocks. However, the degree of underestimation was generally small in view of the wide range of shock durations used.

Matsumoto and Griffin (2005) determined the effect of the magnitude of transient whole-body vibration in the vertical direction on subjective responses of the seated human body. The transient vibrations were formed from one-and-half cycles of a sinusoidal acceleration waveform modulated by a half cycle sinusoidal at unit amplitude with a period three times longer than the period of the sinusoidal acceleration (Figure 2.15). The frequencies of the sinusoidal waveform were 3.15, 4.0, 5.0, 6.3, and 8 Hz. The magnitudes of the transient vibration were defined by the acceleration at the peak (i.e., -0.7, -1.4, and -2.8 ms^{-2}). The method of magnitude estimation was applied to measure the relative discomfort caused by the input stimuli. The frequency of the reference transient vibration was 5 Hz and the magnitudes was the same as that of the test stimulus (i.e., -0.7, -1.4 and -2.8 ms^{-2}).

Statistical analysis showed that there were significant differences in the magnitude estimates obtained with the shock at 3.15 and 4 Hz ($p< 0.05$, Friedman). The median magnitude estimate obtained with the transient vibration having -2.8 ms^{-2} peak were significantly greater than those for transient vibration having -0.7 ms^{-2} and -1.4 ms^{-2} peaks at 3.15 Hz and that for the transient vibrations having -0.7 ms^{-2} peaks at 4 Hz ($p<0.05$, Wilcoxon matched-pairs signed ranks test) (Figure 2.16). The results showed a strong nonlinear characteristic in subjective response to vertical transient vibration caused by different stimulus magnitudes.

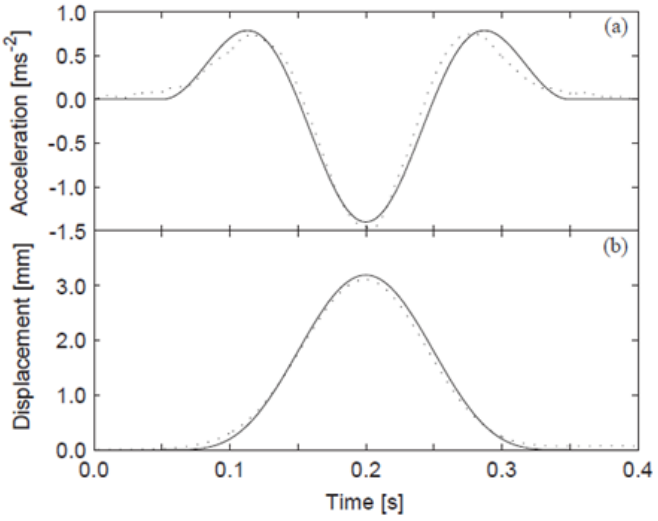

Figure 2.15 An example of the acceleration and displacement waveform of the transient vibration used in the experiment. ——: desired waveform; ·····: measured waveform (Matsumoto and Griffin 2005).

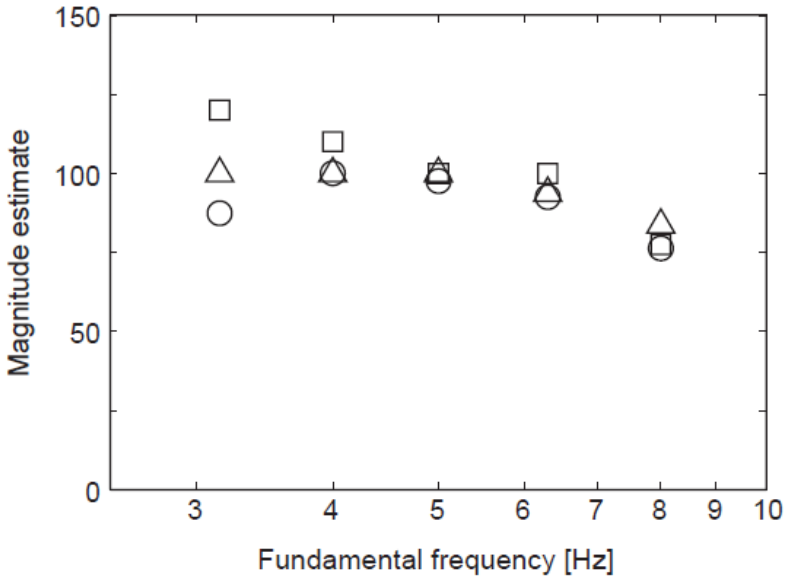

Figure 2.16 Median of magnitude estimates measured with 12 subjects exposed to transient vibration. ○: -0.7 ms^{-2} at peak, -1.4 ms^{-2} at peak and -2.8 ms^{-2} at peak (Matsumoto and Griffin 2005).

Ahn and Griffin (2008) studied the discomfort of 15 seated subjects exposed to a wide range of vertical mechanical shocks. Shocks were produced from responses of single degree-of-freedom models with 16 fundamental frequencies (0.5-16 Hz) and four damping ratios (0.05, 0.1, 0.2 and 0.4) to half-sine force inputs (Figure 2.17). For the highest damping ratio (i.e., 0.4), a reverse direction of shock was also applied. Each type of shock was presented at five unweighted vibration dose values (0.35-2.89 $ms^{-1.75}$). The method of magnitude estimation was used to compare the discomfort produced by the test shocks with the discomfort produced by a reference shock. The reference was a 2.5 Hz shock with a damping ratio of 0.1 and an unweighted VDV of 1.0 $ms^{-1.75}$ (3.1 ms^{-2} peak-to-peak). For each subject at each fundamental frequency and damping ratio, the shock magnitude (in unweighted VDV) corresponding to a magnitude estimate of 100 was determined from the regressions between subjective magnitudes and VDVs.

At each combination of fundamental frequency and damping ratio (including the reversed direction shocks), there were significant correlations between the five magnitudes and the magnitude estimates of discomfort. The median of the exponents, *n* of the Stevens' power law over the 15 subjects at each frequency and at each damping ratio and for the reverse direction shock, are shown in Figure 2.18. For all four damping ratios, and the reverse direction shock, the exponents varied with the shock fundamental frequency.

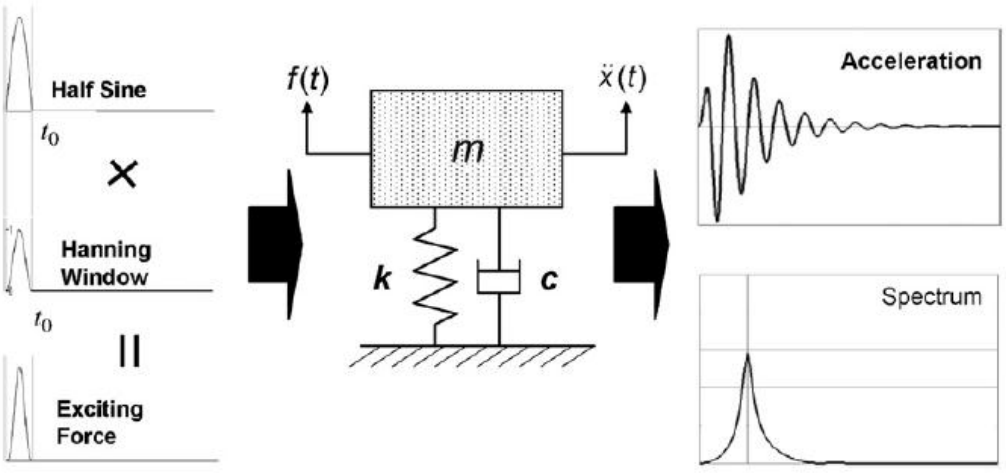

Figure 2.17 One degree-of-freedom vibration model. Hanning-windowed half-sine input and the shock-type response (Ahn and Griffin, 2008)

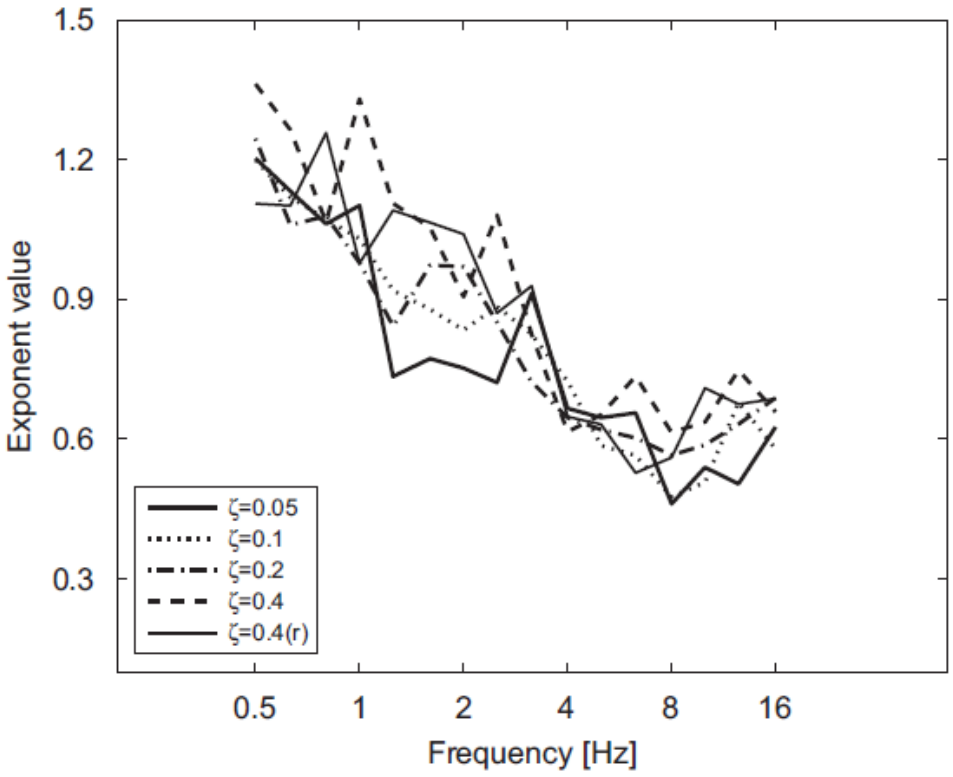

Figure 2.18 Median of exponents in Stevens' power law over the 15 subjects for each frequency, each damping ratio and the reversed direction shocks (Ahn and Griffin, 2008).

2.2.4.2 Effect of frequency

Howarth and Griffin (1991) conducted an analysis of covariance to determine whether the discomfort of mechanical shocks depends on frequency (1, 4 and 16 Hz) for

constant vibration dose values (VDV = 0.6, 1.0, 1.6 and 2.5 $ms^{-1.75}$). The results indicated that both frequency and damping had a significant effect on the magnitude estimates for a constant vibration dose value ($p<0.025$). The magnitude estimate of discomfort was greatest at 1 Hz. They suggested that it may be a result of increased subjective judgements resulting from seeing the greater displacement that occur at 1 Hz than at 4 Hz and 16 Hz. Because subjects were not in a moving cabin and could see their movements relative to the laboratory.

Matsumoto and Griffin (2005) found for transient vibration (details of the experimental conditions have been mentioned in Section 2.2.4.1), the effect of frequency on the magnitude estimates was statistically significant at all magnitudes ($p<0.05$ for -0.7 ms^{-2} peak and $p<0.01$ for -1.4 and -2.8 ms^{-2} peak, Friedman two-way analysis of variance). At all three magnitudes, the median magnitude estimates at 8.0 Hz were lower than those at the other frequencies.

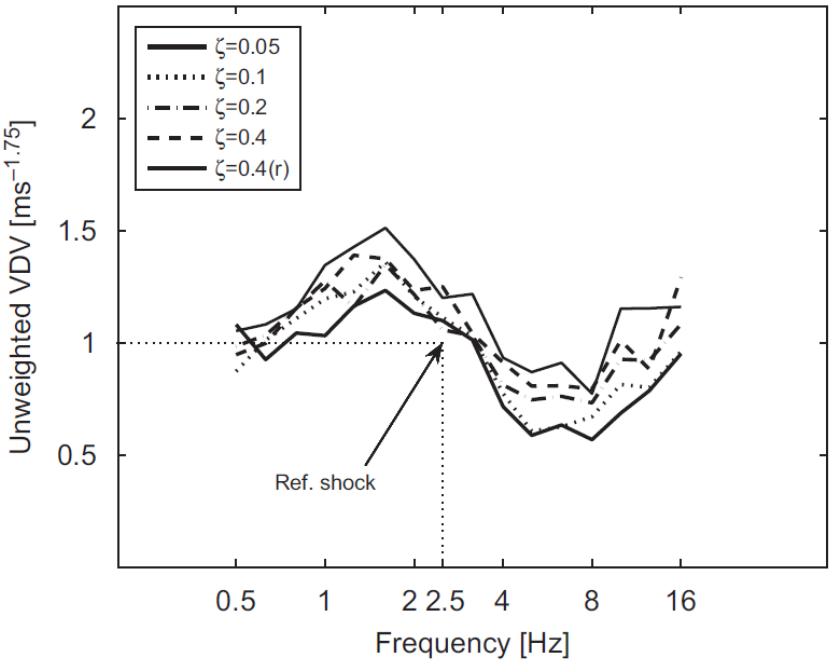

Figure 2.19 Equivalent comfort contours for test shocks (median over 15 subjects for each damping ratio and reversed direction shocks) (Ahn and Griffin, 2008).

Ahn and Griffin (2008) found the magnitude estimate of the subjects to the desired shock magnitudes were highly dependent on the fundamental frequency of the shock. The equivalent comfort contours was shown in Figure 2.19. For the same damping ratio and unweighted VDV, subjects showed greatest discomfort in the range 4-12.5 Hz. The damping had a small but consistent effect, with the more highly damped motions being significantly more comfortable in the range 4-10 Hz.

2.2.4.3 Effect of direction

Howarth and Griffin (1991) found no large difference in subjective response to upward and downward shocks (having nominal frequencies of 1, 4, or 16 Hz) or a large difference in frequency weighting when the VDVs of shocks varied over the range 0.6-4.0 $ms^{-1.75}$.

Ahn and Griffin (2008) showed the shock direction only had a statistically significant effect on the equivalent comfort contour at 0.63, 1.6, 2.0, 3.15, and 12.5 Hz, where the upward shock caused slightly greater discomfort than the downward shock.

2.2.5 Frequency weighting

The effects of the frequency of vibration on subjective responses have previously been studied with single-frequency sinusoidal vibration and with narrow band random vibration so as to obtain frequency weightings that have influenced the evaluation methods for quantifying the severity of whole-body vibration in current standards, such as BS 6841 (1987) and ISO 2631-1 (1997). BS 6841 advocates the use of frequency weighting W_b for the evaluation vertical whole-body vibration. The W_b frequency weighting was derived from equivalent comfort contours determined by Griffin et al (1982) over the frequency range 1-100 Hz and by Corbridge and Griffin (1986) over the range 0.5-5 Hz. The asymptotic version of the W_b frequency weighting is independent of frequency (0 dB per octave) between 0.5 and 2 Hz, increases in proportion to frequency (+6 dB per octave) between 2 and 5 Hz, independent of frequency (0 dB per octave) between 5 and 16 Hz, and decrease inversely proportional to frequency (-6 dB per octave) between 16 and 80 Hz, indicating greatest sensitivity to acceleration at frequencies between 5 and 16 Hz. ISO 2631 uses frequency weighting W_k for the evaluation of some type of vertical vibration. It was based on the preference of some committee members rather than experimental evidence (Figure 2.20). These frequency weightings are used to predict the severity of human response to complex oscillations (e.g. multiple-frequency sinusoidal vibration, random vibration, transient vibration, and shocks) in occupational and leisure environments. However, there are some limitations to the current frequency weightings. For example, the current frequency weightings have the same frequency dependence at all magnitudes (i.e., they are linear) where studies of biodynamic responses and subjective responses suggest the frequency dependence of human response varies with the magnitude of motion.

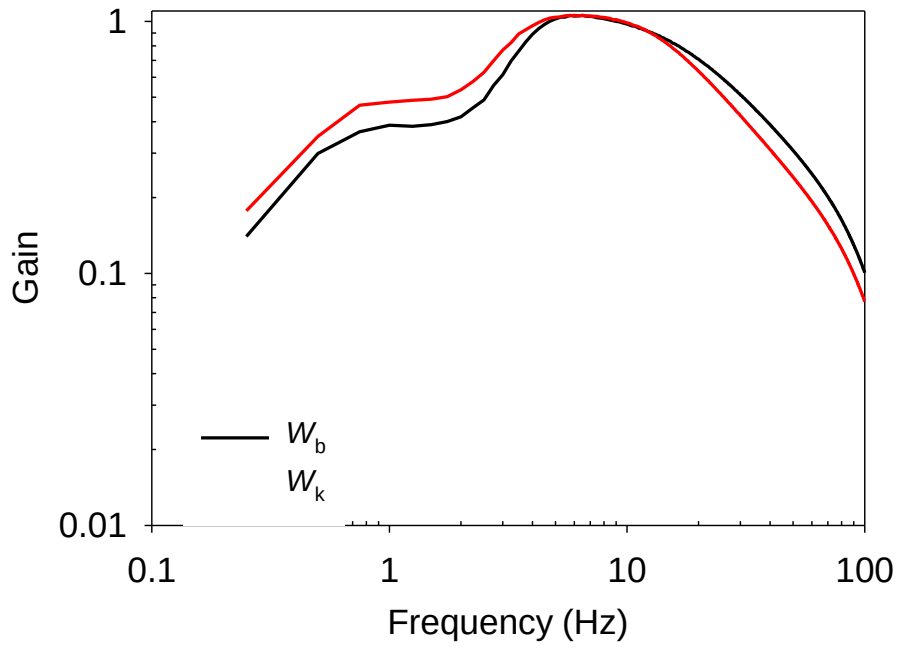

Figure 2.20 Frequency weightings (W_b from BS 6841 (1987) and W_k from ISO 2631-1 (1997))

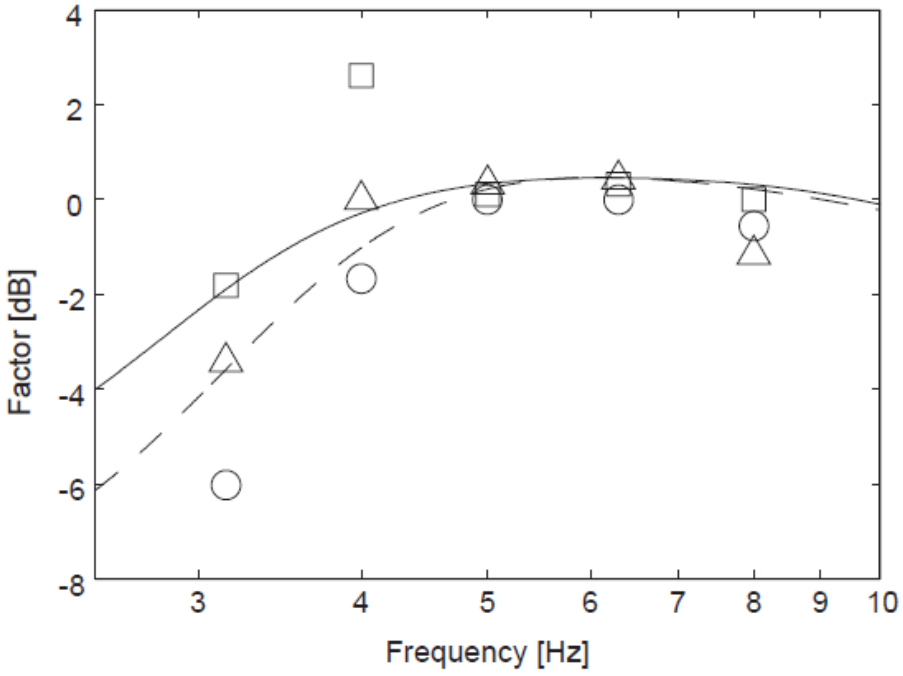

Figure 2.21 Comparison between the standard frequency weighting (——: W_k; — —: W_b) and the median discomfort magnitudes estimates obtained with the sinusoidal vibration expressed in dB. ○: 0.5 ms^{-2} r.m.s.; △: 1.0 ms^{-2} r.m.s.; □: 2.0 ms^{-2} r.m.s. (Matsumoto and Griffin, 2005)

Matsumoto and Griffin (2005) compared the median magnitudes estimates of discomfort obtained with sinusoidal vibration (five frequencies from 3.15 to 8.0 Hz, three magnitudes: 0.5, 1.0 and 2.0 ms^{-2} r.m.s.) with the standardised frequency weighting (e.g., W_b frequency weighting in BS 6841 (1987) and W_k frequency weighting in ISO 2631-1 (1997)) (Figure 2.21). The figure implies that the nonlinearity of subjective responses observed in the study is potentially important when considering frequency weighting for vertical vibration.

Mansfield and Maeda (2005) compared acceleration equal sensation with other studies and W_k frequency weighting (Figure 2.22). All data were scaled to have a value of 0.5 at 8 Hz. The trend was found similar between studies. All data showed the greatest sensation frequency occur between 4 and 8 Hz, and a reduced sensation at higher and lower frequencies. At frequencies of 4 Hz and above, the results in this study was similar with W_k frequency weighting. However, below 4 Hz the W_k frequency weighting shows a more rapid reduction in sensitivity than the results here.

Morioka and Griffin (2006) inverted the equivalent comfort contours for vertical vibration and normalised it to have a value of unity at 5 Hz and overlaid it with the W_b frequency weighting (Figure 2.23). The frequency weighting obtained by this study was in broad agreement with the W_b frequency weighting in the standard, but there was a tendency for the standardised frequency to underestimate discomfort at frequencies greater than about 30 Hz. Because of the magnitude-dependence of equivalent comfort contours, it implied that no single linear frequency weighting can provide an accurate prediction of subjective judgement of discomfort caused by whole-body vibration over a range of vibration frequencies and magnitudes from threshold to levels associated discomfort and injury.

Ahn and Griffin (2008) compared the weightings for the lowest, middle and highest shock with the frequency weighting W_b from BS 6841 in Figure 2.24. The weighting W_b was adjusted to match at 6.3 Hz, the expected magnitude estimates for the lowest shocks (i.e., VDV 0.35 $ms^{-1.75}$), the middle magnitude shocks (i.e. VDV 1 $ms^{-1.75}$), and the highest magnitude (i.e., VDV 2.89 $ms^{-1.75}$). It showed that the frequency weighting W_b was broadly similar to the shock frequency weighting at lower magnitudes but underestimated the discomfort of low frequency (less than 4 Hz) for high magnitude shocks.

The differences between frequency weightings in standards and the equivalent comfort contours from previous studies suggests that current standard frequency

weightings cannot provide an accurate prediction of discomfort caused by whole-body vibration over a range of vibration frequencies and magnitudes.

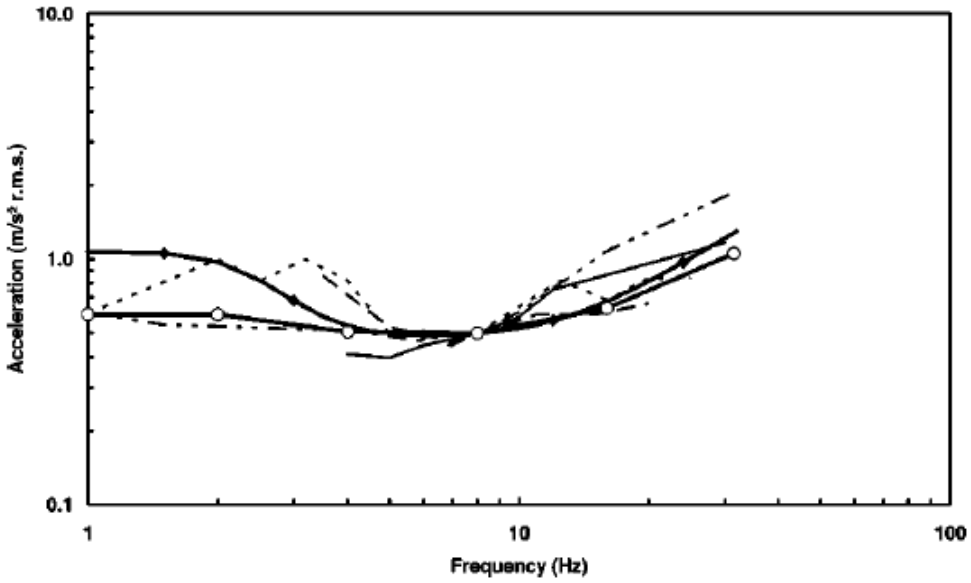

Figure 2.22 Comparison of median equal sensation acceleration data obtained in Mansfield and Maeda (2005; —○—) with data from Miwa (1967; — ▪▪ —), Shoenberger and Harris (1971; — — —), Jones and Saunders (1972; ——), Griffin *et al.* (1982; ▪ ▪ ▪), and an inverted W_k frequency weighting (— ♦ —), all scaled to give a value of 0.5 and 8 Hz. (Mansfield and Maeda, 2005)

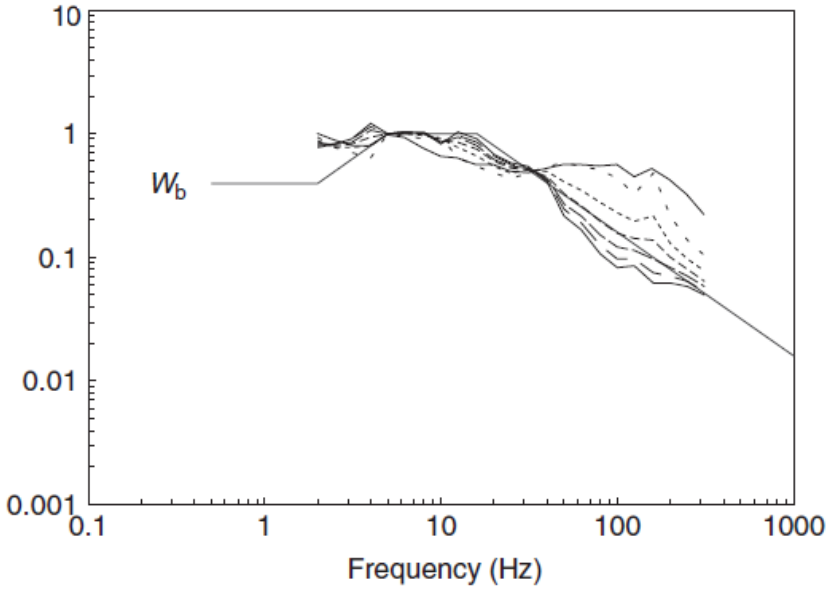

Figure 2.23 Effect of vibration magnitude on frequency weightings (normalised at 5 Hz). A sensation magnitude of 100 is equivalent to the discomfort produced by 0.5 ms^{-2} r.m.s. at 20 Hz. ·····:50, ▪▪▪▪▪▪: 100, — — —: 150, ▬ ▬: 200, ▬ ▪ ▬: 250, ▬▬▬: 300, ——: threshold. (Morioka and Griffin, 2006)

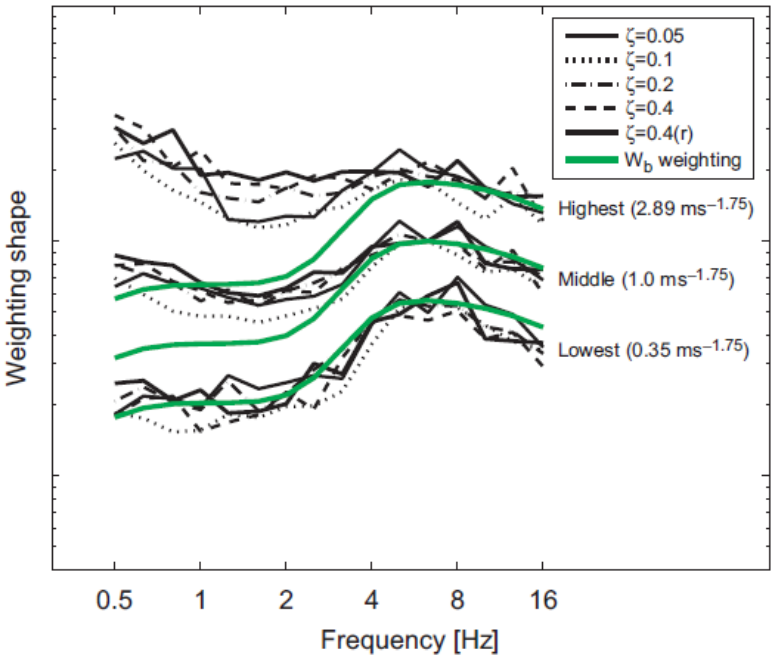

Figure 2.24 Frequency dependence of discomfort caused by shocks compared with frequency weighting W_b in BS 6841(1987) (Ahn and Griffin, 2008).

2.3 Biodynamic responses to vibration

2.3.1 Measurements of dynamic responses of the human body

Driving-point frequency response functions are used to describe relationships between an input signal and an output signal measured at the same point, usually at the interface between the subject and the vibration source. The interface could be the seat surface or backrest for a seated subject, the foot platform for a standing subject, or the recumbent back support for a supine subject. If the acceleration is used as the input at the interface and the dynamic force is the output, the frequency response function represents the 'apparent mass' of the human body. If the velocity is used as the input, the frequency response function represents the 'mechanical impedance'.

The apparent mass (also known as 'driving-point apparent mass' or 'effective mass') at a frequency *f, M*(*f*), is defined as the complex ratio of the output force, *F*(*f*), to the input acceleration, *a*(*f*), measured at the seat-subject interface:

$$M(f) = \frac{F(f)}{a(f)}$$

The mechanical impedance at frequency *f, Z*(*f*), is defined as the complex ratio of the output (or driving) force, *F*(*f*), to the input velocity, *v*(*f*), measured at the seat-subject interface:

$$Z(f) = \frac{F(f)}{v(f)}$$

'Transmissibility' represents the amount of motion transmitted between two locations. Normally the acceleration is used for convenience of measurement. The transmissibility is defined as the complex ratio of the motion measured at the output location to the motion measured at the input reference location. The input reference motion is usually measured at the seat-subject interface. For example:

$$T(f) = \frac{a_{L5}(f)}{a_B(f)}$$

Where $T(f)$ is the transmissibility between the vertical acceleration at the seat base, $a_B(f)$, and the vertical acceleration at the fifth vertebra of lumbar spine, $a_{L5}(f)$.

2.3.2 The vertical apparent mass

Previous studies have investigated the apparent mass of the seated human body exposed to vertical vibration and reported a first resonance frequency at around 4-6 Hz and a second resonance frequency around 8-12 Hz (e.g. Fairley and Griffin, 1989; Kitazaki and Griffin, 1998; Mansfield and Griffin, 2000; Mansfield and Griffin, 2002; Matsumoto and Griffin, 2002a; Matsumoto and Griffin, 2002b; Nawayseh and Griffin 2003, Mansfield and Maeda 2006). Experimental studies have shown that many factors can affect the apparent mass of the human body (e.g., vibration magnitude, vibration spectrum, seating conditions, intra-subject variability and inter-subject variability). The following sections mainly review the effect of vibration magnitude and vibration spectrum on the vertical apparent mass.

2.3.2.1 Effect of vibration magnitude

Research has consistently found that the resonance frequency of the apparent mass of the human body decreases with increasing magnitude of vibration, which has been referred as the biodynamic nonlinearity (e.g. Hinz and Seidel, 1987; Fairley and Griffin, 1989; Mansfield, 1998; Matsumoto and Griffin, 1998; Mansfield and Griffin, 2000; Matsumoto and Griffin, 2002a and 2002b; Matsumoto and Griffin 2005; Nawayseh and Griffin 2005; Subashi *et al*. 2006 and Subashi *et al*. 2009).

Using vertical sinusoidal vibration, Hinz and Seidel (1987) reported a decrease in the average apparent mass resonance frequency of four subjects from 4.5 to 4 Hz with an increase in vibration magnitude from 1.5 to 3.0 ms^{-2} r.m.s.

With random vibration in the range from 1 to 20 Hz, the apparent mass resonance frequency of seated subjects exposed to vertical vibration decreased from about 6 to 4 Hz as the vibration magnitude increased from 0.25 to 2.0 ms^{-2} r.m.s., as shown in Figure 2.25 (Fairley and Griffin, 1989).

Mansfield and Griffin (2000) obtained the apparent masses and transmissibilities of twelve subjects exposed to six magnitudes, 0.25 to 2.5 ms^{-2} r.m.s., of random vibration in the frequency range 0.2-20 Hz. The apparent mass resonance frequency reduced from 5.4 to 4.2 Hz as the magnitude of the vibration increased from 0.25 to 2.5 ms^{-2} r.m.s., as shown in Figure 2.26.

The apparent masses and the transmissibilities of eight male subjects exposed to random vertical vibration in the frequency range 0.5 to 20 Hz at five magnitudes (0.125, 0.25, 0.5, 1.0 and 2.0 ms^{-2} r.m.s.) were investigated by Matsumoto and Griffin (2002a). The resonance frequency of the normalised apparent mass decreased from 6.4 Hz to 4.75 as the vibration magnitude increased from 0.125 to 2.0 ms^{-2} r.m.s. Nonlinearity was also found in the transmissibilities to the body at eight locations: at the head, at the first, fifth and tenth thoracic vertebrae (T1, T5, T10), at the first, third and fifth lumbar vertebrae (L1, L3, L5) and at the pelvis (Figure 2.27). For example, Figure 2.27(f) shows the peak frequency of transmissibility to vertical vibration at L3 decreased from 6.25 to 4.75 Hz when the vibration magnitude increased from 0.125 to 2.0 ms^{-2} r.m.s.

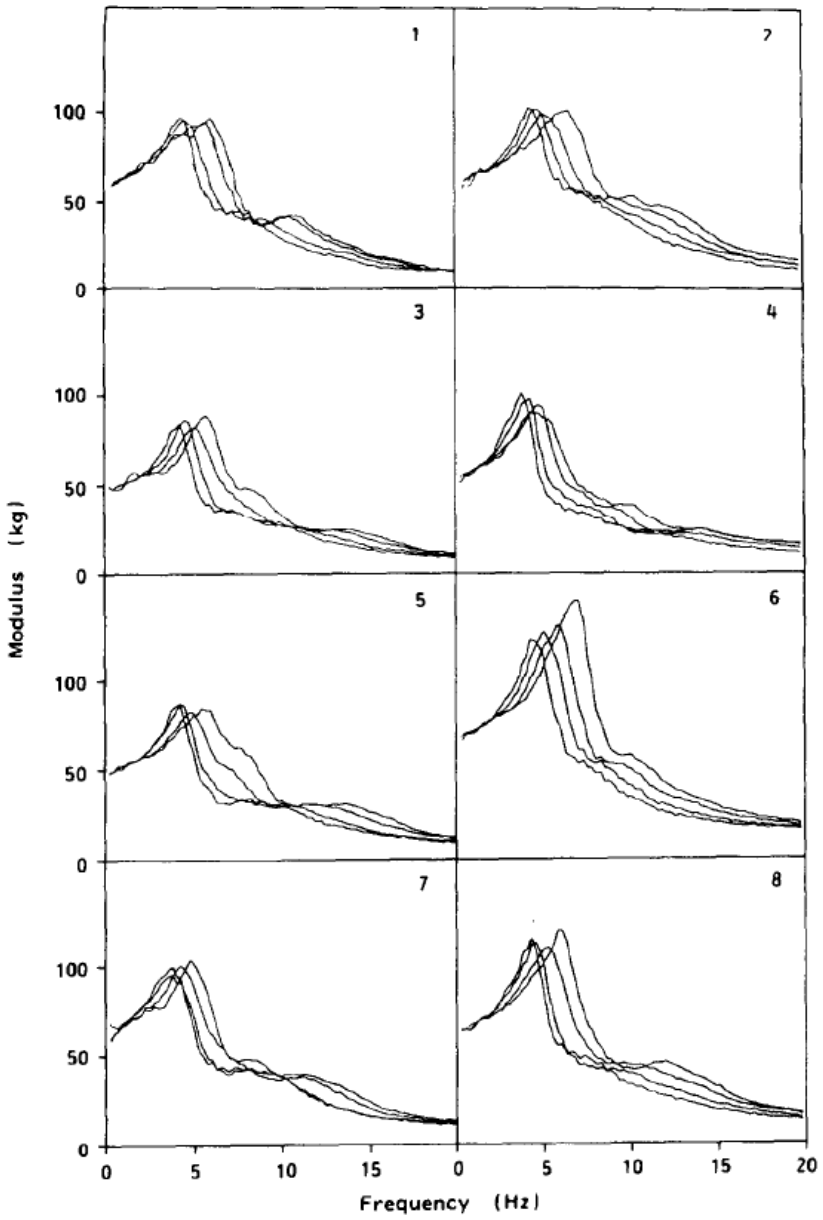

Figure 2.25 Effect of vibration magnitude (0.25, 0.5, 1.0 and 2.0 ms^{-2} r.m.s.) on the apparent mass of eight people — the resonance frequency, and the apparent mass at frequencies above resonance, consistently decrease with increasing magnitude for every person (Fairley and Griffin, 1989).

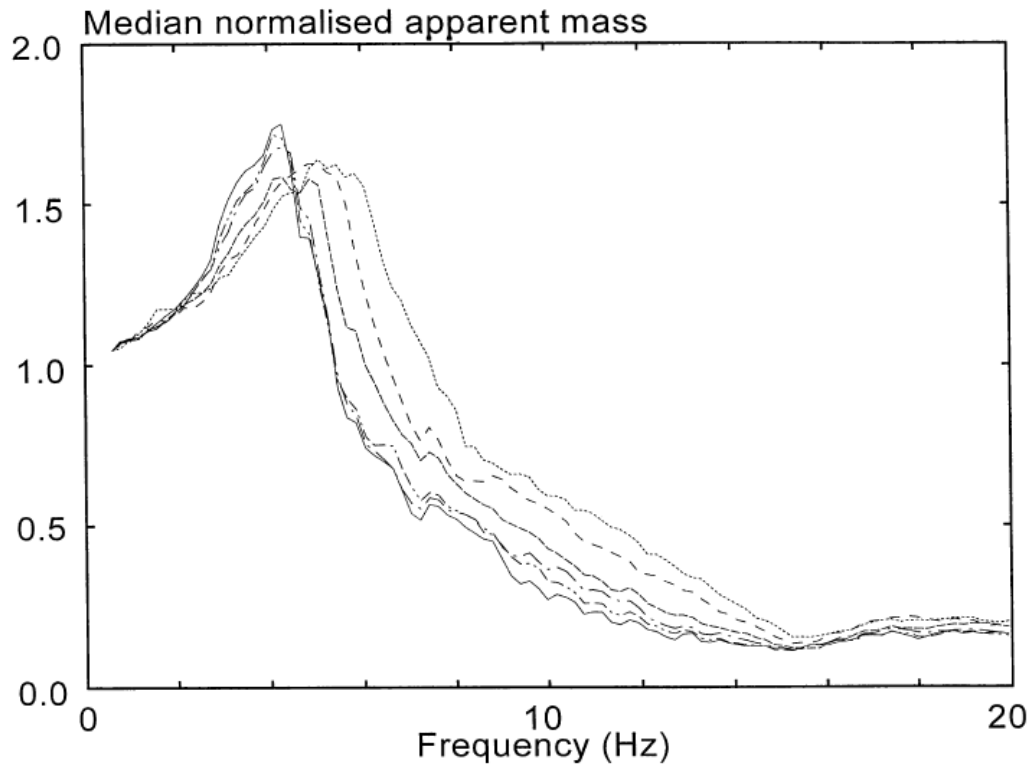

Figure 2.26 Median normalised apparent mass of 12 subjects measured at 0.25 (……), 0.5 (**---**), 1.0 (– – –), 1.5 (– · –), 2.0 (-- · --), 2.5 (——) ms^{-2} r.m.s. Resonance frequencies decrease with increasing vibration magnitude (Mansfield and Griffin, 2000).

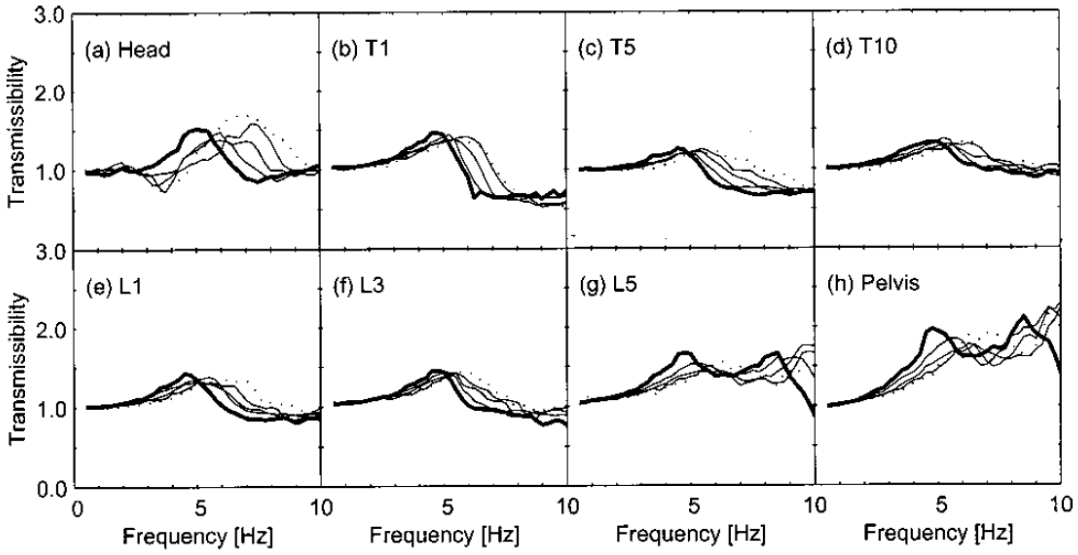

Figure 2.27 Median transmissibilities from vertical seat vibration to vertical vibration at each measurement location at five magnitudes of vibration: **---**, the lowest magnitude (0.125 ms^{-2} r.m.s.); —— the greatest magnitude (2.0 ms^{-2} r.m.s.) (Matsumoto and Griffin, 2002a).

Matsumoto and Griffin (2002b) investigated the effect of muscle tension on nonlinearity in the apparent mass of seated subjects exposed to vertical whole-body vibration. It was found that with increases in the magnitude of random vibration from 0.35 to 1.4 ms^{-2} r.m.s., the apparent mass resonance frequency decreased from 5.25 to 4.25 Hz with normal muscle tension, from 5.0 to 4.38 Hz with the buttocks muscles tensed, and from 5.13 to 4.5 Hz with abdominal muscle tension.

Mansfield and Griffin (2002) investigated the effect of variations in posture and vibration magnitude on apparent mass with vertical random vibration over the frequency range 1.0 to 20 Hz. Each of 12 subjects was exposed to 27 combinations of three vibration magnitudes (0.2, 1.0 and 2.0 ms^{-2} r.m.s.) and nine sitting postures (‘upright’, ‘anterior lean’, ‘posterior lean’, ‘kyphotic’, ’basck-on’, ‘pelvis support’, ‘inverted SIT-BAR’(increased pressure beneath ischial tuberosities), ‘bead cushion’ (decreased pressure beneath ischial tuberosities) and ‘belt’ (wearing an elasticated belt)). In all postures, the resonance frequencies in the apparent mass decreased with increased vibration magnitude, indicating a nonlinear softening system. There were only small changes in apparent mass with changes in posture. The changes in apparent mass caused by changes in vibration magnitude were greater than changes caused by variation in posture.

Matsumoto and Griffin (2005) investigated the effect of the magnitude of continuous and transient whole-body vibration in the vertical direction. Twelve subjects were exposed to sinusoidal continuous vibration at five frequencies (3.15, 4.0, 5.0, 6.3 and 8.0 Hz) and at three magnitudes (0.5, 1.0 and 2.0 ms^{-2} r.m.s.). They were also exposed to transient vibrations that were modulated one-and-half cycle sinusoidal waveforms at the same frequencies as the continuous vibrations and at three magnitudes corresponding to the magnitudes used for the continuous vibrations. At 3.15 and 4 Hz, the normalised mechanical impedance and apparent mass increased significantly with increases in vibration magnitude from 0.5-2.0 ms^{-2} r.m.s. For the transient vibrations, the driving-point dynamic responses were interpreted as responses in frequency bands around the fundamental frequency of the input motion.

Huang and Griffin (2006) investigated the effects of vibration magnitude and voluntary periodic muscle activity on the apparent mass resonance frequency using vertical random vibration in the frequency range 0.5-20 Hz. Each subject was exposed to 14 combinations of two vibration magnitudes (0.25 and 2 ms^{-2} r.m.s.) in seven sitting conditions: two without voluntary periodic movement (A: upright; B: upper-body tensed), and five with voluntary periodic movement (C: back-abdomen bending; D: folding-stretching arms from back to front; E: stretching arms from rest to front; F:

folding arms from elbow; G: deep breathing). Three conditions with voluntary periodic movement significantly reduced the difference in resonance frequency at the two vibration magnitudes compared with the difference in a static sitting condition. Without voluntary periodic movement, the median apparent mass resonance frequency reduced from the 5.47 Hz to 4.39 Hz as the vibration magnitude increased from 0.25 to 2 ms^{-2} r.m.s. With voluntary periodic movement (C: back-abdomen bending), the resonance frequency was 4.69 Hz at the low vibration magnitude and 4.59 Hz at the high vibration magnitude.

2.3.2.2 Effect of vibration spectrum

Most studies have measured the apparent mass of the human body with random vibration (e.g. Fairley and Griffin, 1989; Mansfield and Griffin 2000) while a few have considered response to sinusoidal vibration (e.g., Mansfield and Maeda, 2005).

Mansfield and Maeda (2005) compared the apparent mass of seated humans measured using random and sinusoidal vibration. Twelve male subjects participated in the experiment. For random vibration, the frequency range was from 1 to 40 Hz. The magnitude of the random vibration was 0.1 ms^{-2} r.m.s. (unweighted) and the duration was 60 s. The frequencies of sinusoidal vibration were 1, 2, 4, 8, 16, and 32 Hz. Each sinusoidal vibration had a duration of 4 s. The 1 Hz vibration had a magnitude of 0.2 ms^{-2} r.m.s. W_k weighted, the 2 Hz vibration had a magnitude of 0.4 ms^{-2} r.m.s. W_k weighted; all other frequencies of vibration had a magnitude of 0.5 ms^{-2} r.m.s. W_k weighted. The results showed that the moduli of the apparent mass measured using random vibration and sinusoidal vibration were similar to one another (Figure 2.28 and Figure 2.29). Differences between the apparent mass were significant at 1.0 Hz ($p<0.001$, Wilcoxon) and at 16 Hz ($p<0.05$, Wilcoxon). Generally, there is no difference between the modulus of the apparent masses measured using random or sinusoidal vibration, and the differences were small where it occured. The phase of the apparent mass was similar for the random and sinusoidal vibration at low frequencies. However, at frequencies of 8 Hz and greater, the phase lag with sinusoidal vibration was significantly greater than that measured using random vibration ($p<0.005$, Wilcoxon).

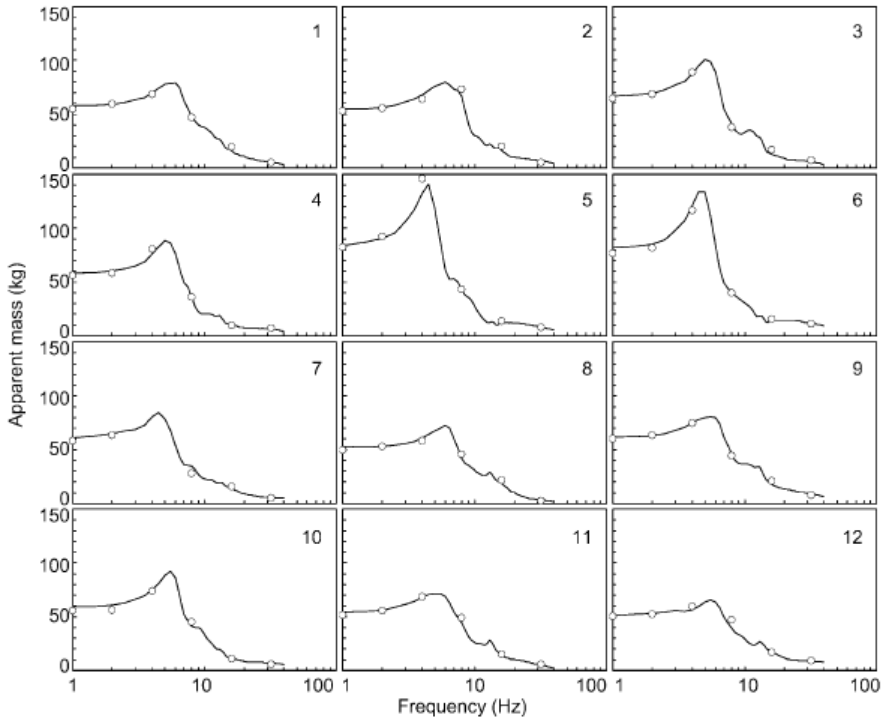

Figure 2.28 Modulus of apparent mass of 12 male subjects measured using random (—) and sinusoidal (○) vibration (Mansfield and Maeda, 2005).

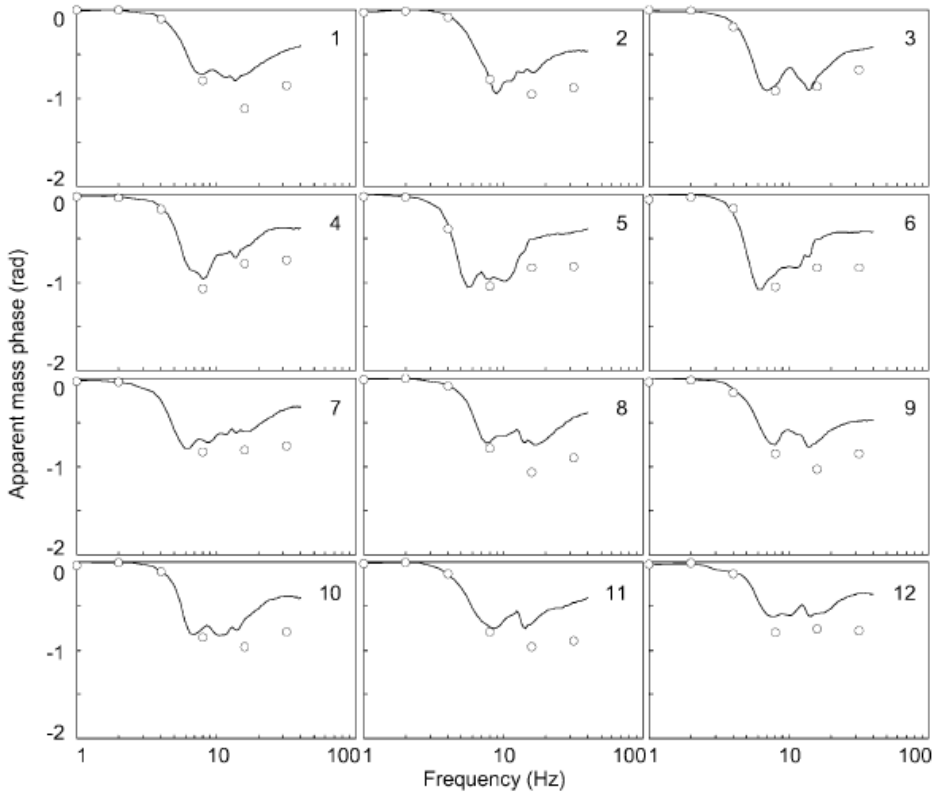

Figure 2.29 Phase of apparent mass of 12 male subjects measured using random (—) and sinusoidal (○) vibration (Mansfield and Maeda, 2005).

Apart from changing with vibration magnitude, different vibration spectra have also been observed to induce nonlinearity in biodynamic responses (e.g. Toward 2002; Mansfield *et al.* 2006).

Toward (2002) investigated the apparent mass of 12 seated subjects exposed to random broadband vibration (0.125 to 25 Hz, at 0.25 ms^{-2} r.m.s.) on which nine 1/2-octave narrow-band inputs were superposed at four magnitudes (0.25, 0.4, 0.63 and 1.0 ms^{-2} r.m.s.). Consistent with other studies, the frequency of the first and second resonances in the apparent mass decreased with increasing input magnitude. The apparent masses of the subjects also depended on the frequency of the narrow-band inputs. The magnitude of vibration at frequency below 4 Hz had the greatest effect on the apparent mass at resonance, while vibration at frequencies below 8 Hz had the greatest effect on the resonance frequency. (Figure 30 and 31).

Mansfield *et al.* (2006) studied the effect of vibration spectra and waveform on the primary resonance frequency in the vertical apparent masses of 12 seated male subjects exposed to vibration where the vibration spectrum was dominated by either low-frequency motion (2-7 Hz), high-frequency motion (7-20 Hz) or a 1.0 ms^{-2} r.m.s. sinusoidal vibration at the frequency of the second peak in the apparent mass (10-14 Hz) added to 0.5 ms^{-2} r.m.s. random vibration. The results showed that both the resonance frequency and peaks of apparent mass were lower for low frequency dominated vibration than high frequency dominated vibration or sinusoidal vibration (Figure 32).

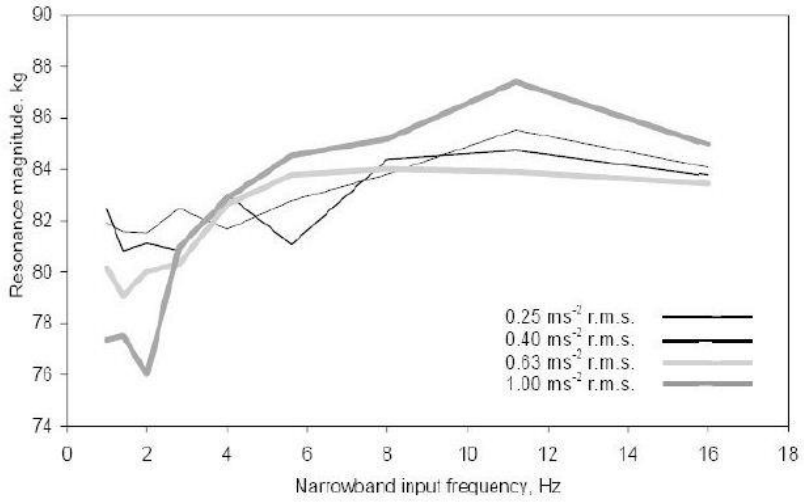

Figure 2.30 Median apparent mass at resonance measured with narrowband inputs at nine 1/2-octave input frequencies (centred at: 1.0, 1.4, 2.0, 2.8, 4.0, 5.6, 8.0, 11.2, 16.0 Hz) and four input magnitudes superimposed on 0.25 ms^{-2} r.m.s. broadband 0.125–25 Hz vibration (Toward, 2002).

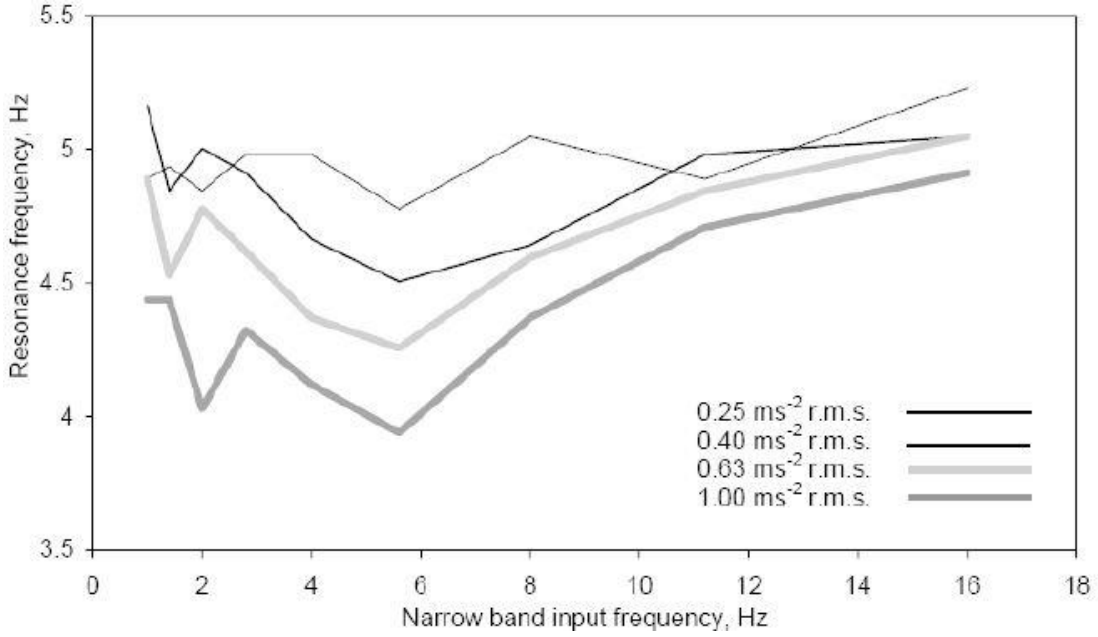

Figure 2.31 Median apparent mass resonance frequency measured with narrow-band inputs at nine ½ octave input frequencies (centred at: 1.0, 1.4, 2.0, 2.8, 4.0, 5.6, 8.0, 11.2, 16.0 Hz) and four input magnitudes superimposed on 0.25 ms-2 r.m.s. broadband 0.125–25 Hz vibration (Toward, 2002).

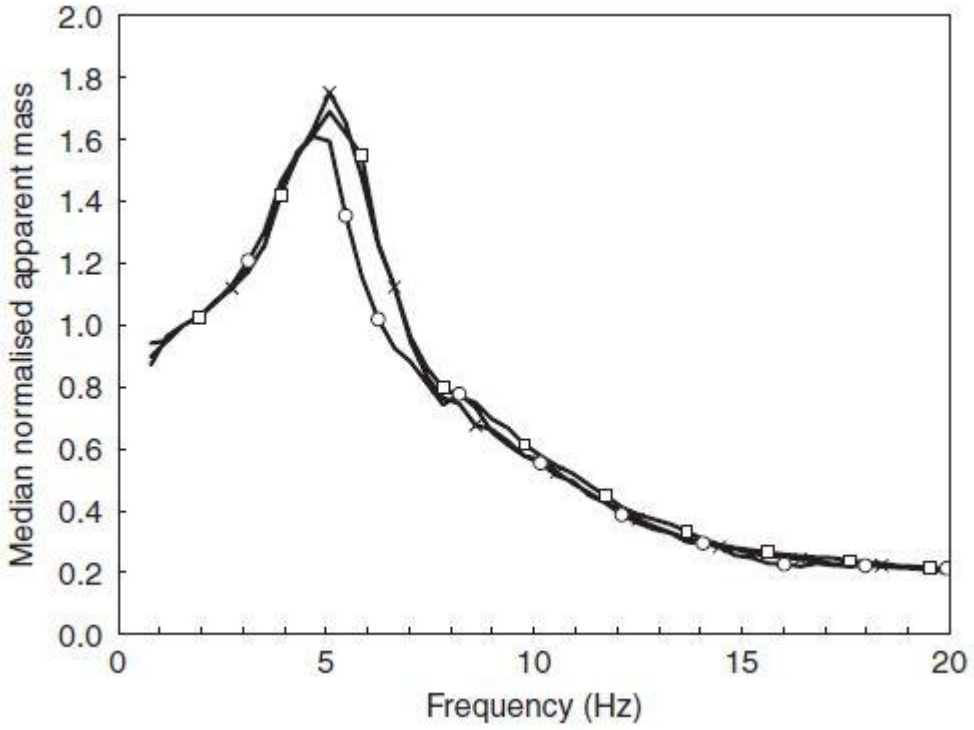

Figure 2.32 Median normalised apparent mass of 12 subjects exposed to random vibration: effect of vibration spectrum in a relaxed upright posture (—□—: high frequency; —○—: low frequency; —×—: sine) (Mansfield *et al.*, 2006).

2.3.3 The fore-and-aft cross axis apparent mass

Many experimental studies show considerable cross-axis forces on a seat induced by vertical whole-body vibration (e.g. Nawayseh and Griffin 2003; Nawayseh and Griffin 2004; Nawayseh and Griffin 2005 and Nawayseh and Griffin 2009). The forces show that the seated human body moves in at least two dimensions when exposed to vertical vibration, consistent with rotational modes of the pelvis, the spine, and the upper body. Such motion will result in both axial and shear cross-axis forces in the spine.

Nawayseh and Griffin (2003) investigated the nonlinearity in the fore-and-aft cross-axis apparent mass of seated human body. Twelve male subjects were exposed to random vibration in the frequency range 0.25-25 Hz at four vibration magnitudes (0.125, 0.25, 0.625 and 1.25 ms^{-2} r.m.s.). The subjects sat in four sitting postures having varying foot heights so as to produce differing thigh contact with the seat (feet hanging, feet supported with maximum thigh contact, feet supported with average thigh contact, and feet supported with minimum thigh contact, Figure 3.33). Forces were measured in the vertical, force-and-aft, and lateral directions on the seat.

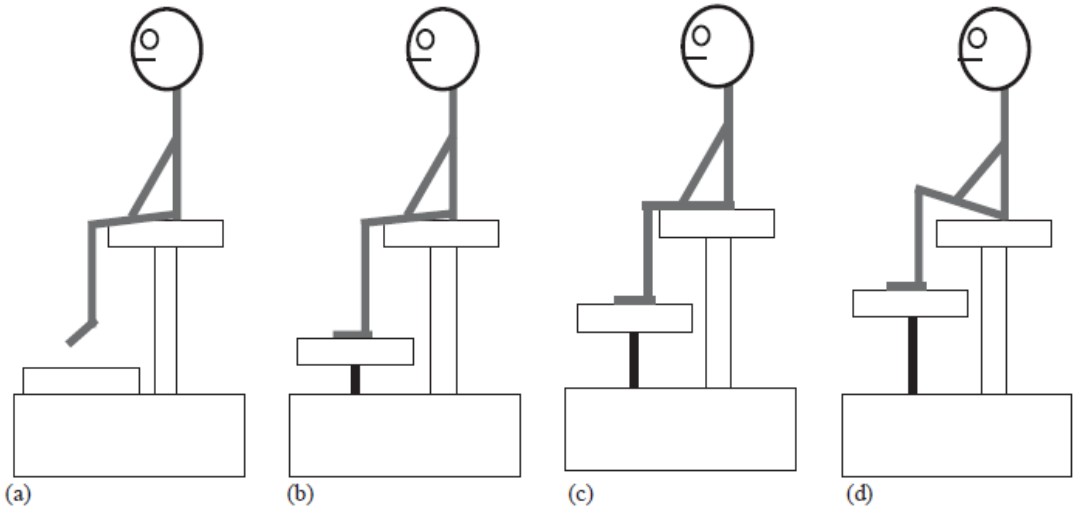

Figure 2.33 Schematic diagrams of the four siting postures: (a) feet hanging; (b) maximum thigh contact; (c) average thigh contact; (d) minimum thigh contact (Nawayseh and Griffin, 2003).

There were considerable forces on the seat in the fore-and-aft direction when the subjects exposed vertical vibrations. In all postures, the resonance frequencies of fore-and-aft apparent mass were around 5 Hz which were similar to that for the vertical apparent mass. There were high correlations between the resonance frequencies in the vertical response and the resonance frequencies of the fore-and-aft response. The resonance frequency in the fore-and-aft cross-axis apparent mass decreased as the

magnitude of vibration increased (Figure 2.34). This suggested that the high forces measured in the fore-and-aft direction might be attributed to some combination of bending or rotational modes of the upper thoracic and cervical spine at the principle resonance frequency or a bending mode of the lumbar and lower thoracic spine.

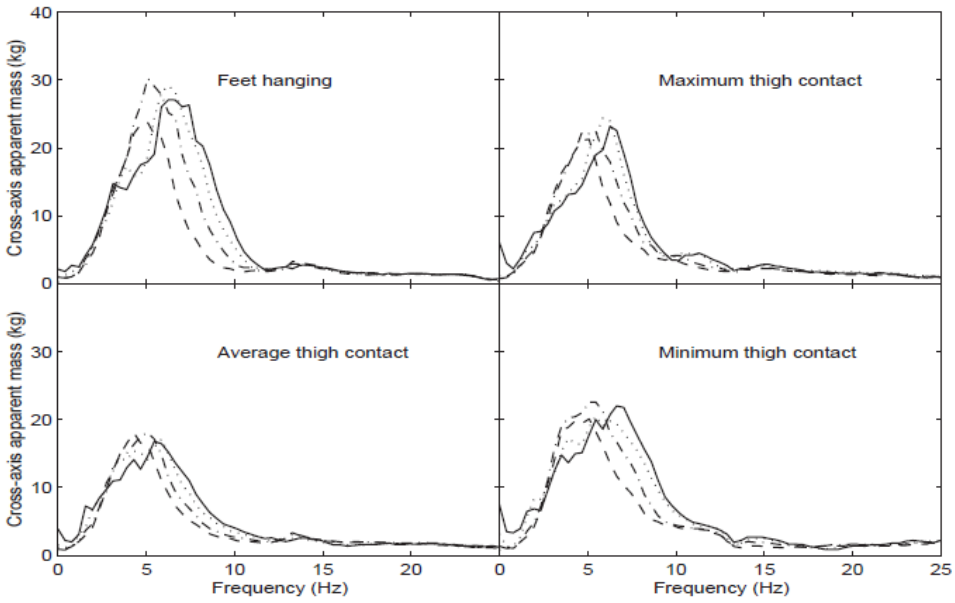

Figure 2.34 Median cross-axis apparent mass of 12 subjects in the fore-and-aft direction: effect of vibration magnitude. ——, 0.125 ms^{-2} r.m.s.; · · · · ·, 0.25 ms^{-2} r.m.s.; — · — ·, 0.625 ms^{-2} r.m.s.; — — —, 1.25 ms^{-2} r.m.s. (Nawayseh and Griffin, 2003).

2.3.4 Causes of the biodynamic nonlinearity

It has been found that the resonance frequency of the apparent mass or transmissibility decreases with increasing vibration magnitude. The variables causing the biodynamic nonlinearity of seated human body exposed to vertical whole-body vibration have been studied (e.g. Fairley and Griffin, 1989: Mansfield and Griffin, 2000; Matsumoto and Griffin, 2002; Nawayseh and Griffin, 2003; Mansfield, 2006; Huang and Griffin, 2006).

Fairley and Griffin (1989) indicated a softening effect with increasing vibration magnitude and suggested a greater movement with high magnitudes of vibration may reduce the stiffness of the musculo-skeletal structure. The resonance frequency changed less at higher magnitudes of vibration. It was suggested that subjects may involuntarily increase muscle tension to reduce the motion, or there may be limited ability to vary body stiffness.

Mansfield and Griffin (2000) observed the nonlinearity along a transmission path common to the spine and the abdomen and the nonlinearity was suggested to be

caused by a combination of following factors: i) softening response of the buttocks tissue; ii) bending or bucking response of the spine (i.e. a geometric nonlinearity – physically an inverted pendulum); iii) different muscular forces at different magnitude of vibration – a doubling of vibration magnitude did not result in a doubling of the muscle activity.

Matsumoto and Griffin (2002) concluded that the nonlinearity in apparent mass was not solely caused by the nonlinearity in the geometric arrangement of the body. Softening characteristics in the passive soft tissues (i.e. thixotropy) and (voluntary and/or involuntary) muscle activity could primarily contribute to the nonlinearity. The transmissibility from vertical seat to vertical, fore-and-aft, and pitch axes along the spine and/or the softening effect of soft tissues along the spine might all contribute to the nonlinearity.

Mansfield and Griffin (2002) designed nine sitting conditions ('upright', 'anterior lean', 'posterior lean', 'kyphotic', 'back-on', 'pelvis support', 'inverted SIT-BAR', 'bead cushion' and 'belt', as shown in (Figure 2.35) to investigate the cause of the nonlinearity in the apparent mass. A similar nonlinearity was found in the vertical-to-pelvis-rotation transmissibility. The pelvis support condition altered the rotation of the pelvis when compared to the upright posture resulting significant difference in the transmissibility resonance frequencies. For the 'belt' condition, visceral movement was restricted by the elasticated belt, the resonance frequencies were significantly higher at 0.2 and 2.0 ms^{-2} r.m.s., but not at 1.0 ms^{-2} r.m.s. The influence of whole-body bending was tested by using the anterior and posterior conditions. The only significant differences in apparent mass resonance frequency in these postures compared to the upright posture was observed for 'anterior lean' at 0.2 ms^{-2} r.m.s. The influence of the dynamics of the tissue beneath the ischial tuberosities was tested using the 'inverted SIT-BAR' and 'cushion' conditions. Increasing the loading area (i.e., the 'cushion' condition) showed a significant decrease in the apparent mass resonance frequencies at 1.0 and 2.0 ms^{-2} r.m.s. when compared to the upright posture. Differences in the nonlinearity were found in some of the postures, however, they were mainly small and inconsistent, and therefore difficult to interpret.

Matsumoto and Griffin (2002) found a slightly reduced degree of nonlinearity with increased muscle tension in the buttocks and abdomen with broadband random vertical vibration. This small change in the nonlinearity might suggest that involuntary changes in muscle activity could alter the nonlinearity. It also found that increasing muscle tension at the buttocks during the sinusoidal vibration showed slightly less degree of nonlinearity than the random vibration.

Nawayseh and Griffin (2003) found that increased pressure in the buttocks tissues slightly reduced the nonlinearity during vertical random vibration. They also found the minimum thigh contact posture gave less degree of nonlinearity than the maximum thigh contact and the feet hanging postures at the two highest magnitudes (0.625 and 1.25 ms^{-2} r.m.s.).

Huang and Griffin (2006) found the voluntary periodic movement significantly reduced the difference in resonance frequency at two vibration magnitudes (0.25 and 2.0 ms^{-2} r.m.s.) compared with the difference in static sitting condition. This suggests that back muscles, or other muscles or tissues in the upper body, influence biodynamic responses of the human body to vibration and that voluntary muscular activity or involuntary movement of these parts can alter their equivalent stiffness.

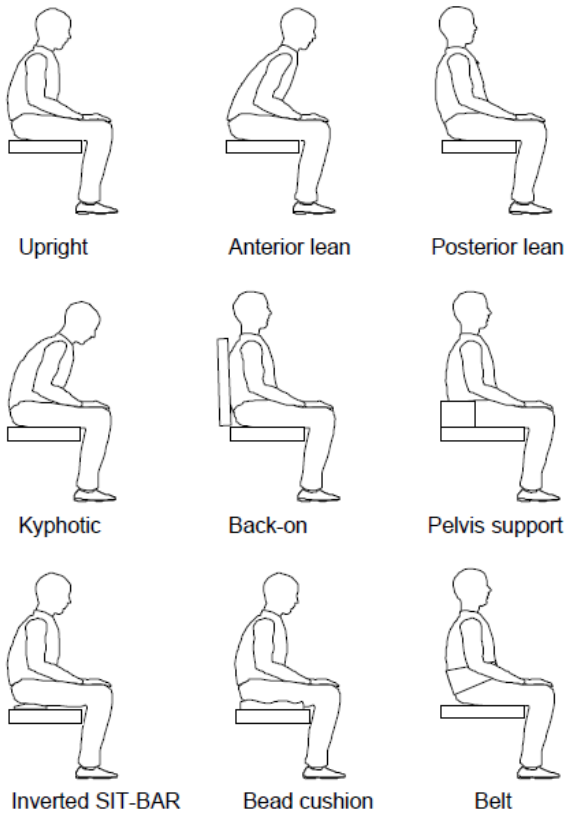

Figure 2.35 Diagrammatic representation of the nine postures used in the experiment. (Mansfield and Griffin, 2002)

Huang and Griffin (2008) investigated the nonlinear dual-axis biodynamic response of the relaxed semi-supine human body exposed to two types of vertical vibration (in the *x*-axis of the semi-supine body): (i) continuous random vibration (0.25-20 Hz) at five magnitudes (0.125, 0.25, 0.5, 0.75 and 1.0 ms^{-2} r.m.s.); (ii) intermittent random vibration (0.25-20 Hz) alternately at 0.25 and 1.0 ms^{-2} r.m.s.. The nonlinearity of the human body was apparent with both types of vibration and in both the vertical (x-axis)

apparent mass and in the horizontal (z-axis) cross-axis apparent mass. The relaxed semi-supine posture was assumed to involve less voluntary and involuntary muscular postural control of the body than sitting and standing postures used in most previous studies of the nonlinearity of the body. The consistent nonlinearity found there suggested that the nonlinearity is not primarily caused by active control of postural muscles but as a result of some passive property of the body (e.g. thixotropy).

Huang and Griffin (2009) designed an experiment to explore the effects of body location on the nonlinearity of the body in the spine posture. In a group of 12 subjects, the apparent mass and transmissibility to the sternum, upper abdomen, and lower abdomen were measured in three postures (relaxed semi-spine, flat supine and constrained semi-spine) with vertical random vibration (0.25-20 Hz) at seven vibration magnitudes (0.0313, 0.0625, 0.125, 0.25, 0.5, 0.75 and 1.0 ms^{-2} r.m.s.). In all three postures, the apparent mass resonance frequencies and the primary peak frequencies of the transmissibilities to the upper and lower abdomen decreased with increasing vibration magnitude. Nonlinearity that was generally apparent in transmissibility to the abdomen was less evident in transmissibility to the sternum and less evident in transmissibilities to the abdomen at vibration magnitudes less than 0.125 ms^{-2} r.m.s.. The nonlinearity was more apparent in the flat supine posture than in the semi-supine postures. The findings are consistent with the nonlinearity being associated with the response of soft tissues, more likely a consequence of passive thixotropy than muscle activity.

2.4 Biodynamic modelling of the human body

The apparent mass and transmissibility have been used to develop biodynamic models of the human body in response to whole-body vibration. The models can be used to predict the forces and movements in the body for a number of purposes: to understand the nature of body movements; to provide information necessary for the optimization of isolation systems and the dynamics of other systems coupled to the body; to predict the influence of variables affecting biodynamic responses, etc.

Based on what information the biodynamic models try to predict, these models can be summarized into three general categories: (i) mechanistic models, which represent the qualitative mechanisms govern the body movement; (ii) quantitative models, which describe the input-output relationships between input stimuli and the resultant biodynamic responses; (iii) effect models, which reflect human discomfort, risk of injury, or performance for specific input stimuli.

A mechanistic model can be defined by a suitable model form with a group of lumped parameters (e.g., discrete masses, springs and dampers) so as to represent the apparent mass or transmissibilities to more than one location and in more than one direction (e.g. Fairley and Griffin, 1989; Wei and Griffin, 1998). More complex finite element models can be used to describe the forces transmitted to and through the spine by comparing the modal parameters of the model with the modal analysis of experimental data (e.g. Kitazaki and Griffin, 1997; Pankoke *et al*., 1998).

In this section, linear and nonlinear lumped parameter models of the response of the sated body to vertical vibration excitation are introduced.

2.4.1 Linear lumped parameter models

Linear mass-spring-damper models can be used to represent the apparent mass of the seated human body in the vertical direction. Fairley and Griffin (1989) developed a model to describe the mean apparent mass and phase of 60 subjects with feet moving with the seat (Figure 2.36). The sprung mass m_1 represented the body mass moving relative to the platform; the unsprung mass m_2 represented the body mass and the legs that did not move relative to the platform. An additional degree of freedom represented the effect of the stationary footrest (m_3). The model was not calibrated to represent the effect of increased muscle tension, contact with backrest, or vibration magnitude.

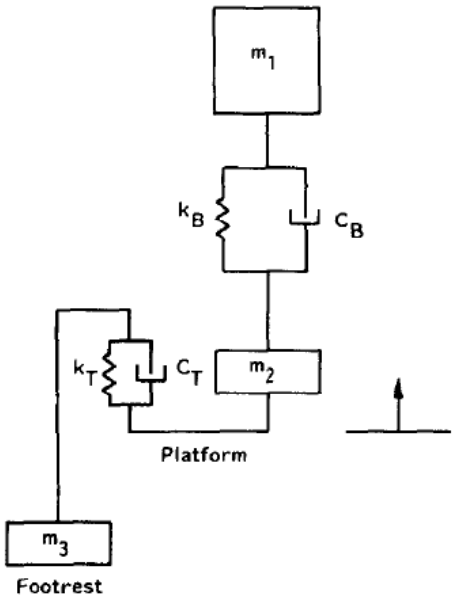

Figure 2.36 Lumped-parameter model of the seated body (Fairley and Griffin, 1989)

Wei and Griffin (1998) derived single- and parallel two-degree-of-freedom models to reproduce the apparent mass to predict the seat transmissibility (Figure 2.37). Model

(a) is a simple linear single-degree-of-freedom model. The mass, m, represents the weight of the person which is supported by tissues represented by the spring, K, and damping, C. An alternative single-degree-of-freedom model is shown in Figure 2.35(b). In this model, the mass of the person is divided into two parts: a support structure, m_1, and a sprung mass, m_2. Figure 2.35 (c) is a two-degree-of-freedom human body model. The mass m_2 consists of the masses of the head and the mass m_1 represents the main part of the body. In Figure 2.35(d), the mass m comprises the skeleton. The model parameters were determined by comparing the model response with the measured (individual and mean) apparent mass modulus and phase of 60 subjects. The apparent masses were obtained by exposing the 60 subjects to 0.25 to 20 Hz broadband random vibration at 1.0 ms^{-2} r.m.s. by Fairley and Griffin 1989. The single-degree-of-freedom model was able to represent the individual apparent mass modulus over the frequency range 0 to 20 Hz (Figure 2.38). The two-degree-of-freedom model improved the fit to the phase at frequencies greater than 8 Hz and resulted in a better fit to the modulus around 5 Hz (Figure 2.39). It was found that including the frame mass (i.e., m in two degree-of-freedom model; m_1 in the single degree of freedom model) could improve the fitting results.

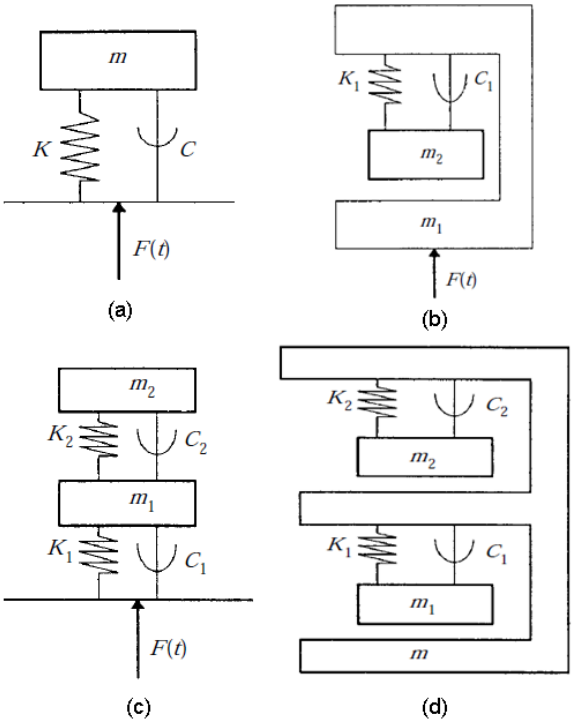

Figure 2.37 The simple linear lumped parameter models. (a) single-degree-of-freedom model; (b) single-degree-of-freedom model with rigid support; (c) two-degree-of-freedom model; (d) two-degree-of-freedom model with rigid support (Wei and Griffin, 1998).

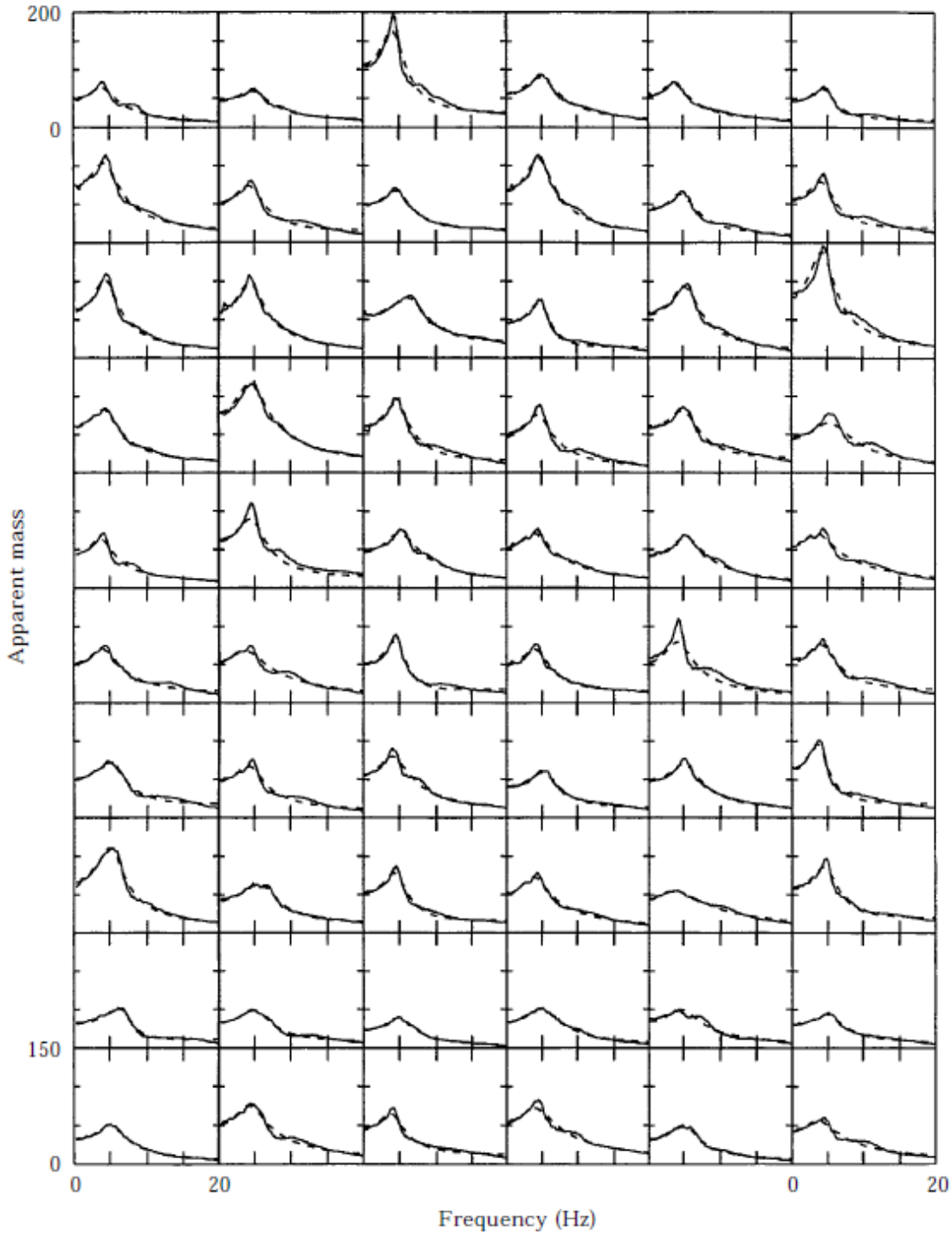

Figure 2.38 Comparison of measured modulus and phase of apparent mass compared with values fitted using single-degree-of-freedom model with rigid support. (——: experimental curves; — —: fitted curves) (Wei and Griffin, 1998)

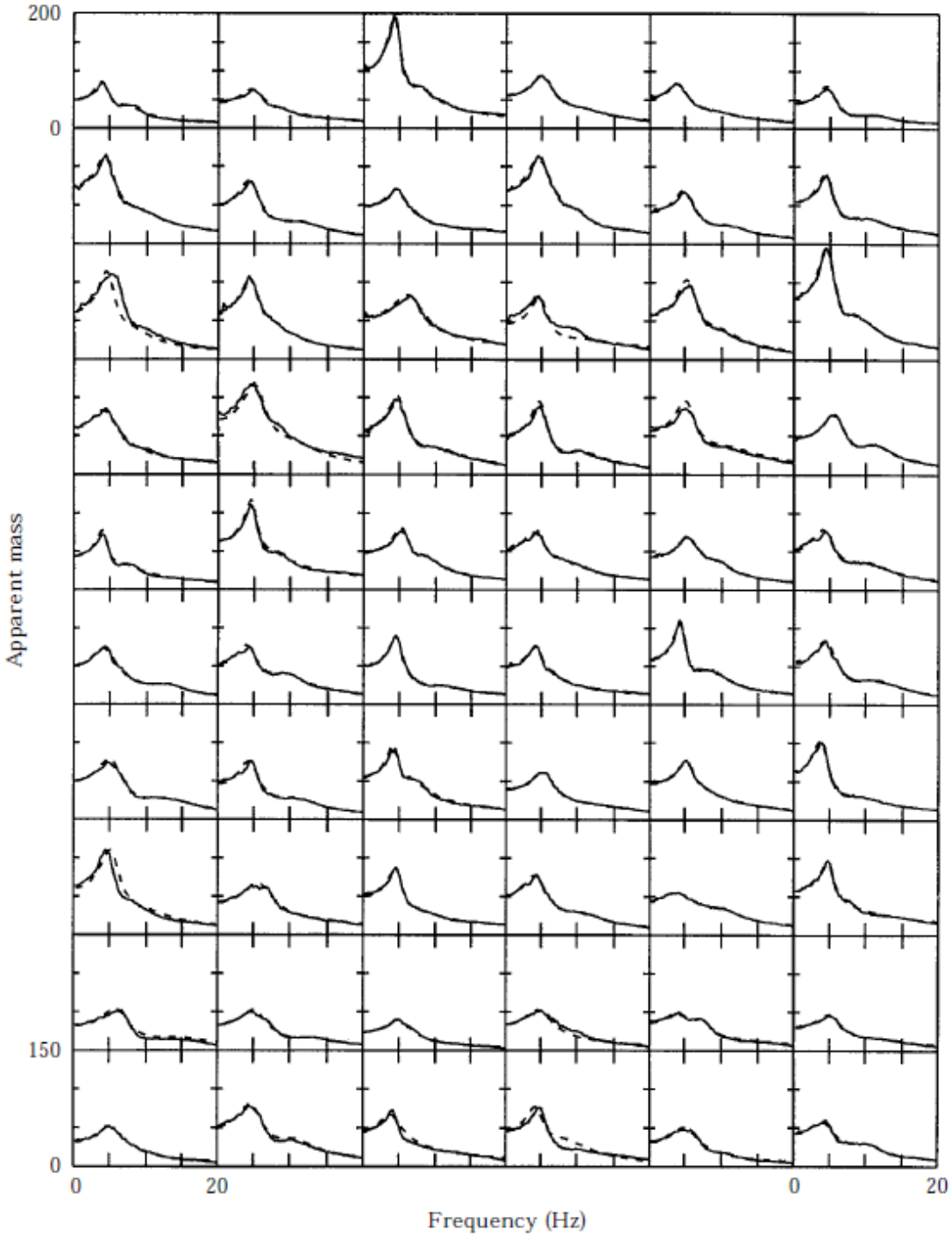

Figure 2.39 Comparison of measured modulus and phase of apparent mass compared with values fitted using two-degree-of-freedom model with rigid support. (—: experimental curves; – –: fitted curves) (Wei and Griffin, 1998)

Because of high fore-and-aft forces on the seat (the fore-and-aft cross-axis apparent mass), Nawayseh and Griffin (2009) defined a model (Figure 2.40) to predict the vertical and fore-and-aft cross-axis apparent mass of the seated human body exposed to vertical vibration. The model is a three degree-of-freedom model with vertical, fore-

and-aft, and rotational motion. The rotational degree of freedom is used to predict the fore-and-aft force on the seat induced by vertical excitation. The translational and rotational springs and dampers used in the model have linear excitation-response relationships. The model is not intended to represent the full complexity of motion occurring in the seated human body exposed to vertical vibration, it is developed to provide an approximation to the vertical apparent mass and cross-axis fore-and-aft apparent mass of the body.

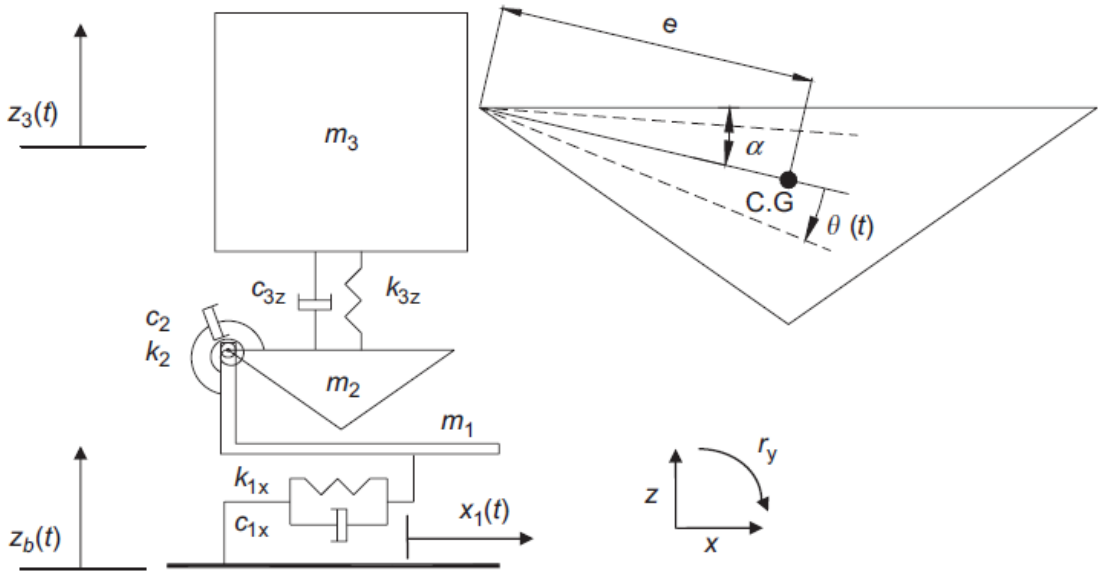

Figure 2.40 Lumped parameter model for the seated human body exposed to vertical vibration (Nawayseh and Griffin, 2009)

The equations of motion of the model were derived using Lagrange's equations. Then the parameters of the model were fitted by comparing the model with the vertical apparent mass and fore-and-aft cross axis apparent mass data obtained by Nawayseh and Griffin (2003).

The results showed that the same model can provide close fits to the responses of each of 12 individual subjects (Figure 2.41 to Figure 2.44).

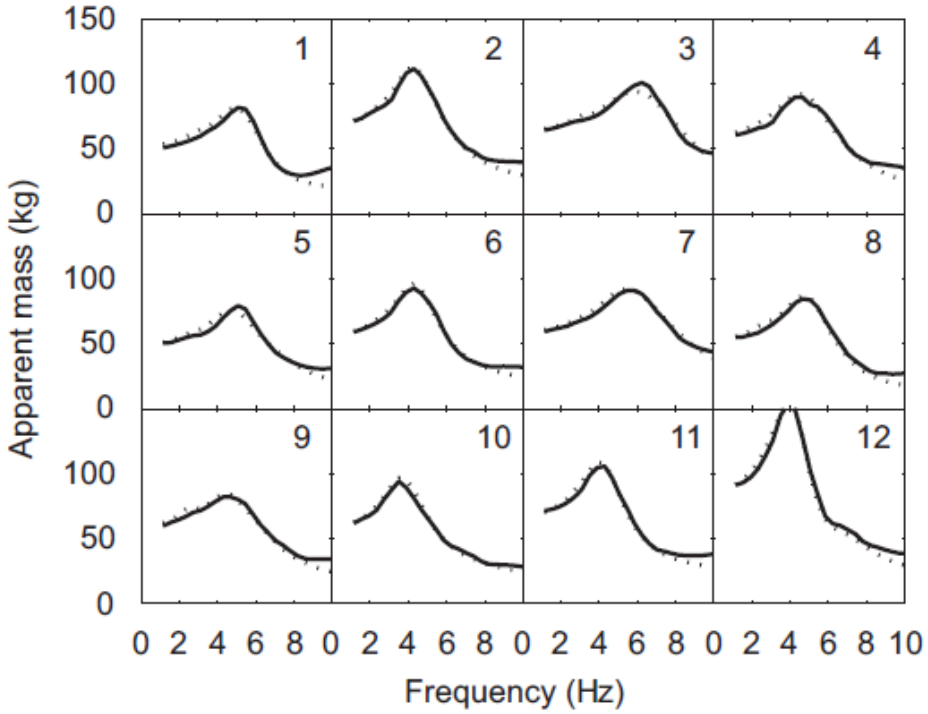

Figure 2.41 Modulus of the vertical apparent mass of 12 subjects: ——: measured; · ····, predicted.

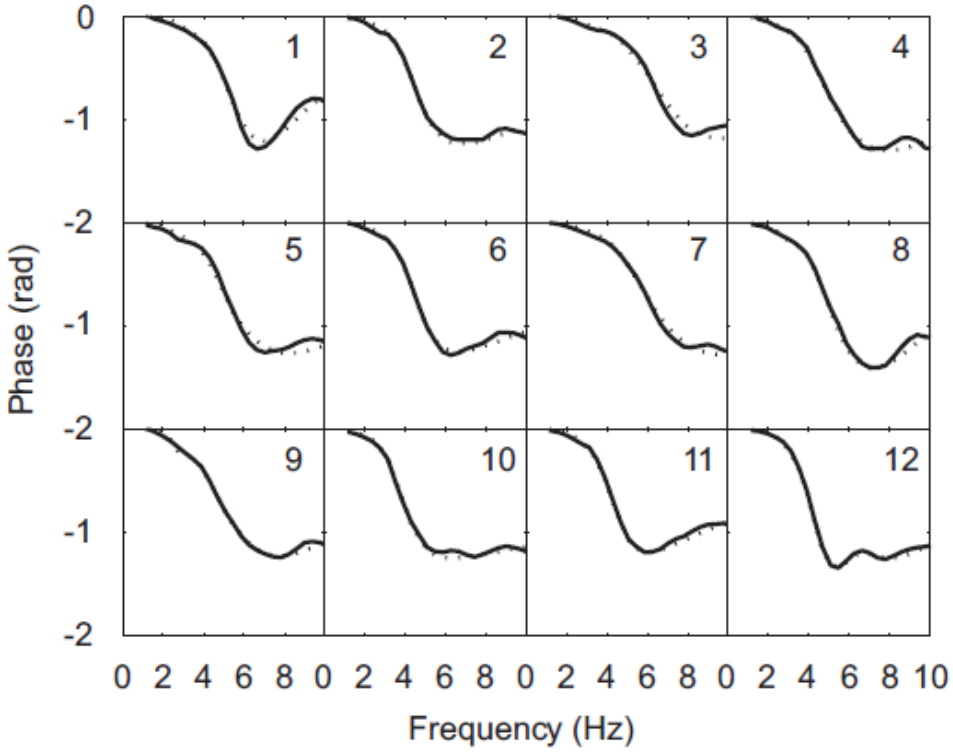

Figure 2.42 Phase of the vertical apparent mass of 12 subjects: ——: measured; · ····, predicted.

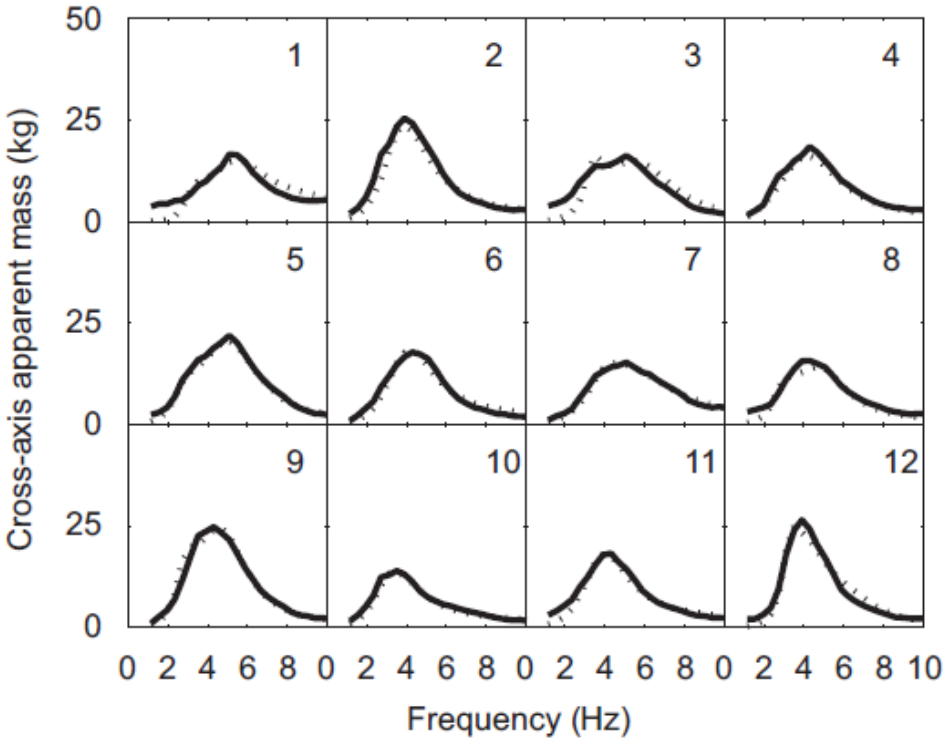

Figure 2.43 Modulus of the for-and-aft cross-axis apparent mass of 12 subjects: ——: measured; ·····, predicted.

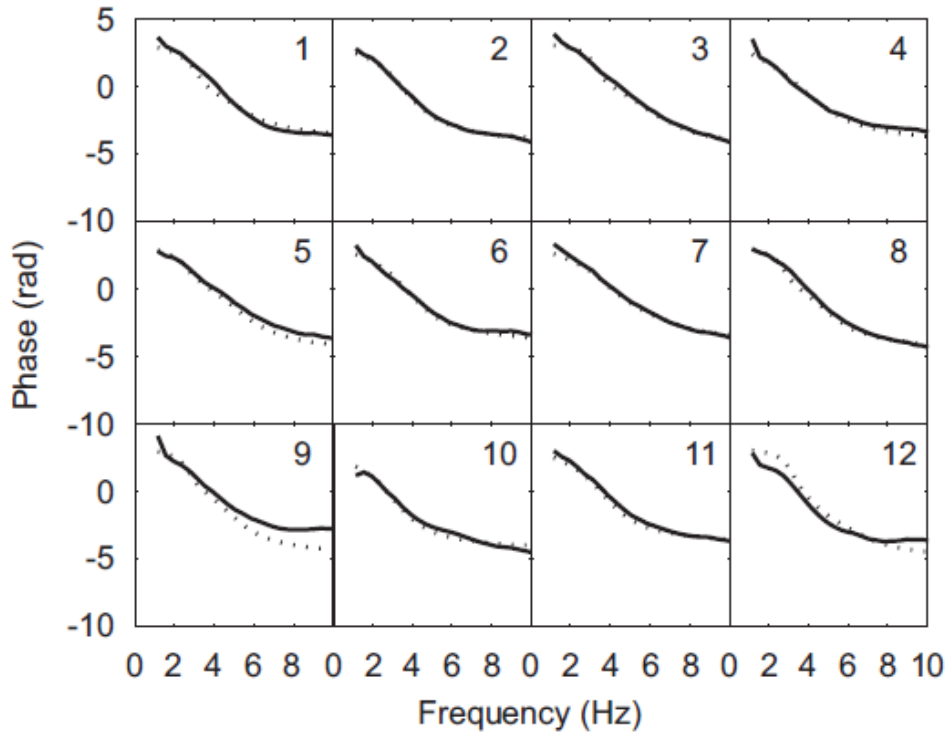

Figure 2.44 Phase of the for-and-aft cross-axis apparent mass of 12 subjects: ——: measured; ·····, predicted.

2.4.2 Nonlinear lumped parameter models

'Nonlinear' means the behaviour of a system that does not obey the principle of superposition. For example, a linear spring will maintain the same stiffness at different ranges of displacement. The stiffness of a nonlinear spring can be dependent on the magnitude of displacement, velocity or acceleration, or alternatively, dependent on some function that is not proportional to the displacement (e.g. a cubic stiffness spring). The shift of the resonance frequency of the frequency response functions due to vibration magnitude is one form of nonlinear behaviour. Models with embedded nonlinear components or nonlinear geometric arrangements have been employed to represented particular nonlinear behaviour of the body (e.g. Hopkins, 1971; Muksian and Nash, 1974; Muksian and Nash, 1976; Mansfield, 1998).

Muksian and Nash (1974) defined a lumped-parameter model of the seated human body which included the head, vertebral column, upper torso, abdomen, thorax viscera, pelvis and legs (Figure 2.45). With cubic stiffness and damping, the response of the model to sinusoidal seat displacement gave reasonable agreement with the head to seat transmissibility published by Goldman and von Gierke (1960) and Pradko et al (1966, 1967). The agreement was good for frequencies between 1 and approximately 7 Hz but was divergent from approximately 7 to 30 Hz. By estimating the sensitivity of the model to the damping coefficient, the results showed that a good fit to the experimental data would be obtained by using the original damping coefficient for input frequencies up to approximately 8 Hz and the higher damping coefficient (increased by 50% the originally estimated damping coefficient) for higher input frequencies. The results implied that a frequency-dependent damping coefficient should be included in lumped-parameter models of the human.

Muksian and Nash (1976) presented a three degree-of-freedom model of the human body in the sitting position that contained a parallel connection between the pelvis and the head (Figure 2.46). It included the head (m_1), body (m_2) and pelvis (m_3) connected in series. The arms and legs were neglected. It was assumed that: all springs (k_{p1}, k_{p2} and k_{p3}) are linear in the frequency range between 1 and 30 Hz; the damping between the head and body (c_{p2}) was zero; all other dampers (c_{p1} and c_{p3}) were linear between 1 and 6 Hz but nonlinear between 6 and 30 Hz. The values of the masses were obtained from Hertzberg and Clauser (1964). The spring stiffness and damping coefficients were determined by matching the head to seat transmissibility published by Goldman and von Gierke (1960) and Magid et al (1962). For each single frequency, the model fitted well with the experimental data. However, since the damping depended on the input

frequencies, the model may be difficult to fit to multi-frequency data input (e.g., random vibration).

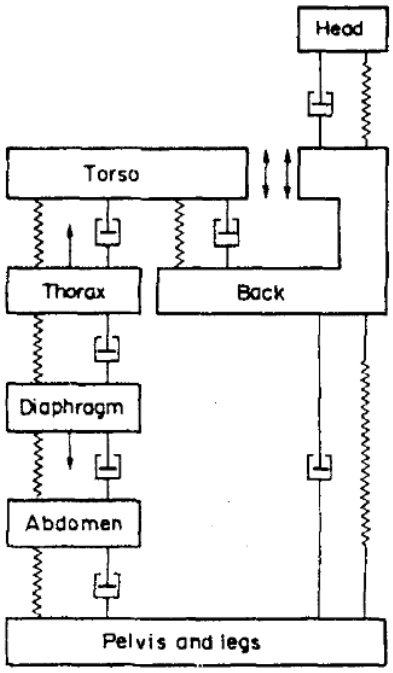

Figure 2.45 A nonlinear model of the human body in the sitting position. Muskian and Nash (1974)

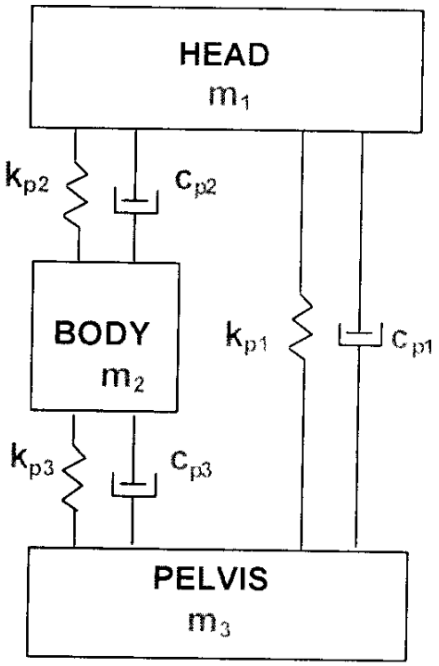

Figure 2.46 A dual pelvis to head path model of the human body in the sitting position

Based on a single-degree-of-freedom model, Mansfield (1998) used a linear quasi-static variable parameter procedure and a nonlinear quasi-static variable parameter

procedure to predict the median apparent mass modulus at six magnitudes (0.25, 0.5, 1.0, 1.5, 2.0 and 2.5 ms^{-2} r.m.s.) of broadband random vibration (0.5 to 20 Hz). In the linear procedure, a set of mass, stiffness, and damping parameters were obtained by minimizing the error between the median apparent mass and the predicted apparent mass at all six magnitudes. Then the optimized parameters were fixed and one parameter at a time was allowed to vary to minimize the error at each magnitude. It was found that optimizing the stiffness and mass had greater effect of reducing the error than changing the damping. When optimizing all parameters, the error was further reduced. The stiffness and the damping decreased with increasing vibration magnitude. The nonlinear procedure started with the optimized parameters determined by the linear procedure. Then one of the nonlinear parameters (a softening cubic spring, a nonlinear friction damper, a nonlinear sprung mass) at a time was allowed to change to minimize the error at each magnitude (Figure 2.47). The error was reduced by varying the stiffness or the sprung mass, but not the damping. The results suggested that the change in the apparent mass resonance frequency due to vibration magnitude could be caused by variations in the effective stiffness or in the effective sprung mass of the body, or both.

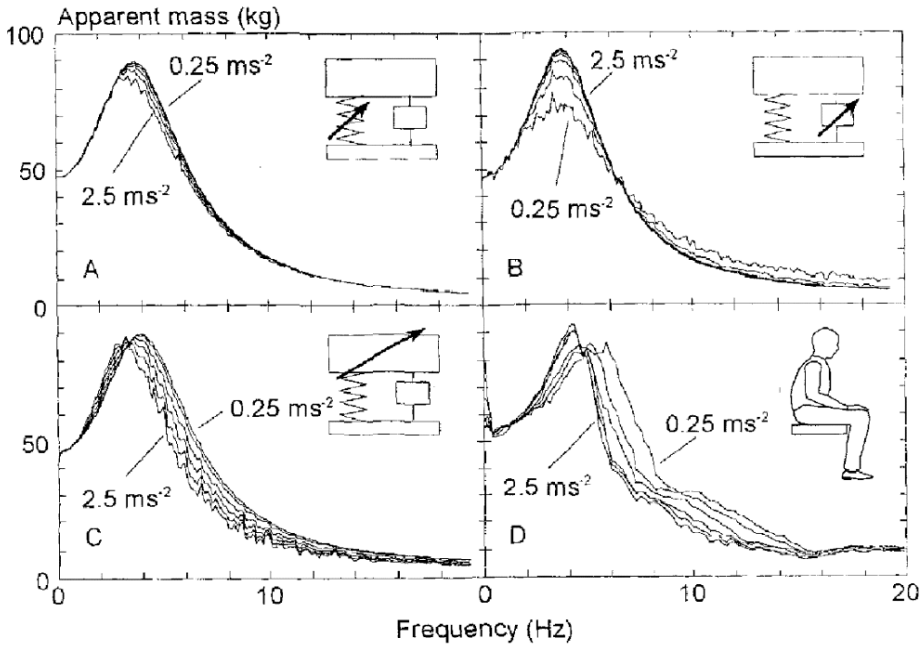

Figure 2.47 The predicted apparent masses at six magnitudes of vibration ((0.25, 0.5, 1.0, 1.5, 2.0 and 2.5 ms^{-2} r.m.s.) using single-degree-of-freedom model by (A) varying the nonlinear stiffness only; (B) varying the nonlinear damping only; (C) varying the sprung mass; and (D) measured median apparent mass of twelve upright seated subjects (Mansfield, 1998).

2.5 Correlation between subjective and biodynamic responses

The previous sections show nonlinearity in subjective and biodynamic response of the human body exposed to whole-body vibration. The biodynamic responses of the body (e.g., apparent mass, mechanical impedance and transmissibility) represent the movement of human body. It is reasonable to consider there may be some relation between the vibration discomfort and biodynamic response of body.

Griffin and Whitham (1978) found evidence of a relation between the seat-to-head transmissibility and subjective responses. The relative vibration discomfort between 16 Hz sinusoidal vibration and 4 Hz reference vibration was obtained in three groups of subjects (56 men, 28 women, and 28 children). The seat-to-head transmissibility at 16 Hz was also measured. It was found that subjects with high transmissibility at 16 Hz required lower magnitude of vibration at 16 Hz for equivalence with the reference vibration at 4 Hz.

Matsumoto and Griffin (2005) investigated the relation between subjective and biodynamic responses of the human body exposed to continuous and transient whole-body vibration in the vertical direction at five frequencies (3.15-8 Hz). Vibration discomfort was measured by the method of magnitude estimation with reference stimuli at 5 Hz. The mechanical impedance and apparent mass of seated body were also measured and divided by the response at reference stimuli so that they could be compared with the subjective responses. For continuous vibrations, the normalised apparent mass and mechanical impedance show similar trends to the relative discomfort, all of them increased significantly with increasing vibration magnitude from 0.5-2.0 ms^{-2} r.m.s. The magnitude estimation showed greater correlation with the normalised mechanical impedance than with the normalised apparent mass. For the transient vibrations, the relative discomfort was more similar to the normalised nominal apparent mass than the normalised nominal mechanical impedance in the trend caused by the changes in stimulus magnitude. The magnitude estimates show greater correlation with the normalised nominal apparent mass than the normalised nominal mechanical impedance. At higher frequencies, the local vibration at various parts of the body dominate discomfort, the vibration discomfort is unlikely associated with the whole-body biodynamic response (e.g., apparent mass or mechanical impedance).

Subashi et al (2009) studied the relation between the relative vibration discomfort and the normalised apparent mass in the horizontal direction. In the fore-and-aft direction, the magnitude estimates of vibration were affected by the magnitude of vibration similarly to the normalised apparent mass. The results suggest the increases in the

apparent mass with increasing vibration magnitude might be attributed to increases in the ratio of motion of the body segments to seat motion or increases in the parts of the body mass excited by input vibration, or both. Increases in the motion of the body segments relative to the seat, or increasing in the body portions excited, may also expect to increase discomfort. Except for the low vibration magnitude, there were significant positive correlations between the median magnitude estimates and the median normalised apparent mass at 2.0, 2.5, 3.15 and 5.0 Hz. This suggests the magnitude-dependence of relative discomfort was associated with the nonlinearity in the apparent mass. At higher frequencies, the local vibration of different body parts may become dominant, and the vibration discomfort is not likely associate with the apparent mass of the whole body.

2.6 Discussions and Conclusions

Equivalent comfort contours showing the effect of the frequency of vibration on the vibration discomfort of seated people have been constructed in several studies. Nonlinearities in the equivalent comfort contours (the shapes of equivalent comfort contours vary with the magnitude of vibration) have been studied at medium and high frequencies (e.g. Morioka and Griffin 2006a) and at low frequencies (e.g. Matsumoto and Griffin, 2005). However, the effects of the magnitude of vibration in the low frequency range (i.e. 1 – 16 Hz) have not been systematically studied.

The acceleration based frequency weightings in current International and British standards cannot reflect the nonlinearity of subjective response to vibration which restricts the application of the standards. The ideal frequency weightings should be different for low and high vibration magnitudes.

Experimental studies of subjective responses to vibration have mainly been conducted with rigid seats and using acceleration equivalent comfort contours. Unlike rigid seats, the acceleration measured above a soft seat may vary with the location over the seat surface. It is worth seeking a better predictor for vibration discomfort.

For biodynamic studies, random vibrations have mainly been used for investigating the nonlinearity of the body (i.e., the resonance frequency of vertical and fore-and-aft cross-axis apparent mass decreased with increasing vibration magnitude). The biodynamic responses of human body exposed to other types of vibration are still unclear because of the nonlinearity of human body.

According to the above discussion, this thesis was designed to answer the following questions:

1. How does the discomfort caused by vertical whole-body vibration depend on the frequency and magnitude of the vibration at low frequencies (e.g., 1 to 16 Hz)?
2. Is the force is a better predictor of vibration discomfort than acceleration – because it avoids the nonlinearity and can predict the influence of soft seats on vibration discomfort more accurately than acceleration?
3. How does the biodynamic response of body depend on the different types of vibration (e.g., random vibration, sinusoidal vibration, and mechanical shocks)?
4. How does the nonlinearity in subjective responses to vibration relate to the nonlinearity in biodynamic responses to vibration?

Chapter 3 Apparatus and Analysis

3.1 Introduction

This chapter describes the apparatus and equipment used in the experimental work. All experiments were approved by the Human Experimentation, Safety and Ethics Committee of the Institute of Sound and Vibration Research at the University of Southampton. It also shows the data acquisition and analysis techniques used to collect and present the data from the experiments.

3.2 Experimental apparatus

3.2.1 One-meter vertical electro-hydraulic vibrator

The vibrator was used to produce vibration in the vertical direction. The 1-meter vertical electro-hydraulic vibrator was capable of accelerations up to ±10 ms^{-2}, a peak to peak displacement of 1 m, a dynamic load of 10 kN with a preload of 8.8 kN in the vertical direction. The magnitude of background noise was about 0.003 ms^{-2} r.m.s.. The distortion of the vibration varied with the magnitude and type of the stimuli. Details can be found in the following chapters.

A 150.0×89.0×1.5 cm aluminium alloy vibrator platform was bolted rigidly on the top of the vibrator. The seat used in the experiments was mounted on the aluminium alloy plate (Figure 3.1).

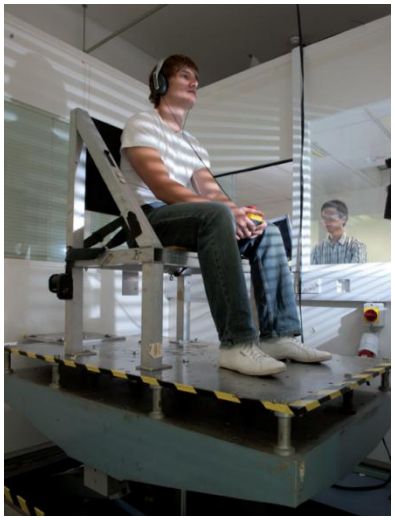

Figure 3.1 One-meter vertical electro-hydraulic vibrator. From http://www.southampton.ac.uk/hfru/lab_facilities/vertical_vibrator.html

During the experiment, white noise was presented to the subjects via calibrated headphones (65 dB(A)) to mask noise around. The subjects were also asked to close their eyes to prevent vision affecting their reaction to the motion.

3.2.2 Transducers

The force and acceleration were required for both subjective and biodynamic studies in this thesis. Hence, force transducers and accelerometers were used to measure the signals during all the experiments.

3.2.2.1 Force transducers

A Kistler 9281 B 12-channel force platform was used to measure the dynamic forces between subjects and the seat surface (Figure 3.2). The force platform was capable of measuring force in three directions (i.e., in the *x*-, *y*-, and *z*-axes of the seated body) simultaneously, the specifications of the force platform are shown in Table 3.1. Force signals from the transducers in the four corners were summed separately in three axes and conditioned using three charge amplifiers. In this study, only vertical and fore-and-aft date were analysed and presented. The charge amplifier had two modes (high amplification mode and low amplification mode). The amplification factors were chosen according to the maximum force that would be measured during the experiment. Low amplification factor was chosen to get larger range when measuring high magnitude of force, high amplification factor was chosen to get better signal to noise ratio when measuring low magnitude of force. In this study, for low magnitude vibration session, the range of measured force was set to about 250 N; for higher magnitude vibration session, the range of measured force was set to about 1250 N.

The force platform was calibrated statically and dynamically in the *y*- and *z*-axis to measure the fore-and-aft and vertical forces, respectively. The force platform was covered by rectangular aluminium plate which weight 31.5 kg. In vertical direction, the static calibration was carried out with 5 kg and 10 kg rigid mass. The mass of aluminium plate was eliminated by resetting the force signal back to zero before the calibration was conducted. In horizontal direction, the static calibration was carried out with a pulley system (Figure 3.3).

In vertical direction, the dynamic calibration was carried out by measuring apparent mass of the aluminium plate on the force platform with random vibration (0.5 to 20 Hz, 0.4 ms^{-2} r.m.s.). As the aluminium plate was highly rigid over the above frequency range, the measured modulus of the plate apparent mass was roughly constant (31.5 kg), and the measured phase of the apparent mass was close to zero except a little

shift at higher frequencies (lag about 0.1 radian at 16 Hz). All the calibrations need to be done twice for both high amplification mode and low amplification mode.

Table 3.1 Specifications of Kistler 9281 B 12-channel force platform

Parameter		Specification
Range	F_x, F_y	-10 to 10 kN
	F_z	-10 to 20 kN
Overload	F_x, F_y	-15/15 kN
	F_z	-10/25 kN
Crosstalk	F_x <-> F_y	<±1.5%
	F_x, F_y -> F_z	<±1.5%
	F_z -> F_x, F_y	<±0.5%
Rigidity	x-axis (a_y=0)	≈250 N/µm
	y-axis (a_x=0)	≈400 N/µm
	z-axis (a_x= a_y=0)	≈30 N/µm
Natural frequency	f_n (x, y)	≈1000 Hz
	f_n (z)	≈1000 Hz
Operating temperature range		0 – 60 ℃

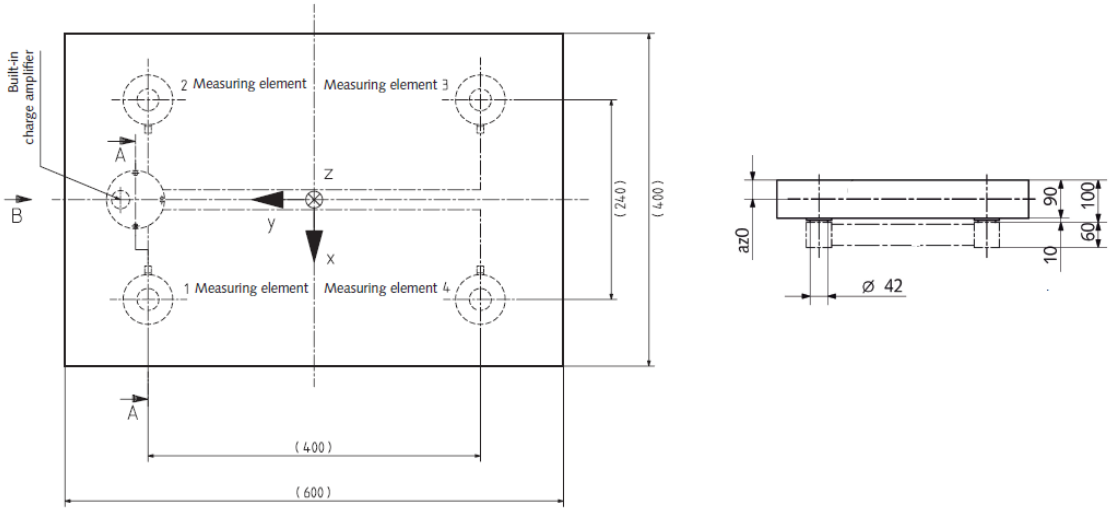

Figure 3.2 Kistler 9281 B 12-channel force platform.

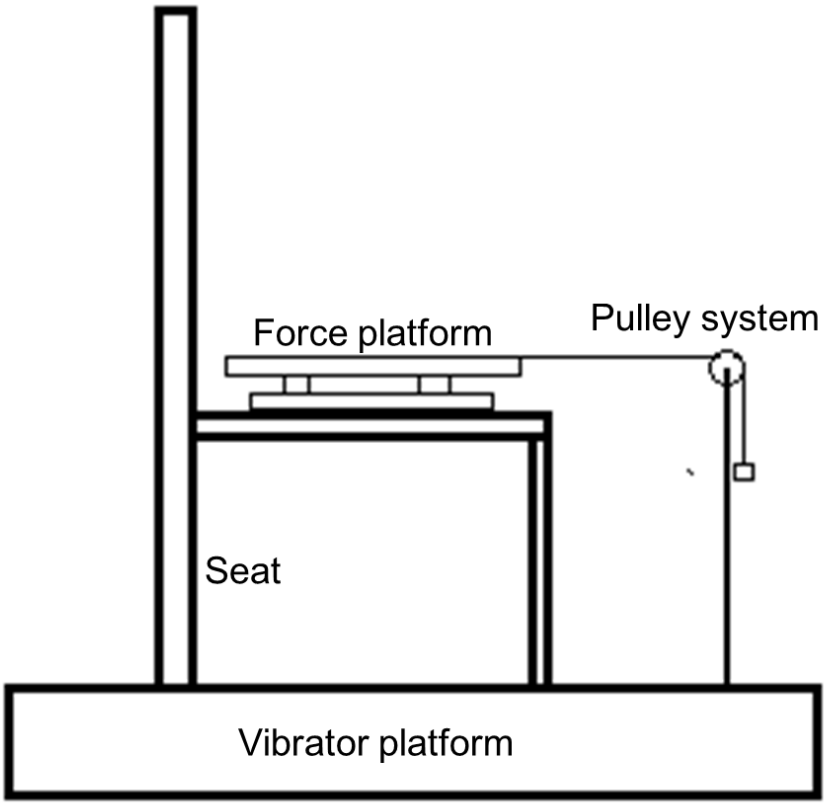

Figure 3.3 Pulley system used to calibrate the force platform in horizontal direction using 1.0 kg weight.

3.2.2.2 Accelerometers

In experiments with a rigid seat, the vibration was measured using a capacitive micro-machined accelerometer Silicon Designs Model 2260-002 (Figure 3.4). The specification of the accelerometer is shown in Table 3.2. The accelerometers were calibrated to give zero reading when its bottom surface was attached to a horizontal surface, -2 g when its top surface was attached to the horizontal surface.

Table 3.2 Specifications of Silicon Designs Model 2260-002

Parameter	Specification
Range	±2 g
Sensitivity	2000 mv/g
Frequency response	0-400 Hz
Output noise	13 μg/(root Hz)
Maximum Mechanical shock	2000 g

Cross Axis Sensitivity	3% (maximum)
Non-Linearity (-90 to +90% of Full Scale)	1.0%
Mass (not including cable)	6 grams

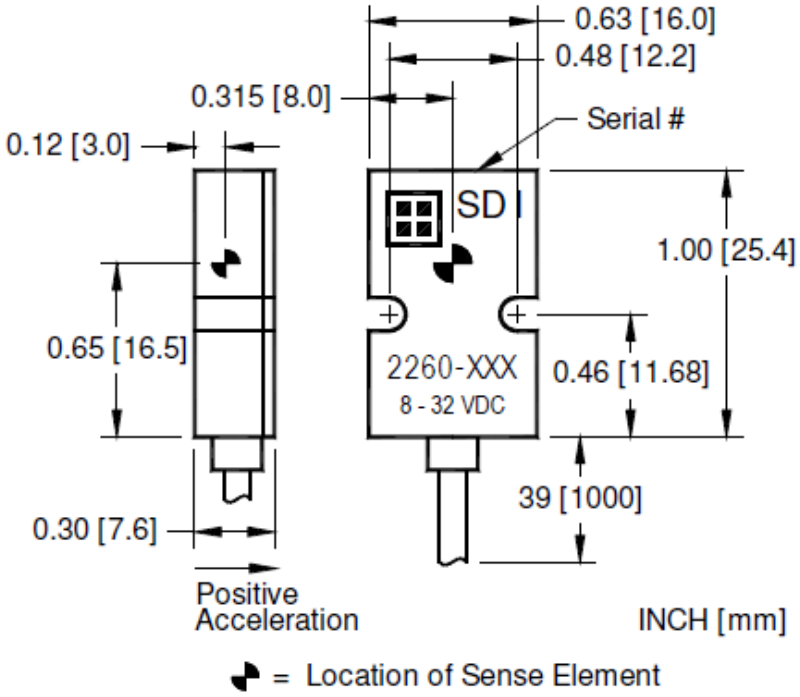

Figure 3.4 Single-axis capacitive micro-machined accelerometer Silicon Designs Model 2260-002

During measurements with a soft seat, the acceleration above foam was measured by a SIT-pad. The construction of the SIT-pad with embedded accelerometer (Willow Technologies KXD94-2808) is shown in Figure 3.5. The SIT-pad was calibrated to give zero reading when its flat surface was attached to a upward horizontal surface, -2 g when its flat surface was attached to a downward horizontal surface.

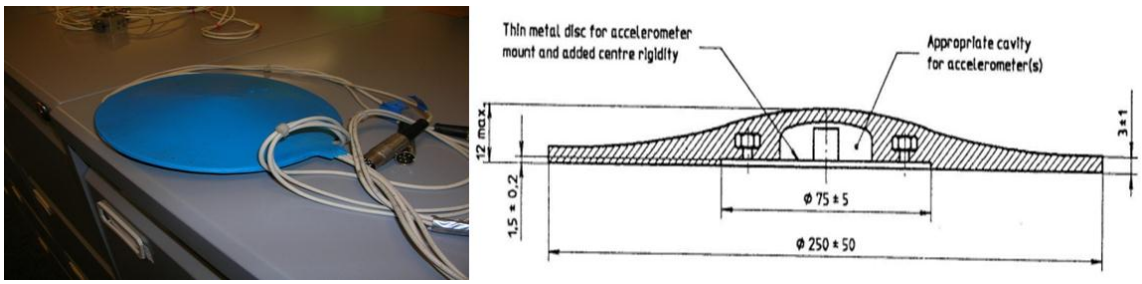

Figure 3.5 SIT-pad and its construction. ISO 10326-1 (1992)

3.3 Signal generation and data acquisition

A self-developed MATLAB programme was used to control the vibrator via the original Pulsar Digital Controller (Servotest Test System, Egham, UK). During experiment, a trigger was used to send each vibration signal to the controller and also activate data acquisition system (*HVL*ab Data acquisition system, version 1.0), as shown in Figure 3.6. The signals were generated and acquired at 512 samples/second after low-pass filtering at 50 Hz.

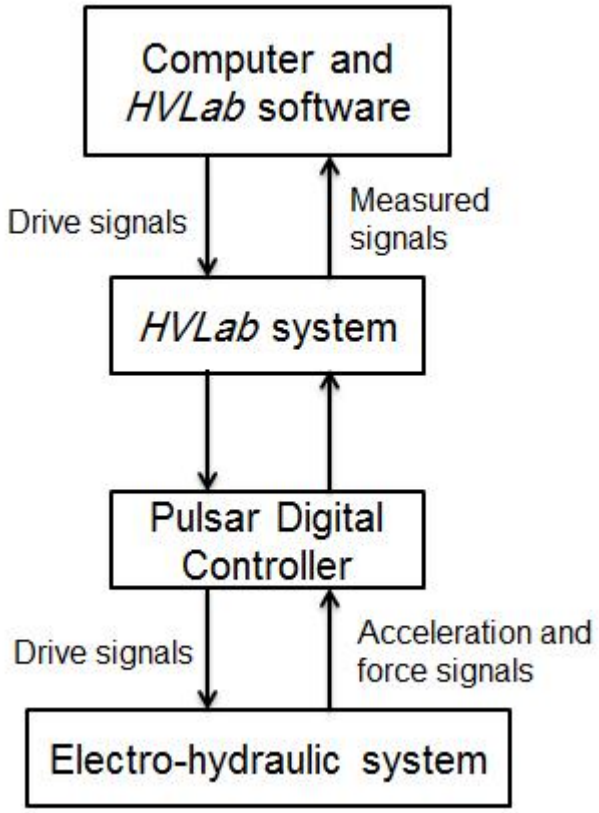

Figure 3.6 Experimental setup for signal generation and data acquisition

3.4 Data analysis

3.4.1 Frequency response function

Frequency response function (i.e., apparent mass) which has been defined in Section 2.3 is applied in this study to present biodynamic response of human body exposed to vertical vibration. The cross spectral density (CSD) method is used to calculate to apparent mass:

$$H(f) = S_{io}(f) / S_{ii}(f) \tag{3.1}$$

Where, f is the frequency, in Hz; $H(f)$ is the apparent mass; $S_{io}(f)$ is the cross spectral density between the output (i.e., force) and the input excitation acceleration; $S_{ii}(f)$ is the power spectral density of the input excitation acceleration at the vibrator platform.

The modulus and phase of the apparent mass can be calculated as:

$$Modulus = \sqrt{(\mathrm{Re}(H(f))^2 + (\mathrm{Im}(H(f)))^2)} \tag{3.2}$$

$$Phase = \tan^{-1}(\mathrm{Im}(H(f))/\mathrm{Re}(H(f))) \tag{3.3}$$

Where $Re(H(f))$ and $Im(H(f))$ are the real and imaginary parts of the frequency response function $H(f)$.

3.4.2 Statistical analysis

Non-parametric statistical analysis was applied in this study as the distribution of the population was unknown (Siegel and Castellan, 1988).

The Friedman two-way analysis of variance was used to test the null hypothesis that k matched sample have been drawn from the same population. For example, it can be used to test the effect of vibration magnitude (more than 2 magnitudes) to the resonance frequency of apparent mass, or the effect of vibration magnitude (more than 2 magnitudes) to the rate of growth of discomfort.

The Wilcoxon matched-pairs signed ranks test was used to examine whether two related samples were different with each other. For example, if the Friedman test has shown that there was a significant effect of vibration magnitude on the resonance frequency, the Wilcoxon test would be used to identify the significant difference happened in which two vibration magnitudes.

The Spearman rank-order correlation test was used to compare the ranking of data between two variables (samples) and to identify whether the two are related. For example, the Spearman rank-order correlation can be used to examine the correlation between the resonance frequency of vertical apparent mass and the resonance frequency of fore-and-aft cross-axis apparent mass of the seated human body exposed to vertical vibration, it also can be used to examine the correlation between the biodynamic response and subjective responses of human body exposed to vibration.

Chapter 4 Biodynamic responses to sinusoidal and random vibration

4.1 Introduction

During whole-body vertical vibration, the resonance frequency evident in the vertical apparent mass of the human body decreases with increasing magnitude of vibration excitation, a phenomenon referred to as a biodynamic nonlinearity (e.g., Hinz and Seidel 1987, Fairley and Griffin 1989, Mansfield and Griffin 2000, Matsumoto and Griffin 2002, Nawayseh and Griffin 2003). With random vibration in the frequency range 1 to 20 Hz, Fairley and Griffin (1989) found that the principal resonance frequency in the vertical apparent masses of 60 seated subjects (24 men, 24 women and 12 children) decreased from about 6 Hz to about 4 Hz as the vibration magnitude increased from 0.25 to 2.0 ms^{-2} r.m.s. A second resonance in the vertical apparent mass, evident in the frequency range 8 to 12 Hz, has also been observed to reduce as the magnitude of vibration excitation increases (e.g., Fairley and Griffin 1989, Mansfield and Griffin, 2000).

When the seated body is excited by random vertical vibration, there are significant forces on the seat in the fore-and-aft direction. These forces also show a nonlinear relationship to the vibration magnitude during random vertical excitation (e.g., Matsumoto and Griffin 2002a, 2002b, Nawayseh and Griffin 2003, Hinz *et al*. 2006).

There have been few studies of biodynamic nonlinearity during exposure to vertical sinusoidal vibration. The resonance frequency in the apparent mass averaged over four subjects decreased from 4.5 to 4 Hz as the magnitude of sinusoidal vertical vibration increased from 1.5 to 3.0 ms^{-2} r.m.s. (Hinz and Seidel 1987). Increasing the magnitude of sinusoidal vibration (over the range 0.5 to 2.0 ms^{-2} r.m.s.) increased the apparent mass at 3.15 Hz but decreased the apparent mass at 5.0, 6.3, and 8.0 Hz (Matsumoto and Griffin 2005).

During excitation by sinusoidal vibration, the dominant body motions occur at different locations in the body according to the frequency of the vibration excitation. During excitation by random vibration there is a more distributed movement of all parts of the body, with some parts experiencing more movement and other parts experiencing less movement than during excitation by any single frequency of sinusoidal vibration at the same acceleration magnitude. The nonlinearity observed in the apparent mass with random vibration does not identify which frequencies, or which movements, are

associated with the nonlinearity. For example, nonlinearity observed at 16 Hz during random vibration may be caused by the 16-Hz vibration within the spectrum or it may be caused by the influence of vibration at another frequency. Although the vertical apparent mass of the human body has occasionally been measured with both sinusoidal and random vibration (e.g., Mansfield and Maeda, 2005), there has been little consideration of the nonlinearity in the apparent mass with different vibration waveforms.

Whereas biodynamic studies have mostly investigated responses to random vibration, studies of subjective reactions to vibration (i.e., judgments of vibration discomfort) have mostly investigated responses to sinusoidal vibration. The subjective studies have also observed nonlinearities (e.g., Matsumoto and Griffin 2005, Morioka and Griffin 2006, Subashi *et al.* 2009). In their working and leisure activities, people are exposed to non-sinusoidal vibration, so the applicability of the subjective studies (that employ sinusoidal vibration to obtain 'weightings' from the subjective judgements at each frequency) depends on an understanding of the nonlinearity, and whether the nonlinearity is similar with sinusoidal and non-sinusoidal vibration. Although the nonlinearity can have a large influence, the mechanisms responsible are not yet understood, so there are doubts as to the applicability to real environments of some of the findings from laboratory studies of human responses to sinusoidal vibration.

The effects of subject characteristics on the apparent mass of the body have been investigated in various studies (e.g., Fairley and Griffin 1989, Boileau *et al*. 1998, Paddan and Griffin 1998, Holmlund *et al*. 2000, Wang *et al*. 2004, Toward and Griffin 2011). Variability induced by differences in body mass, age, gender, height, and size among subjects are classified as inter-subject variability. In a group of 60 subjects, the principal resonance frequencies were found to be negatively correlated with the total body weights and static sitting weights of subjects divided by their sitting height (Fairley and Griffin 1989). In a group of 80 subjects, the principal resonance frequency in the vertical apparent mass was most consistently associated with age and with body mass index (BMI) (Toward and Griffin 2011). The only subject characteristic found to influence the biodynamic nonlinearity has been gender: the reduction in resonance frequency with increasing vibration magnitude was less in females than in males, but only when seated with a reclined rigid backrest (Toward and Griffin 2011). It was speculated that the difference in nonlinearity between the genders might have been caused by anatomical differences having a greater influence when supported by a reclined rigid backrest, consistent with the BMI affecting the resonance frequency in this posture.

Similar to biodynamic responses, subjective responses to vibration also depend on the magnitude of vibration excitation. Some nonlinearities in vibration discomfort (i.e., changes in the frequency-dependence of discomfort with changing magnitude of vibration excitation) appear to be associated with the nonlinearity in the biodynamic responses of human body (e.g., Matsumoto and Griffin 2005, Subashi *et al.* 2009).

This study was primarily designed to compare the biodynamic nonlinearity, as reflected in the vertical apparent masses and the fore-and-aft cross-axis apparent masses of seated people, during random and sinusoidal vertical vibration excitation. The nonlinearity was quantified by changes in the measured apparent masses, the principal resonance frequencies, and the parameters of a simple mathematical model of the vertical apparent mass. It was hypothesised that: (i) with both sinusoidal and random vibration, the equivalent stiffness and equivalent damping of the body would decrease with increasing magnitude of vibration excitation, and that there would be a corresponding reduction in the principal resonance frequencies of both the vertical apparent mass and the fore-and-aft cross-axis apparent mass; (ii) with both sinusoidal and random vibration, the principal resonance frequency in the vertical apparent mass would correlate with the principal resonance frequency in the fore-and-aft cross-axis apparent mass; (iii) at each magnitude of vibration, the different distributions of vibration in the body with random and sinusoidal vibration would result in different apparent masses measured with the two waveforms. In view of a reported difference in nonlinearity in males and females, the study had the subsidiary objective of comparing nonlinearity in males and females.

4.2 Method

4.2.1 Apparatus

A 1-metre stroke vertical electrohydraulic vibrator was employed to generate vertical vibration of a rigid flat seat. An accelerometer (Silicon Designs 2260-002) measured vertical acceleration and a force platform (Kistler 9281B) measured the vertical and fore-and-aft forces between the seat and subjects.

Sinusoidal vibration and random vibration were generated by a Servotest Pulsar system and acquired using an *HVLab* data acquisition and analysis system (version 1.0; University of Southampton, UK). The measured force and acceleration were acquired at 512 samples per second via 50-Hz anti-aliasing filters. The distortions of the sinusoidal acceleration waveforms were examined by fitting measured waveforms

to the desired waveforms. For all sinusoidal waveforms, the difference, δ_a, between the measured and desired acceleration was calculated from:

$$\delta_a = \frac{\int (a_d(t) - a_m(t))^2 dt}{\int (a_d(t))^2 dt} \times 100\% \quad (4.1)$$

where $a_d(t)$ is the desired acceleration, and $a_m(t)$ is the measured acceleration. For the session of the experiment using low magnitude stimuli, the median difference between the measured acceleration waveform and the desired acceleration waveform (i.e., δa) was 1.7% (with a 5%-95% range from 0.43% to 5.5%). The distortions were less with the greater magnitude stimuli employed in the sessions with medium and high magnitudes.

Subjects sat on the seat without making contact with the backrest (Figure 4.1). They rested their feet on a rigid footrest that was attached to the vibrator table.

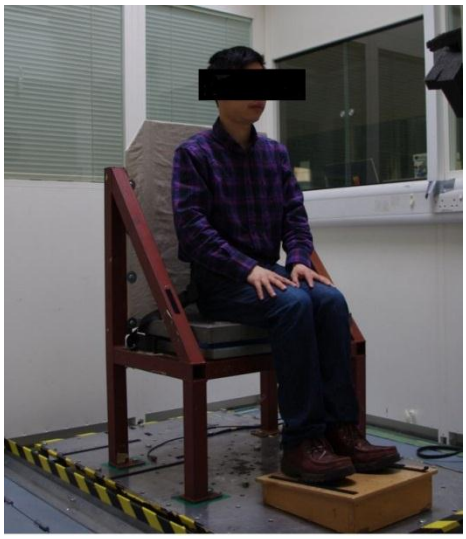

Figure 4.1 Experiment setup

4.2.2 Subjects

Twenty male and twenty female subjects, students and staff at the University of Southampton, participated in the study. The subject characteristics are shown in Table 4.1.

Subjects were exposed to white noise at 65 dB(A) via a pair of headphones. During exposure to vibration, they closed their eyes to prevent vision influencing their reactions to the motion.

Table 4.1 Characteristics of 20 males and 20 females: medians (range)

	Age (years)	Weight (kg)	Stature (cm)	Sitting height* (cm)
Males	26.5 (22-41)	70.5 (48-107)	173 (165-202)	90 (78-102)
Females	23.5 (20-30)	55.8 (45-72)	165 (149 - 183)	86 (80-92)

* from surface of seat to vertex of head

4.2.3 Experimental design

The experiment had three sessions conducted on different days. In each session, subjects were exposed to a series of vertical sinusoidal vibrations of 6-s duration, with the first and last second tapered by cosine functions. The sinusoidal motions were presented at each of 13 frequencies (1, 1.25, 1.6, 2, 2.5, 3.15, 4, 5, 6.3, 8, 10.0, 12.5 or 16 Hz) and at various magnitudes (including 0.1, 0.2, 0.4, 0.8 and 1.6 ms^{-2} r.m.s.). The order of presenting the vibration frequencies and vibration magnitudes was randomized.

At the end of the final session, subjects were exposed to random vertical vibration at five magnitudes (0.1, 0.2, 0.4, 0.8, and 1.6 ms^{-2} r.m.s.). The random vibration had an approximately flat constant bandwidth spectrum that was band-limited (Butterworth filter cut-off frequencies of 0.5 Hz and 18 Hz with 24 dB/octave attenuation rates). Each magnitude of random vibration was presented for 60 s. The order of presenting the magnitudes of random vibration was randomized.

The experiment was also designed to obtain the subjective responses of the subjects to the sinusoidal vibration stimuli. The subjective responses are reported separately (Chapter 5). The experiment was approved by the Human Experimentation Safety and Ethics Committee of the Institute of Sound and Vibration Research at the University of Southampton. Informed consent to participate in the experiment was given by all subjects.

4.2.4 Analysis

With random vibration, the vertical apparent mass was calculated by the cross-spectral density method:

$$M(f) = S_{af}(f)/S_{a}(f) \tag{4.2}$$

where $M(f)$ is the apparent mass, is $S_{af}(f)$ is the cross spectral density function between the vertical seat acceleration and the vertical force at the seat surface, and $S_a(f)$ is the power-spectral density function of the vertical seat acceleration, all calculated using a frequency resolution of 0.25 Hz. The effect of the mass of the top plate on the force platform was eliminated by subtracting the vertical acceleration multiplied by the mass of the top plate of the force platform (i.e., 31.5 kg) from the measured vertical force. The fore-and-aft cross-axis apparent mass was calculated similarly, with $S_{af}(f)$ the cross spectral density function between the vertical seat acceleration and the fore-and-aft force. A fore-and-aft mode in the response of the hydraulic vibrator impeded accurate measurement of fore-and-aft cross-axis apparent mass around 16 Hz, so all measures of fore-and-aft cross-axis apparent mass are limited to the range 1 to 12.5 Hz.

With sinusoidal vibration, the vertical apparent mass was calculated from the ratio of the r.m.s. values of the vertical seat acceleration and the vertical force at the seat surface after mass cancellation:

$$M_{zz} = F_{z\text{-}rms}/A_{z\text{-}rms} \tag{4.3}$$

where M_{zz} is the vertical apparent mass, $F_{z\text{-}rms}$ is the r.m.s. value of the vertical force at the seat surface, and $A_{z\text{-}rms}$ is the r.m.s. value of the vertical seat acceleration. Mass cancellation was performed by subtracting the product of the mass of the top plate of the force platform and the vertical seat acceleration time history from the measured vertical force time history. The phase of the apparent mass was calculated from the maximum in the cross-correlation function between the force, after mass cancellation, and the acceleration.

With sinusoidal vibration, the fore-and-aft cross-axis apparent mass was calculated from the ratio of the r.m.s. values of the vertical seat acceleration and the fore-and-aft force at the seat:

$$M_{xz} = F_{x\text{-}rms}/A_{z\text{-}rms} \tag{4.4}$$

where M_{xz} is the cross-axis apparent mass, $F_{x\text{-}rms}$ is the r.m.s. value of the force at the seat in the fore-and-aft direction, and $A_{z\text{-}rms}$ is the r.m.s. value of the vertical seat acceleration.

To compare the apparent masses of males and females, the ‘normalised apparent mass’ of each subject was calculated by dividing their apparent mass by the modulus of their vertical apparent mass at 1 Hz. This gives a normalised vertical apparent mass of unity at 1 Hz.

The apparent mass obtained at the highest magnitude of vibration (i.e., 1.6 ms^{-2} r.m.s.) was expressed as a ratio of the apparent mass obtained at the lowest magnitude of vibration (i.e., 0.1 ms^{-2} r.m.s.) so as to quantify the nonlinearity, *n*, at each frequency:

$$n(f) = M(f)_{1.6} / M(f)_{0.1} \quad . \tag{4.5}$$

4.2.5 Curve fitting

To quantify the biodynamic nonlinearity, a one-degree-of-freedom parametric model (model 1b, Wei and Griffin, 1998, Figure 4.2) was used to fit the vertical apparent masses and phases (from 1 to 16 Hz) with both random and sinusoidal vibration so as to obtain the stiffness and damping of the model at each of the five magnitudes (i.e., 0.1, 0.2, 0.4, 0.8 and 1.6 ms^{-2} r.m.s.). It was assumed there was no mass transfer during vibration, and the masses m_1 and m_2 could be constrained to 15% and 85% of the sitting masses of subjects, in accord with the findings of Wei and Griffin (1998). The sitting masses were obtained from the measured apparent mass of each subject at 1 Hz.

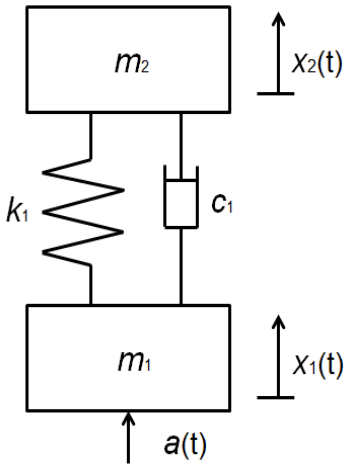

Figure 4.2 Single-degree-of-freedom model

A constrained minimum error search command 'fmincon()' from the optimisation toolbox of MATLAB (version R2010a) was used for curve fitting. The target error, *E*(*f*), was calculated by summing the squared errors in the modulus and phase at each frequency between the measured data and the fitted curve (i.e., Huang and Griffin, 2006):

$$E(f) = \sum_{N} \left[M_m(f) - M_s(f) \right]^2 + \sum_{N} \left[PH_m(f) - PH_s(f) \right]^2 \tag{4.6}$$

where $E(f)$ is the overall target error between the fitted curve and measured apparent mass, N is the number of frequency points in the measured apparent mass (61 points for random vibration, 13 points for sinusoidal vibration corresponding to the frequency range 1-16 Hz), $M_m(f)$ and $PH_m(f)$ are the apparent mass modulus and phase of the model at each frequency, $M_s(f)$ and $PH_s(f)$ are the measured apparent mass modulus and phase. The initial guesses and bounds of the stiffness and damping were determined from published data where the parameters m_1, m_2, k_1, c_1 had been determined by fitting the model in the frequency domain to the apparent mass measured with random vibration (Wei and Griffin, 1998). In 24 male subjects, they found optimum stiffness and optimum damping in the ranges 29,409 to 77,829 Nm^{-1} and 675 to 2,345 Nsm^{-1}, respectively. Considering the variability between subjects, the lower and upper bounds of the stiffness and damping in the present study were set to 10,000 to 200,000 Nm^{-1} and 100 to 10,000 Nsm^{-1}, respectively. In order to avoid optimisation to local minima, different start points were used in a 'Global Search' algorithm in MATLAB (version R2010a).

A two-degree-degree-of-freedom parametric model (model 2b from Wei and Griffin, 1998) was also fitted to the measured apparent masses, with both constrained and un-constrained masses.

4.3 Results

4.3.1 Vertical apparent mass

Sinusoidal vibration

The principal resonance in the vertical apparent mass during sinusoidal vertical excitation was in the region of 5 Hz, but with variability within the 20 males and within the 20 females (Figure 4.3).

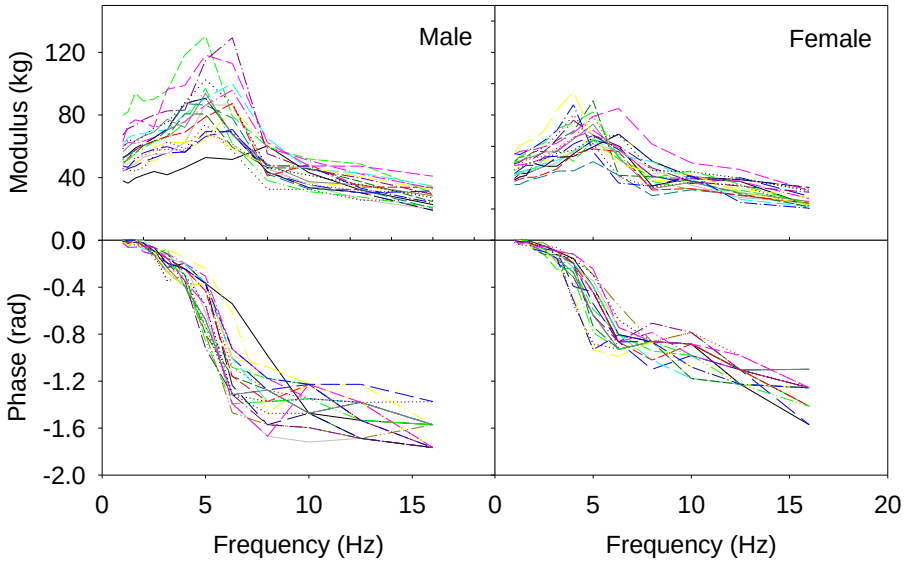

Figure 4.3 Inter-subject variability in the vertical apparent masses of 20 male and 20 female subjects exposed to sinusoidal vertical vibration at 0.4 ms^{-2} r.m.s

With increasing magnitude of sinusoidal vibration, the phase lag of the apparent mass tended to increase (Figure 4.4).

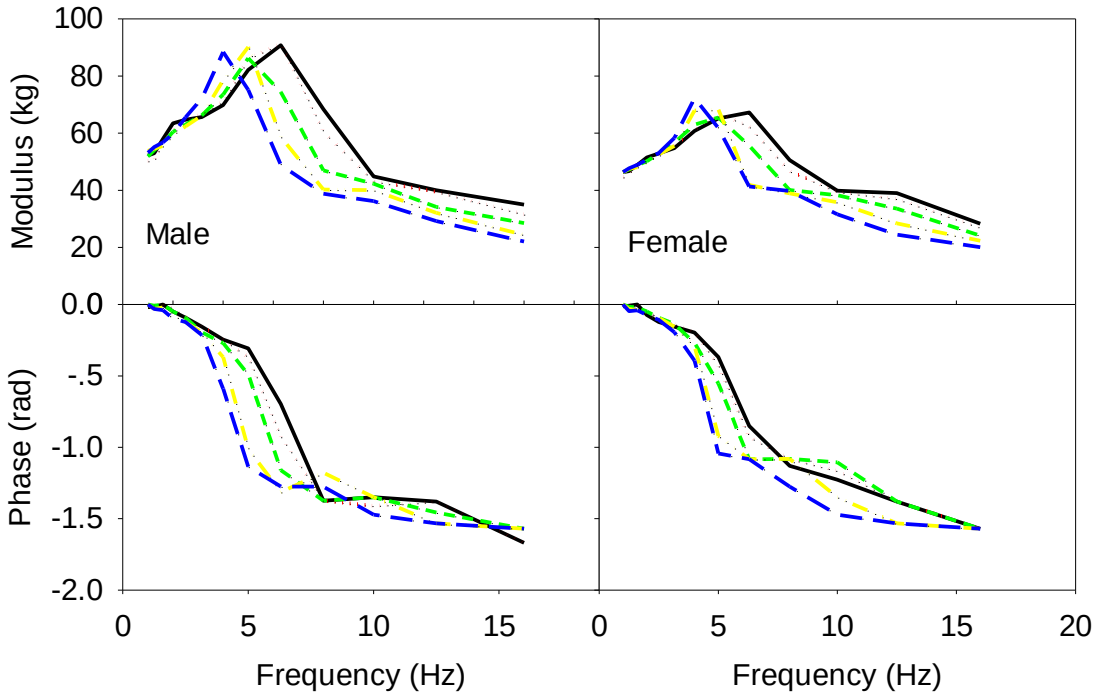

Figure 4.4 Median modulus and phase of apparent mass for subjects exposed to sinusoidal vibration at five different magnitudes of random vibration (—— 0.1 ms^{-2} r.m.s., ● ● ● 0.2 ms^{-2} r.m.s., — — — 0.4 ms^{-2} r.m.s., — ● — 0.8 ms^{-2} r.m.s., — — — 1.6 ms^{-2} r.m.s.). Median values for 20 males and 20 female

The resonance frequency in the vertical apparent mass reduced with increasing magnitude of sinusoidal excitation in both males and females (p<0.001 Friedman; Table 4.2). As the magnitude of sinusoidal vibration increased from 0.1 to 1.6 ms^{-2} r.m.s., the median resonance frequency evident in the modulus of the apparent mass decreased from 6.3 Hz to 4 Hz in both males and females.

Random vibration

The principal resonance in the vertical apparent mass during random vibration was also in the vicinity of 5 Hz, with variability within the males and within the females (Figure 4.5).

Table 4.2 Resonance frequencies and apparent masses at resonance with sinusoidal and random vibration at five magnitudes (0.1, 0.2, 0.4, 0.8, and 1.6 ms^{-2} r.m.s.). (Median of individual values of the resonance frequencies and apparent masses at resonance from 20 males and 20 females)

Direction		Vertical apparent mass				Fore-and-aft cross-axis apparent mass			
Vibration		Sinusoidal		Random		Sinusoidal		Random	
	Magnitudes (ms^{-2} r.m.s.)	M	F	M	F	M	F	M	F
Resonance Frequency (Hz)	0.1	6.3	6.3	6.5	6.3	6.3	6.3	6.4	6.4
	0.2	6.3	5.0	6.1	5.9	6.3	6.3	6.3	5.9
	0.4	5.0	5.0	5.8	5.5	5.0	5.0	6.0	5.5
	0.8	5.0	5.0	5.0	5.0	5.0	5.0	5.3	5.1
	1.6	4.0	4.0	4.5	4.5	4.0	4.0	4.5	4.8
Apparent mass at resonance (kg)	0.1	92.5	71.5	99.4	74.3	59.8	49.9	59.1	49.3
	0.2	95.1	69.4	95.8	74.5	58.7	46.2	56.4	41.7
	0.4	87.3	68.9	91.7	73.8	56.6	48.4	54.7	47.6
	0.8	93.3	75.1	93.0	74.2	48.8	45.7	50.2	38.8
	1.6	94.9	74.6	93.5	79.8	40.6	33.1	45.5	36.2

M: males; F: females

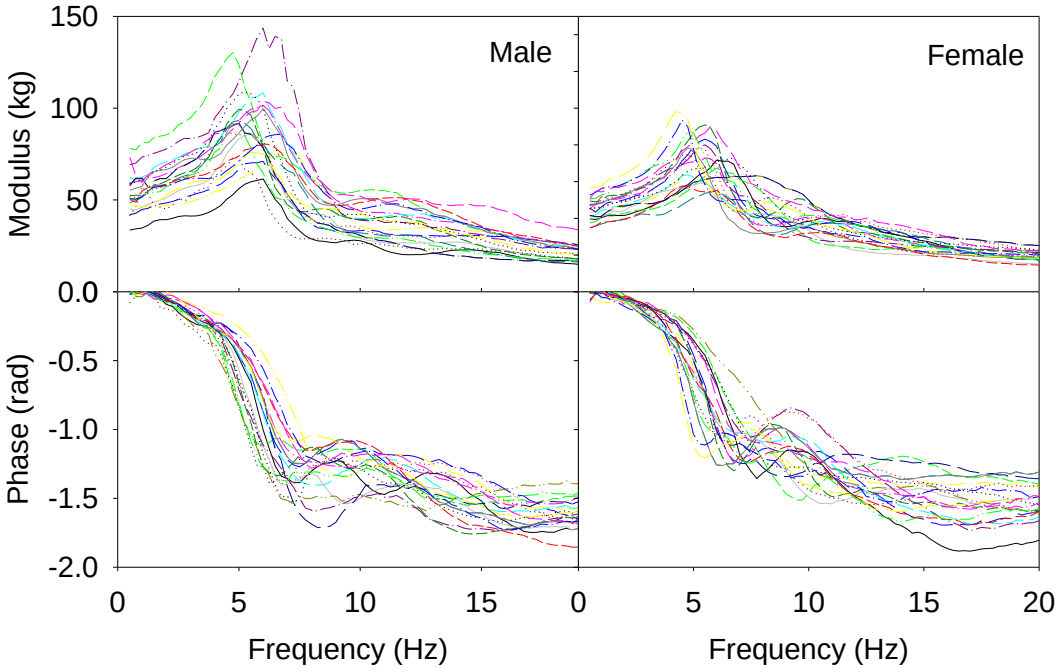

Figure 4.5 Inter-subject variability in the vertical apparent masses of 20 male and 20 female subjects exposed to random vertical vibration at 0.4 ms^{-2} r.m.s.

With increasing magnitude of vibration, the modulus of the apparent mass shows nonlinearity with the resonance frequency decreasing with increasing magnitude of vibration (Table 4.2, Figure 4.6, and Figure 4.7). As the magnitude of random vibration increased from 0.1 to 1.6 ms^{-2} r.m.s., the median resonance frequency of the apparent mass decreased from 6.5 Hz to 4.5 Hz in males and decreased from 6.25 to 4.5 Hz in the females (p<0.001 for both males and females, Friedman). There were significant differences in the resonance frequency within both males and females with every increment in vibration magnitude (i.e., between 0.1 and 0.2 ms^{-2} r.m.s., between 0.2 and 0.4 ms^{-2} r.m.s., between 0.4 and 0.8 ms^{-2} r.m.s., between 0.8 and 1.6 ms^{-2} r.m.s.; Wilcoxon, p<0.005).

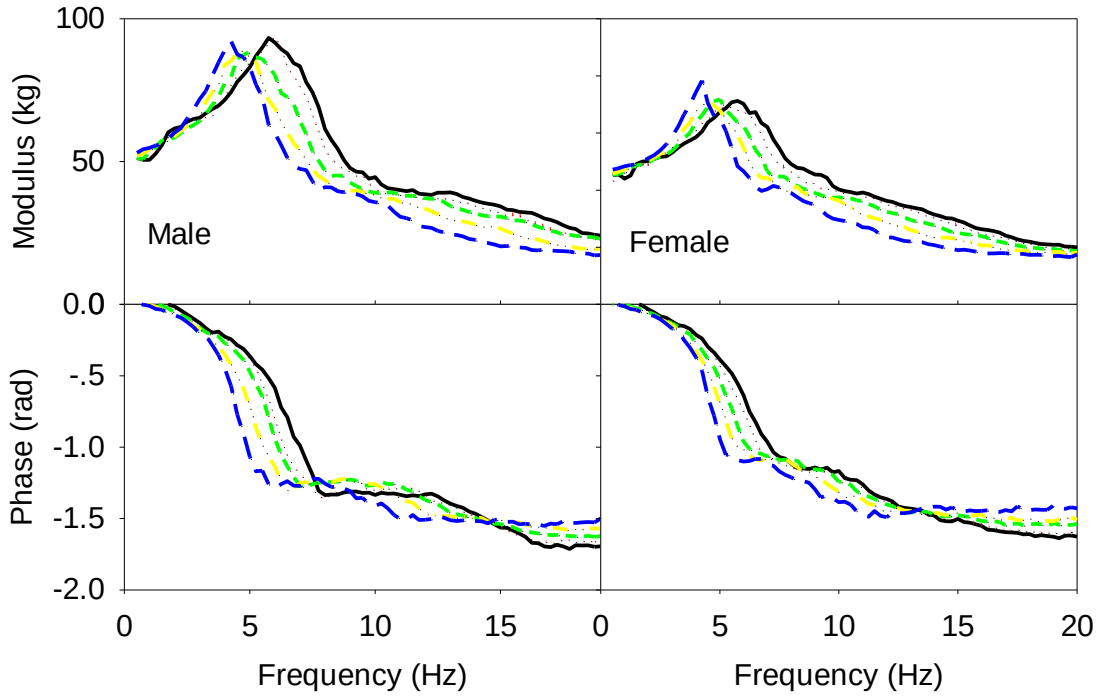

Figure 4.6 Median modulus and phase of apparent mass for subjects exposed to random vibration at five different magnitudes of random vibration (—— 0.1 ms^{-2} r.m.s., ● ● ● 0.2 ms^{-2} r.m.s., — — — 0.4 ms^{-2} r.m.s., — ● ● — 0.8 ms^{-2} r.m.s., — — — 1.6 ms^{-2} r.m.s.). Median values for 20 males and 20 females.

With increasing magnitude of vibration excitation, the apparent mass at resonance showed a trend to decrease and then increase in the males (p=0.0189, Friedman) but increase in the females (p=0.00043, Friedman).

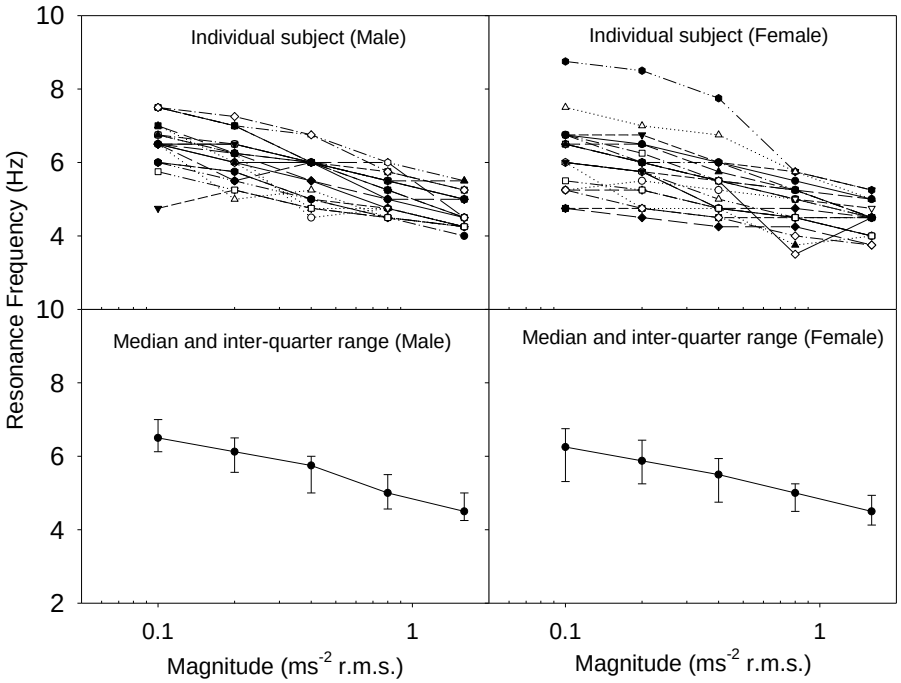

Figure 4.7 Individual (top) and median and inter-quarter range (bottom) of resonance frequencies for 20 males and 20 females exposed to random vibration at five magnitudes (0.1, 0.2, 0.4, 0.8 and 1.6 ms^{-2} r.m.s.)

Comparing sinusoidal and random vibration

The median moduli and phases of the apparent mass measured with sinusoidal and random vibration were similar at all five magnitudes of vibration, for both males and females (Figures 4.8 and 4.9). After correction of *p*-values for multiple-comparisons, there were no significant differences at any frequency between the moduli or the phases of the apparent mass measured with sinusoidal and random vibration at the same r.m.s. magnitude.

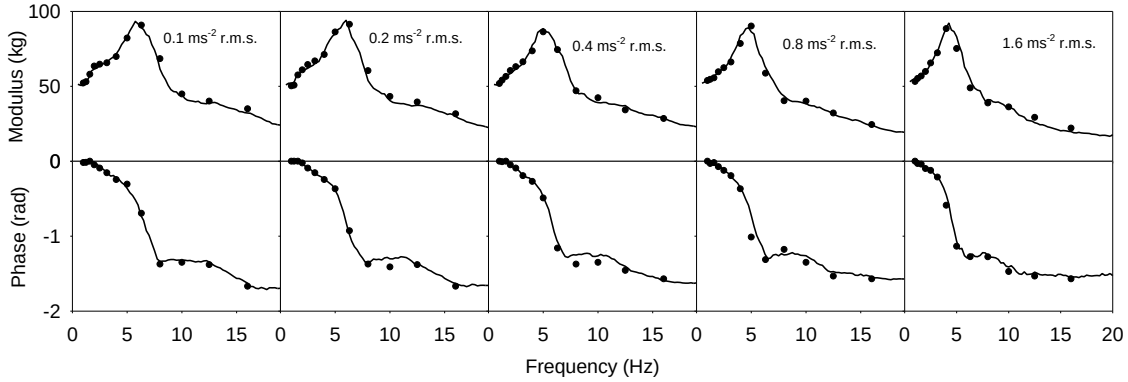

Figure 4.8 Comparison of the modulus and phase of the apparent mass between sinusoidal vibration and random vibration at five vibration magnitudes (median values for 20 males).

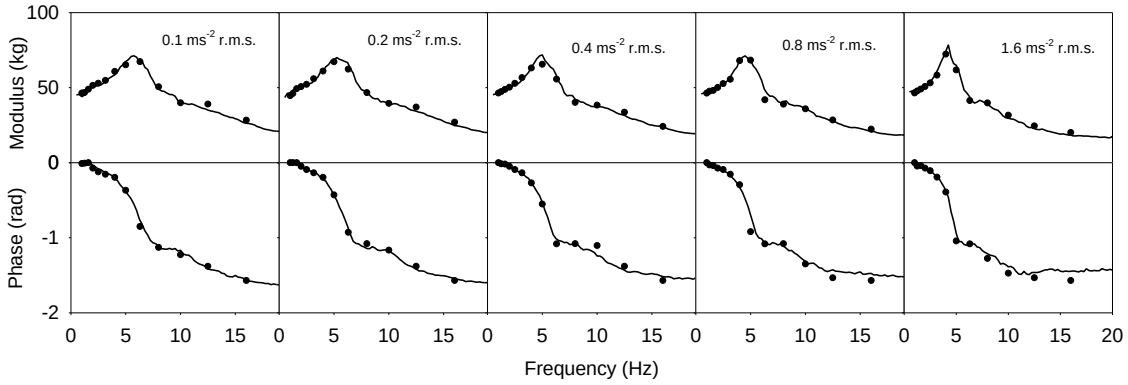

Figure 4.9 Comparison of the modulus and phase of the apparent mass between sinusoidal vibration and random vibration at five vibration magnitudes (median values for 20 females).

Effect of subject physical characteristics

There were no significant differences in the normalised vertical apparent mass between male and female subjects with either sinusoidal or random vibration at any of the five magnitudes of vibration at any frequency (p>0.05, Mann-Whitney U-test, Figures 4.10 and 4.11). There were also no significant differences in the resonance frequencies of the normalised apparent mass between males and females at any of the five magnitudes of vibration with either sinusoidal or random vibration (p>0.05, Mann-Whitney U-test).

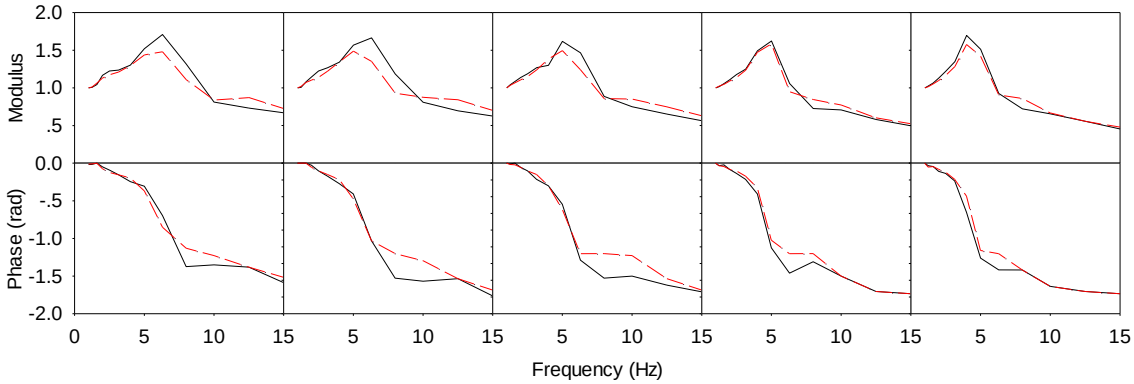

Figure 4.10 Comparison the modulus of the normalised vertical apparent mass between male and female subjects for sinusoidal vibration at five magnitudes (from left to right: 0.1, 0.2, 0.4, 0.8 and 1.6 ms^{-2} r.m.s.). Median values for 20 males (——) and 20 females (– – –).

The biodynamic measurements (i.e., the apparent masses at different frequencies and the resonance frequency of the apparent mass) at each of the five magnitudes of random and sinusoidal vibration were compared with the physical characteristics of the

40 subjects (i.e., age, total-weight, sitting-weight, knee-height, sitting-height, body mass index). There was no significant correlation between subject age and any of the biodynamic measurements (i.e., apparent masses at different frequencies, resonance frequency of apparent mass) at any of the five vibration magnitudes (p>0.05, Kendall's τ_b correlation coefficient). There were significant positive correlations between total-weight, sitting-weight, knee-height, sitting-height, BMI and the apparent masses at 1, 10, and 16 Hz and also the resonance frequency (p<0.05, Kendall's τ_b correlation coefficient).

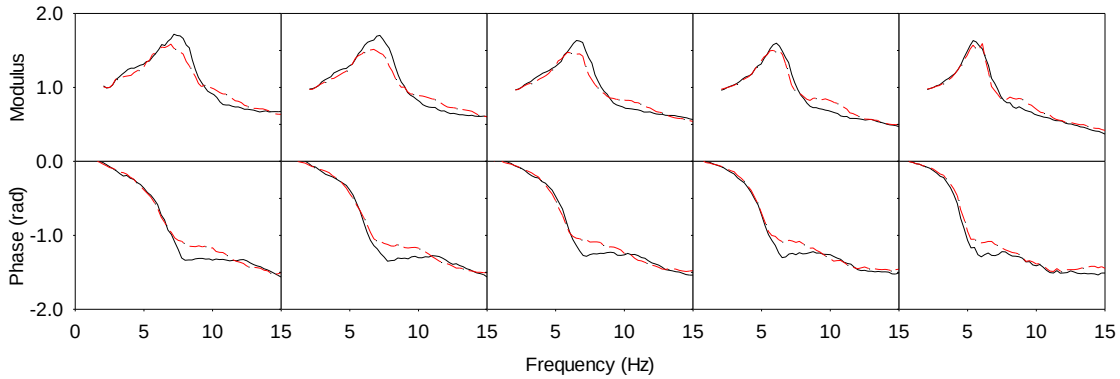

Figure 4.11 Comparison the modulus of the normalised vertical apparent mass between male and female subjects for sinusoidal vibration at five magnitudes (from left to right: 0.1, 0.2, 0.4, 0.8 and 1.6 ms-2 r.m.s.). Median values for 20 males (——) and 20 females (– – –)

4.3.2 Fore-and-aft cross-axis apparent mass

Sinusoidal vibration

Similar to the vertical apparent mass, the principal resonance in the fore-and-aft cross-axis apparent mass during sinusoidal vertical excitation was in the region of 5 Hz, but with variability within the 20 males and within the 20 females (Figure 4.12).

The modulus of the fore-and-aft cross-axis apparent mass varied with the magnitude of the vertical vibration excitation at all frequencies in the males and at all frequencies except 4 Hz in the females (p<0.05, Friedman; Figure 4.13).

The median resonance frequencies in the fore-and-aft cross-axis apparent mass at resonance decreased from 6.3 to 4.0 Hz as the magnitude of vibration increased from 0.1 to 1.6 ms^{-2} r.m.s. in both the males and the females (p<0.001 Friedman; Table 4.2).

The median fore-and-aft cross-axis apparent mass at resonance also decreased as the vibration magnitude increased from 0.1 to 1.6 ms^{-2} r.m.s. in both males and females (Figure 4.13; p<0.001 Friedman).

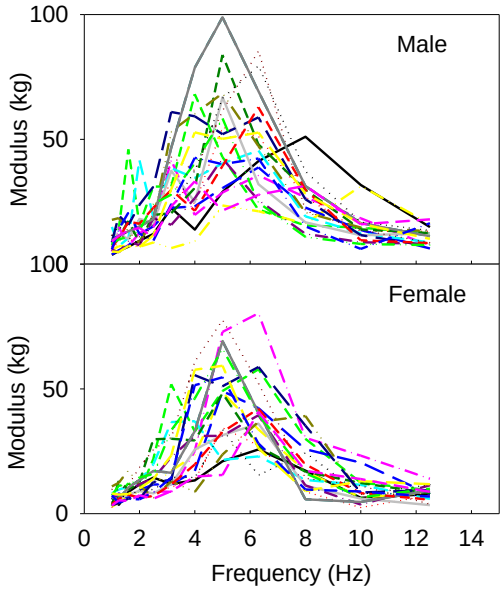

Figure 4.12 Inter-subject variability in the fore-and-aft cross-axis apparent masses of 20 male and 20 female subjects exposed to sinusoidal vertical vibration at 0.4 ms^{-2} r.m.s.

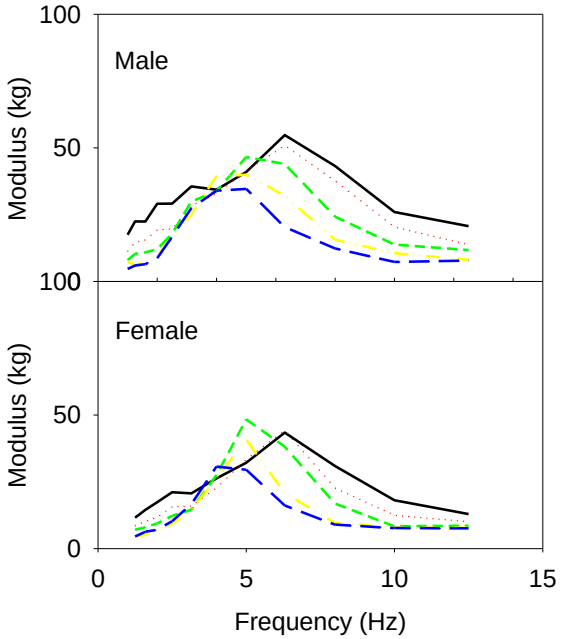

Figure 4.13 Modulus of the fore-and-aft cross-axis apparent mass with sinusoidal vibration at five different magnitudes (—— 0.1 ms^{-2} r.m.s., ····· 0.2 ms^{-2} r.m.s., — · — 0.4 ms^{-2} r.m.s., — — 0.8 ms^{-2} r.m.s., ▬▬ 1.6 ms^{-2} r.m.s.). (Medians of the measured apparent masses of 20 males and 20 females)

Random vibration

The modulus of the fore-and-aft cross-axis apparent mass during random vibration also varied between subjects (Figure 4.14) and was highly dependent on the magnitude of vibration, with the frequency of the peak in the cross-axis apparent mass decreasing with increasing magnitude of vibration (Figure 4.15, Table 4.2).

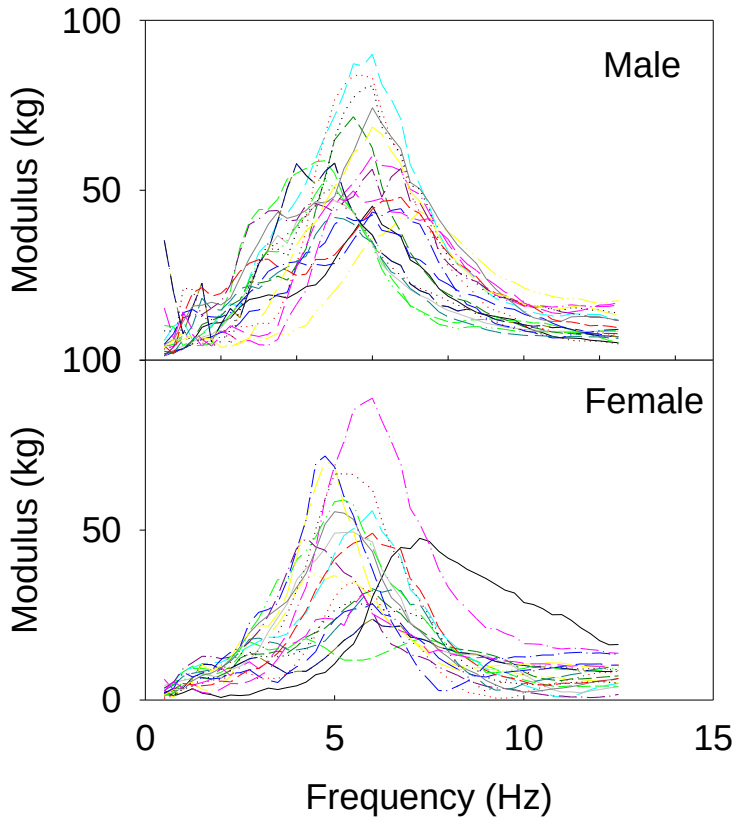

Figure 4.14 Inter-subject variability in the fore-and-aft cross-axis apparent masses of 20 male and 20 female subjects exposed to random vertical vibration at 0.4 ms^{-2} r.m.s.

The median resonance frequencies in the fore-and-aft cross-axis apparent mass at resonance decreased from 6.4 to 4.5 Hz as the vibration magnitude increased from 0.1 to 1.6 ms^{-2} r.m.s. in male subjects and decreased from 6.4 to 4.8 Hz in female subjects (Table 2). There were significant differences in the resonance frequency with every change of vibration magnitude (i.e., between 0.1 and 0.2 ms^{-2} r.m.s., between 0.2 and 0.4 ms^{-2} r.m.s., between 0.4 and 0.8 ms^{-2} r.m.s., between 0.8 and 1.6 ms^{-2} r.m.s.) in both males and females (p<0.05, Wilcoxon), except between 0.1 and 0.2 ms^{-2} r.m.s. in male subjects. The median fore-and-aft cross-axis apparent mass at resonance also decreased as the vibration magnitude increased from 0.1 to 1.6 ms^{-2} r.m.s. in both the males and females (Figure 4.15; p<0.001 Friedman).

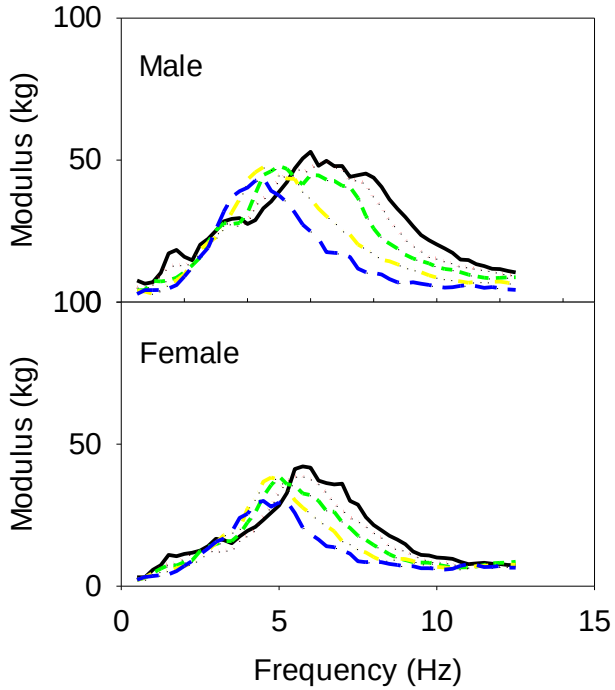

Figure 4.15 Modulus of the fore-and-aft cross-axis apparent mass with random vibration at five vibration magnitudes (——— 0.1 ms^{-2} r.m.s., ● ● ● 0.2 ms^{-2} r.m.s., — — 0.4 ms^{-2} r.m.s., — ● ● — 0.8 ms^{-2} r.m.s., — — — 1.6 ms^{-2} r.m.s.). (Medians of the measured apparent masses of 20 males and 20 females)

Comparing sinusoidal and random vibration

The fore-and-aft cross-axis apparent mass shows small but systematic differences between sinusoidal and random excitation at most of the 12 frequencies, with greater apparent mass with sinusoidal excitation at the two lower magnitudes (i.e., 0.1 ms^{-2} r.m.s. and 0.2 ms^{-2} r.m.s.; Figure 4.16 and Table 4.3).

Effect of subject physical characteristics

There were no significant differences in the normalised cross-axis apparent masses of the males and females at any of the 12 frequencies at any of the five magnitudes of sinusoidal or random vibration (p>0.05, Mann-Whitney U-test; Figure 4.17). There were also no significant differences in the resonance frequencies of the normalised fore-and-aft cross-axis apparent mass between the males and females at any of the five magnitudes of vibration with either sinusoidal or random vibration (p>0.05, Mann-Whitney U-test).

The fore-and-aft cross-axis biodynamic measurements (i.e., the fore-and-aft cross-axis apparent masses at different frequencies and the resonance frequency of the apparent

mass) at each of the five magnitudes of random and sinusoidal vibration were also compared with the physical characteristics of the 40 subjects (i.e., age, total-weight, sitting-weight, knee-height, sitting-height, body mass index). There were significant positive correlations between total-weight, sitting-weight, knee-height, sitting-height, BMI and the apparent masses at 10 Hz and also at the resonance frequency (p<0.05, Kendall's τ_b correlation coefficient).

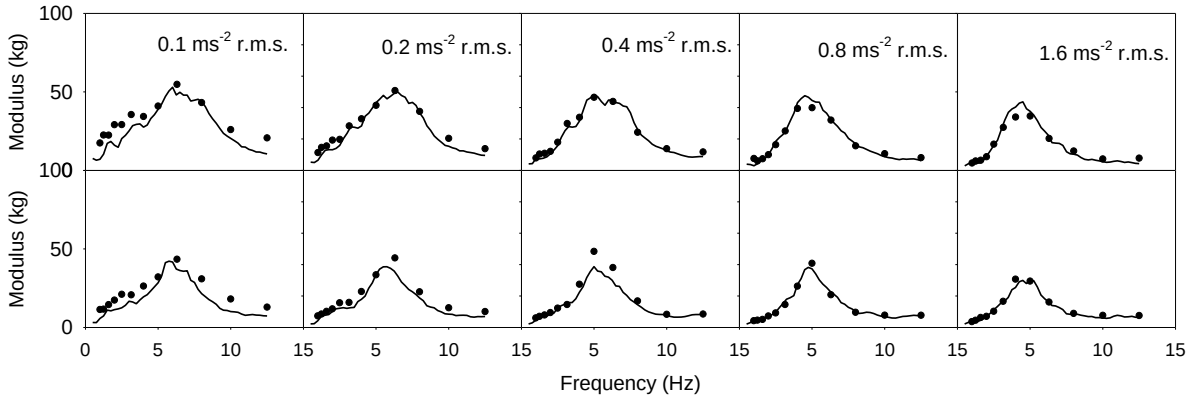

Figure 4.16 Comparison the modulus of the fore-and-aft cross-axis apparent mass between sinusoidal and random vibration for males (upper) and females (lower) at five vibration magnitudes. Median values for 20 males and 20 females.

Table 4. 3 Statistical significance of differences in fore-and-aft cross-axis apparent mass between sinusoidal vibration excitation and random vibration excitation at 12 frequencies (Wilcoxon matched-pairs signed-ranks test).

Frequency (Hz)	Males (ms^{-2} r.m.s.)					Females (ms^{-2} r.m.s.)				
	0.1	0.2	0.4	0.8	1.6	0.1	0.2	0.4	0.8	1.6
1	***	***	-	**	**	***	***	-	-	-
1.25	***	**	-	-	**	***	**	-	-	-
1.6	**	**	-	-	**	**	**	**	-	**
2	***	***	-	-	-	***	**	**	-	**
2.5	***	**	-	-	-	***	**	-	-	-
3.15	***	-	-	-	-	***	**	-	-	-
4	-	-	-	-	-	***	-	**	-	-
5	-	-	-	-	**	-	-	-	-	-
6.3	**	-	-	-	-	-	-	-	-	-
8	-	-	-	-	***	***	**	-	-	-
10	***	**	-	-	**	***	***	-	-	-
12.5	***	***	-	-	***	***	**	-	-	-

*: p<0.05, **: p<0.01, ***:p<0.005; -: p>0.05

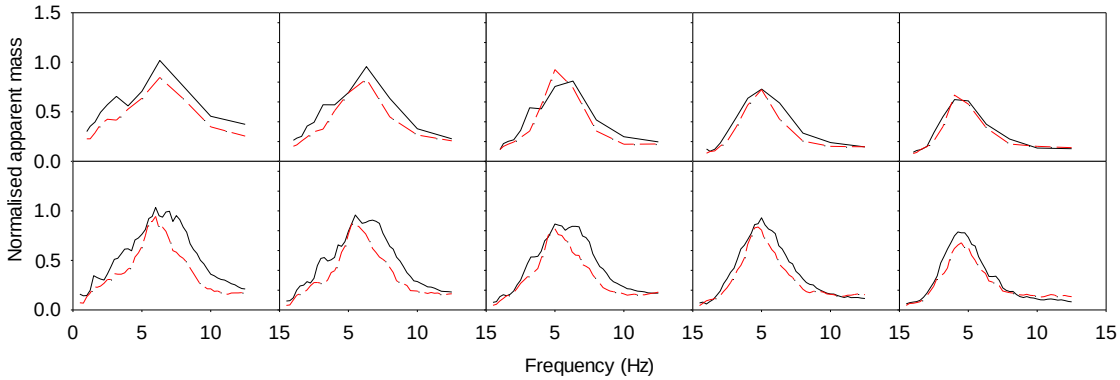

Figure 4.17 Comparison the modulus of the normalised fore-and-aft cross-axis apparent mass between male and female subjects for sinusoidal vibration (upper figures) and random vibration (lower figures) at five magnitudes (from left to right: 0.1, 0.2, 0.4, 0.8 and 1.6 ms^{-2} r.m.s.). Median values for 20 males (——) and 20 females (– – –).

4.3.3 Comparing vertical apparent mass and fore-and-aft cross-axis apparent mass

There were no significant differences between the primary resonance frequencies in the vertical apparent mass and fore-and-aft cross-axis apparent mass with either random or sinusoidal vibration at any of the five magnitudes investigated (p>0.05, Wilcoxon). Over the 40 subjects, the resonance frequencies of the vertical apparent mass were correlated with the resonance frequencies of the fore-and-aft apparent mass with all five magnitudes of random vibration and with four magnitudes of sinusoidal vibration (i.e., except 0.4 ms^{-2} r.m.s.; Figure 4.18).

4.3.4 Parameters of the one-degree-of-freedom model

Individual and median values of the stiffness, k, and damping, c, of the one degree-of-freedom model fitted to the apparent mass measured with vertical random and sinusoidal vibration at five magnitudes (0.1, 0.2, 0.4, 0.8 and 1.6 ms^{-2} r.m.s.) are shown in Tables 4.4 and 4.5. These values may be used to construct apparent mass models for each of the 20 males and 20 females used in this biodynamic study and the associated study of vibration discomfort (Chapter 5).

With both sinusoidal and random vibration, the stiffness, k, and the damping, c, decreased with increasing magnitude of vibration (p<0.001, Friedman). The stiffness decreased with each increment in magnitude, whereas the decrease in damping was not statistically significant between 0.1 and 0.2 ms^{-2} r.m.s. for sinusoidal vibration

(p=0.78, Wilcoxon) or between 0.2 and 0.4 ms^{-2} r.m.s. for either waveform (p=0.22 for sinusoidal vibration; p=0.15 for random vibration).

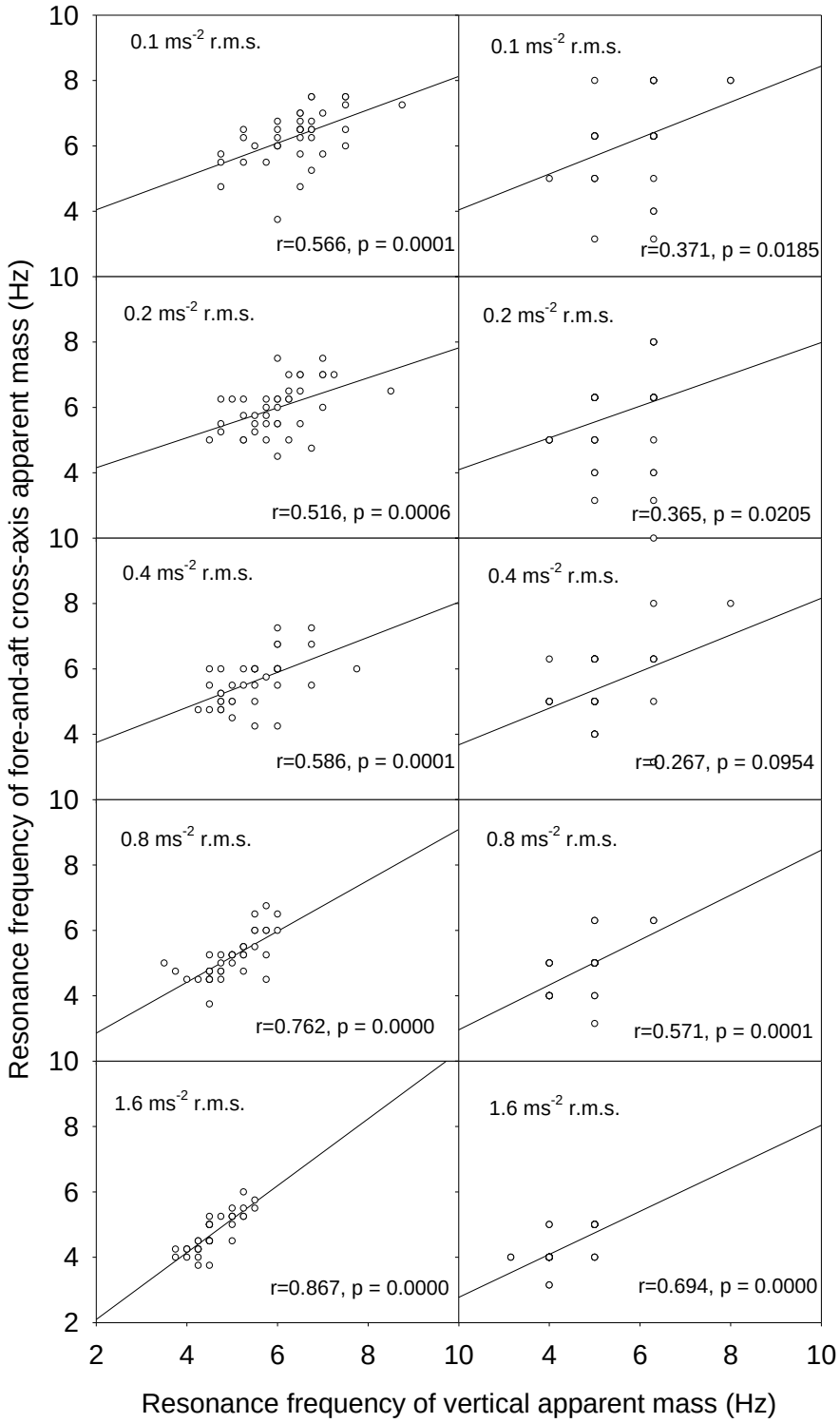

Figure 4.18 Correlation of resonance frequencies between the vertical apparent masses and the fore-and-aft apparent masses of 40 subjects exposed to random vibration (left) and sinusoidal vibration (right). Correlation coefficients r and p-values were obtained using Spearman rank correlation.

Table 4.4 Individual and median stiffness (k, Nm^{-1}) of the single degree-of-freedom model fitted to the apparent mass with vertical random and sinusoidal vibration at five magnitudes (0.1, 0.2, 0.4, 0.8, and 1.6 ms^{-2} r.m.s.).

		Sinusoidal (ms^{-2} r.m.s.)					Random (ms^{-2} r.m.s.)				
Subject	Gender	0.1	0.2	0.4	0.8	1.6	0.1	0.2	0.4	0.8	1.6
1	F	87173	74026	63118	46489	38097	103809	90465	78638	61728	48089
2	F	76639	72133	56852	48308	43190	68109	70477	63002	52332	43630
3	F	69204	72179	52799	51656	35634	84670	79316	69267	60808	49673
4	F	80776	74301	61140	58884	46666	74545	72721	55785	46601	42305
5	F	85515	72767	64004	43300	41903	91257	84105	69202	59256	49822
6	F	81486	81612	61559	59158	53961	88585	73492	58019	50632	41794
7	F	75004	68611	65734	41654	33572	83130	82174	58286	47827	42049
8	F	81412	73177	62020	54992	48062	76439	63147	51531	39944	38108
9	F	49553	40964	38371	28765	27054	76179	63443	56337	43426	34929
10	F	73564	69018	47719	48663	45954	83368	74901	68102	53739	48515
11	F	88640	73799	61929	51643	41914	142505	133300	109502	80766	65168
12	F	77567	69007	59913	44590	38010	78298	69778	58290	49828	41950
13	F	64062	59764	46501	35484	35889	83889	84497	78091	58191	38578
14	F	57082	46012	48786	34366	28963	64516	50064	41949	35453	31012
15	F	81285	77829	80233	60793	51722	94183	87490	79463	65571	57137
16	F	77247	58670	52733	39927	31311	72062	58506	50717	38705	34525
17	F	64681	57030	51737	41421	35924	78744	74999	62827	50094	40575
18	F	68914	58199	42005	36705	32278	64714	60347	49649	43497	38079
19	F	53884	48005	34220	33945	27680	55761	52231	47003	40368	35004
20	F	111856	86146	96683	68034	53247	103483	99927	85227	71261	61792
21	M	73180	73122	92126	49264	42599	66310	55209	45634	32716	27290
22	M	82619	72752	58613	43362	35049	83887	68182	60282	43406	36002
23	M	105319	100113	75443	64953	52456	83730	84653	74881	64719	58109
24	M	119433	102761	81525	63130	53721	106386	95681	89723	69560	55499
25	M	86698	77896	65998	49207	42088	86261	80744	62514	50639	41747
26	M	123712	107229	92324	79009	66208	110111	101947	89663	78632	64167
27	M	90497	101008	91906	77021	63161	95636	82727	84406	68614	62838
28	M	72188	70833	58624	43754	35357	70217	68932	57678	43843	35742
29	M	53074	54773	49325	29151	26258	78611	61530	39395	34473	30390
30	M	83871	84261	60885	49250	42670	75497	78223	63445	53093	45245
31	M	87290	76434	53942	60994	53541	78352	69083	53660	47217	43892
32	M	109955	108955	88882	64624	54008	134328	112336	95099	82454	57179
33	M	83876	68727	58520	43340	33802	83826	74617	63271	54958	43415
34	M	80176	65044	61851	48953	39709	111149	105423	90826	73874	62447
35	M	77940	76542	67486	45687	35607	84336	78016	68872	50532	44071
36	M	85092	84278	69286	66700	56286	132079	122207	109504	85517	73413
37	M	75045	80406	50443	43315	34900	64516	57849	50019	41272	36906
38	M	103790	94949	75544	65902	51541	94176	90641	73599	60527	53738

39	M	107662	100896	75165	48879	40625	143048	124174	103655	71503	62363
40	M	107996	101537	81496	63316	53686	132920	129397	112953	94088	81177
Median		81349	73488	61705	48916	41909	83857	78120	63358	52713	43761

Table 4.5 Individual and median damping (c, Nsm^{-1}) of the single degree-of-freedom model fitted to the apparent mass with vertical random and sinusoidal vibration at five magnitudes (0.1, 0.2, 0.4, 0.8 and 1.6 ms^{-2} r.m.s.).

		Sinusoidal (ms^{-2} r.m.s.)					Random (ms^{-2} r.m.s.)				
Subject	Gender	0.1	0.2	0.4	0.8	1.6	0.1	0.2	0.4	0.8	1.6
1	F	1344	1261	1447	1183	859	1648	1600	1608	1367	1227
2	F	2508	2443	1810	1673	1343	2469	2501	2370	1831	1466
3	F	1491	1598	1496	1192	1451	1449	1348	1407	1417	1294
4	F	1547	1763	1675	1618	1420	1712	1682	1654	1619	1494
5	F	1421	1300	1638	942	1253	1604	1638	1544	1453	1335
6	F	2986	2677	1845	1818	1565	2286	2123	1802	1613	1291
7	F	1455	1374	1466	1562	1421	1967	2041	1884	1744	1446
8	F	1647	1792	1401	1447	1273	1464	1487	1422	1347	1164
9	F	1589	1161	1335	1101	934	1816	1707	1709	1515	1188
10	F	1293	1760	1313	1556	1326	1720	1818	1760	1674	1522
11	F	2111	1653	2603	1101	1006	1544	1556	1594	1570	1423
12	F	2171	2256	1715	1200	1149	1554	1519	1515	1436	1284
13	F	1842	1682	1685	1563	920	2183	1980	2142	1938	1467
14	F	1521	1691	1620	1236	1048	1626	1671	1510	1409	1265
15	F	1857	1717	1947	1398	1266	1664	1674	1640	1522	1447
16	F	1786	1537	1215	1094	808	1795	1539	1416	1160	983
17	F	1150	1162	1361	1223	935	1817	1735	1685	1505	1290
18	F	1800	1565	1397	1293	1095	1964	1770	1660	1509	1298
19	F	1624	1622	1426	1437	1313	1924	1756	1652	1473	1306
20	F	2146	2475	2048	1704	1017	2432	2304	2060	1984	1586
21	M	1142	1648	1404	961	1238	1265	1241	1271	1179	1036
22	M	1559	2499	2126	1347	1050	1460	1591	1575	1459	1225
23	M	2112	2325	1988	1887	1321	2792	2515	2438	2163	1876
24	M	1084	1581	1286	1435	1523	1736	1647	1822	1684	1327
25	M	1508	1420	1420	1447	1283	1678	1842	2001	1922	1643
26	M	2522	1722	1958	1646	1725	2212	1903	1979	1779	1598
27	M	1612	1716	1772	1562	1478	1995	1979	1804	1704	1472
28	M	788	832	758	764	590	848	987	1129	1119	973
29	M	1282	999	1263	861	755	1989	1207	1357	1226	1168
30	M	1001	1121	1674	1197	1157	1550	1546	1537	1492	1326
31	M	1237	1124	1089	1290	995	1225	1101	1116	1042	1001
32	M	1242	1089	1311	1171	1239	1222	1082	1260	1249	1063
33	M	1153	1065	1144	845	866	1353	1273	1276	1251	1124
34	M	1347	1425	1567	792	723	2209	2252	2119	1750	1375

35	M	894	1195	1286	1111	780	1353	1440	1443	1275	1176
36	M	1201	1235	1259	1174	1184	2178	2154	2362	1916	1648
37	M	1585	1798	948	987	973	1306	1336	1224	1086	989
38	M	1828	1820	2394	1679	1305	2181	2162	1990	1707	1397
39	M	2511	1998	1729	1562	1353	2058	1960	1884	1286	1217
40	M	2463	1880	1241	1450	1291	2713	2857	2725	2397	1964
Median		1553	1635	1456	1292	1211	1728	1678	1653	1507	1302

Between sinusoidal vibration and random vibration there were no significant differences in the stiffnesses at the three lower magnitudes (p=0.058 at 0.1 ms^{-2} r.m.s., p=0.085 at 0.2 ms^{-2} r.m.s., p=0.076 at 0.4 ms^{-2} r.m.s., Wilcoxon). At two higher magnitudes, the stiffness was significantly greater with random vibration than with sinusoidal vibration (p=0.005 at 0.8 ms^{-2} r.m.s., p<0.001 at 1.6 ms^{-2} r.m.s.). The damping was significantly lower with sinusoidal vibration than with random vibration at all magnitudes except 0.2 ms^{-2} r.m.s. (p=0.053, Wilcoxon). The fitted parameters (both stiffness and damping) obtained with sinusoidal vibration and with random vibration were correlated (Table 4.6, Figures 4.19 and 4.20).

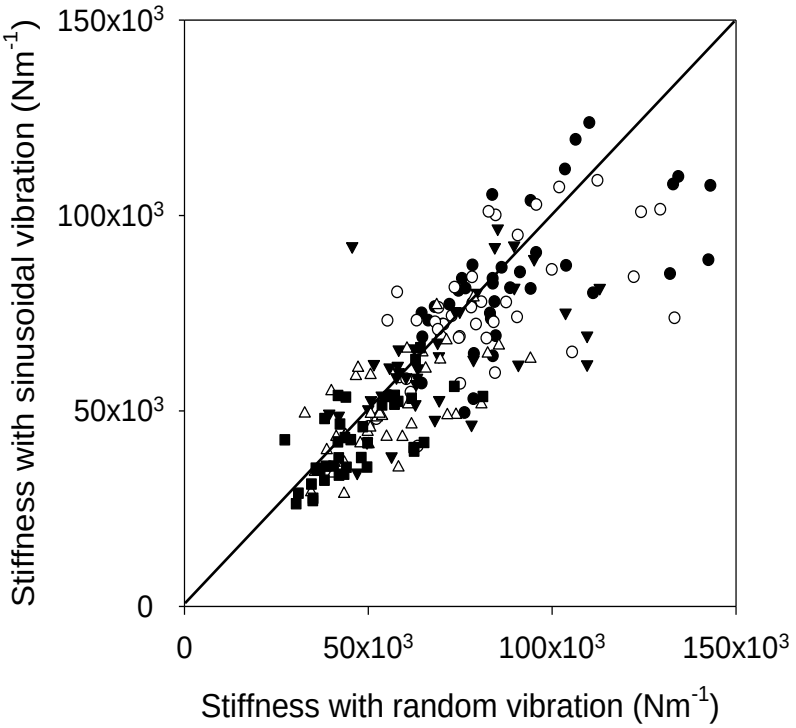

Figure 4.19 Correlation between the stiffnesses of an equivalent single degree-of-freedom model of biodynamic response to random vibration and biodynamic response to sinusoidal vibration (●: 0.1 ms^{-2} r.m.s.;○ : 0.2 ms^{-2} r.m.s.; ▼: 0.4 ms^{-2} r.m.s.; ∆: 0.8 ms^{-2} r.m.s.; ■: 1.6 ms^{-2} r.m.s.)

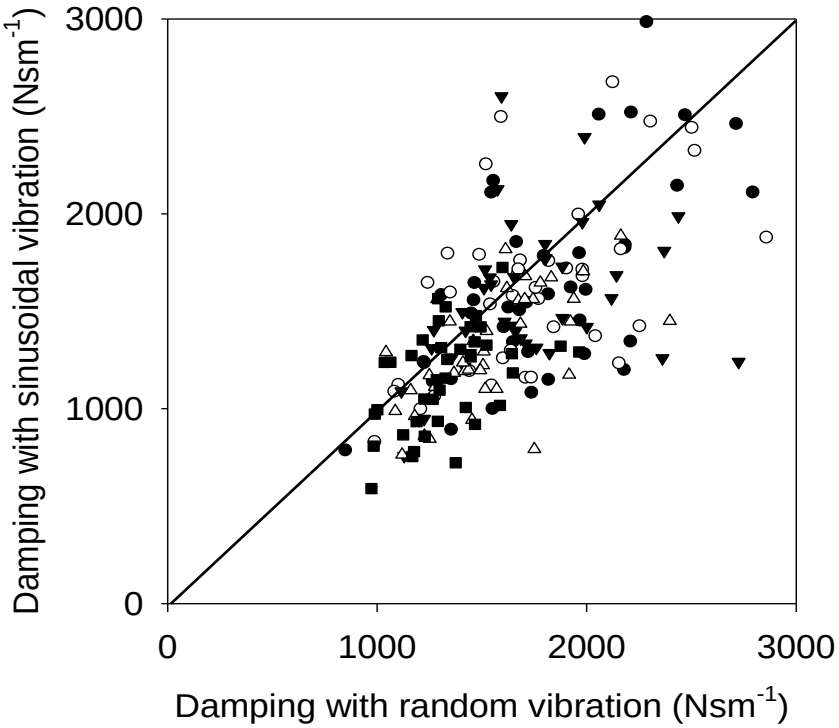

Figure 4.20 Correlation between the damping of an equivalent single degree-of-freedom model of biodynamic response to random vibration and biodynamic response to sinusoidal vibration (●: 0.1 ms^{-2} r.m.s.;○ : 0.2 ms^{-2} r.m.s.; ▼: 0.4 ms^{-2} r.m.s.; ∆: 0.8 ms^{-2} r.m.s.; ■: 1.6 ms^{-2} r.m.s.)

Table 4.6 Kendall's correlation coefficient τ_b between the model parameters (i.e., stiffness and damping) obtained with random vibration and sinusoidal vibration.

Magnitude (ms^{-2} r.m.s.)	stiffness		damping	
	τ_b	*p*-value	τ_b	*p*-value
0.1	0.54	<0.001	0.42	<0.001
0.2	0.45	<0.001	0.37	<0.001
0.4	0.45	<0.001	0.32	<0.005
0.8	0.49	<0.001	0.48	<0.001
1.6	0.58	<0.001	0.36	<0.001

Similar conclusions were obtained when fitting the two-degree-degree-of-freedom parametric model (model 2b from Wei and Griffin, 1998) to the measured vertical apparent masses of all individual subjects. When constraining the masses of the model (i.e., m, m_1, and m_2 to be 12%, 65%, and 23% of the subject sitting mass), the stiffness k_1 and damping c_1 reduced as the magnitude of vibration increased, but the stiffness k_2 and damping c_2 (associated with the mass m_2) did not show a clear trend. When un-constraining the masses of the model, the stiffness k_1 reduced as the magnitude of

vibration increased, but the stiffness k_2 and damping c_1 and c_2 did not show a clear trend.

4.4 Discussion

4.4.1 Nonlinearity in the vertical apparent mass

Nonlinearity in the vertical apparent mass is clearly evident with both the sinusoidal and the random vibration excitation. With sinusoidal vibration, as the magnitude of vibration increased from 0.1 to 1.6 ms^{-2} r.m.s., the median resonance frequency of the apparent mass decreased from 6.3 Hz to 4.0 Hz for both males and females. With random vibration, as the magnitude of vibration increased from 0.1 to 1.6 ms^{-2} r.m.s., the median resonance frequency of the apparent mass decreased from 6.5 Hz to 4.5 Hz in the males and from 6.25 Hz to 4.5 Hz in the females. This 'softening' behaviour of the apparent mass of the human body with increased vibration magnitude is similar to that found in previous studies of both the apparent mass of the body and the transmissibility to the spine (Fairley and Griffin 1989, Matsumoto and Griffin 2002a).

The nonlinearity is also evident in the phase of the apparent mass. With both vibration waveforms, the phase lag increased rapidly with increases in the frequency of the vibration excitation around the resonance frequency. As the vibration magnitude increased from 0.1 to 1.6 ms^{-2} r.m.s., there was a reduction in the frequency at which the phase started to increase. The changes in the phase of the apparent mass are consistent with the changes in the modulus of the apparent mass (Figures 4.4 and 4.6).

The mechanism responsible for the nonlinear biodynamic responses of the human body has been considered previously. It has been speculated that with increased magnitudes of vibration the thixotropic-like behaviour of the musculoskeletal structure reduces the dynamic stiffness of the body (Fairley and Griffin 1989). Both the stiffness, k, and the damping, c, of the one degree-of-freedom model reduced with increasing magnitude of both sinusoidal vibration and random vibration (Tables 4.4 and 4.5). The stiffness of such a model has been found to reduce with increasing magnitude of vibration in previous studies (e.g., Huang and Griffin 2006), and one study has reported a significant reduction in the damping (Toward and Griffin, 2010).

Nonlinearity along the vibration transmission path common to the spine and the abdomen allows the possibility that the nonlinearity might be caused by a combination of factors: a softening response of the buttocks tissue, a bending or buckling response of the spine (i.e., a geometric nonlinearity), and different muscular forces at different

magnitudes of vibration (a doubling of vibration magnitude not resulting in a doubling of muscle activity) (Mansfield and Griffin 2000). The nonlinearity appears to decrease with voluntary increases in muscle tension around the buttocks, suggesting these tissues may be partly responsible for the nonlinearity (Matsumoto and Griffin 2002b). During vertical vibration excitation, nonlinearity in the apparent masses of seated subjects is slightly reduced when pressure on the tissues at the ischial tuberosities is increased, also consistent with these tissues being involved in the nonlinearity (Nawayseh and Griffin 2003). Other studies also suggest that passive thixotropy of soft tissues, rather than geometric nonlinearity or voluntary or involuntary muscular activity, is the most likely primary cause of the nonlinearity in biodynamic responses of the human body to whole-body vibration (Huang and Griffin 2008, Huang and Griffin 2009). The present study shows that the nonlinearity is similar with sinusoidal and random vibration, which also suggests it is unlikely that changes in muscle activity are the principal cause of the nonlinearity.

By determining the parameters of a single degree-of-freedom model that fit the vertical apparent mass of the body at different magnitudes of vibration, the results can be applied to the specification of anthropodynamic dummies for replacing people when measuring seat transmissibility. In many situations the variation in apparent mass associated with the relevant range of vibration magnitudes is likely to be greater than the differences in apparent mass between a single degree-of-freedom model and a two degree-of-freedom model. It might therefore be argued that unless an anthropodynamic dummy is appropriately nonlinear, or the range of magnitudes of vibration is very narrow, there is no justification for developing an anthropodynamic dummy with more than a single degree-of freedom.

4.4.2 Nonlinearity in the fore-and-aft cross-axis apparent mass

There was similar nonlinear behaviour in the fore-and-aft cross-axis apparent mass as in the vertical apparent mass: a decrease in the resonance frequency with each increase in vibration magnitude (Figures 4.6 and 4.15). At all frequencies, and with both sinusoidal and random vibration at all magnitudes, the fore-and-aft cross-axis apparent mass was less than the vertical apparent mass (compare Figures 4.4 and 4.13, and Figures 4.6 and 4.15). However, it is clear that vertical excitation caused substantial fore-and-aft forces during both sinusoidal and random excitation, especially over the range 4 to 10 Hz.

Different mechanisms could be responsible for the nonlinearity in the vertical apparent mass and the fore-and-aft cross-axis apparent mass. With random vertical vibration

excitation at 1.7 ms^{-2} r.m.s. from 0.5 to 30 Hz, and measuring the motion of the head, spine, pelvis, and viscera in the mid-sagittal planes of eight subjects, Kitazaki and Griffin (1998) found separate vibration modes at 3.4 and 4.9 Hz produced by two different mechanisms. The mode at 3.4 Hz was a bending mode of the entire spine, with fore-and-aft motion of the pelvis in phase with fore-and-aft motion of the head. The mode at 4.9 Hz was the principal mode and in phase with a vertical visceral mode. Tensing the muscles of the tissues beneath the pelvis appears to affect the nonlinearity in the vertical direction but not the nonlinearity in the fore-and-aft direction (Matsumoto and Griffin 2002b), and increasing pressure on the tissue beneath the pelvis (sitting on a seat with minimum thigh contact) appears to reduce the nonlinearity in only the vertical direction (Nawayseh and Griffin 2003).

Although some studies have found differences suggestive of different mechanisms for nonlinearity in the vertical apparent mass and the fore-and-aft cross-axis apparent mass, in the present study, the primary resonance frequencies in the vertical apparent mass were highly correlated with the primary resonance frequency in fore-and-aft cross-axis apparent mass with both random vibration and sinusoidal vibration at each of the five magnitudes investigated (Figure 4.18). The correlation coefficients were greater with random vibration, consistent with the finer frequency resolution, and increased with increasing magnitude of vibration. In part, differences between the resonances in each direction may be due to difficulty in identifying the resonance frequency in some individuals (Figures 4.3, 4.5, 4.12, 4.14). Resonance frequencies in the fore-and-aft cross-axis apparent mass have also been found to be correlated with resonances in the vertical in-line apparent mass by Qiu and Griffin (2010).

4.4.3 Effect of vibration waveform on the apparent mass

Many previous studies have found nonlinearities in the apparent mass when using random vibration, including a reduction in the resonance frequency with increasing magnitude of vibration. This study shows that changes in the magnitude of sinusoidal vibration cause similar nonlinear changes. This is broadly consistent with changes in the frequency-dependence of subjective responses associated with increases in the magnitude of vibration excitation at some frequencies (e.g., Matsumoto and Griffin 2005, Subashi *et al*. 2009).

The energy in a random vibration is distributed across a range of frequencies whereas a sinusoidal vibration has energy concentrated at one frequency. For random and sinusoidal vibrations of the same r.m.s. acceleration, as in this study, at each frequency of the sinusoidal vibration the energy is greater than with random vibration of the same

r.m.s. magnitude (Figure 4.21). Notwithstanding the large differences, the apparent masses obtained with the two very different waveforms of vibration are remarkably similar at all five magnitudes of acceleration (i.e., at 0.1, 0.2, 0.4, 0.8, and 1.6 ms^{-2} r.m.s.; Figures 4.8, 4.9 and 4.16). Superficially, the results may appear to suggest that the same apparent mass is obtained with very different waveforms (i.e., sinusoidal or random) when the r.m.s. magnitude of the vibration acceleration is the same.

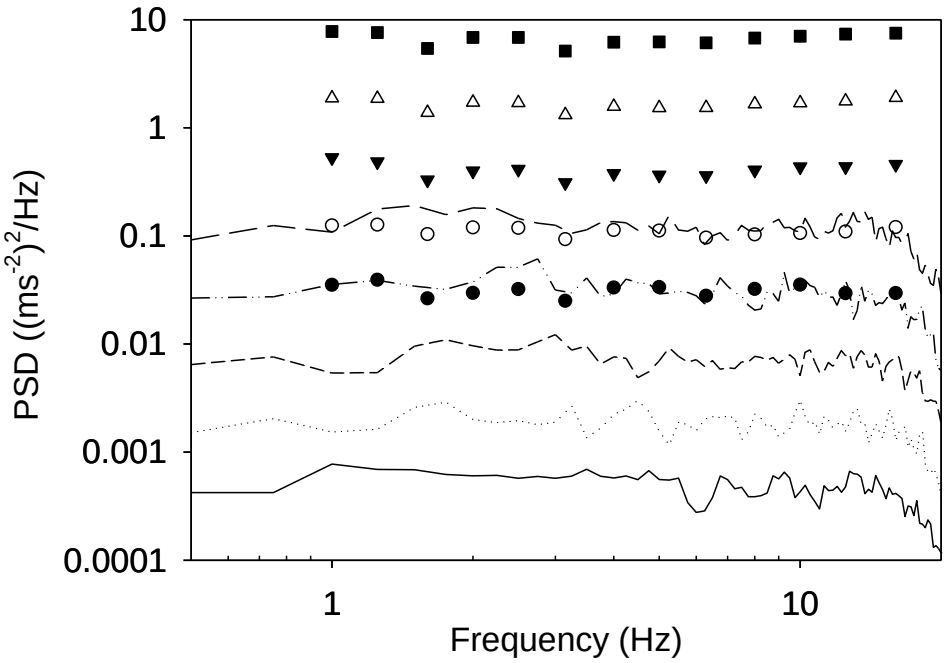

Figure 4.21 Comparison of acceleration power spectral densities between sinusoidal vibration (• 0.1 ms^{-2} r.m.s.; ○ 0.2 ms^{-2} r.m.s.; ▼ 0.4 ms^{-2} r.m.s.; Δ 0.8 ms^{-2} r.m.s.; ■ 1.6 ms^{-2} r.m.s.) and random vibration (—— 0.1 ms^{-2} r.m.s., ····· 0.2 ms^{-2} r.m.s., — — 0.4 ms^{-2} r.m.s., — ·· — 0.8 ms^{-2} r.m.s., —— —— 1.6 ms^{-2} r.m.s.) analysed with 0.25-Hz frequency resolution.

The nonlinearity that is observed at any frequency may be presumed to arise from magnitude-dependent dynamic characteristics in a part of the body that influences the apparent mass with that frequency of vibration. The nonlinearity in the apparent mass has been reported to be influenced more by some frequencies of vibration than by other frequencies of vibration (e.g., Toward 2002). In the present study, the ratio of the apparent masses obtained at the highest and the lowest magnitude at each frequency varied with the frequency of both the sinusoidal vibration and the random vibration (Figure 4.22). At frequencies less than 2.5 Hz, the ratio is close to unity, so the magnitude of vibration did not greatly affect the apparent mass, and the response of the human body is close to linear. At frequencies greater than about 2.5 Hz, the ratio

differs from unity, indicating nonlinearity. A ratio greater than unity means the apparent mass is greater with higher magnitudes, whereas a ratio less than unity means the apparent mass is greater with lower magnitudes. As the magnitude of vibration increased, the apparent mass resonance frequency reduced, so the ratio was greater than unity at frequencies less than the resonance frequency (around 5 Hz) and less than unity at frequencies greater than the resonance frequency. Even though the distribution of vibration within the body differs greatly over the frequency range investigated here, it is clear from Figure 4.22 that nonlinearity influenced the apparent mass of the body at all frequencies greater than about 2.5 Hz. The median values of the model parameters (stiffness *k* and damping *c;* Tables 4.4 and 4.5) obtained by curve fitting to the measured vertical apparent masses of the individual subjects (males and females) were used to calculate the apparent mass of the one-degree-of-freedom model at the highest and lowest magnitudes with both sinusoidal and random vibration (Figure 4.22 (c)). At each frequency, the ratios of the apparent mass fitted from the single degree-of-freedom model at the highest and lowest magnitudes of vibration are close to the experimental data obtained with both sinusoidal vibration and random vibration. This means that, although the body is much more complex than a single degree-of-freedom model, a single degree-of-freedom model in which the stiffness and damping reduce with increasing magnitude of vibration can provide a useful prediction of the nonlinearity in the vertical apparent mass of the seated human body at all frequencies up to 16 Hz.

A random vibration with a wider or a narrower bandwidth (or with a different spectral shape) than used in this study but with the same overall acceleration magnitude may be expected to produce a different apparent mass. The close similarity in the apparent mass obtained with sinusoidal and random vibration in the present study is therefore limited, to some extent, to random vibration with an approximately flat constant bandwidth acceleration spectrum within a bandwidth of approximately 1.0 to 16 Hz.

There is scope for improved understanding of the mechanisms involved in the nonlinearity but, for practical purposes, the present results suggest that when the dominant interest is in biodynamic responses to vertical excitation at frequencies in the range 1 to 16 Hz, the apparent mass obtained with random vibration may be broadly similar to that with other waveforms, including sinusoidal vibration excitation, if the r.m.s. magnitudes of the acceleration are similar.

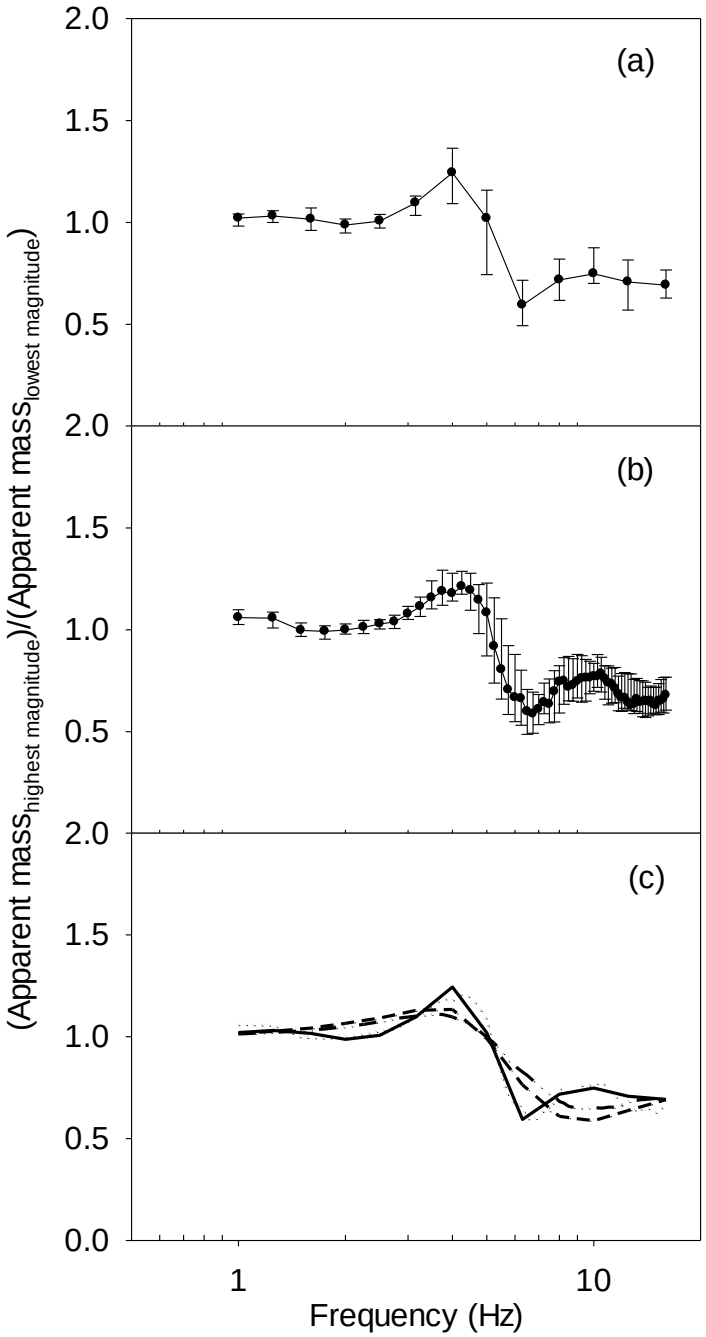

Figure 4.22 Ratios of apparent masses obtained at the highest and lowest magnitudes of vibration (i.e., 1.6 and 0.1 ms^{-2} r.m.s.): (a) sinusoidal vibration (medians and inter-quarter ranges for 40 subjects); (b) random vibration (medians and inter-quarter ranges for 40 subjects); (c) comparison of the median ratio from four conditions: measured sinusoidal vibration (——), measured random vibration (·····), fitted sinusoidal vibration (— —) and fitted random vibration (— · · —).

4.4.4 Effect of subject characteristic

The nonlinearity evident in the vertical apparent mass and the fore-and-aft cross-axis apparent mass obtained with both random and sinusoidal vibration was similar in males and females. There were no significant differences between males and females in their vertical apparent masses or their fore-and-aft cross-axis apparent masses (after normalisation to correct for subject mass) at any of the five vibration magnitudes (i.e., 0.1, 0.2, 0.4, 0.8 and 1.6 ms^{-2} r.m.s.). There were also no significant differences between males and females in the principal resonance frequencies in the vertical apparent mass or fore-and-aft cross-axis apparent mass for either random or sinusoidal vibration at any of the five vibration magnitudes. This finding is similar to Fairley and Griffin (1989) who concluded that the mean normalised apparent masses of men, women, and children are similar. After controlling for other factors (i.e., age and body mass index), the resonance frequencies in the vertical apparent masses of males and females have also been found to be similar with three different backrest conditions (i.e., sitting upright with no backrest, sitting upright with a rigid backrest, and sitting with a foam backrest reclined to 15°) (Toward and Griffin 2011). However, with a reclined rigid backrest the reduction in resonance frequency with increased vibration magnitude was significantly less in females than in males. It was suggested that the effects of anatomical differences between genders may be more pronounced when supported by a reclined rigid backrest.

The physical characteristics of the subjects (e.g., total-weight, sitting-weight, knee-height, sitting-height and BMI) were positively correlated with their vertical apparent masses at 1, 10 and 16 Hz, but there was no correlation with their resonance frequencies. Fairley and Griffin (1989) also found no statistically significant correlation between subject weight and the apparent mass resonance frequency, although seat-to-head transmissibility has been reported to be negatively correlated with subject weight and subject height (Griffin *et al*. 1982). In the present study there were no significant correlations between the ages of the 40 subjects and their measured biodynamic responses. In a study with 80 subjects, Toward and Griffin (2011) found the frequency of the principal resonance increased by 0.27 Hz per 10 years increase of age. Whereas the present study investigated subjects aged 22 to 41 years, Toward and Griffin (2011) investigated subjects aged 18 to 65 years and it seems that the principal influence of age occurred in their subjects who were older than about 40 years.

4.5 Conclusions

During vertical vibration excitation of the seated human body, the vertical apparent mass, the fore-and-aft cross-axis apparent mass, and the associated nonlinearity, are broadly similar with sinusoidal and random vibration. With both sinusoidal and random vibration, the principal resonance frequencies evident in the vertical apparent mass and the fore-and-aft cross-axis apparent mass are correlated and decrease as the magnitude of vibration excitation increases.

Both the stiffness and the damping of an equivalent single degree-of-freedom lumped parameter model of the body reduce with increasing magnitude of vibration excitation. Consequently, changes in the vertical apparent mass of the body with changes in the magnitude of vertical excitation depend on the frequency of the vibration excitation, with relatively little nonlinearity at frequencies less than about 2.5 Hz (where the apparent mass is little affected by stiffness or damping) but greater nonlinearity at higher frequencies (where the apparent mass is highly dependent on both stiffness and damping). It seems reasonable to expect that the changes in the stiffness and the damping are associated with some measure of relative motion at one or more location in the body. This relative motion will depend on the frequency of vibration, and so the nonlinearity in apparent mass obtained with random vibration may be expected, in general, to depend on the spectrum of the vibration excitation. The apparent mass of the body measured with the same magnitudes of random and sinusoidal vibration could therefore differ. However, for the spectrum of 1- to 16-Hz random vibration used in this study, the vertical apparent mass of the seated human body was similar to that with sinusoidal vibration of a similar magnitude, and there was similar nonlinearity with both waveforms (i.e., sinusoidal and random).

With both sinusoidal and random vibration there are no large or systematic differences between males and females in either their vertical apparent masses or their fore-and-aft cross-axis apparent masses after normalisation (i.e., correction for differences in sitting weight). There are also no large differences between males and females in the principal resonance frequencies evident in their vertical and fore-and-aft apparent masses during either random or sinusoidal vibration excitation.

Chapter 5 Discomfort caused by sinusoidal vibration

5.1 Introduction

Human responses to whole-body vibration are dependent on many factors including the frequency of the vibration. From understanding of the frequency-dependence of the discomfort caused by vibration, frequency weightings have been developed, standardised (in British Standard 6841:1987, International Standard 2631-1:1997), and built into commercially available meters for measuring and evaluating exposures to whole-body vibration.

Understanding of the frequency-dependence of the discomfort caused by whole-body vibration is based on experimental studies that have determined the acceleration required to produce similar discomfort over a range of frequencies of vibration (i.e., equivalent comfort contours). Early studies asked subjects to estimate the extent of their sensations, discomfort, annoyance, etc. using semantic scales. More recent studies have mostly asked subjects to compare vibration stimuli so as to determine their relative importance in terms of some subjective response (e.g., Miwa 1967, Shoenberger and Harris 1971, Griffin *et al*. 1982, Corbridge and Griffin 1986, Howarth and Griffin 1988, Morioka and Griffin 2006a,b).

The relation between the physical magnitude of a stimulus and the sensations it produces may be expressed by Stevens' power law, in which the 'objective magnitude', φ, of the stimulus and the 'subjective magnitude', Ψ, of the response are assumed to be related by a power function:

$$\Psi = k\,\varphi^{n} \qquad (5.1)$$

where the 'rate of growth of discomfort' with increasing magnitude of vibration is given by the exponent, *n*. With fore-and-aft, lateral, and vertical vibration of both seated and standing people, the exponent, *n*, varies with the frequency of vibration (e.g., Morioka and Griffin 2006a, Wyllie and Griffin 2007, 2009, Thuong and Griffin 2011). The frequency-dependence of the exponent means that equivalent comfort contours have a different frequency-dependence at different magnitudes. Although this implies the frequency weightings should be different for low and high magnitude vibration this is not reflected in the frequency weightings in current standards.

The nonlinearity in the weightings may be caused by several different phenomena. It seems likely that with some motions the neurophysiological mechanisms responsible for the sensations causing discomfort differ at low and high magnitudes of vibration. For example, while the sensations produced by low magnitudes of high frequency vibrotactile stimulation may be mediated by the Pacinian channel, higher magnitudes may be mediated by another tactile channel with a different frequency-dependence. This may explain the magnitude-dependence of equivalent comfort contours seen in the exponents for hand-transmitted vibration (Morioka and Griffin 2006b) and high frequency whole-body vibration (Morioka and Griffin 2006a). With low frequency non-vertical vibration (e.g., roll or lateral oscillation), a change in the part of the body experiencing most discomfort as the magnitude of the oscillation increases may change the rate of increase in discomfort with increasing magnitude of oscillation (Wyllie and Griffin 2007).

Biodynamic studies have found that the mechanical responses of the body are also nonlinear, with the resonance frequencies for whole-body vibration reducing as the magnitude of vibration increases. This nonlinearity has been seen with fore-and-aft, lateral, and vertical vibration of seated, standing and recumbent subjects (e.g., Fairley and Griffin 1989, Mansfield 1998, Matsumoto and Griffin 1998, Mansfield and Griffin 2000, Matsumoto and Griffin 2002a and 2002b, Matsumoto and Griffin 2005, Nawayseh and Griffin 2005, Subashi *et al.* 2006, 2009).

If the location in the body at which a vibration causes principal discomfort is distant from the location of the input (e.g., the supporting seat surface), the biodynamic nonlinearity between the input and the location of discomfort may be expected to contribute to the frequency-dependence in the rate of growth of sensation, *n*. Matsumoto and Griffin (2005) found similar nonlinearities in the discomfort and the driving-point dynamic response associated with the principal body response to vertical vibration in the range 3.15 to 8 Hz. They concluded that the nonlinearity in discomfort may be partially caused by the nonlinear dynamic response of the body and suggested the variation is sufficiently great to require consideration in methods of predicting the discomfort caused by vertical whole-body vibration. Subashi *et al.* (2009) found the magnitude of vibration had a similar effect on how vibration discomfort and apparent mass depend on the frequency of fore-and-aft and lateral whole-body vibration over the range 1.6 to 10 Hz. There were significant correlations between discomfort and the normalised apparent mass.

When predicting vibration discomfort from the frequency-weighted acceleration at the supporting seat surface it is assumed that the same frequency weighting is appropriate

at all vibration magnitudes. However, nonlinearity in the response of the human body means that equivalent comfort contours have different frequency-dependence at different magnitudes and so the ideal frequency weighting is different for low magnitudes and high magnitude vibration. This study seeks to quantify the extent of the nonlinearity when predicting discomfort using acceleration at the seat surface. For the frequencies of vibration where discomfort arises from movements of body parts that have a large influence on the apparent mass of the body (i.e., frequencies up to and around the principal resonance of the body) it might be anticipated that the dynamic force would reflect the nonlinearity in vibration discomfort and provide a more accurate prediction of vibration discomfort.

This study was designed to determine equivalent comfort contours and the frequency-dependence of the rate of growth of discomfort for both acceleration and force measured at the surface supporting the seated human body. The apparent mass of the body was determined so as to quantify the biodynamic nonlinearity and investigate the extent to which the frequency-dependence of the rate of change of discomfort could be attributed to the biodynamic nonlinearity. Assuming part of the nonlinearity in subjective responses is caused by biodynamic nonlinearity, it was hypothesised that equivalent comfort contours expressed in terms of dynamic force would show less nonlinearity than equivalent comfort contours expressed in terms of acceleration.

5.2 Method

5.2.1 Apparatus

A 1-metre stroke vertical electrohydraulic vibrator generated vertical vibration of a flat rigid seat. An accelerometer (Silicon Designs 2260-002) mounted on the lower surface of the seat measured acceleration in the direction of excitation. A force platform, Kistler 9281B, mounted on the seat measured the force at the interface between the seat (i.e., top surface of the force platform) and the subject in the vertical and fore-and-aft directions. Sinusoidal vibration was generated by a Servotest Pulsar system and acquired using an *HVLab* data acquisition and analysis system (version 1.0) to a computer.

Subjects sat on the top surface of the seat without making contact with the backrest (Figure 5.1). They rested their feet on a footrest that was attached to the vibrator table.

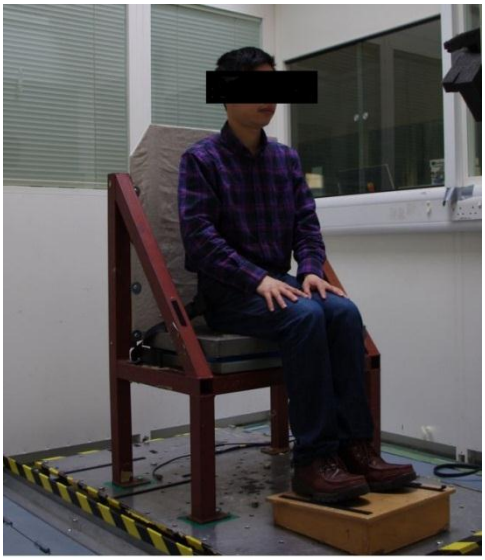

Figure 5.1 Experiment setup

The distortions of the sinusoidal acceleration waveforms were examined by fitting measured waveforms to the desired waveforms. For all sinusoidal waveforms, the difference, δ_a, between the measured and desired acceleration was calculated from:

$$\delta_a = \frac{\int (a_d(t) - a_m(t))^2 dt}{\int (a_d(t))^2 dt} \times 100\% \quad (5.2)$$

where $a_d(t)$ is the desired acceleration, and $a_m(t)$ is the measured acceleration. For the session of the experiment using low magnitude stimuli, the median difference between the measured acceleration waveform and the desired acceleration waveform (i.e., δa) was 1.7% (with a 5%-95% range from 0.43% to 5.5%). The distortions were less with the greater magnitude stimuli employed in the sessions with medium and high magnitudes (see below).

5.2.2 Subjects

Twenty male and twenty female subjects, students and staff at the University of Southampton, participated in the study. Subject characteristics are shown in Table 5.1.

Subjects were exposed to white noise at 65 dB(A) via a pair of headphones. During exposure to vibration, subjects were asked to close their eyes to prevent vision affecting their reaction to the motion.

The experiment was also designed to measure the nonlinearity in the vertical apparent mass and the fore-and-aft cross-axis apparent mass with both sinusoidal and random vibration. These biodynamic responses are reported separately (Chapter 4). The experiment was approved by the Human Experimentation Safety and Ethics Committee

of the Institute of Sound and Vibration Research at the University of Southampton. Informed consent to participate in the experiment was given by all subjects.

Table 5.1 Subjects details (median (min-max))

	Age (years)	Weight (kg)	Standing height (cm)	Sitting height (cm)
Male	26.5 (22-41)	70.5 (47.5-107)	173 (165-202)	90 (78-102)
Female	23.5 (20-30)	55.8 (45-72)	165 (149 - 183)	85.5 (80-92)

5.2.3 Experiment design

Subjects attended three sessions on three different days. In each session they were exposed to a series of sinusoidal vibrations presented in pairs: a 6-s 'reference' motion followed by a 6-s 'test' motion, with the first 1 s and last 1 s of both stimuli tapered by cosine functions. The two stimuli were separated by an interval of 1 s.

The 'reference motion' had a frequency of 4 Hz and was presented at one of three magnitudes (0.125, 0.315, or 0.8 ms^{-2} r.m.s.), with the magnitude constant within a session. The three sessions are referred to as the 'low magnitude session', 'medium magnitude session', and 'high magnitude session'. The 'test' motions were presented at each of 13 preferred one-third octave centre frequencies from 1.0 to 16 Hz. At each frequency, the test motion was presented at nine magnitudes (equi-spaced on a logarithmic scale) that varied according to the frequency of the test motion (so as to produce an approximately similar range of subjective responses at each frequency, assuming the frequency-dependence of frequency weighting W_b). The magnitudes of the test motion at 4 Hz (the frequency of the reference motion) varied from 40% of the magnitude of the reference motion to 250% of the magnitude of the reference motion (Table 5.2). In each session, subjects experienced 117 test motions in a completely randomised order over about 45 minutes.

Judgements of discomfort were obtained using the method of magnitude estimation, assuming the magnitude of discomfort caused by the reference motion was 100. For example, if a test motion was half as uncomfortable as the reference motion it should be assign a value of 50, and a test motion twice as uncomfortable as the reference motion should be assigned a value of 200. If subjects could not feel a 'test' vibration, they were asked to give it a value of 0, and their response was excluded from further analysis. Less than 2% of responses were excluded because subjects could not feel the lowest magnitude of vibration at some frequencies.

Table 5.2 Magnitudes of test motions at each frequency in the three sessions with different magnitudes of the reference motion (ms^{-2} r.m.s.)

Frequency of test motion (Hz)	Magnitude of 4-Hz reference motion (ms^{-2} r.m.s.)					
	Low magnitude (0.125 ms^{-2} r.m.s.)		Medium magnitude (0.315 ms^{-2} r.m.s.)		High magnitude (0.8 ms^{-2} r.m.s.)	
	Minimum	Maximum	Minimum	Maximum	Minimum	Maximum
1.0	0.1	0.63	0.25	1.6	0.63	4.0
1.25	0.1	0.63	0.25	1.6	0.63	4.0
1.6	0.1	0.63	0.25	1.6	0.63	4.0
2.0	0.1	0.63	0.25	1.6	0.63	4.0
2.5	0.08	0.5	0.2	1.25	0.5	3.2
3.15	0.063	0.4	0.16	1.0	0.4	2.5
4.0	0.05	0.315	0.125	0.8	0.315	2.0
5.0	0.04	0.25	0.1	0.63	0.25	1.6
6.3	0.04	0.25	0.1	0.63	0.25	1.6
8.0	0.04	0.25	0.1	0.63	0.25	1.6
10.0	0.04	0.25	0.1	0.63	0.25	1.6
12.5	0.04	0.25	0.1	0.63	0.25	1.6
16.0	0.04	0.25	0.1	0.63	0.25	1.6

5.2.4 Analysis

For each frequency of vibration and each subject, the relation between the vibration acceleration, φ, and the individual magnitude estimate of discomfort, Ψ, was determined using Stevens' Power law. Linear regression was performed at each frequency after logarithmic transformation of Equation (5.1) to:

$$\log_{10} \Psi = n.\log_{10} \varphi + \log_{10} k \tag{5.3}$$

The vertical apparent mass of each subject at each frequency was calculated by dividing the r.m.s. value of the measured force in vertical direction (after mass cancellation) by the r.m.s. value of the measured acceleration in the vertical direction:

$$AM(f) = F_{\text{rms}}(f) / A_{\text{rms}}(f) \tag{5.4}$$

where $AM(f)$ is the apparent mass at frequency f, and $F_{\text{rms}}(f)$ and $A_{\text{rms}}(f)$ are the r.m.s. values of the force and acceleration respectively. Mass cancellation was performed by subtracting the product of the mass of the top plate of the force platform and the vertical seat acceleration time history from the measured vertical force time history.

Statistical analysis was performed using non-parametric statistics. The Friedman two-way analysis of variance and the Wilcoxon matched-pairs signed ranks test were used to investigate differences between related samples and the Mann-Whitney U-test was

to investigate differences between independent samples. Associations between variables were investigated with Spearman's rank correlation. The *p*-values shown are uncorrected for multiple comparisons.

5.3 Results

5.3.1 Rate of growth of discomfort with increasing acceleration

The rate of growth of discomfort, *n*, and the constant, *k,* did not differ between male and female subjects at any of the 13 frequencies with any of the three magnitudes of the reference motion ($p>0.05$, Mann-Whitney U-test). The median exponent, *n*, and the constant, *k* over all 40 subjects are shown in Table 5.3. The medians and inter-quarter range of the rates of growth of discomfort, *n*, from all three magnitudes of the reference vibration are shown in Figure 5.2. With all three magnitudes of the reference vibration, the exponent, *n*, was highly dependent on the frequency of vibration ($p<0.0001$; Friedman). With all three magnitudes of the reference, at any frequency in the range 1 to 5 Hz the exponent was greater than at any frequency in the range 6.3 to 16 Hz ($p<0.05$, Wilcoxon). At two frequencies, the exponent depended on the magnitude of the reference vibration ($p<0.003$ at 1.0 and 1.25, Friedman).

5.3.2 Rate of growth of discomfort with increasing force

For each vibration frequency and each subject, the relation between the measured force in the vertical direction, φ, and the individual sensation magnitude, Ψ, was also determined using Stevens' Power law. The rate of growth of discomfort, *n,* and the constant *k*, did not differ between males and females at any of the 13 frequencies with any of the three magnitudes of the reference motion ($p>0.05$, Mann-Whitney U-test). The median exponent, *n*, and the constant, *k,* over all 40 subjects are shown in Table 5.4. The medians and inter-quarter range of the rates of growth of discomfort with increasing force are shown in Figure 5.3. With all three magnitudes of the reference motion, the rate of growth of discomfort, *n*, was highly dependent on the frequency of vibration ($p< 0.0001$; Friedman). Similar to acceleration, at two frequencies, the exponent depended on the magnitude of the reference vibration ($p<0.003$ at 1.0 and 1.25, Friedman).

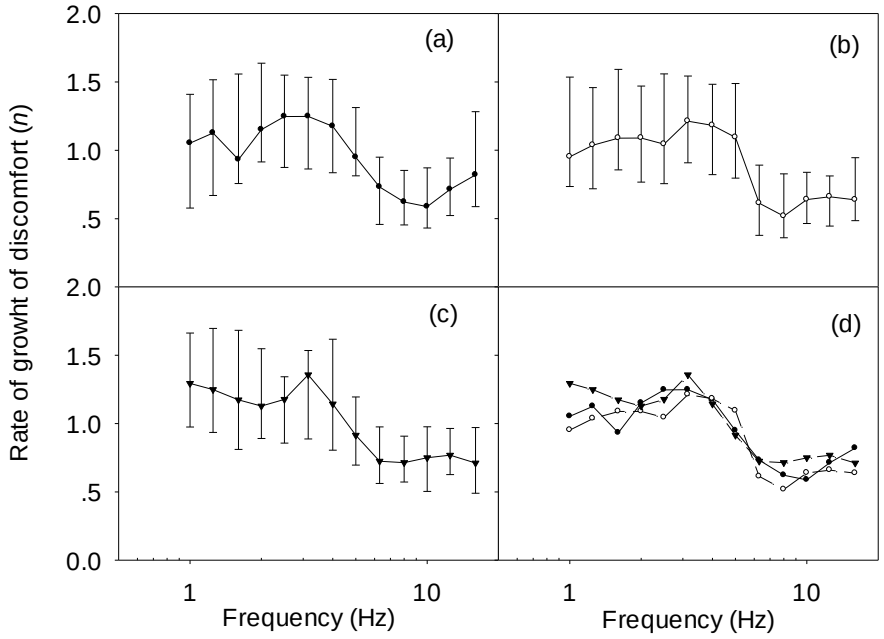

Figure 5.2 Median and inter-quartile range of rate of growth of discomfort, *n*, for vertical vibration acceleration with three magnitudes of 4-Hz reference vibration. (a) Low magnitude session; (b) Medium magnitude session; (c) High magnitude session; (d) Median data for all three sessions, ●: low magnitude (0.125 ms^{-2} r.m.s. 4-Hz reference); ○: medium magnitude (0.315 ms^{-2} r.m.s. 4-Hz reference); ▼: high magnitude (0.8 ms^{-2} r.m.s. 4-Hz reference).

Table 5.3 Median exponent, *n*, and constant, *k*, for acceleration in each session (Low: 0.125 ms^{-2} r.m.s. 4-Hz reference; Medium: 0.315 ms^{-2} r.m.s. 4-Hz reference; High: 0.8 ms^{-2} r.m.s. 4-Hz reference).

Frequency (Hz)	Exponent (*n*)			Constant (*k*)		
	Low	Medium	High	Low	Medium	High
1	1.05	0.95	1.29	370.58	194.52	65.27
1.25	1.13	1.04	1.25	374.09	177.97	59.62
1.6	0.93	1.09	1.17	433.36	172.90	64.73
2	1.15	1.09	1.13	460.42	167.21	71.06
2.5	1.25	1.04	1.18	561.30	211.23	80.77
3.15	1.25	1.21	1.36	655.09	291.44	96.44
4	1.18	1.18	1.14	763.12	363.77	135.61
5	0.95	1.09	0.91	892.19	542.23	192.97
6.3	0.73	0.61	0.73	783.35	364.48	179.24
8	0.62	0.52	0.71	604.26	330.94	169.86
10	0.59	0.64	0.75	573.23	368.15	164.76
12.5	0.71	0.66	0.77	693.75	333.37	163.14
16	0.82	0.64	0.71	809.73	358.39	159.35

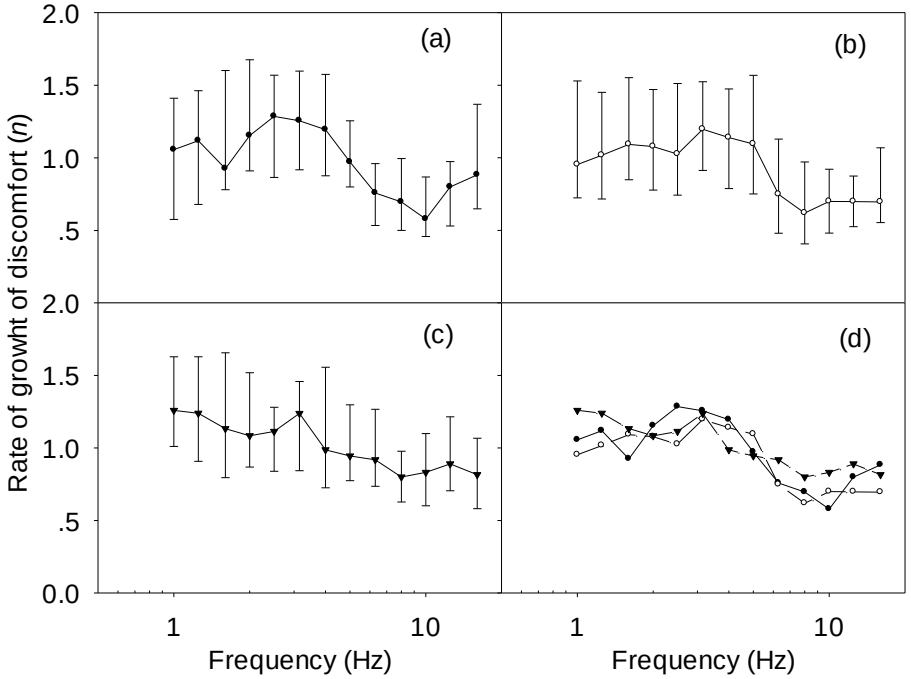

Figure 5.3 Median and inter-quartile range rate of growth of discomfort, *n*, for vertical vibration force with three magnitudes of 4-Hz reference vibration. (a) Low magnitude session; (b) Medium magnitude session; (c) High magnitude session; (d) Median data for all three sessions, ●: low magnitude; ○: medium magnitude; ▼: high magnitude.

Table 5.4 Median exponent, *n,* and constant, *k*, for force in each session (Low: 0.125 ms^{-2} r.m.s. 4-Hz reference; Medium: 0.315 ms^{-2} r.m.s. 4-Hz reference; High: 0.8 ms^{-2} r.m.s. 4-Hz reference).

Frequency (Hz)	Exponent (*n*)			Constant (*k*)		
	Low	Medium	High	Low	Medium	High
1	1.06	0.95	1.26	6.53	3.55	0.47
1.25	1.12	1.02	1.24	3.68	2.34	0.47
1.6	0.93	1.09	1.13	6.24	1.73	0.60
2	1.15	1.08	1.08	4.39	2.16	1.04
2.5	1.29	1.03	1.11	3.11	3.04	0.77
3.15	1.26	1.20	1.24	4.66	1.87	0.55
4	1.20	1.14	0.99	6.24	2.73	1.88
5	0.97	1.10	0.94	11.66	5.09	3.38
6.3	0.76	0.75	0.92	31.98	20.96	4.44
8	0.70	0.62	0.80	34.67	30.01	8.70
10	0.58	0.70	0.83	58.99	29.89	10.36
12.5	0.80	0.70	0.89	50.00	28.98	9.68
16	0.88	0.70	0.82	37.85	33.25	12.63

5.3.3 Comparison of the rate of growth of discomfort between force and acceleration

The rate of growth of discomfort, *n*, differed between force and acceleration at most frequencies with all three magnitudes of the reference motion (Table 5.5 and Figure 5.4). At frequencies less than 5 Hz, the exponent for force was generally less than the exponent for acceleration, whereas at frequencies greater than 5 Hz, the exponent for force was generally greater than the exponent for acceleration. Although the differences were small they were statistically significant at most frequencies. With the greatest magnitude of the reference motion, the difference was highly significant at all frequencies except 5 Hz (p<0.001; Wilcoxon).

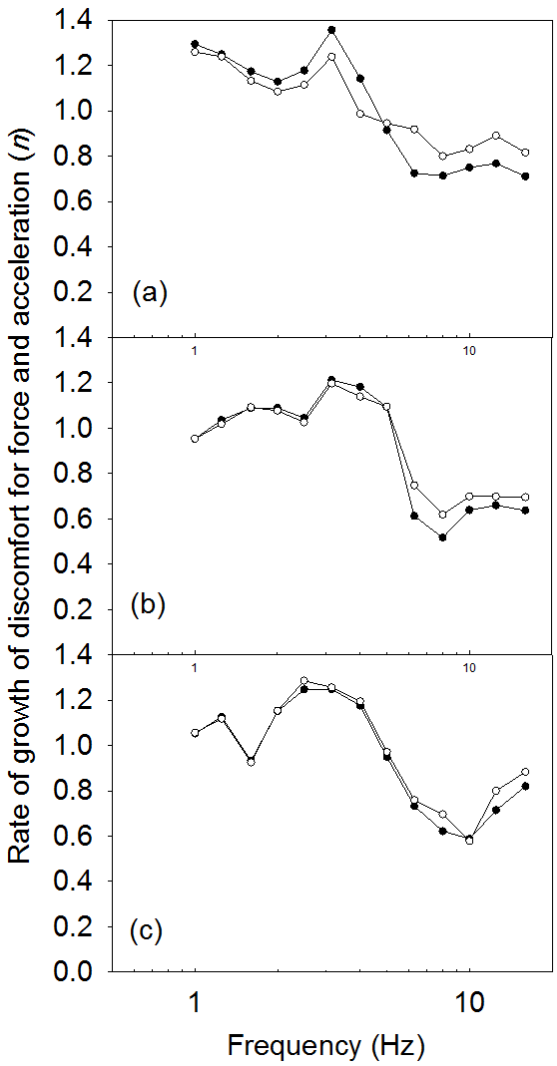

Figure 5. 4 Comparison of the rates of growth of discomfort for force and acceleration obtained with three magnitudes of 4-Hz reference vibration. Median data: ●: acceleration; ○: force. (a): high magnitude (0.8 ms^{-2} r.m.s.); (b) medium magnitude (0.315 ms^{-2} r.m.s.); (c) low magnitude (0.125 ms^{-2} r.m.s.).

Table 5.5 Statistical significance of differences in the rate of growth of discomfort, *n*, between force and acceleration (*p* value; Wilcoxon matched-pairs signed ranks test). (Low: 0.125 ms^{-2} r.m.s. 4-Hz reference; Medium: 0.315 ms^{-2} r.m.s. 4-Hz reference; High: 0.8 ms^{-2} r.m.s. 4-Hz reference).

	Frequency (Hz)												
Magnitude	1.0	1.25	1.6	2.0	2.5	3.15	4.0	5.0	6.3	8.0	10	12.5	16
Low	-	-	-	**	*	-	-	-	**	***	-	***	***
Medium	***	*	-	-	-	***	***	-	***	***	**	***	***
High	***	***	***	***	***	***	***	*	***	***	***	***	***

***p<0.0005, **p<0.005, *p<0.05, - not significant

5.3.4 Equivalent comfort contours for acceleration

Equivalent comfort contours for acceleration were determined for each subject by calculating the vibration acceleration, φ, corresponding to nine subjective magnitudes, ψ, from 40 to 250 at each vibration frequency (from 1 to 16 Hz) using equation (5.1). The equivalent comfort contours illustrate the vibration magnitudes required to produce the same strength of sensation across the frequency range. With each magnitude of the reference motion, the acceleration equivalent comfort contours for all sensation magnitudes varied with frequency (p<0.001, Friedman; Figure 5.5).

The acceleration equivalent comfort contours are roughly constant from 1 to 2 Hz and then reduce as the frequency increases. As the magnitude of vibration increased, the frequency at which the acceleration produced most discomfort decreased. The individual, median, and inter-quartile ranges of the equivalent comfort contours for acceleration (for Ψ=100) are shown in Appendix B.1.

Some of the contours in Figure 5.5 are lower than the lowest vibration magnitudes presented in a session of the study, especially for the lowest magnitudes at frequencies from 6.3 to 12.5 Hz. However, the lowest 'extrapolated contours' with the 0.8 ms^{-2} r.m.s. reference are within the range of magnitudes studied with the 0.315 ms^{-2} r.m.s. reference. Similarly, the lowest 'extrapolated contours' with the 0.315 ms^{-2} r.m.s. reference are within the range of magnitudes studied with the 0.125 ms^{-2} r.m.s. reference. Overlapping these contours shows reasonable agreement, suggesting Stevens' power law can be used to make moderate extrapolations, at least at these higher magnitudes.

5.3.5 Equivalent comfort contours for force

Equivalent comfort contours for vertical force were determined for each subject by calculating the force, φ, corresponding to the same nine subjective magnitudes, ψ, from 40 to 250 at each vibration frequency (1 to 16 Hz) using equation (5.1). With all three magnitudes of the reference motion, the force equivalent comfort contours for all sensation magnitudes varied with frequency (p<0.0001, Friedman; Figure 6). Again, parts of some contours, especially for the lowest magnitudes at frequencies from 6.3 to 12.5 Hz, are extrapolated to forces below the range of forces the subjects experienced.

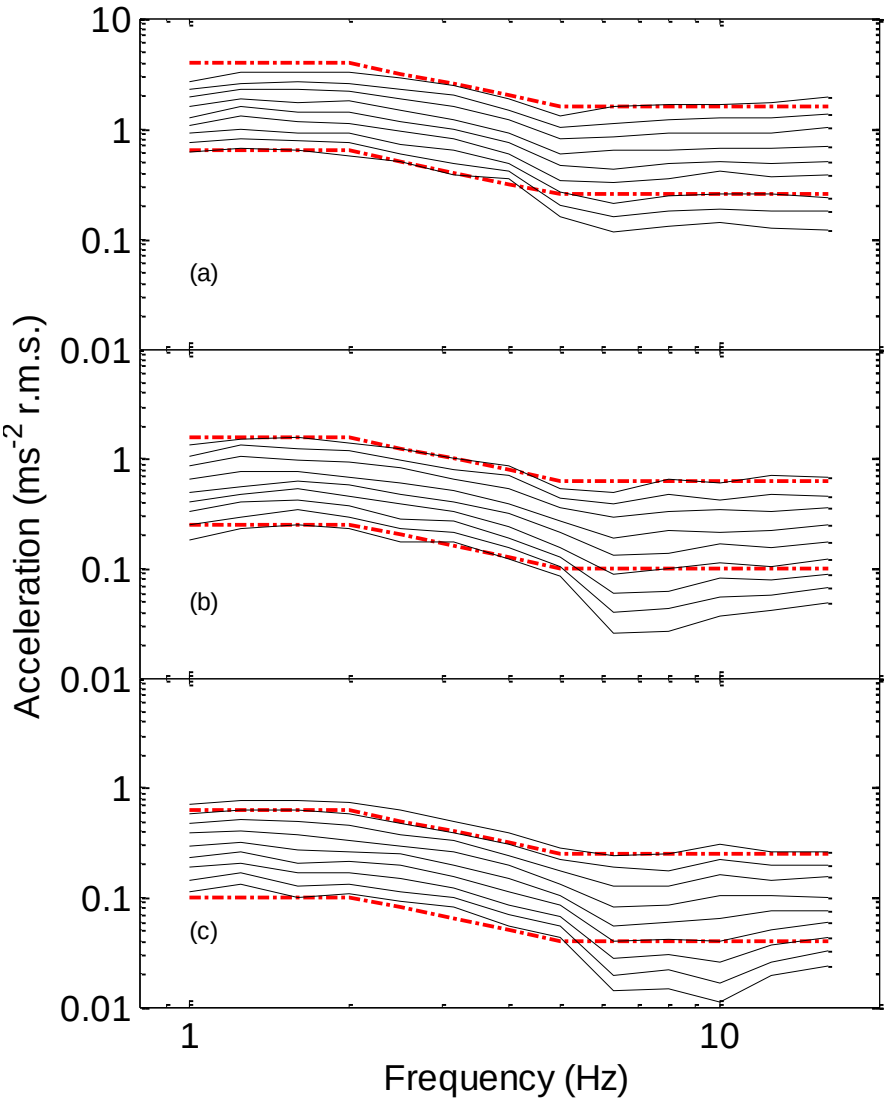

Figure 5.5 Median acceleration equivalent comfort contours. Contours are shown for subjective magnitudes, ψ, of 40, 50, 63, 80, 100 125, 160, 200 and 250 with three magnitudes of 4-Hz reference vibration. (a): high magnitude (0.8 ms^{-2} r.m.s.); (b) medium magnitude (0.315 ms^{-2} r.m.s.); (c) low magnitude (0.125 ms^{-2} r.m.s.). The dot lines show the ranges of magnitudes of the test motions in each session.

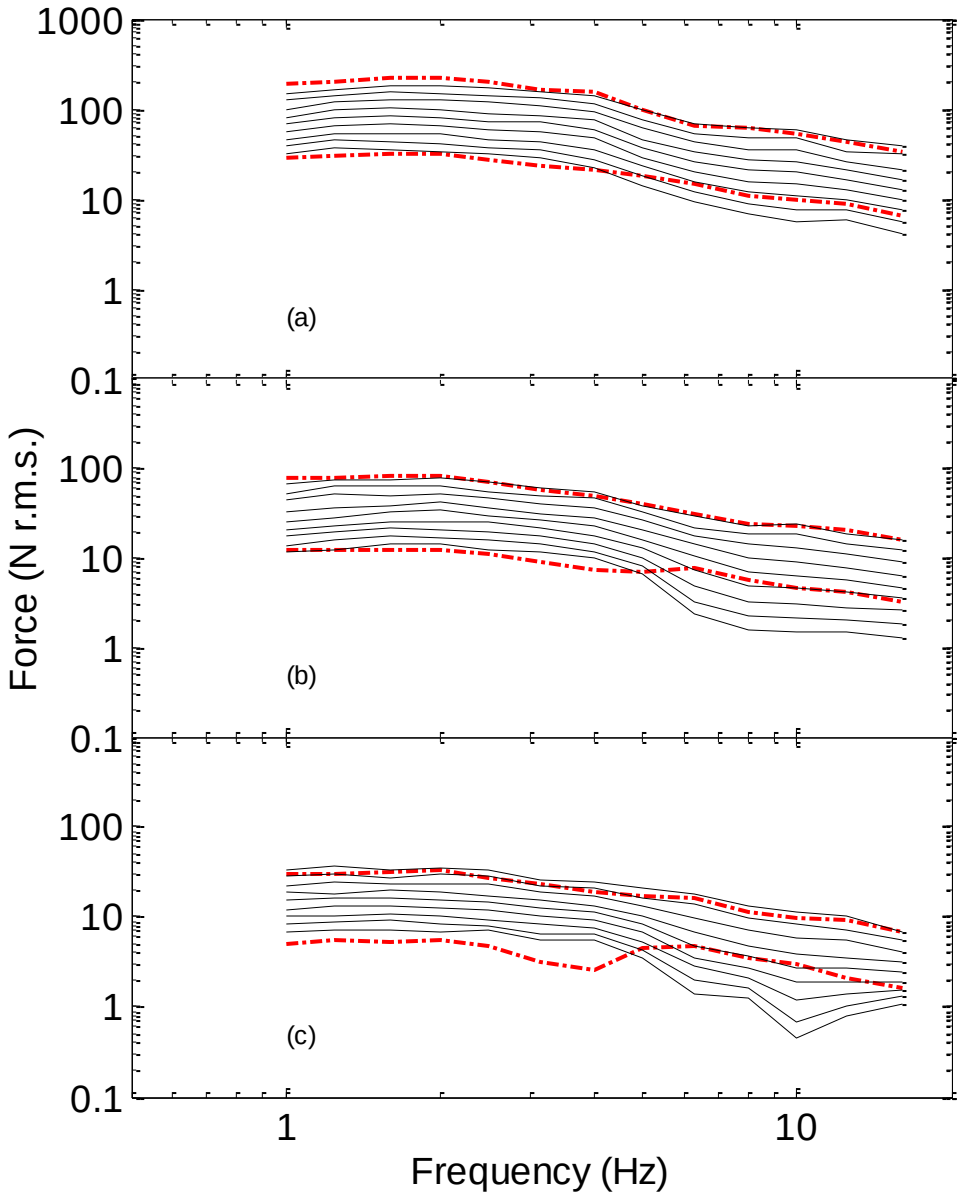

Figure 5.6 Median force equivalent comfort contours. Contours are shown for subjective magnitudes, ψ, of 40, 50, 63, 80, 100 125, 160, 200 and 250 with three magnitudes of 4-Hz reference vibration. (a) 0.8 ms^{-2} r.m.s. reference; (b) 0.315 ms^{-2} r.m.s. reference; (c) 0.125 ms^{-2} r.m.s. reference. The dot lines show the maximum and minimum force at each frequency (median values over 40 subjects).

Similar to the acceleration equivalent comfort contours, the force equivalent comfort contours are roughly constant at low frequencies and reduce as the frequency increases. Subjects were most sensitive to force at 16 Hz, except for a few of the lowest magnitudes of vibration. Comparing Figures 5.5 and 5.6 it can be seen that the force equivalent comfort contours are more parallel than the acceleration equivalent comfort contours, suggesting the force equivalent comfort contours are more 'linear'.

The individual, median, and inter-quartile ranges of the equivalent comfort contours for force (for Ψ=100) are shown in Appendix B.2.

5.3.6 Location of discomfort

Most discomfort was generally felt in either the buttocks or the upper body (Figure 5. 7, Table 5.6). As the magnitude of vibration increased, the location of most discomfort moved from the lower-body to the upper-body. At most frequencies in the low magnitude session, there were some subjects who said they could not feel where the discomfort was located. In the middle frequency range, most subjects felt the discomfort in the buttocks or the upper-body during medium and high magnitude vibration.

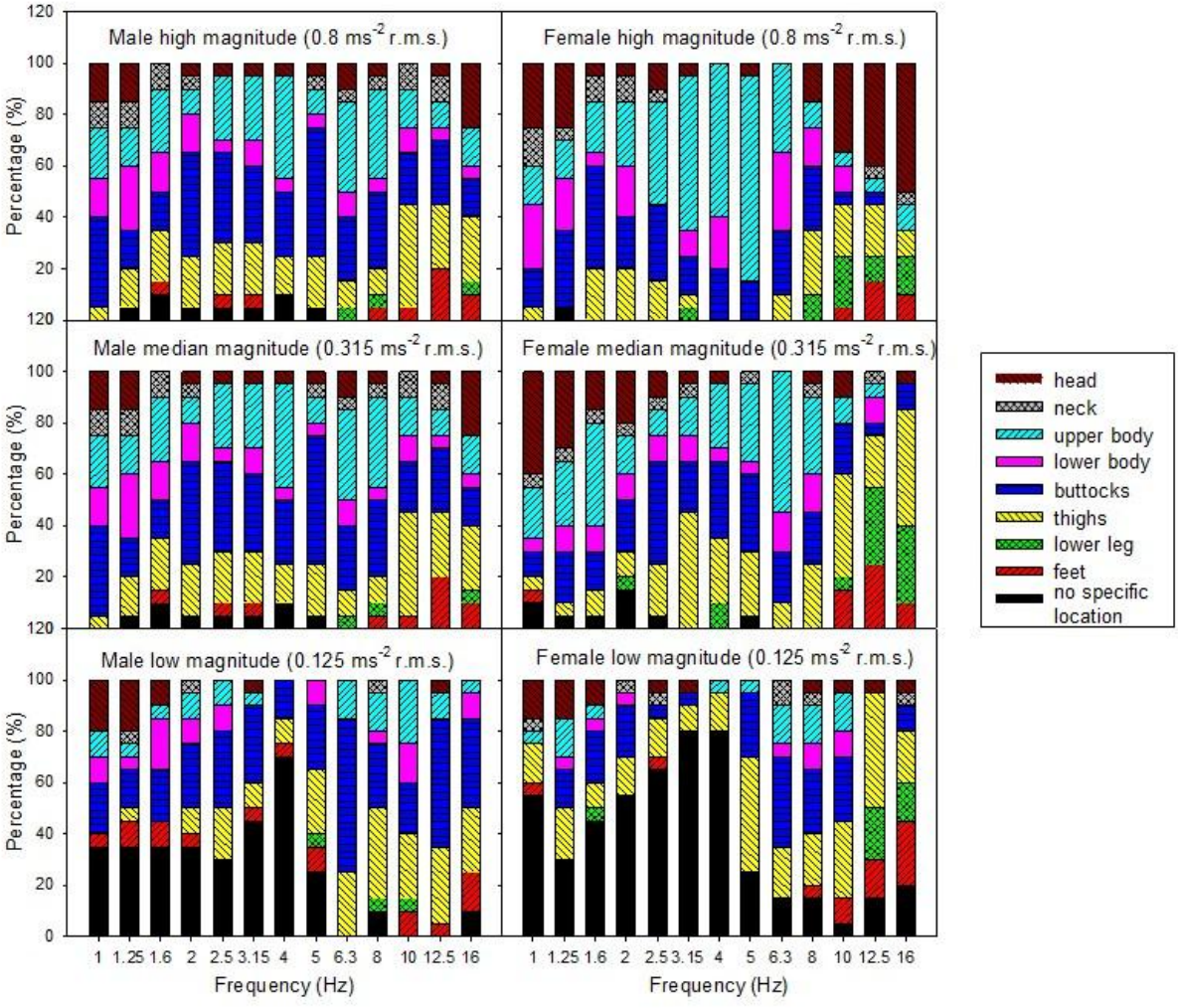

Figure 5.7 Locations of discomfort arising from exposure to vertical vibration at three different vibration magnitudes for both male and female subjects.

Table 5.6 Locations in the body where most subjects felt discomfort. (Low: 0.125 ms^{-2} r.m.s. 4-Hz reference; Medium: 0.315 ms^{-2} r.m.s. 4-Hz reference; High: 0.8 ms^{-2} r.m.s. 4-Hz reference).

Frequency (Hz)		1.0	1.25	1.6	2.0	2.5	3.15	4.0	5.0	6.3	8.0	10	12.5	16
Low	Males	1	1	1	1	1	1	1	1	5	4	4	5	5
	Females	1	1	1	1	1	1	1	4	5	5	4	4	2
Medium	Males	5	6	7	5	5	5	7	5	7	7	4	4	4
	Females	9	9	7	5	5	4	5	5	7	7	4	3	4
High	Males	5	6	7	5	5	5	7	5	7	7	4	4	4
	Females	6	5	5	7	7	7	7	7	7	4	9	9	9

1: no specific location; 2: feet; 3: lower legs; 4: thighs; 5: buttocks; 6: lower body; 7: upper body; 8: neck; 9: head

5.3.7 Association between relative discomfort and normalised apparent mass

The association between subjective responses and biodynamic responses was investigated by calculating correlations between the ratio of apparent masses at two frequencies and the ratio of the subjective responses between the same two frequencies. The ratios were calculated for all possible pairs of frequencies for all subjects when exposed to the middle magnitude of vibration in each of the three sessions.

In the session with the greatest vibration magnitudes, there were no statistically significant negative correlations but distinct patterns of statistically significant positive correlations between the relative apparent mass and the relative subjective response (Table 5.7). For example, the ratio of the apparent mass at 4 Hz to the apparent mass at higher frequencies (6.3 Hz to 16 Hz) was positively correlated with the ratio of the subjective response at 4 Hz to the subjective response at these higher frequencies ($p<0.05$; Spearman). This indicates that subjects having a proportionately greater apparent mass at 4 Hz relative to their apparent mass at the higher frequencies were likely to be relatively more uncomfortable at 4 Hz. Similarly, the ratio of the apparent mass at 6.3 Hz to the apparent mass at all lower frequencies (1.0 to 5.0 Hz) was positively correlated with the ratio of the subjective response at 6.3 Hz to the subjective response at all lower frequencies ($p<0.05$; Spearman). This indicates that subjects having a proportionately greater apparent mass at 6.3 Hz relative to their apparent mass at lower frequencies were likely to be relatively more uncomfortable at 6.3 Hz. It can also be inferred that subjects having a proportionately greater apparent mass at 16

Hz relative to their apparent mass at frequencies less than 5 Hz were likely to be relatively more uncomfortable at 16 Hz.

In the sessions with medium vibration magnitudes the trends were similar, but the correlations with 4 Hz were only statistically significant at 8, 10, and 16 Hz, the correlations with 6.3 Hz were only significant at 5 and 8 Hz, and the correlations with 16 Hz were significant at 3.15, 4, 5, and 12.5 Hz. In the session with the lowest vibration magnitudes the correlations with 4 Hz were only statistically significant at 10, 12.5 and 16 Hz, the correlations with 6.3 Hz were only significant at 1.0 Hz, and the correlations with 16 Hz were only significant at 4 and 5 Hz.

5.4 Discussion

5.4.1 Vibration discomfort for acceleration

5.4.1.1 Effect of acceleration magnitude

The rate of growth for vertical vibration (i.e., the exponent in Stevens' power law) has been investigated previously for acceleration (Figure 5.8), but not for dynamic force. Over the preferred one-third octave centre frequencies between 2 and 315 Hz Morioka and Griffin (2006a) found the greatest rate of growth of discomfort for vertical vibration around the principal resonance frequency of the body, broadly consistent with this study. Similar values of the exponent were found at frequencies in the range 6.3 to 16 Hz, but much greater values at lower frequencies in the present study, possibly because low frequency discomfort in the earlier study may have been influenced by relative motion between the seat and the stationary feet whereas there was no such relative motion in the present study (i.e., the feet and the seat moved with the same magnitude). Over the range of 4 to 63 Hz at magnitudes from 0.04 to 0.4 ms^{-2} r.m.s., Howarth and Griffin (1988) found no significant variation in the exponent with the frequency of vibration, unlike the present study with higher magnitudes of vibration where there were significant differences over the range 4 to 16 Hz.

Because the rate of growth of discomfort varied with the frequency of vibration, the shapes of the equivalent comfort contours varied with the magnitude of the vibration. A similar trend was observed with all three magnitudes of the reference vibration and for both male and female subjects, providing further evidence of nonlinearity in acceleration equivalent comfort contours. Shoenberger and Harris (1971) concluded that as the magnitude of a reference vibration increased, the frequency corresponding to the minimum of each acceleration contour decreased. Over the range 2 to 315 Hz,

Table 5.7 Spearman correlation coefficients between the ratio of apparent mass at two frequencies and the ratio of the subjective responses between the same two frequencies (high magnitude session: 0.8 ms^{-2} r.m.s. 4-Hz reference).

Frequency (Hz)	1	1.25	1.6	2	2.5	3.15	4	5	6.3	8	10	12.5	16
1	--	-0.04	-0.02	-0.07	0.03	0.22	0.15	-0.02	0.32*	0.13	-0.05	0.23	0.30
1.25		--	0.15	0.06	-0.11	0.22	0.22	-0.07	0.55***	0.23	-0.07	0.21	0.35*
1.6			--	-0.13	-0.05	0.15	0.30	-0.03	0.51***	0.30	0.15	0.14	0.31
2				--	-0.17	0.06	0.12	0.22	0.48***	0.49**	0.33*	0.21	0.44**
2.5					--	-0.01	0.20	-0.12	0.44**	0.43**	0.22	0.14	0.40*
3.15						--	0.17	0.05	0.51***	0.49**	0.30	0.36*	0.59***
4							--	0.22	0.71***	0.60***	0.38*	0.32*	0.58***
5								--	0.46**	0.18	-0.02	0.12	0.19
6.3									--	0.13	0.17	0.10	0.09
8										--	-0.14	-0.16	-0.09
10											--	-0.07	0.11
12.5												--	-0.07
16													--

*: $p<0.05$; **: $p<0.01$; ***: $p<0.001$

Morioka and Griffin (2006a) found equivalent comfort contours similar to absolute perception thresholds with low magnitudes of acceleration (i.e., similar acceleration over the frequency range) but, with increasing sensation magnitudes, the contours changed to approximately similar velocity (i.e., acceleration increasing in proportion to frequency) over the frequency range 16 to 315 Hz.

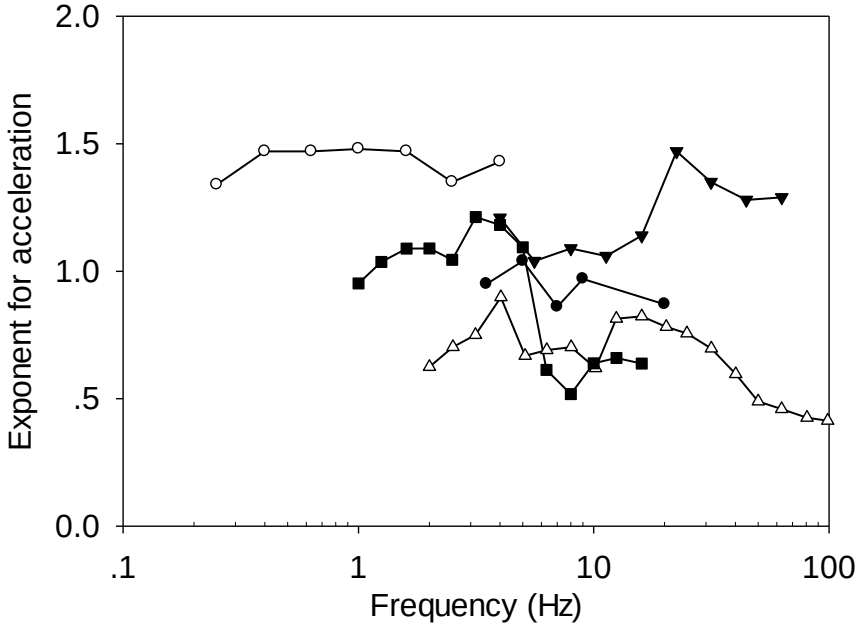

Figure 5.8 Comparison of the exponent, *n*, from Stevens' power law for acceleration with previous studies (○: Shoenberger and Harris (1971); ●: Shoenberger (1975); ▼: Howarth and Griffin (1988); ∆: Morioka and Griffin (2006a); ■: Present study (medium magnitude session)).

5.4.1.2 Effect of frequency

The median equivalent comfort contours (obtained for Ψ=100 with each of the three magnitudes of the reference vibration) are compared in Figure 5.9. As the magnitude of the reference vibration increased, the frequency of acceleration producing greatest discomfort decreased. However, with all three magnitudes of vibration, greater discomfort was caused by acceleration at 5 Hz than acceleration at 4 Hz.

Greater sensitivity to vertical vibration acceleration at 5 Hz than at lower frequencies has been reported previously. This is apparent in contours equivalent to 0.75 ms^{-2} r.m.s. at 10 Hz obtained with 10 males at the nine preferred one-third octave centre frequencies from 3.15 to 20 Hz (Griffin 1976), in contours equivalent to 0.8 ms^{-2} r.m.s. at 10 Hz from 18 males and 18 females at preferred third-octave centre frequencies

from 1 to 100 Hz (Griffin et al. 1982), in contours equivalent to 0.25 and 0.75 ms^{-2} r.m.s. with 20 males and 20 females over the 11 preferred one-third octave centre frequencies from 0.5 to 5.0 Hz (Corbridge and Griffin 1986), and in contours equivalent to 0.5 ms^{-2} r.m.s. 20 Hz vibration with 12 males over the 23 preferred one-third octave centre frequencies from 2 to 315 Hz (Morioka and Griffin 2006a).

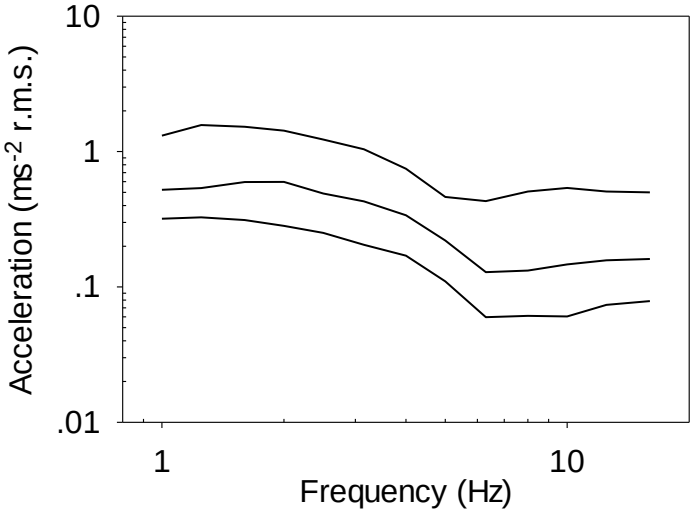

Figure 5.9 Median equivalent comfort contours obtained for Ψ=100 with the three magnitudes of reference vibration

The median acceleration equivalent comfort contours (for Ψ=100) from the three sessions with the three different magnitudes of the reference vibration are compared with the findings of previous studies in Figure 5.10. With low frequency vibration, the equivalent comfort contours from the present study show similarities with the contours of Corbridge and Griffin (1986), where subjects also had no relative motion between the feet and the seat. The equivalent comfort contours from the present study also show close similarity to the contours of Griffin (1976) and Griffin *et al.* (1982) at frequencies greater than 3.15 Hz and Morioka and Griffin (2006a) at frequencies greater than about 5 Hz. The subjects participating in these three studies had stationary feet and so relative motion between the seat and their feet may be expected to have increased subject discomfort at low frequencies (see Jang and Griffin 1999, 2000).

The realisable forms of the W_b and W_k frequency weightings were inverted and normalised so that the accelerations at 4 Hz were the same as the reference vibration in each session (i.e., either 0.125, 0.315, or 0.8 ms^{-2} r.m.s.). The median equivalent comfort contours equivalent to the reference vibration (i.e., ψ = 100) from each session

were overlaid so that they could be compared with the inverted frequency weightings (Figure 5.11). With all three magnitudes of vibration, the W_b and W_k frequency weightings are broadly similar to the equivalent comfort contour at frequencies from 1 to 4 Hz. The frequency weightings tend to underestimate discomfort from 4 to 16 Hz at all vibration magnitudes, but especially with lower magnitudes of vibration.

Other studies also have questioned the applicability of currently standardised frequency weightings for the evaluation of low magnitude vibration (e.g., Morioka and Griffin 2006b).

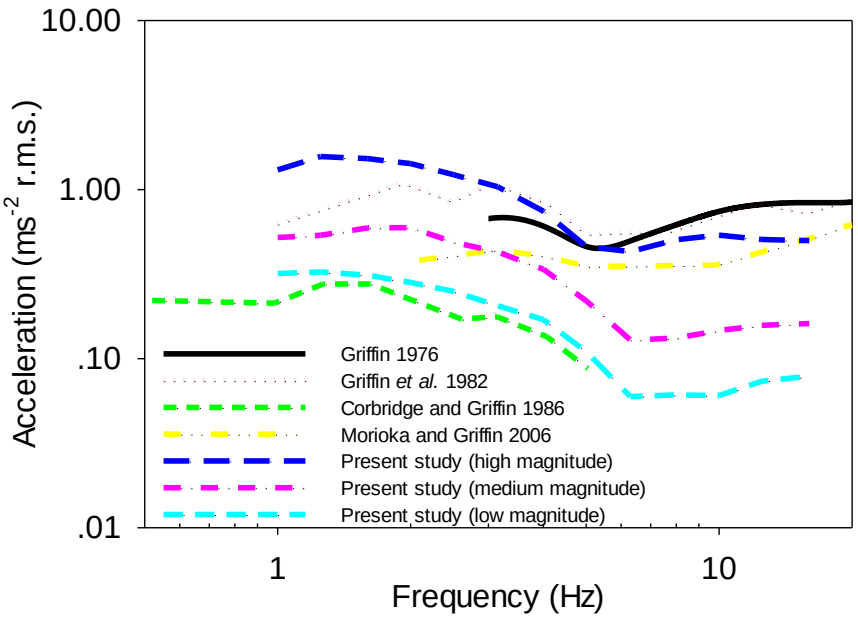

Figure 5.10 Comparison of equivalent comfort contours from present study with previous studies.

5.4.2 Vibration discomfort for force

Similar to the equivalent comfort contours for acceleration, nonlinearity was also evident in the force equivalent comfort contours, although mostly with the lower magnitudes of vibration. The nonlinearity is less evident in the force contours in Figure 5.6 than in the acceleration contours in Figure 5.5, especially with greater magnitudes of vibration.

The dynamic force required to cause any degree of discomfort was almost constant at frequencies less than about 5 Hz, but progressively decreased at frequencies greater than 5 Hz (Figure 5.6), consistent with the findings of Mansfield and Maeda (2005). It seems that less vertical force is required to cause discomfort as the frequency of

vibration increases above the principal resonance in the vertical apparent mass of the seated human body around 5 Hz. In this study, greatest sensitivity to vertical dynamic force occurred at the highest frequency studied (i.e., 16 Hz). The head is the location where most discomfort was felt by seated subjects exposed to 16-Hz vertical vibration (Figure 5.7, and Whitham and Griffin 1978). Movement of the relatively low mass of the head requires less dynamic force than movement of the greater masses lower in the body that are responsible for discomfort at lower frequencies.

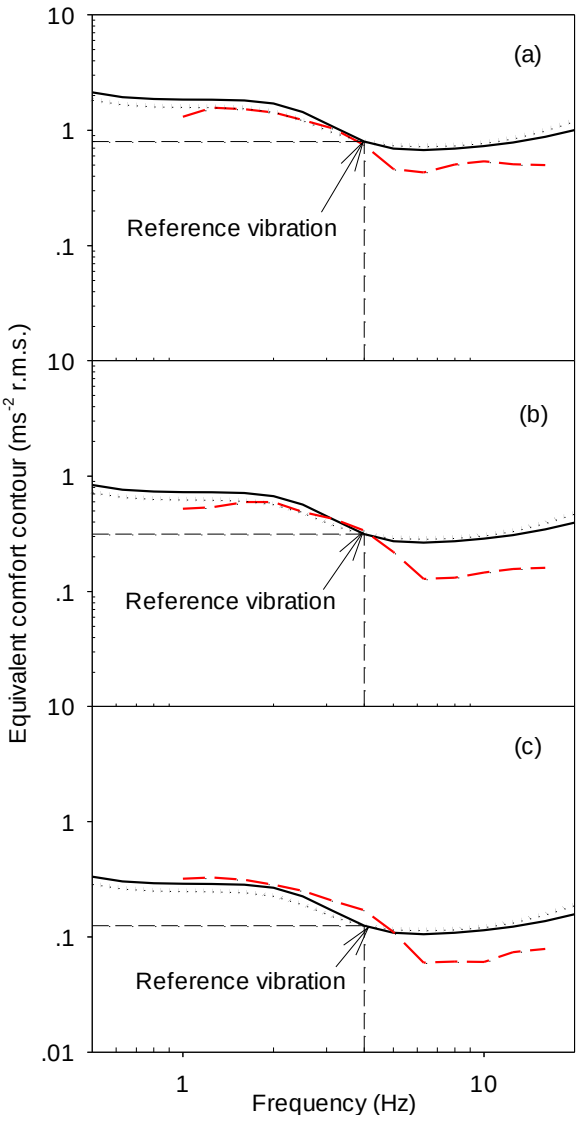

Figure 5.11 Comparison of the median equivalent comfort contour (φ=100) with the inverted and normalised frequency weighting W_b and W_k (– –: equivalent comfort contour; ——: inverted and normalised frequency weighting W_b; ••••: inverted and normalised frequency weighting W_k). (a) 0.8 ms^{-2} r.m.s. reference; (b) 0.315 ms^{-2} r.m.s. reference; (c) 0.125 ms^{-2} r.m.s. reference.

Current standards offer a six-point scale of discomfort (from 'not uncomfortable' to 'extremely uncomfortable') associated with various magnitudes of frequency-weighted acceleration (BS 6841, 1987; ISO 2631-1, 1997). Obviously, this scale should not be converted to a scale of force without recognising that forces are dependent on subject apparent mass, and therefore subject weight. Although force has some advantages over acceleration (e.g., less nonlinearity in the equivalent comfort contours) it cannot be used directly to predict discomfort without understanding the relation between subject mass and vibration discomfort. A doubling of dynamic force may approximately double vibration discomfort if it is associated with a doubling of acceleration, but probably not if it is associated with a doubling of subject mass.

5.4.3 Gender

The absence of significant differences in the acceleration comfort contours for males and females in the present study is reasonably consistent with the findings of previous studies. Similar contours were obtained from 18 male and 18 female subjects at one-third octave centre frequencies over the range 1 to 100 Hz (Griffin et al. 1982). With 20 males and 20 females providing contours equivalent to 0.25 and 0.75 ms^{-2} r.m.s. over the 11 preferred one-third octave centre frequencies from 0.5 to 5.0 Hz, Corbridge and Griffin (1986) found females relatively more sensitive at 3.15, 4.0 and 5.0 Hz with a 0.75 ms^{-2} r.m.s. 2-Hz reference motion and more sensitive at 5.0 Hz with a 0.25 ms^{-2} r.m.s. 2-Hz reference motion.

The male subjects in the present study were significantly heavier than the female subjects (p<0.0005, Mann-Whitney U-test), so there were greater dynamic forces with the males, but these greater forces also occurred with the reference frequency, so were 'normalised'. Greater forces in heavier subjects might reasonably be expected to result in a greater risk of injury, but it is not clear whether they will also produce greater discomfort. The present study did not obtain absolute judgements of discomfort, merely judgements of discomfort relative to that caused by the reference frequency. The similarity in the equivalent comfort contours of the males and females is consistent with a similarity in the normalised apparent masses of these subjects (i.e., apparent mass divided by subject weight) as reported in Chapter 4. Other studies have also found similar vertical apparent masses for males and females after normalisation (e.g., Fairley and Griffin, 1989, Toward and Griffin, 2011).

There were no significant differences in the rates of growth of discomfort, n, or the constant k, in Steven's Power law between males and females, so gender did not influence the shapes of the force equivalent comfort contours.

5.4.4 Frequency weightings

The acceleration frequency weightings in current standards assume that the same frequency-dependence is appropriate at all vibration magnitudes. In fact, the nonlinear response of human body means that equivalent comfort contours have a different frequency-dependence at different magnitudes and so the frequency weightings should differ at low and high vibration magnitudes. The equivalent comfort contours for force are less dependent on vibration magnitude, consistent with the biodynamic nonlinearities of the body (i.e., reductions in the resonance frequency with increasing vibration magnitude) contributing to the nonlinearity in the acceleration equivalent comfort contours. However, the nonlinearity evident in different rates of increase of discomfort with increasing vibration magnitude may also be due to differing sensitivity to changes in vibration magnitude in different parts of the body. Irrespective of the absolute threshold for perceiving vibration, the discomfort increases at a rate that depends on which part of the body produces the greatest sensation, which is dependent on the frequency of excitation and the magnitude of excitation. It seems likely that people find the vibration of some parts of their body more uncomfortable (or more unusual, or more concerning) than the vibration of other parts of their body and that the rate of growth of discomfort is greater when vibration excites these 'more sensitive' parts.

Consistent with various previous studies, the results show greater discomfort with acceleration at 5 Hz than acceleration at 4 Hz, which is also consistent with the use of frequency weighting W_b for predicting vibration discomfort in preference to the use of frequency weighting W_k (see BS 6841:1987 and ISO 2631-1). This difference in sensitivity between 4 Hz and 5 Hz is relatively large (i.e., 65% with the low magnitude vibration and 62% with the high magnitude vibration used in this study) and occurs at a frequency where seats often have resonances. The use of an inappropriate frequency weighting will prevent the optimisation of seat transmissibility.

The equivalent comfort contours for acceleration and force developed from this study can be constructed from the *n* and *k* values provided in Tables 5.3 and 5.4 and used to develop frequency weightings if required.

5.4.5 Association between subjective and biodynamic response

Associations between judgements of vibration discomfort and the apparent mass of the body have been found when investigating the nonlinearity of the body at low frequencies. Varying the magnitudes of whole-body vertical sinusoidal vibration and

mechanical shocks, it was found that with increasing magnitude of excitation both the apparent mass normalised to 5 Hz and the discomfort normalised to 5 Hz increased at frequencies less than about 5 Hz (Matsumoto and Griffin 2005). In a linear system there would be no change in either the normalised discomfort or the normalised apparent mass when the magnitude of the excitation changes. This association between subjective and objective measures suggested the nonlinearity in the subjective response might be due to the nonlinearity in the apparent mass. A similar study investigated the relation between vibration discomfort and the apparent mass of the human body (both normalised at 4 Hz) during fore-and-aft and lateral whole-body vibration (Subashi et al. 2009). With variations in the magnitude of the excitation, normalised judgements of vibration discomfort were again correlated with the normalised apparent mass at frequencies less than 5 Hz. In both studies the correlations were less at higher frequencies, suggesting local motions in the body dominated discomfort at higher frequencies and did not greatly influence the forces measured at the seat and, therefore, the apparent mass. In a study of discomfort caused by whole-body vibration at frequencies over a wider range of frequencies (1 to 100 Hz), it was concluded that increased seat-to-head transmissibility tended to be associated with increased subject discomfort (Griffin et al. 1982).

The present study adds additional evidence of the biodynamic responses of the body influencing vibration discomfort. For example, subjects having a proportionately greater apparent mass at 4 Hz were likely to be relatively more uncomfortable at 4 Hz and subjects having a proportionately greater apparent mass at 6.3 Hz were likely to be relatively more uncomfortable at 6.3 Hz (Table 5.7). Although the finding is unsurprising, it is helpful in giving confidence to the use of biodynamic measures to predict factors that will influence subjective responses. The present associations show that biodynamic differences between subjects (reflected in differences in the forces at the seat when the acceleration is the same) influence the frequency-dependence of discomfort caused by vertical vibration at frequencies over the range 1 to 16 Hz.

5.5 Conclusions

With vertical whole-body vibration in the frequency range 1 to 16 Hz, the frequency dependence of equivalent comfort contours, expressed in terms of either acceleration or force, vary with the magnitude of vibration. However, equivalent comfort contours for force show less variation with vibration magnitude, consistent with the biodynamic

nonlinearity of the body contributing to the magnitude-dependence of equivalent comfort contours.

Over the range of magnitudes commonly encountered by seated passengers and operators, sensitivity to vertical acceleration is greater at 5 Hz than at lower frequencies, although this is not well reflected in the current International Standard.

Over the frequency range 1 to 16 Hz, inter-subject differences in subjective responses to vertical vibration are associated with inter-subject variability in biodynamic responses.

Chapter 6 Biodynamic responses to mechanical shocks

6.1 Introduction

The biodynamic responses of the human body indicate how vibration is transmitted through the body and contribute to understanding of the effects of vibration on comfort, performance, and health. The transmission of vibration to the body through seating and other non-rigid structures is dependent on the biodynamic responses of the body.

The biodynamic responses of the human body to low frequency vibration are nonlinear. For example, with vertical excitation of the body the principal resonance frequency decreases if the magnitude of the vibration excitation is increased. This nonlinear softening effect has been found with both random and sinusoidal vibration (e.g., Hinz and Seidel, 1987; Fairley and Griffin, 1989; Matsumoto and Griffin, 2005; Toward and Griffin, 2011; Chapter 4). With random vibration in the range 1 to 20 Hz, Fairley and Griffin (1989) found that the mean apparent mass resonance frequencies of 8 seated subjects decreased from about 6 Hz to 4 Hz as the vibration magnitude increased from 0.25 to 2.0 ms^{-2} r.m.s. The frequency of a second resonance in the vertical apparent mass in the frequency range 8 to 12 Hz has also been observed to reduce as the magnitude of vibration excitation increases (e.g., Fairley and Griffin, 1989; Mansfield and Griffin, 2000).

With sinusoidal vibration (13 frequencies from 1 to 16 Hz at five magnitudes from 0.1 to 1.6 ms^{-2} r.m.s.) and with random vibration (1 to 16 Hz) at the same magnitudes, this study has measured the dependence of the apparent mass of the seated human body on the frequency, magnitude, and waveform of vertical vibration in 20 males and 20 females (Chapter 4). The apparent mass was similar with random and sinusoidal vibration, but with increasing magnitude of vibration, the resonance frequency decreased from 6.5 to 4.5 Hz. The change in biodynamic response with increasing vibration magnitude (i.e., the nonlinearity) depended on the frequency of the vibration excitation. Males and females had similar apparent mass (after adjusting for subject weight) and a similar principal resonance frequency with both random and sinusoidal vibration.

The apparent mass of the body has mostly been determined with random vibration, although it seems the frequency-dependence and magnitude-dependence of the apparent mass are similar with random and sinusoidal vibration. Few studies have

investigated biodynamic responses to mechanical shocks, but with vertical transients at 4.0, 5.0, 6.3, or 8 Hz, the nominal apparent mass of the seated body was observed to decrease with increasing magnitude of the transient excitation (Matsumoto and Griffin, 2005). The limited investigation of human responses to shock restricts the modelling of biodynamic responses to mechanical shocks that are often associated with discomfort or injury,

Simple linear mass-spring-damper models provide surprisingly accurate representations of the modulus and phase of the vertical apparent mass of the seated human body exposed to random vibration (e.g., Fairley and Griffin, 1989; Toward and Griffin, 2009; Chapter 4), although the addition of a second degree-of-freedom provides a small improvement (Wei and Griffin, 1998). Such models have been developed to also represent the fore-and-aft forces on a seat during vertical excitation, by the addition of a rotational degree-of-freedom to represent the rotation of body segments during vertical excitation (e.g., Matsumoto and Griffin, 2001; Nawayseh and Griffin, 2009). Nonlinearity in the response of the human body implies that the response depends on the type of excitation (e.g., random or shock) and that a linear model representing the apparent mass of the body will require different parameters according to the magnitude of the excitation and the waveform of the excitation.

This study sought to identify what form of biodynamic model is required to represent the relation between force and acceleration when the seated human body is exposed to vertical shocks. For two alternative lumped-parameter time-domain models it was hypothesised that the parameters of the models would depend on both the magnitude of the shock and the nominal frequency of the shock, reflecting the decrease in the resonance frequency of the apparent mass of the human body observed with increasing magnitudes of sinusoidal and random vibration. There are no known previous studies of the apparent mass of the human body exposed to mechanical shocks using time domain methods.

6.2 Experimental method and model description

6.2.1 Apparatus

A 1-metre stroke vertical electrohydraulic vibrator generated vertical vibration of a flat rigid seat that was measured by an accelerometer (Silicon Design 2260-002). A force platform (Kistler 9281B) mounted on the seat measured the force at the interface between the seat and the subject in the vertical direction. The effect of the mass of the

top plate on the force platform was eliminated by subtracting the vertical acceleration multiplied by the mass of the top plate of the force platform (i.e. 31.5 kg) from the measured vertical force in the time domain (i.e., mass cancellation). Vibrations were generated by a Servotest Pulsar system and acquired using an *HVLab* data acquisition and analysis system (version 1.0) to a computer.

Subjects sat on the top surface of the seat without making contact with a backrest (Figure 6.1). They rested their feet on a footrest that was attached to the vibrator table. The footrest was adjusted so that the upper surfaces of the upper legs were horizontal.

Figure 6.1 Experiment setup

6.2.2 Subjects

Twenty male subjects, students at the University of Southampton, participated in the study. The median subject age was 24.5 years (range 22 - 33 years), mass 71.1 kg (range 48 - 107 kg), stature 1.75 m (range 1.65 – 1.97 m) and body mass index 23.1 kg/m^2 (range 17.6 kg/m^2 – 27.6 kg/m^2).

During exposure to shocks, subjects were asked to close their eyes to prevent vision affecting their reaction to the motion. They were exposed to white noise at 65 dB(A) via a pair of headphones.

The experiment was approved by the Human Experimentation Safety and Ethics Committee of the Institute of Sound and Vibration Research at the University of Southampton. Informed consent to participate in the experiment was given by all subjects.

6.2.3 Experimental design

To obtain the shock acceleration waveforms, 1½-cycle sinusoidal waveforms were modulated by a half cycle sinusoid with a period three times longer than the period of the sinusoidal acceleration (Figure 6.2).

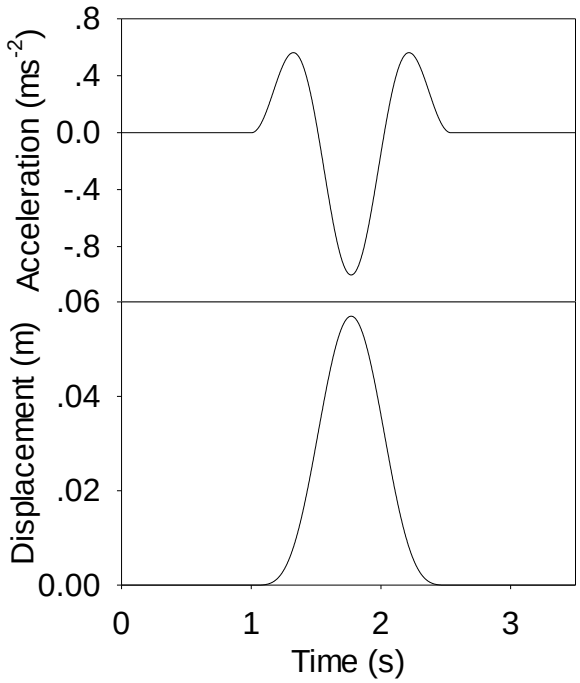

Figure 6.2 Example acceleration and displacement of the shocks.

Subjects attended two sessions on different days. In both sessions, subjects experienced 117 vertical shocks in the upward direction (an upward displacement as shown in Figure 6.2) and 117 vertical shocks in the downward direction in a completely random order over about 30 minutes. Different magnitude ranges of shocks were presented in the two sessions.

Each of the 1½-cycle sinusoidal vibration waveforms had a frequency at one of the 13 preferred one-third octave centre frequencies in the range 1 to 16 Hz. At each frequency, the shock was presented at nine magnitudes with the magnitude adjusted to produce the same frequency-weighted vibration dose value (i.e., VDV) at each frequency (using the W_b frequency weighting in ISO 8041:2005) (Table 6.1).

Table 6.1 The peak acceleration (ms^{-2}) and vibration dose value ($ms^{-1.75}$) of each stimulus in the two sessions

	Low magnitude session									High magnitude session								
VDV ($ms^{-1.75}$)	0.05	0.063	0.08	0.1	0.125	0.16	0.2	0.25	0.315	0.315	0.4	0.5	0.63	0.8	1	1.25	1.6	2
Frequency (Hz)	Peak acceleration (ms^{-2} r.m.s.)																	
1.0	0.2	0.25	0.32	0.40	0.50	0.64	0.8	1.00	1.26	1.26	1.60	2.00	2.52	3.20	4.00	4.99	6.39	7.99
1.25	0.21	0.26	0.33	0.41	0.51	0.66	0.82	1.03	1.30	1.30	1.65	2.06	2.6	3.30	4.12	5.15	6.59	8.24
1.6	0.21	0.26	0.33	0.41	0.52	0.66	0.83	1.03	1.30	1.30	1.65	2.07	2.61	3.31	4.14	5.17	6.62	8.27
2.0	0.19	0.24	0.31	0.39	0.48	0.62	0.77	0.97	1.22	1.22	1.55	1.94	2.44	3.10	3.87	4.84	6.19	7.74
2.5	0.17	0.21	0.27	0.34	0.42	0.54	0.68	0.84	1.06	1.06	1.35	1.69	2.13	2.70	3.38	4.22	5.41	6.76
3.15	0.14	0.18	0.23	0.29	0.36	0.46	0.57	0.72	0.90	0.90	1.15	1.44	1.81	2.30	2.87	3.59	4.59	5.74
4.0	0.13	0.16	0.20	0.25	0.32	0.41	0.51	0.63	0.80	0.80	1.01	1.27	1.6	2.03	2.53	3.17	4.06	5.07
5.0	0.12	0.15	0.19	0.24	0.30	0.39	0.48	0.60	0.76	0.76	0.96	1.20	1.52	1.93	2.41	3.01	3.85	4.81
6.3	0.12	0.15	0.19	0.24	0.30	0.39	0.48	0.61	0.76	0.76	0.97	1.21	1.53	1.94	2.42	3.03	3.88	4.85
8.0	0.13	0.16	0.21	0.26	0.32	0.41	0.51	0.64	0.81	0.81	1.03	1.28	1.62	2.05	2.56	3.21	4.10	5.13
10.0	0.14	0.18	0.22	0.28	0.35	0.45	0.56	0.70	0.88	0.88	1.12	1.40	1.76	2.24	2.80	3.50	4.48	5.59
12.5	0.16	0.20	0.25	0.31	0.39	0.50	0.63	0.78	0.99	0.99	1.25	1.57	1.97	2.51	3.13	3.92	5.02	6.27
16.0	0.18	0.23	0.29	0.37	0.46	0.59	0.73	0.92	1.15	1.15	1.47	1.83	2.31	2.93	3.66	4.58	5.86	7.33

After being exposed to all the shocks, subjects were exposed to random vertical vibration at five magnitudes (0.1, 0.2, 0.4, 0.8 and 1.6 ms^{-2} r.m.s.). The random vibration had approximately flat constant-bandwidth acceleration power spectra over the frequency range 1 to 16 Hz. The 60-s stimuli were presented in random order.

The experiment was also designed to measure the nonlinearity in the subjective responses to the vertical mechanical shocks. These subjective responses are reported in Chapter 7.

6.2.4 Model description

A single-degree-of-freedom model and a two-degree-of-freedom model were used to represent the biodynamic response of human body exposed to mechanical shock (Figure 6.3).

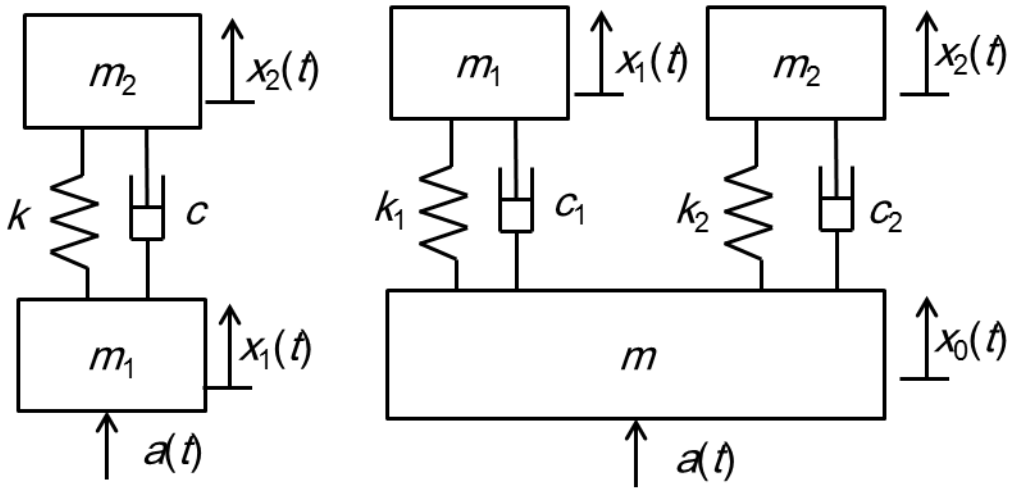

Figure 6.3 Single degree-of-freedom and two degree-of-freedom models

The motion equations for single-degree-of-freedom model are:

$$m_1\ddot{x}_1+c(\dot{x}_1-\dot{x}_2)+k(x_1-x_2)=F(t) \tag{6.1}$$

$$m_2\ddot{x}_2+c(\dot{x}_2-\dot{x}_1)+k(x_2-x_1)=0 \tag{6.2}$$

The motion equations for two-degree-of-freedom model are:

$$m\ddot{x}_1+c_1(\dot{x}-\dot{x}_1)+k(x-x_1)+c_2(\dot{x}-\dot{x}_2)+k_2(x-x_2)=F(t) \tag{6.3}$$

$$m_1\ddot{x}_1+c(\dot{x}_1-\dot{x})+k(x_1-x)=0 \tag{6.4}$$

$$m_2 \ddot{x}_2 + c(\dot{x}_2 - \dot{x}) + k(x_2 - x) = 0 \tag{6.5}$$

6.2.5 Procedure to determine model parameters

6.2.5.1 Single-degree-of-freedom model

The second-order ordinary differential equations ((1), (2)) were recast to a system of first order differential equations by introducing new variables:

$$y_1 = x_1, \quad y_2 = \dot{x}_1, \quad y_3 = x_2, \quad y_4 = \dot{x}_2 \tag{6.6}$$

The above motion equations were transferred to:

$$\dot{y}_1 = y_2 \tag{6.7}$$

$$\dot{y}_2 = \frac{F(t) - c(y_4 - y_2) - k(y_3 - y_1)}{m_1} \tag{6.8}$$

$$\dot{y}_3 = y_4 \tag{6.9}$$

$$\dot{y}_4 = \frac{c(y_2 - y_4) + k(y_1 - y_3)}{m_2} \tag{6.10}$$

In the above equations, the force at the subject-seat interface is $F(t)$. The four model parameters (m_1, m_2, c, k) are unknown. To minimise the risk of optimisation to inappropriate local minimum, the masses m_1 and m_2 were constrained to be 15% and 85% of the sitting masses of subjects, in accord with the findings of Wei and Griffin (1998). The sitting mass (i.e., m_1 + m_2) was obtained from the measured vertical apparent mass of the subjects at 1 Hz measured using random vertical vibration (with a spectrum of 1 to 16 Hz at a magnitude of 0.4 ms^{-2} r.m.s.). The stiffness, k, and the damping, c, were determined by optimisation using the function (fmicon) provided in MATLAB (version R2010a). The interior point algorithm was used. The initial guesses and bounds of the stiffness and damping were determined from published data where the parameters m_1, m_2, k, and c had been determined by fitting the model in the frequency domain to the apparent mass measured with random vibration (Wei and Griffin, 1998). In 24 male subjects, they found optimum stiffness in the range 29,409 to 77,829 Nm^{-1} and optimum damping in the range 675 to 2,345 Nsm^{-1}. Considering the variability between subjects, the lower and upper bounds of the stiffness and damping in the present study were set to the range from 10,000 to 200,000 Nm^{-1} and 100 to 10,000 Nsm^{-1}, respectively.

In each optimisation iteration, the above four first order differential equations were solved using a 4th order Runge-Kutta method, and the velocity of m_1 (i.e., y_2) was obtained, then the acceleration of m_1 was calculated by differentiating the velocity of m_1. The model parameters were obtained by minimizing the difference between the fitted acceleration and the measured acceleration over the duration of the shock and the following second, because the human body did not stop movement immediately after the end of a shock.

2.5.2 Two-degree-of-freedom model

Similar to the above single-degree-of-freedom model, the second-order differential equations ((3) to (5)) were also recast to a system of first order differential equations. The seven model parameters (m, m_1, m_2, c_1, k_1, c_2, k_2) are unknown. To minimise the risk of optimisation to inappropriate local minimum, the masses m, m_1 and m_2 were constrained to be 12%, 23% and 65% of the sitting masses of subjects, in accord with the findings of Wei and Griffin (1998). The values of the stiffness, k_1, k_2, and the damping, c_1 and c_2 were determined by optimisation as described above. The above two models are referred to as time-domain models.

6.2.6 Apparent mass

Based on the motion equations of the single degree-of-freedom model (Equations (6.1) and (6.2)), the equivalent apparent mass of the human body exposed to shocks at each nominal frequency can be obtained from:

$$AM_{1\text{dof}}(i\omega) = \left[m_1 + m_2 \left(\frac{k + c_1 i\omega}{k - m_2\omega^2 + ci\omega} \right) \right] \tag{6.11}$$

Then the apparent mass at each nominal frequency can be calculated using the fitted parameters (c, k) of the single degree-of-freedom model.

Similarly, with the motion equations of the two degree-of-freedom model (Equations (6.3) to (6.5)), the apparent mass can be obtained by:

$$AM_{2\text{dof}}(i\omega) = \frac{D + E + (F + G)i}{A + Bi} \tag{6.12}$$

where:

$$A = k_1 k_2 - \omega^2 (k_1 m_2 + k_2 m_1) + m_1 m_2 \omega^4 - c_1 c_2 \omega^2 \tag{6.13}$$

$$B = \omega(k_1 c_2 + k_2 c_1) - \omega^3 (m_1 c_2 + m_2 c_1) \tag{6.14}$$

$$D = (m + m_1 + m_2)k_1k_2 - (mm_2k_1 + mm_1k_2 + m_1m_2k_1 + m_1m_2k_2)\omega^2 \quad (6.15)$$

$$E = mm_1m_2\omega^4 - (mc_1c_2 + m_1c_1c_2 + m_2c_1c_2)\omega^2 \quad (6.16)$$

$$F = (m + m_1 + m_2)(k_1c_2 + k_2c_1)\omega \quad (6.17)$$

$$G = -(mm_1c_2 + mm_2c_2 + m_1m_2c_1 + m_1m_2c_2)\omega^3 \quad (6.18)$$

Then the apparent mass at each nominal frequency can be calculated using the fitted parameters (k_1, k_2, c_1, c_2) of the two degree-of-freedom model.

Because a shock contains more than one frequency, each frequency mentioned here is the nominal frequency of the shock (i.e., the frequency of the 1½-cycle sinusoidal motion used to generate the shock). The apparent mass obtained here is therefore the 'nominal apparent mass' for that frequency.

With random vibration, the vertical apparent mass, $AM_{random}(\omega)$, was also calculated by the cross-spectral density method:

$$AM_{random}(\omega) = \frac{S_{io}(\omega)}{S_{ii}(\omega)} \quad (6.19)$$

using a frequency resolution of 0.25 Hz with similar mass cancellation in the time domain.

The stiffness and damping in the above single degree-of-freedom model were also obtained by fitting the model to the vertical apparent masses and phases measured with random vibration. The target error, $E(f)$, was calculated by summing the squared error in the modulus and the phase at each frequency between the measured data and the fitted response:

$$E(f) = \sum_N \left[M_m(f) - M_s(f)\right]^2 + \sum_N \left[PH_m(f) - PH_s(f)\right]^2 \quad (6.20)$$

where N is the number of frequency points in the measured apparent mass (61 points for random vibration corresponding to the frequency range 1-16 Hz), $M_m(f)$ and $PH_m(f)$ are the apparent mass modulus and phase of the model at each frequency, and $M_s(f)$ and $PH_s(f)$ are the measured apparent mass modulus and phase. The constrained minimum error search command 'fmincon()' from the optimisation toolbox of MATLAB (version R2010a) was used for curve fitting. The constrained of masses, initial guesses and bounds of the stiffness and damping were the same as described in Section 6.2.5.

6.3 Results

6.3.1 Waveform of shock

Examples of the measured input force, the measured output acceleration, and the fitted output acceleration when using a single degree-of-freedom model are shown for shocks having nominal frequencies of 4 Hz and 16 Hz and the greatest magnitude (i.e., 2.0 $ms^{-1.75}$) in Figure 6.4.

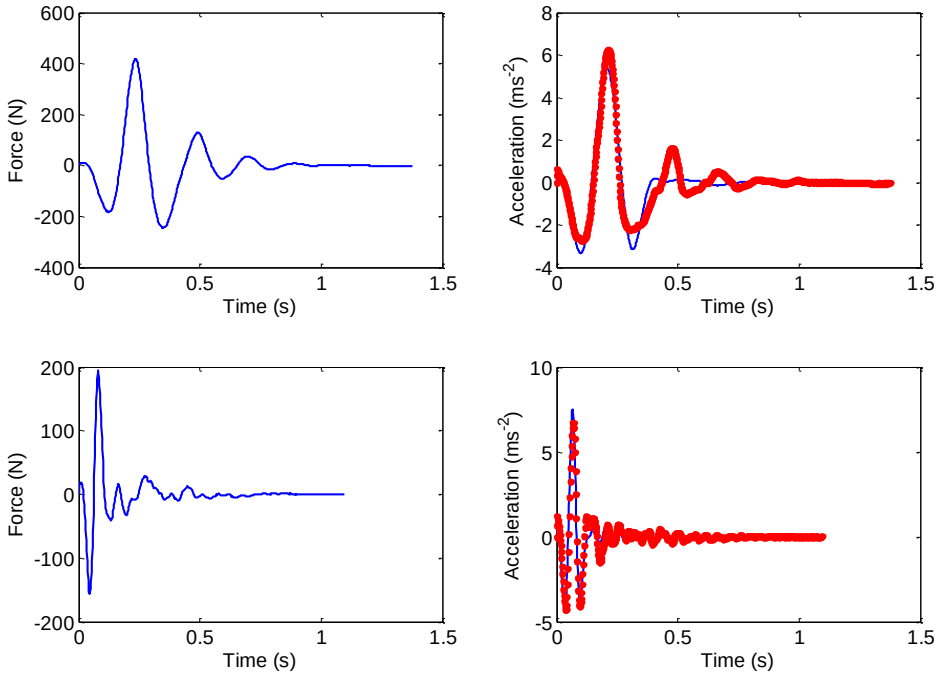

Figure 6.4 Examples of the measured input force, the measured output acceleration, and the predicted output acceleration waveforms for two shocks (upper graphs: 4-Hz nominal frequency with a VDV of 2.0 $ms^{-1.75}$; lower graphs: 16-Hz nominal frequency with a VDV of 2.0 $ms^{-1.75}$); left: measured input force waveforms; right: measured output acceleration waveforms (——) and fitted output acceleration waveforms for a single degree-of-freedom model (●).

The error between the measured acceleration waveform, $a_m(t)$, and the fitted output acceleration waveform $a_f(t)$, δ_a, was examined using the following equation:

$$\delta_a = \left(\frac{\int_{t1}^{t2} (a_d(t) - a_m(t))^2 dt}{\int_{t1}^{t2} (a_d(t))^2 dt} \right)^{1/2} \times 100\% \tag{6.21}$$

where t_1 is the start time of the shock, t_2 is the end time of the shock plus an additional one second.

With both a single degree-of-freedom model and two degree-of-freedom model, the median error between the measured acceleration waveform and the fitted acceleration waveform (i.e., δ*a*) varied with the magnitude of the shock and the nominal frequency of the shock (Figures 6.5 and 6.6): δ*a* decreased as the magnitude of the shock increased but increased as the nominal frequency increased, except for the high magnitude upward shocks with a nominal frequency around 2 Hz where the acceleration peaks approached 1 g. When the acceleration approached 1 g, a sudden jump in the force was measured. This is assumed to have occurred because subjects left the seat (due to their downward acceleration under gravity being momentarily less than the downward acceleration of the vibrator) and then subsequently impacted with the seat. To develop the biodynamic models in this study, the force was assumed to be the input, so the fitted acceleration did not provide a good fit to the measured acceleration waveform for these shocks with high magnitudes. For both models, the worst fit occurred at the higher frequencies where the phase difference between the measured acceleration and the fitted acceleration had a greater effect of the error.

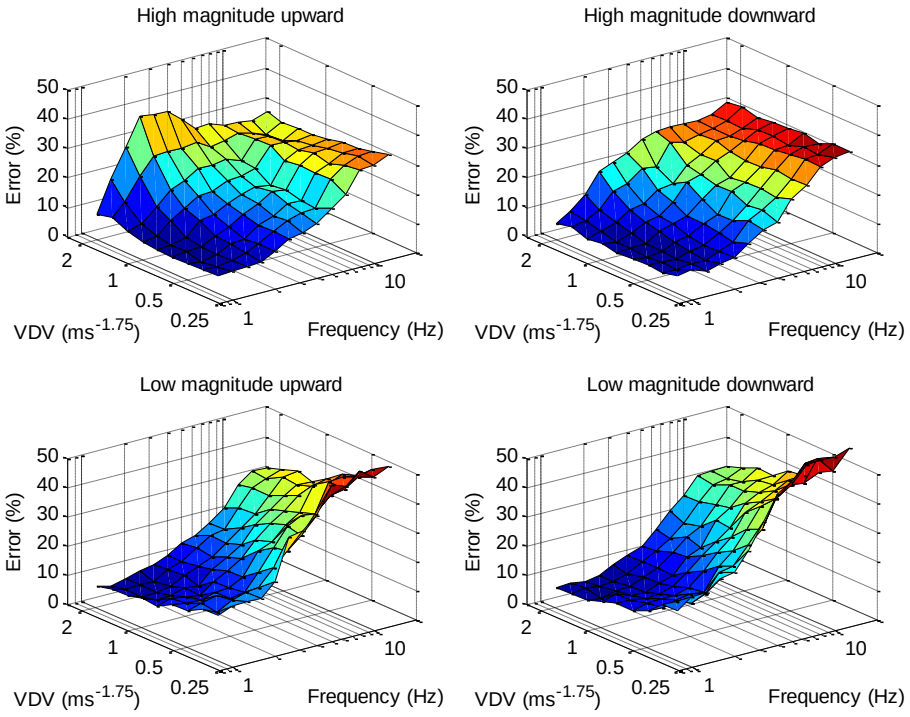

Figure 6.5 Median error between the measured acceleration waveform and the fitted acceleration waveform (i.e., δ*a*) of single degree-of-freedom model at each frequency with lower magnitude shocks (lower figures) and higher magnitude shocks (upper figures) for upward shocks (left figures) and downward shocks (right figures). Median values over 20 subjects at each of nine magnitudes of shock shown in Table 6.1.

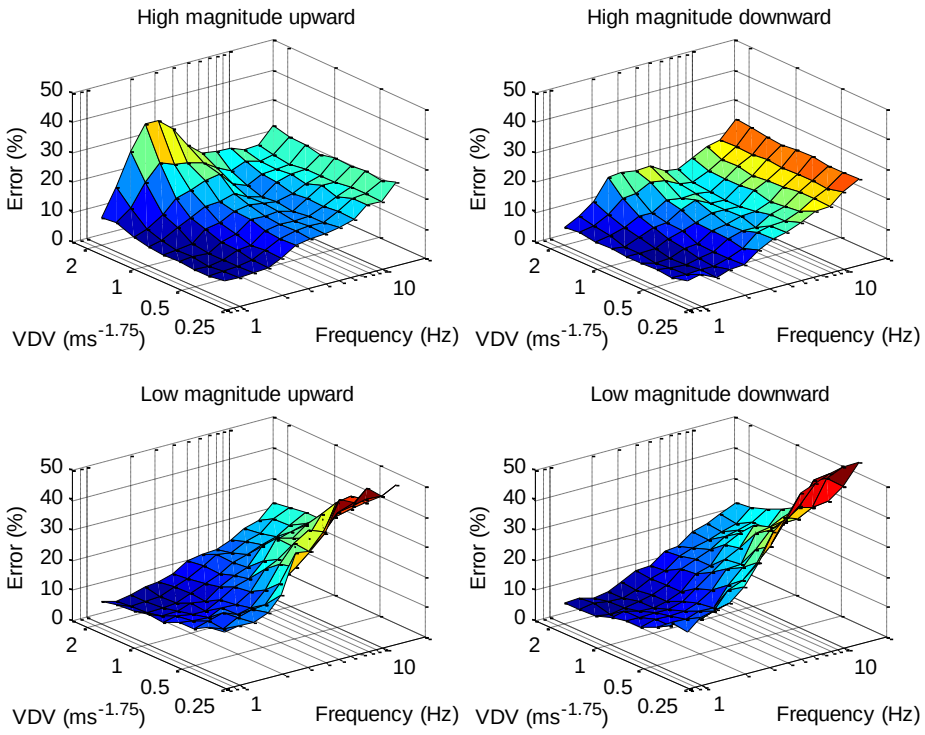

Figure 6.6 Median error between the measured acceleration waveform and the fitted acceleration waveform (i.e., δ*a*) of two degree-of-freedom model at each frequency with lower magnitude shocks (lower figures) and higher magnitude shocks (upper figures) for upward shocks (left figures) and downward shocks (right figures). Median values over 20 subjects at each of nine magnitudes of shock shown in Table 6.1.

6.3.2 Effect of shock magnitude and shock frequency on the stiffness, *k*

The stiffness, *k*, of the equivalent single degree-of-freedom model as obtained by curve fitting varied with both the frequency and the magnitude of the shocks (Figure 6.7; the stiffness calculated for 1-Hz and 1.25-Hz shocks are excluded because the human body was nearly rigid at these frequencies). As the nominal frequency of shocks increased from 1.6 to 16 Hz, the optimum stiffness generally increased. At frequencies greater than 2 Hz, there are negative correlations between the magnitude of the shock and the median optimum stiffness over the 20 subjects at each frequency, for both upward shocks and downward shocks in both the lower and the higher range of magnitudes (Table 6.2).

The stiffnesses, k_1, and k_2, of the equivalent two degree-of-freedom model as obtained by curve fitting varied with both the frequency and the magnitude of the shocks (Figure 6.8). Similar to the single degree-of-freedom model, as the nominal frequency of

shocks increased from 1.6 Hz to 16 Hz, the optimum value of both stiffnesses (k_1 and k_2) generally increased. At frequencies greater than 1.6 Hz, as the magnitude of the shocks increased, the stiffnesses tended to reduce (Table 6.2). The trend is more evident in the high magnitude session than in the low magnitude session, and also more evident with k_2 than with k_1.

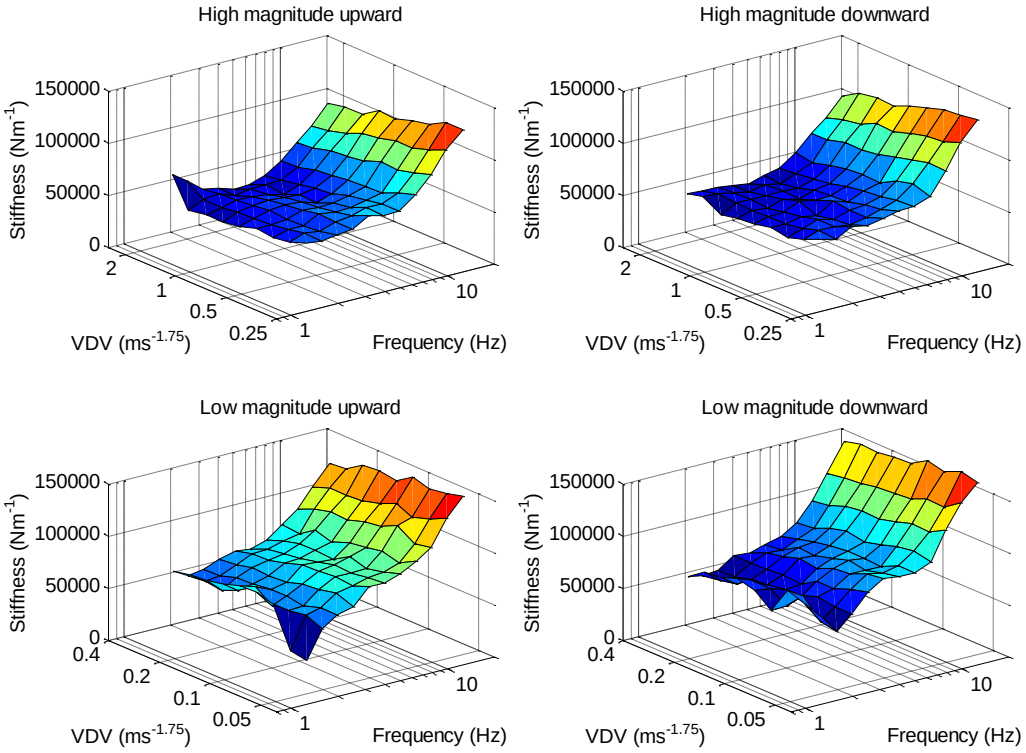

Figure 6.7 Optimum stiffness, *k*, of a single degree-of-freedom model for each magnitude and nominal frequency of shock: lower magnitude shocks (lower figures) and higher magnitude shocks (upper figures) for upward shocks (left figures) and downward shocks (right figures). Median values over 20 subjects.

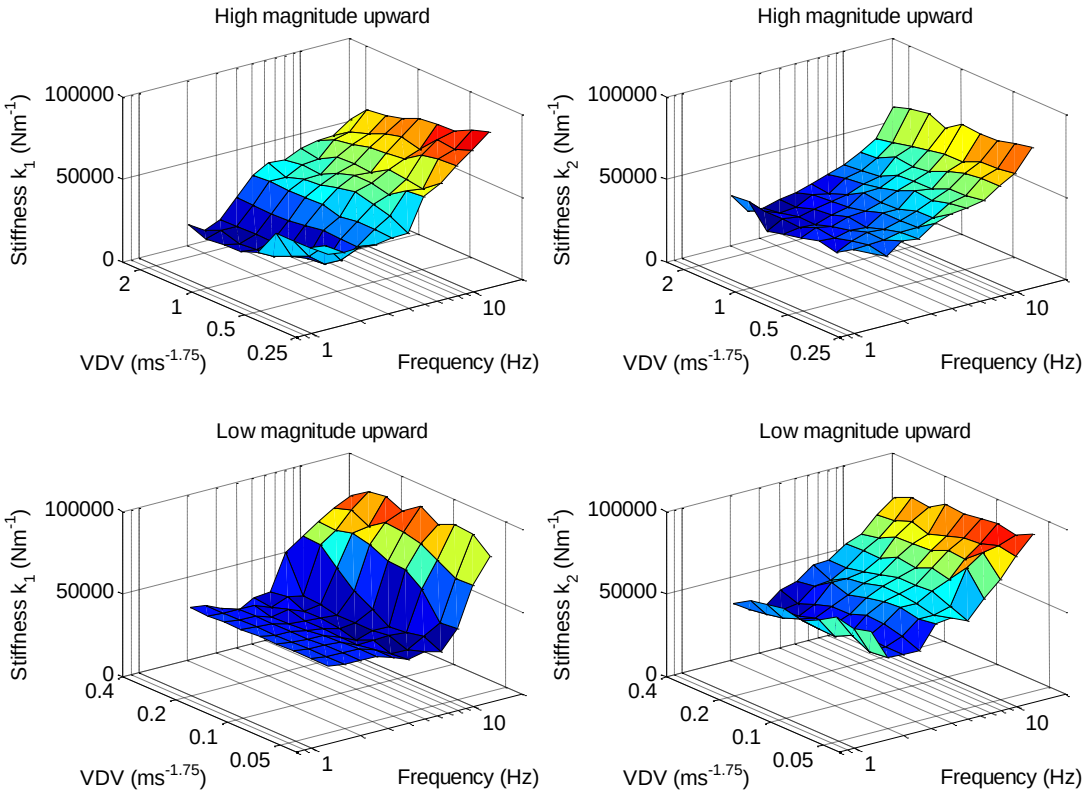

Figure 6.8 Optimum stiffnesses, k_1 and k_2 of a two degree-of-freedom model for each magnitude and nominal frequency of shock: lower magnitude shocks (lower figures) and higher magnitude shocks (upper figures) for upward shocks. Median values over 20 subjects.

Table 6.2 Spearman rank correlations between the optimum stiffness (k for single degree-of-freedom model, k_1 and k_2 for two degree-of-freedom model) and the magnitudes of the shocks.

Frequency (Hz)	Low magnitude						High magnitude					
	Upward			Downward			Upward			Downward		
	1 dof	2 dof		1 dof	2 dof		1 dof	2 dof		1 dof	2 dof	
	k	k_1	k_2	k	k_1	k_2	k	k_1	k_2	k	k_1	k_2
1.6	0.12	-0.35	-0.78*	-0.67	-0.90**	-0.93***	-0.37	-0.63	-0.10	-0.48	-0.88**	-0.18
2.0	-0.57	-0.93***	-0.77*	-0.22	-0.95***	-0.73	-0.37	-0.42	-0.83*	-0.77*	-0.88**	-0.88**
2.5	-0.93***	-0.88**	-0.95***	-0.92**	-0.87**	-0.92**	-0.95***	-0.17	-0.98***	-0.93***	-0.67	-0.97***
3.15	-0.88**	-0.93***	-0.85*	-0.93***	-0.82*	-0.40	-0.93***	0.02	-0.98***	-0.87**	-0.78*	-0.97***
4.0	-0.98***	0.58	-0.67	-0.98***	-0.02	-0.90*	-1.00***	0.78*	-1.00***	-0.88**	0.70*	-0.98***
5.0	-0.98***	0.92**	-0.95***	-0.97***	0.70*	-0.63	-0.95***	0.95***	-0.98***	-0.98***	-0.02	-0.93***
6.3	-0.88**	0.93***	-0.60	-0.93***	0.67	-0.35	-1.00***	0.05	-0.98***	-1.00***	-0.93***	-0.98***
8.0	-0.92**	0.78*	-0.35	-0.93***	0.93***	-0.70*	-0.98***	-0.68	-0.98***	-0.92***	-0.87**	-1.00***
10.0	-0.85*	0.87**	-0.88**	-0.98***	0.93***	-0.88**	-0.98***	-0.93***	-1.00***	-0.97***	-1.00***	-0.98***
12.5	-0.93***	0.47	-0.98***	-0.98***	0.58	-0.97***	-0.98***	-1.00***	-0.98***	-0.98***	-0.93***	-0.98***
16.0	-0.90**	0.08	-0.97***	-0.90**	-0.12	-0.85*	-0.97***	-1.00***	-0.93***	-0.98***	-1.00***	-0.90**

*: p<0.05; **: p<0.005; ***: p<0.0005

6.3.3 Effect of shock magnitude and shock frequency on the damping, *c*

The damping, *c*, of the equivalent single degree-of-freedom model as obtained by curve fitting also varied with both the frequency and the magnitude of the shocks (Figure 6.9, the damping obtained at 1 Hz and 1.25 Hz is excluded because the human body is nearly rigid at these frequencies). The median optimum damping over the 20 subjects tended to decrease with increasing shock magnitude, especially with the higher range of shock magnitudes and with the higher frequencies of shock (Table 6.3).

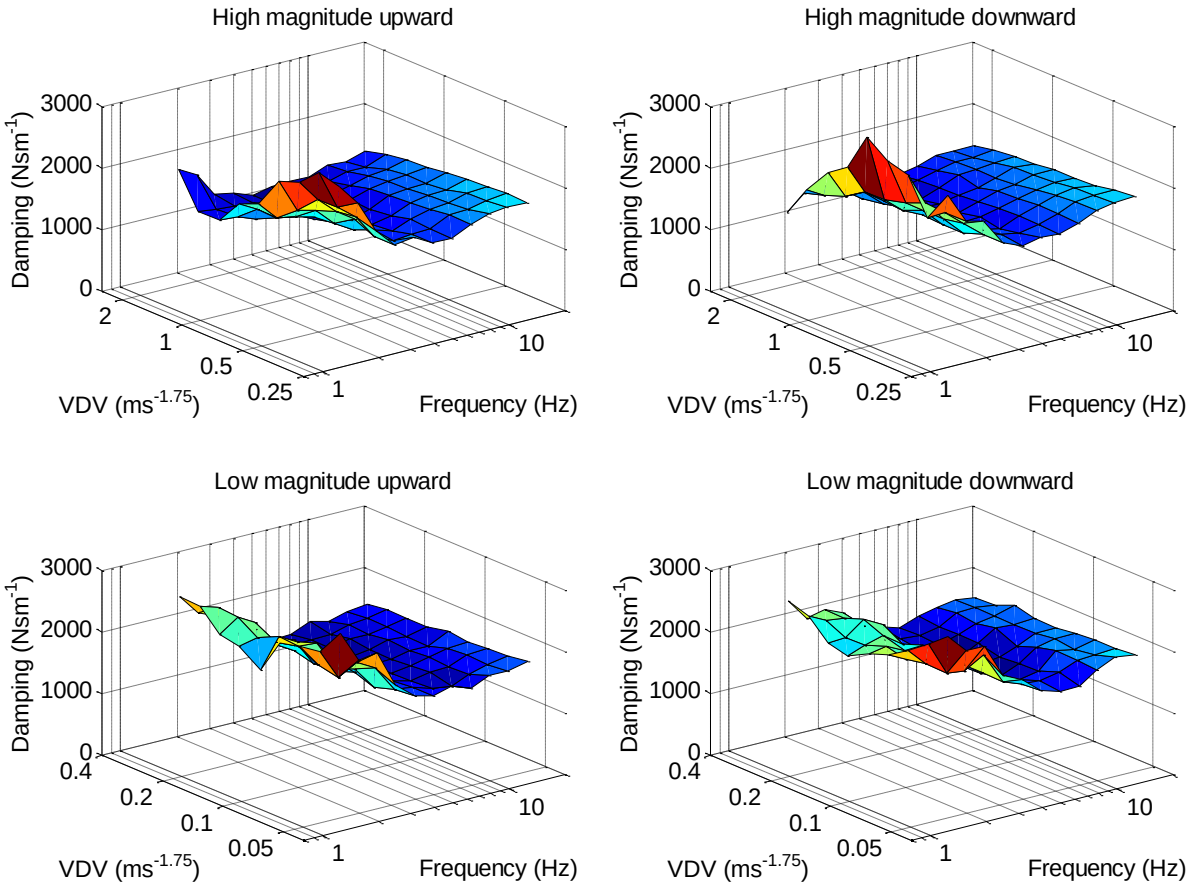

Figure 6. 9 Optimum damping, *c*, of single degree-of-freedom model for each magnitude and nominal frequency of shock: lower magnitude shocks (lower figures) and higher magnitude shocks (upper figures) for upward shocks (left figures) and downward shocks (right figures). Median values over 20 subjects.

Table 6.3 Spearman rank correlations between the optimum damping (c for single degree-of-freedom model, c_1 and c_2 for two degree-of-freedom model) and the magnitudes of the shocks.

Frequency (Hz)	Low magnitude						High magnitude					
	Upward			Downward			Upward			Downward		
	1 dof	2 dof		1 dof	2 dof		1 dof	2 dof		1 dof	2 dof	
	c	c_1	c_2	c	c_1	c_2	c	c_1	c_2	c	c_1	c_2
1.6	-0.52	0.20	-0.32	-0.57	-0.63	-0.52	-0.80*	-0.78*	-0.68	-0.53	-0.72*	-0.10
2.0	0.10	-0.63	-0.12	-0.45	-0.47	-0.12	-0.82*	-0.58	-0.78*	-0.93***	-0.97***	0.22
2.5	-0.48	-0.67	-0.33	-0.02	-0.22	-0.23	-0.88**	-0.48	-0.80*	-0.93***	-0.98***	-0.83*
3.15	-0.73	-0.13	-0.88**	-0.48	-0.27	-0.82*	-0.92**	-0.82*	-0.82*	-0.85**	-0.93***	-0.80*
4.0	-0.65	-0.73*	-0.48	-0.72*	0.42	-0.93***	-0.95***	-0.90**	-0.98***	-0.88**	-0.98***	-0.98***
5.0	-0.90**	-0.78*	-0.83*	-0.55	0.88*	-0.95***	-0.97***	-0.73*	-0.98***	-0.90**	-0.95***	-0.95***
6.3	-0.92**	0.40	-0.93***	-0.18	0.50	-0.88**	-0.92**	0.27	-0.98***	-0.93***	-0.85*	-0.97***
8.0	-0.17	0.23	-0.93***	0.15	0.72	-0.98***	-0.98***	0.70*	-0.95***	-0.93***	-0.85*	-0.93***
10.0	-0.60	0.40	-0.92**	-0.65	0.20	-0.98***	-1.00***	0.52	-0.88**	-0.98***	-0.88**	-0.87**
12.5	-0.75*	-0.93***	-0.82*	-0.78	-0.62	-0.83*	-0.98***	-0.32	-0.82*	-1.00***	-0.17	-0.72*
16.0	-0.83*	-0.58	-0.88**	-0.73	-0.25	-0.87**	-0.98***	-0.22	-0.58	-1.00***	-0.42	-0.73*

*: p<0.05; **: p<0.005; ***: p<0.0005

The damping, c_1, and c_2, of the equivalent two degree-of-freedom model as obtained by curve fitting varied with both the frequency and the magnitude of the shocks (Figure 6.10). Similar to the stiffnesses (k_1 and k_2), there are generally negative correlations between the damping and the magnitude of the shock. The trend is more evident in c_2 than c_1.

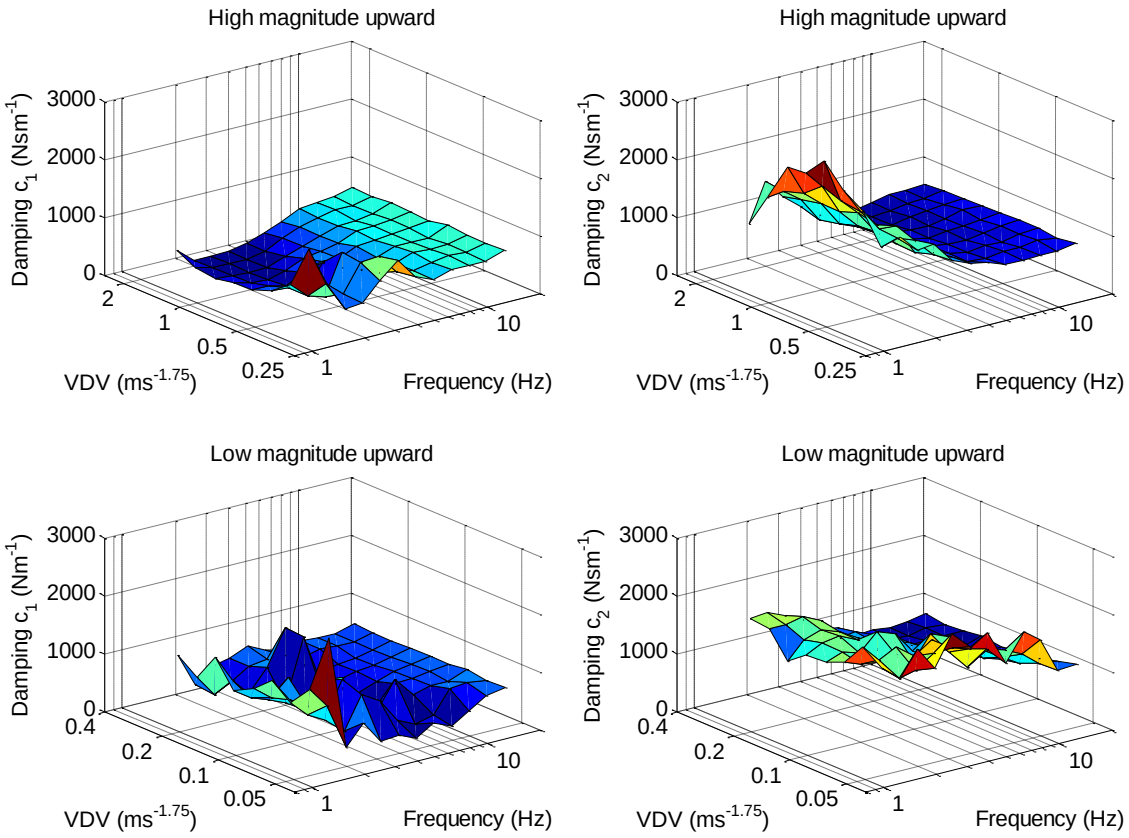

Figure 6.10 Optimum damping, c_1 and c_2 of a two degree-of-freedom model for each magnitude and nominal frequency of shock: lower magnitude shocks (lower figures) and higher magnitude shocks (upper figures) for upward shocks. Median values over 20 subjects.

6.3.4 Nominal apparent mass during shock excitation

With the obtained values of the stiffness, k, and the damping, c, the modulus and phase of the nominal apparent mass, AM_{1dof}, of the body during shocks at each magnitude and each frequency were calculated using Equations (11). An example of the inter-subject variability in AM_{sdof} is shown in Figure 6.11.

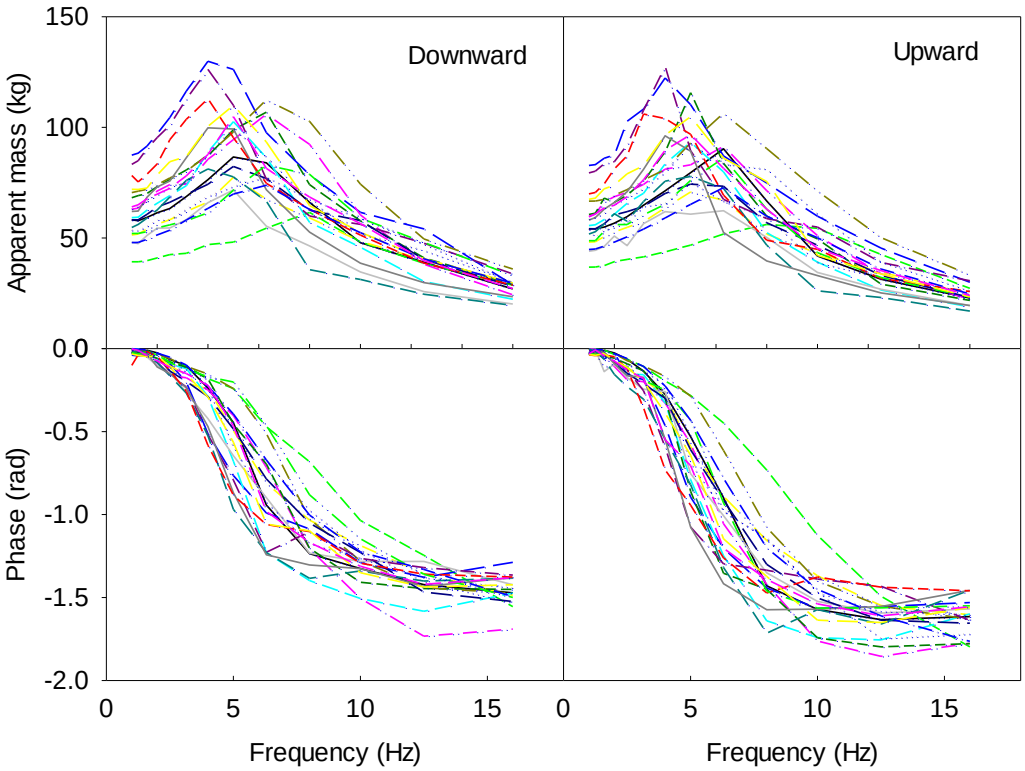

Figure 6.11 Inter-subject variability in the vertical apparent mass, $AM_{sdof}(\omega)$ (the nominal apparent mass measured assuming a single degree-of-freedom model), during downward shocks (left figures) and upward shocks (right figures) having VDVs of 0.315 $ms^{-1.75}$. Data from 20 subjects.

To investigate the effect of shock magnitude on the nominal apparent mass, five magnitudes (i.e., 0.05, 0.125, 0.315, 0.8 and 2.0 $ms^{-1.75}$ VDV) were chosen instead of all magnitudes used in Table 6.1. The greater magnitude difference was used to assist the illustration of the effect of vibration magnitude. As the magnitude of the shocks increased from 0.05 $ms^{-1.75}$ to 2.0 $ms^{-1.75}$ VDV, the median resonance frequency of the nominal apparent mass, $AM_{1dof}(\omega)$ (the nominal apparent mass measured assuming a single degree-of-freedom model) decreased from 6.3 Hz to 4 Hz with both downward and upward shocks (p<0.001, Friedman, Figure 6.12). There was no significant difference in the resonance frequency of the nominal apparent mass between downward and upward shocks at any magnitude, except at 2.0 $ms^{-1.75}$ VDV where the resonance frequency was lower with the upward shocks (p= 0.028, Wilcoxon)

An example of the inter-subject variability in $AM_{2dof}(\omega)$ (the nominal apparent mass measured assuming a 2 degree-of-freedom model) is shown in Figure 6.13. The individual resonance frequencies are in the range 4 to 6 Hz.

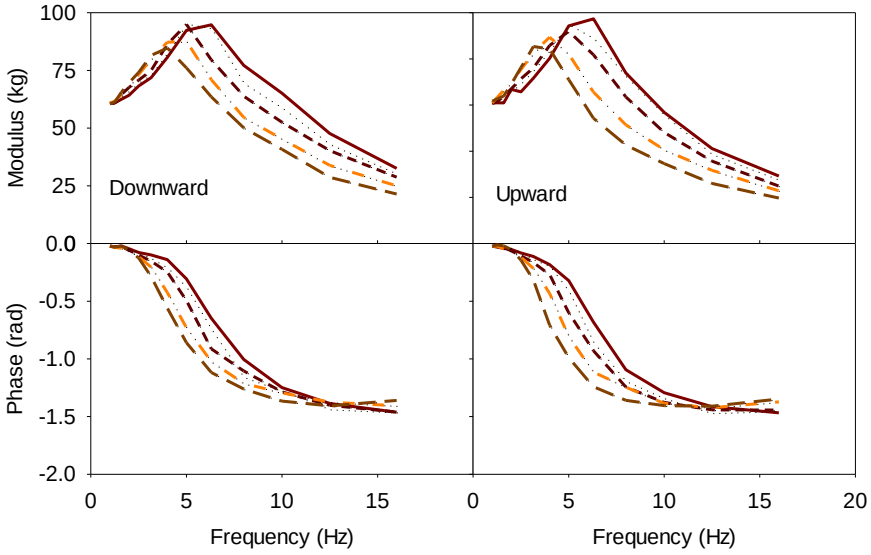

Figure 6.12 Median modulus and phase of the nominal apparent mass, $AM_{sdof}(\omega)$ (the nominal apparent mass measured assuming a single degree-of-freedom model), for subjects exposed to downward shocks (left figures) and upward shocks (right figures) at five magnitudes (—: 0.05 $ms^{-1.75}$; •••: 0.125 $ms^{-1.75}$; — —: 0.315 $ms^{-1.75}$; — •• —: 0.8 $ms^{-1.75}$; —— ——: 2.0 $ms^{-1.75}$).

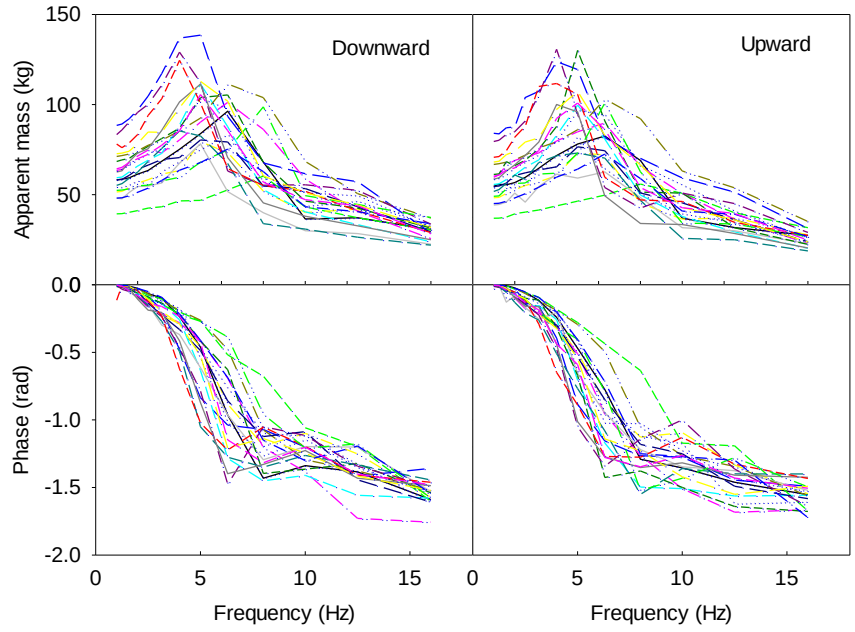

Figure 6.13 Inter-subject variability in the vertical apparent mass, $AM_{2dof}(\omega)$ (the nominal apparent mass measured assuming a 2 degree-of-freedom model) during downward shocks (left figures) and upward shocks (right figures) having VDVs of 0.315 $ms^{-1.75}$. Data from 20 subjects.

As the magnitudes of the shocks increased from 0.05 $ms^{-1.75}$ to 2.0 $ms^{-1.75}$ VDV, the median resonance frequency of the nominal apparent mass AM_{2dof} also decreased from 6.3 Hz to 4 Hz with both downward and upward shocks (p<0.001, Friedman, Figure 6.14). There was no significant difference in the resonance frequency of the nominal apparent mass between the downward and upward shocks at any magnitude.

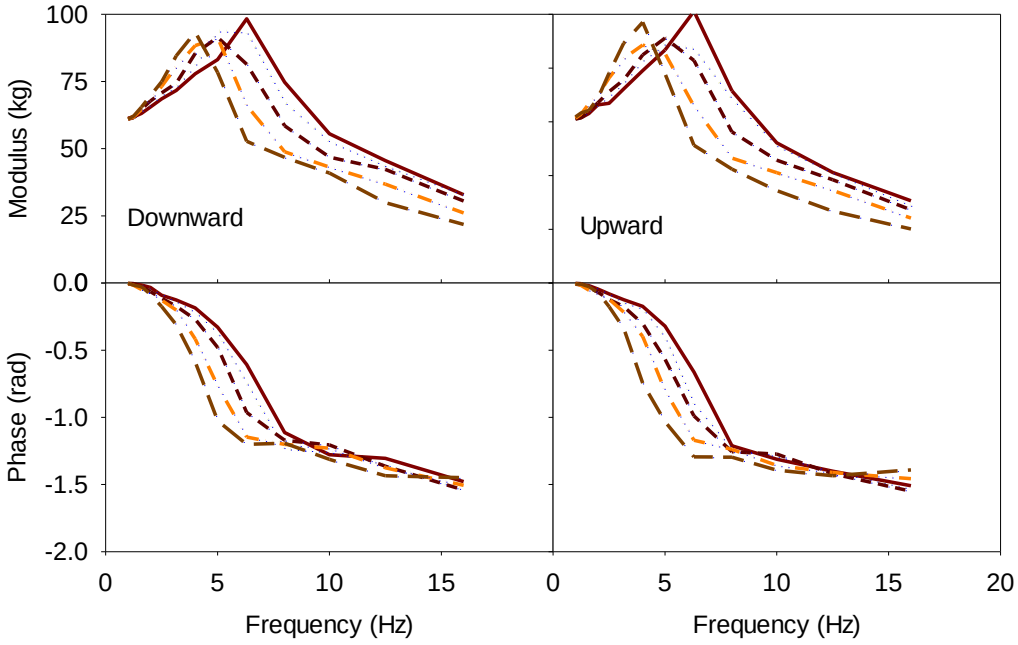

Figure 6.14 Median modulus and phase of the apparent mass, $AM_{2dof}(\omega)$ (the nominal apparent mass measured assuming a 2 degree-of-freedom model), for subjects exposed to downward shocks (left figures) and upward shocks (right figures) at five magnitudes (—: 0.05 $ms^{-1.75}$; •••: 0.125 $ms^{-1.75}$; – –: 0.315 $ms^{-1.75}$; – •• –: 0.8 $ms^{-1.75}$; ——: 2.0 $ms^{-1.75}$).

There were no significant differences in the resonance frequency obtained with AM_{1dof} and AM_{2dof} at any of the five magnitudes in either direction (p>0.05, Wilcoxon). An example of the comparison between AM_{sdof} and AM_{2dof} is shown in Figure 6.15.

6.3.5 Apparent mass during random excitation

The principal resonance in the vertical apparent mass during random vibration was in the vicinity of 5 Hz, but varied between subjects (Figure 6.16).

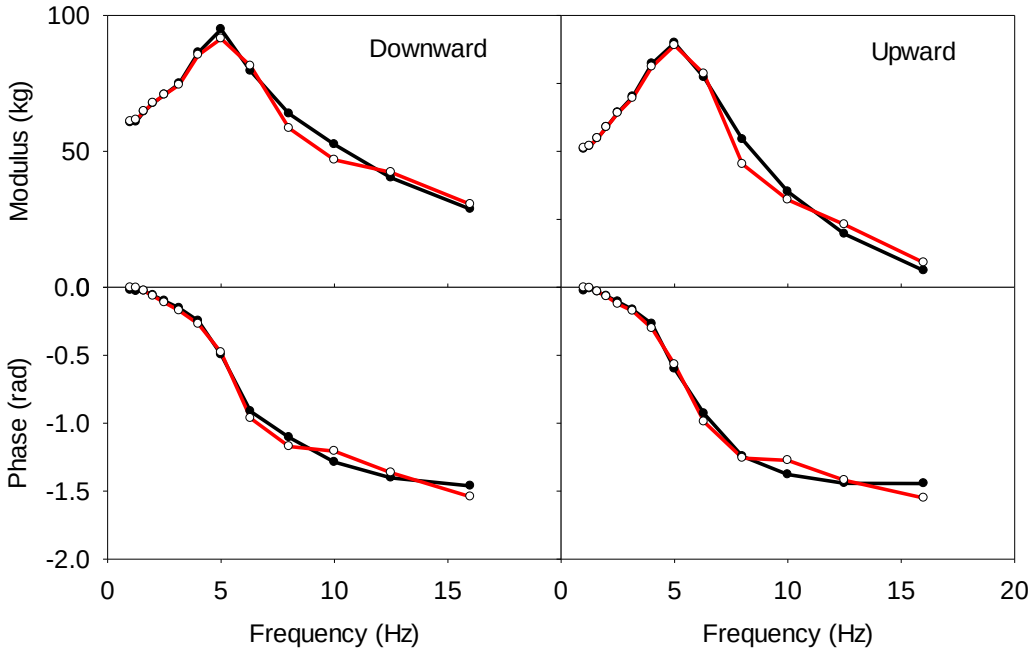

Figure 6.15 Example comparison of $AM_{sdof}(\omega)$ (—●—) and $AM_{2dof}(\omega)$ (—○—). The data are from the median apparent masses of 20 subjects at 0.315 $ms^{-1.75}$.

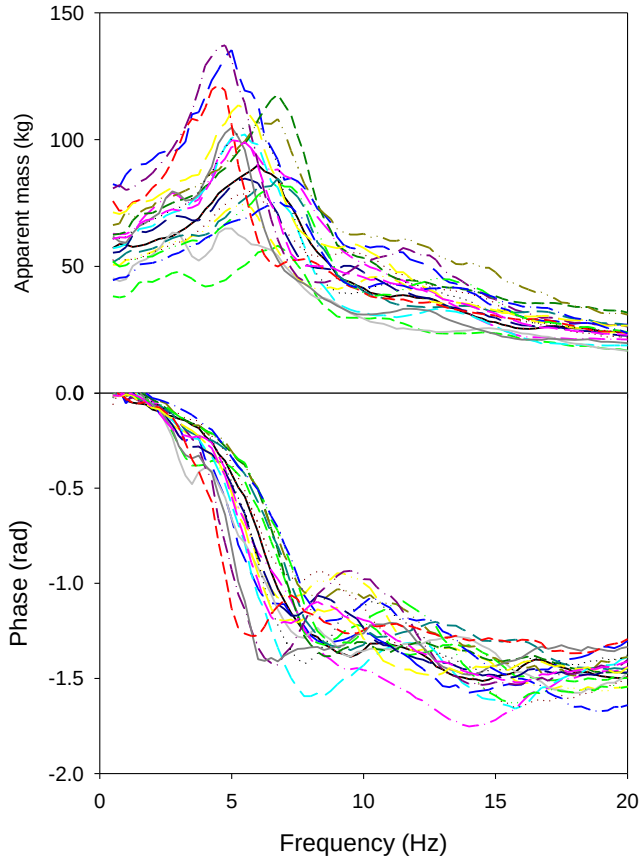

Figure 6.16 Inter-subject variability in the vertical apparent masses of 20 male subjects exposed to random vertical vibration at 0.4 ms^{-2} r.m.s.

Similar to the apparent mass during shock excitation, the resonance frequency evident in the apparent mass during random excitation reduced as the magnitude of the excitation increased (Figure 6.17). As the magnitude of the random vibration increased from 0.1 to 1.6 ms^{-2} r.m.s., the median resonance frequency decreased from 6.5 Hz to 4.5 Hz (p<0.001, Friedman).

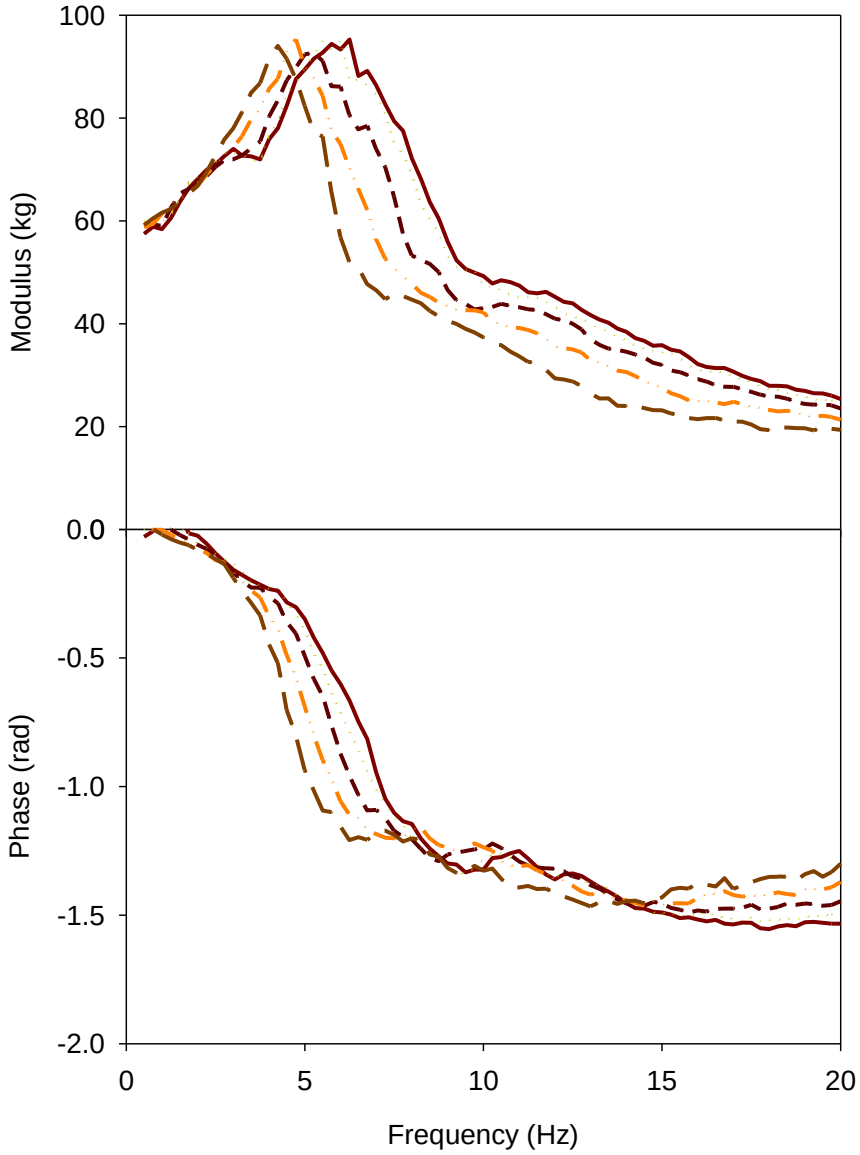

Figure 6.17 Median modulus and phase of the apparent mass of subjects exposed to vertical random vibration at five magnitudes (—: 0.05 $ms^{-1.75}$; •••: 0.125 $ms^{-1.75}$; — —: 0.315 $ms^{-1.75}$; — •• —: 0.8 $ms^{-1.75}$; —— ——: 2.0 $ms^{-1.75}$)

6.3.6 Model parameters during random excitation

With random vibration, the optimum stiffness and optimum damping of the single degree-of-freedom model (i.e., frequency-domain model) decreased with increasing magnitude of vibration (p<0.001, Friedman, Figure 6.18).

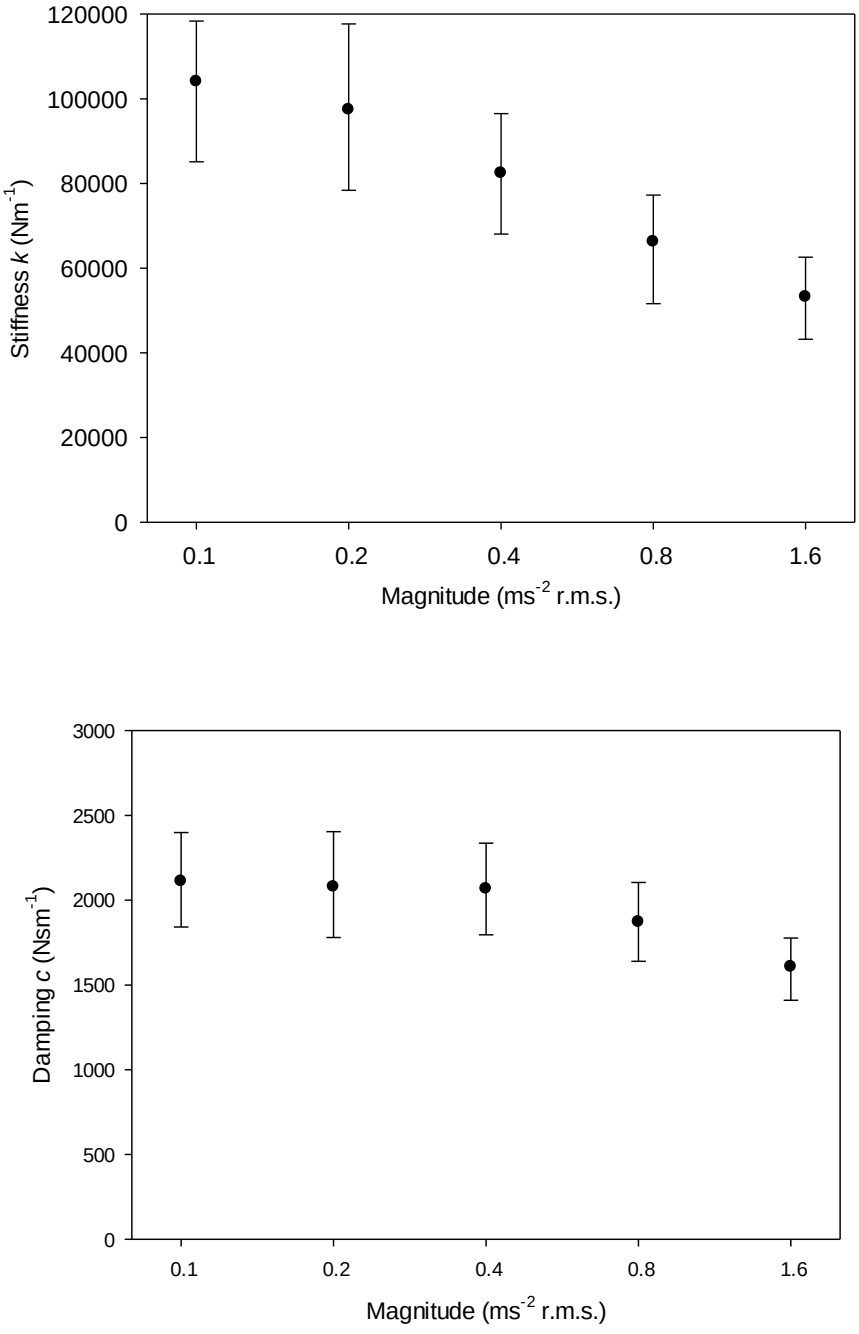

Figure 6.18 Median and inter-quarter range of optimum stiffness and damping of the single degree-of-freedom model from five magnitudes of random vibration

For each of the 20 subjects, the optimum stiffness and optimum damping obtained by fitting their measured response to 4-Hz downward shocks at 0.315 $ms^{-1.75}$ VDV (the greatest magnitude in the low magnitude downward session) were compared with the optimum stiffness and optimum damping fitted to their response to random vibration at 0.1 ms^{-2} r.m.s. (VDV of 0.324 $ms^{-1.75}$). For both the stiffness and the damping, there were statistically significant positive correlations between values obtained during random vibration and the corresponding values obtained in response to shocks with nominal frequencies of shock greater than 2.5 Hz (p<0.05; Spearman, Figure 6.19).

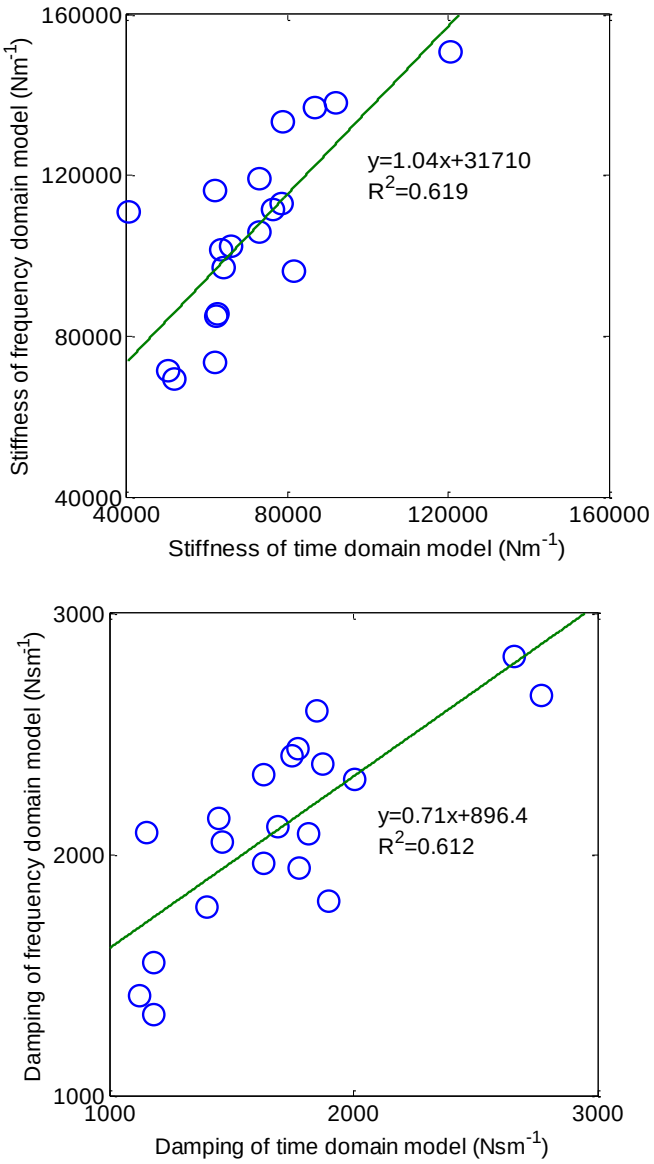

Figure 6.19 Example correlations between the optimum stiffness and optimum damping of a frequency-domain single degree-of-freedom model of response to random vibration (at 0.1 ms^{-2} r.m.s.; 0.324 $ms^{-1.75}$) and the corresponding optimum parameters of a time-domain single degree-of-freedom model of response to a downward shock (4-Hz nominal frequency; 0.315 $ms^{-1.75}$). Data from 20 subjects.

For these motions having similar vibration dose values, both the stiffness and the damping were greater with random vibration than with shocks (p<0.05, Wilcoxon). With other magnitudes of random vibration and other magnitudes of the shocks, the correlations between the optimum values for random vibration and the optimum values for shocks were similar, for both stiffness and damping.

6.3.7 Curve fitting of shock waveform with frequency-domain model

The optimum stiffness and optimum damping obtained by fitting a single degree-of-freedom model to the apparent mass obtained with random vibration (with a magnitude of 0.1 ms^{-2} r.m.s.) were also used to predict the acceleration waveform for shocks in the low magnitude session.

The error between the measured acceleration waveform, $a_m(t)$, and the predicted acceleration waveform $a_p(t)$, δa, was examined using equation (6.21). Similar to Figure 6.5, the median error between the measured acceleration waveform and the fitted acceleration waveform (i.e., δa) decreased as the magnitudes of the shocks increased but increased as the nominal frequencies of the shocks increased (Figure 6.20). However, the median error is somewhat greater than the median error obtained by fitting using the single degree-of-freedom time-domain model.

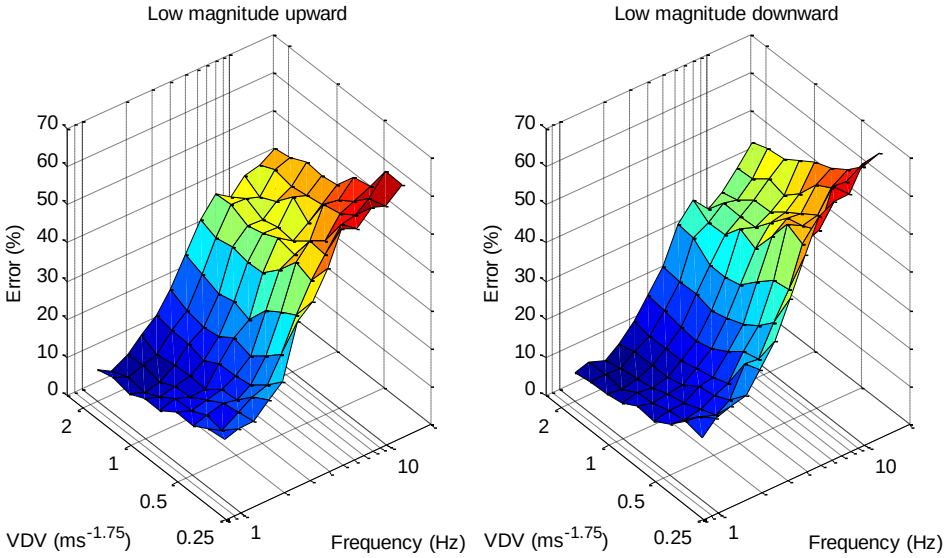

Figure 6.20 Median error between the measured acceleration waveform and the fitted acceleration waveform (i.e., δa) at each frequency with lower magnitude upward shocks (left figure) and low magnitude downward shocks (right figure) using single degree-of-freedom frequency domain model with optimum stiffness and damping obtained at 0.1 ms^{-2} r.m.s.

6.3.8 Associations between subject characteristics and biodynamic responses

There was no clear pattern of correlations between the characteristics of the subjects (e.g., total-weight, stature, and body mass index) and the optimum stiffness with the two medium magnitudes of shock (i.e., 0.125 $ms^{-1.75}$ in the low magnitude session, 0.8 $ms^{-1.75}$ in the high magnitude session) at any frequency in any of the four sessions of the experiment. However, with both two time-domain models, there were distinct patterns of statistically significant positive correlations between the above subject characteristics and the optimum damping for shocks having nominal frequencies greater than 10 Hz. There were no statistically significant correlations between the characteristics of the subjects (i.e., total-weight, stature, and body mass index) and the optimum stiffness or optimum damping of the model obtained for any of the five magnitudes of random vibration.

With each shock magnitude (i.e., 0.05, 0.125, 0.315, 0.8, and 2 $ms^{-1.75}$ VDV), the resonance frequency and the apparent mass at resonance were calculated from the stiffness and damping of a single degree-of-freedom model fitted to the shock response with both directions (upward and downward shocks). There were positive correlations between some of the physical characteristics of subjects (total-weight, stature, and body mass index) and both the resonance frequency of the apparent mass and the apparent mass at resonance frequency at all five magnitudes with both directions of shock (Kendall's τ_b $p<0.05$). With random vibration at all five magnitudes, there were also significant positive correlations between these three physical characteristics and the apparent mass at resonance. However, with random vibration the resonance frequency of the apparent mass had significant positive correlations with the total weight and the body mass index of subjects only at low magnitudes (i.e., 0.1, 0.2, and 0.4 ms^{-2} r.m.s.).

6.4 Discussion

6.4.1 Proposed model

The two time-domain models developed in this study provided reasonable fits the measured time domain data, but with poorer fits at higher frequencies (Section 6.3.1). The greater error at high frequencies seems to be associated with increased phase difference between the fitted acceleration waveforms and the measured acceleration waveforms at higher frequencies. Example comparisons between waveforms are shown in Figure 6.21.

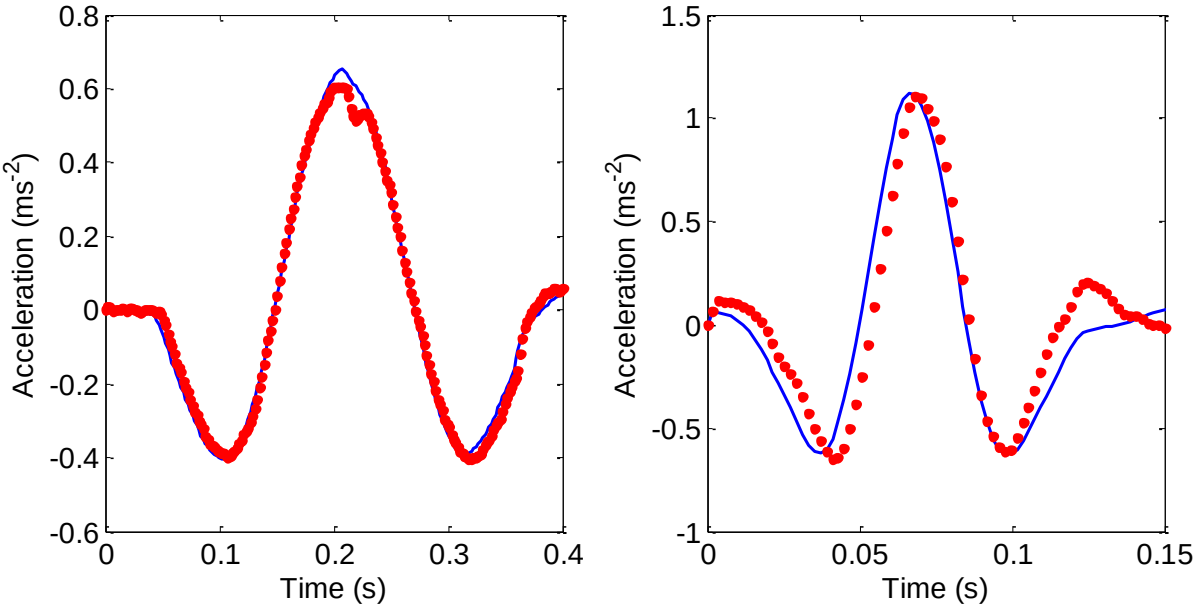

Figure 6.21 Comparison of fitted acceleration waveforms and measured acceleration waveforms (left: 4 Hz; right: 16 Hz). Data from one subject at low magnitude upward session. Output acceleration waveforms (——) and fitted output acceleration waveforms using a single degree-of-freedom time-domain model (●).

As should be expected, the error between the measured and the fitted acceleration waveforms was less with the two degree-of-freedom model than with the single degree-of-freedom model (Figures 6.5 and 6.6). However, this is not sufficient to conclude that the two degree-of-freedom model is better than the single degree-of-freedom model. The optimum stiffness and optimum damping of the single degree-of-freedom model had more distinct patterns of statistically significant negative correlations with the magnitude of shocks (Tables 6.2 and 6.3). This suggests the single degree-of-freedom model might be more useful for simple representations of the nonlinearity of the body. The less clear pattern with the greater number of variables in the two degree-of-freedom model suggests a more complex model is required to represent biodynamic responses of body exposed to a wide range of shock stimuli. Studies with vibration excitation have shown that the response of the body is much more complex than a single degree-of-freedom model (e.g., Kitazaki and Griffin, 1998; Matsumoto and Griffin, 2001; Nawayseh and Griffin, 2003).

At frequencies greater than 2.5 Hz, the optimum stiffness and the optimum damping in a single degree-of-freedom model of the response of the body to mechanical shocks were both positively correlated with the optimum stiffness and the optimum damping in the same model of response to random vibration (Figure 6.19). This shows subjects

with greater stiffness and greater damping in response to random vibration tend to also have greater stiffness and greater damping in response to shocks. However, the stiffness and damping were greater during random vibration – possibly because the random vibration contained more high frequency components and more low frequency components than any shock, resulting in greater optimum stiffness (Figure 6.8) and greater optimum damping (Figure 6.9).

The measured acceleration waveforms were more closely approximated by acceleration waveforms obtained by fitting the time-domain model to the response to each shock than by using the frequency-domain model fitted to the response to a single random vibration (compare Figures 6.5 and 6.20). The maximum median error overall stimuli is around 50% for the single degree-of-freedom time-domain model, and the maximum median error overall stimuli reaches up to 70% for the single degree-of-freedom frequency-domain model. However, whereas in the time-domain model there were 117 pairs of optimum stiffness and optimum damping, the frequency-domain model used only one value of stiffness and one value of damping to fit all 117 waveforms. The frequency-domain approach using the response to random vibration may be sufficient for practical application, but the time-domain approach is valuable for further investigating the frequency-dependence and magnitude-dependence biodynamic responses of the human body exposed to mechanical shocks.

6.4.2 Nonlinearity in the vertical nominal apparent mass

The study shows clear evidence of similar biodynamic nonlinearity in response to both mechanical shocks and random vibration. With shocks, as their magnitude increased from 0.05 $ms^{-1.75}$ to 2.0 $ms^{-1.75}$ VDV, the median resonance frequency of the nominal apparent mass reduced from 6.3 Hz to 4 Hz. With random vibration, as the magnitude of vibration increased from 0.1 to 1.6 ms^{-2} r.m.s., the median resonance frequency of the apparent mass reduced from 6.5 Hz to 4.5 Hz. This ‘softening’ behaviour is similar to that found previously with random vibration (e.g., Fairley and Griffin, 1989), with sinusoidal vibration (e.g., Hinz and Seidel, 1987; Zhen and Griffin, 2014), and a few shocks similar to those in the present study (Matsumoto and Griffin, 2005).

The stiffness and the damping of both an optimum single degree-of-freedom model and an optimum two degree-of-freedom model reduced with increasing shock magnitude, except for the lowest frequencies of shock (Tables 6.2 and 6.3). It has been suggested that passive thixotropy of soft tissues, rather than geometric nonlinearity of the body or either voluntary or involuntary muscular activity, is the most likely primary cause of the nonlinearity in biodynamic responses to whole-body vibration (e.g., Matsumoto and

Griffin, 2002; Huang and Griffin, 2008, 2009). The reduction in the stiffness and damping with increasing magnitudes of shock is consistent with the thixotropic explanation.

With shocks of constant vibration dose value, the optimum stiffness increased greatly as the frequency increased above 3.15 Hz (Figures 6.7 and 6.8). It can be seen that the optimum stiffness was more dependent on the nominal frequency of shock than the magnitude of the shock. The relative motion between body parts is dependent on the frequency of the excitation as well as the magnitude of the excitation, and tends to decrease with increasing frequency of excitation. The reduction in the relative displacement with increasing frequency of excitation may contribute to the increased equivalent stiffness at high frequencies, merely due to the nonlinearity of the body. However, the large increase in the optimum stiffness with increasing frequency is greater than would be expected if nonlinearity was the only explanation (see Figures 6.7 and 6.8). It seems likely that part of the increase in equivalent stiffness with increasing frequency arises because the model has been constrained to one or two degrees of freedom with fixed masses.

Previous studies have modelled the nonlinearity of the human body in the frequency domain with the Laplace transform. Since this is a linear operator, such models do not have nonlinear characteristics, merely different model parameters at different magnitudes. Nonlinear frequency-domain methods of modelling exist (e.g., Worden and Tomlinson, 2000), but their mathematical complexity is difficult to translate into physical meaning. The time-domain modelling method used in the present study (i.e., fitting model parameters directly using the motion equations) avoids these limitations. To model nonlinearities in biodynamic responses of the seated human body, explicit time-domain modelling may be simpler and more straightforward. Although the models used in present study are linear, they may be developed into nonlinear models by adding nonlinear elements. This allows the development of a single model that represents the biodynamic response with varying magnitudes, frequencies, and waveforms.

6.5 Conclusions

Notwithstanding the nonlinearity and complexity of the dynamic response of the human body, the relation between the force and the acceleration at the input to a seated person excited by vertical mechanical shocks can be well represented by either a single degree-of freedom model or a two degree-of-freedom model in which the

optimum stiffness and optimum damping vary with the magnitude of the shock and the nominal frequency of the shock. The optimum stiffness and optimum damping obtained with a time-domain model of response to shocks are correlated with the optimum stiffness and optimum damping obtained with a frequency-domain model of response to random vibration. The frequency-domain model can also been used to predict the biodynamic responses to mechanical shocks. Similar to biodynamic responses to whole-body random vibration and whole-body sinusoidal vibration, the resonance frequency evident in the equivalent apparent mass of the body during mechanical shocks reduces as the magnitude of the excitation increases.

Chapter 7 Discomfort caused by mechanical shocks

7.1 Introduction

The prediction of discomfort caused by whole-body vibration and mechanical shock has applications in the design and operation of land, sea, and air transport and civil engineering structures (e.g., buildings and bridges). In standardised methods of evaluating the severity of vibration, the dependence of discomfort on the frequency of vibration is reflected in frequency weightings derived from studies of responses to sinusoidal vibration. There have been few studies of the applicability of the frequency weightings to non-sinusoidal vibration.

For the evaluation of statistically stationary vibration, it is convenient to predict human responses to vibration from the root-mean-square of the frequency-weighted acceleration. However, because an 'average' measure is inappropriate for quantifying transients, including shocks, and the duration-dependence in r.m.s. averaging underestimates the severity of mechanical shocks, British Standard 6841 (1987) and International Standard 2631 (1997) suggest the severity of vibration containing mechanical shocks may be predicted from the vibration dose value:

$$\text{vibration dose value (VDV)} = \left[\int_{t=0}^{t=T} a_w{}^4(t)\,\mathrm{d}t \right]^{\frac{1}{4}} \qquad (7.1)$$

where $a_w(t)$ is the frequency-weighted acceleration and T is the period during which a person is exposed. If the frequency-dependence implicit in the frequency weighting, and the fourth-power duration-dependence implicit in the vibration dose value, are appropriate for all magnitudes and all directions, shocks will produce similar discomfort when their vibration dose values are similar.

The relation between the physical magnitude of a stimulus and the sensations it produces may be expressed by Stevens' power law, in which the 'objective magnitude', φ, of the stimulus and the 'subjective magnitude', ψ, of the response are assumed to be related by a power function:

$$\Psi = k\,\varphi^n \qquad (7.2)$$

The exponent, n, indicates the rate of growth of sensation with increasing magnitude of vibration and is often assumed to be constant for each type of stimulus (Stevens,

1975). However, experimental studies with whole-body vibration have found the rate of growth may vary with the frequency of vibration (e.g., Jones and Saunders 1974; Shoenberger, 1975; Morioka and Griffin, 2006a), the magnitude of vibration (e.g., Miwa, 1968; Shoenberger and Harris, 1971; Morioka and Griffin, 2006a), the direction of vibration (e.g., Ahn and Griffin 2008), and the duration of vibration (e.g., Miwa, 1968; Griffin and Whitham, 1980).

The dependence of the rate of growth of discomfort on the frequency of vibration means the frequency-dependence of vibration discomfort depends on the magnitude of vibration, referred to as a nonlinearity in subjective response (e.g., Matsumoto and Griffin, 2005; Morioka and Griffin, 2006a; Chapter 5). Although this implies frequency weightings should differ for low magnitude and high magnitude vibration this is not reflected in current standards where the same frequency weighting is used at all magnitudes (e.g., British Standards Institution, 1987; International Organization for Standardization, 1997). Considering the wide range of magnitudes experienced with mechanical shocks it is reasonable to question how well the vibration discomfort caused by mechanical shocks can be predicted using current frequency weightings.

Mechanical shocks may be considered to be vibration of very short duration. The discomfort caused by whole-body vibration increases if the duration of vibration is increased without any change in the magnitude or waveform of the motion. For example, the sensations produced by sinusoidal vibration have been reported to increase as the duration increases up to 2.0 s (for 2 – 60 Hz stimuli), and up to 0.8 s (for 60 - 200 Hz stimuli) (Miwa, 1968). Other studies with sinusoidal whole-body vertical vibration found that discomfort increased with increasing duration up to at least 32 s, with some variations in the rate of increase between vibration stimuli of 4, 8, 16, and 32 Hz (Griffin and Whitham, 1980). The slope of the duration-dependency was, very approximately, a fourth-power relationship such that a 16-fold increase in duration required a 2-fold reduction in vibration magnitude to maintain similar discomfort.

Investigating the discomfort caused by vertical mechanical shocks of various waveforms at nominal frequencies of 1, 4, and 16 Hz with vibration dose values ranging from 0.6 to 4.0 $ms^{-1.75}$, it was found that although discomfort depended on the frequency, duration, and direction of vibration, the rate of growth of discomfort, *n*, showed little variation, with a value close to unity in most conditions (Howarth and Griffin, 1991). For the conditions investigated, this suggested a frequency weighting for predicting the discomfort caused by mechanical shocks need not depend on the magnitude of the shocks. However, with subjects exposed to a wider range of vertical mechanical shocks (16 nominal frequencies from 0.5 to 16 Hz, five peak magnitudes

from ±0.28 to ±2.3 ms^{-2}, a range of damping ratios, and a reversed direction shock) the exponent, *n*, was later found to reduce progressively with increases in the nominal frequency of the shock up to about 8 Hz (Ahn and Griffin, 2008).

Biodynamic studies show that the mechanical responses of the body are also nonlinear, with the resonance frequencies in the apparent mass of the body reducing as the magnitude of vibration increases (e.g., Fairley and Griffin, 1989; Mansfield and Griffin, 2000). Some of the nonlinearity in the biodynamic response is similar to some of the nonlinearity in the subjective response (e.g., Matsumoto and Griffin, 2005; Chapter 5), but it is not clear to what extent the biodynamic nonlinearities explain the nonlinearities in subjective responses.

It might be expected that the direction of a shock (i.e., upward or downward) will have a large effect on discomfort, but more than one study has found that subjective responses to upward shocks are similar to subjective responses to downward shocks of the same magnitude and waveform. Using the transient response of a single-degree-of-freedom damped systems to a step input (giving damped sine waves at nominal frequencies of 1, 4, or 16 Hz, with damping ratios of 0.125, 0.250 and 0.707 and VDVs ranging from 0.6 to 4.0 $ms^{-1.75}$), no large differences were found in subjective responses to upward and downward shocks (Howarth and Griffin, 1991). Using the transient response of single degree-of-freedom damped systems to half-sine force inputs (with 16 nominal frequencies from 0.5 to 16 Hz and four damping ratios from 0.05 to 0.4), equivalent comfort contours for upward shocks were also found to be similar to those for downward shocks (Ahn and Griffin, 2008).

This study was designed to determine the frequency-dependence of the rate of growth of discomfort and equivalent comfort contours for both acceleration and force measured at the surface supporting the seated human body during exposure to vertical mechanical shocks. It was hypothesised that the discomfort caused by mechanical shocks would depend on the nominal frequency of the shock, the magnitude of the shock, and the direction of the shock. Assuming part of the nonlinearity in subjective responses is caused by biodynamic nonlinearity, it was hypothesised that equivalent comfort contours expressed in terms of dynamic force would show less nonlinearity than equivalent comfort contours expressed in terms of acceleration.

7.2 Method

7.2.1 Apparatus

A 1-metre stroke vertical electrohydraulic vibrator generated vertical vibration of a flat rigid seat. An accelerometer (Silicon Design 2260-002) mounted on the seat measured acceleration in the direction of excitation. A force platform (Kistler 9281B) mounted on the seat measured force at the interface between the seat (i.e., top surface of the force platform) and the subject in the vertical direction. The effect of the mass of the top plate of the force platform was eliminated by subtracting from the measured vertical force the measured vertical acceleration multiplied by the mass of the top plate (i.e., 31.5 kg) in the time domain (i.e., mass cancellation). The vibrator was controlled by a Servotest Pulsar system that generated mechanical shocks. The resultant acceleration and force were acquired to a separate computer using an *HVLab* data acquisition and analysis system (version 1.0).

Subjects sat on the seat without making contact with the backrest (Figure 7.1). They rested their feet on a footrest that was attached to the vibrator table. The footrest was adjusted so that the upper surfaces of the upper legs were horizontal.

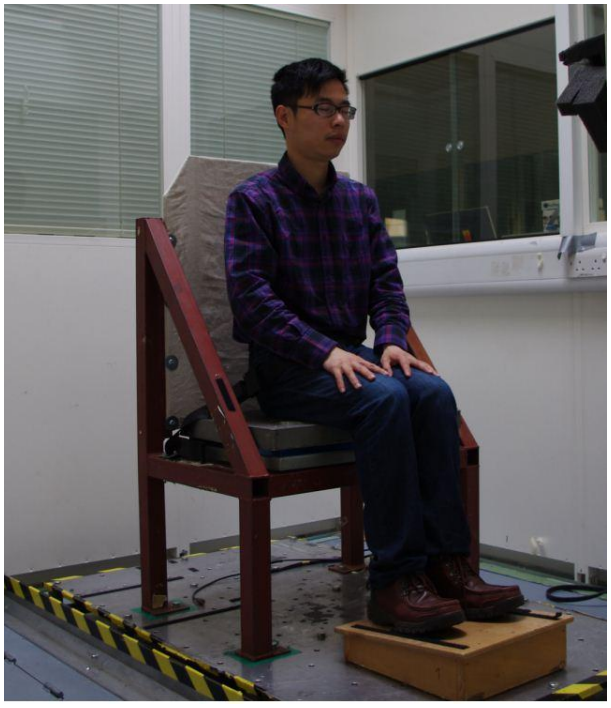

Figure 7.1 Experimental setup

7.2.2 Subjects

Twenty male subjects, students at the University of Southampton, participated in the study. The median subject age was 24.5 years (range 22-33 years), the median subject mass was 71.1 kg (range 48-107 kg), and the median stature was 1.75 m (range 1.65-1.97 m).

Subjects were exposed to white noise at 65 dB(A) via a pair of headphones. During exposure to shocks, subjects were asked to close their eyes to prevent vision affecting their reaction to the motion.

The experiment was approved by the Human Experimentation Safety and Ethics Committee of the Institute of Sound and Vibration Research at the University of Southampton. Informed consent to participate in the experiment was given by all subjects.

7.2.3 Shocks

To obtain the shock acceleration waveforms, sinusoidal waveforms with 1½ cycles were modulated by a half cycle sinusoid with a period three times longer than the period of the sinusoidal acceleration (Figure 7.2).

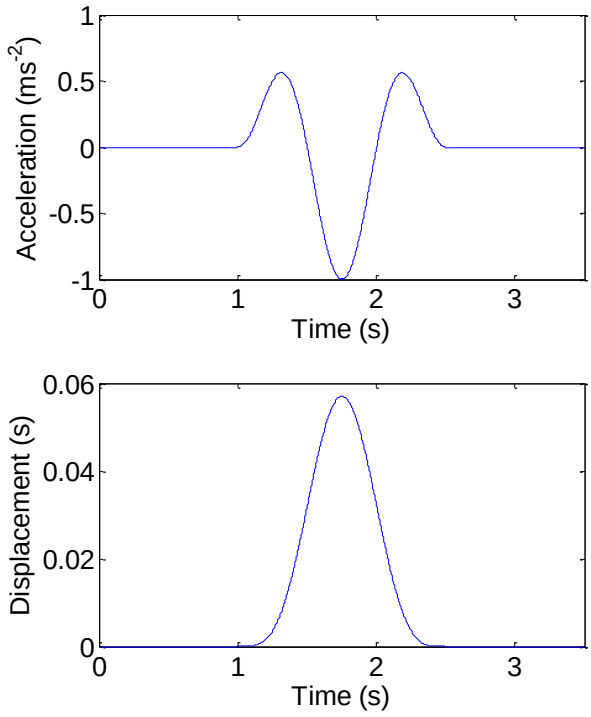

Figure 7.2 Example acceleration and displacement waveforms of the shocks used in the experiment.

The frequencies of the sinusoidal waveforms were at 13 preferred one-third octave centre frequencies from 1.0 to 16 Hz. The study was conducted with a range of 'lower magnitude' shocks and a range of 'higher magnitude' shocks (Table 7.1). With both ranges, at each nominal frequency the shock was presented at nine magnitudes with peak values adjusted to produce the same frequency-weighted VDV at each frequency. The 'W_b' weighting was used so that, in accord with to BS 6841 (1987), shocks with the same VDV would be expected to produce similar discomfort.

7.2.4 Experiment design

Subjects attended four 15-minute sessions on two different days. On each day, in one session they experienced 117 vertical shocks in the upward direction (i.e., an upward displacement as shown in Figure 7.2) and in the other session they experienced 117 vertical shocks in the downward direction. Subjects were exposed to the lower magnitude shocks on one day, and exposed to the higher magnitude shocks on the other day. During all sessions, the shocks were presented in a completely random order. The four sessions are referred to as 'high magnitude upward session', 'high magnitude downward session', 'low magnitude upward session', and 'low magnitude downward session'.

The absolute method of magnitude estimation was used. Subjects were asked to estimate the subjective magnitude (i.e., the discomfort) for each stimulus using any numerical value, but with greater values for greater discomfort. In each day, before the experiment commenced, the subjects practiced magnitude estimation by rating the lengths of lines drawn on paper and then practiced judging the discomfort caused by some of the shocks included in the experiment so as to become familiar with the experimental procedure and the sensations produced by the range of stimuli used in the experiment.

7.2.5 Analysis

For each session, the subjective responses of each individual subject were normalised by dividing each magnitude estimate by the median of the 117 magnitude estimates.

Table 7.1 Unweighted peak accelerations corresponding to the frequency-weighted vibration dose values of the stimuli used at each frequency (ms^{-2}).

	Lower magnitude session									Higher magnitude session								
VDV ($ms^{-1.75}$)	0.05	0.063	0.08	0.1	0.125	0.16	0.2	0.25	0.315	0.315	0.4	0.5	0.63	0.8	1.0	1.25	1.6	2.0
Frequency (Hz)	Peak acceleration (ms^{-2} r.m.s.)																	
1.0	0.2	0.25	0.32	0.40	0.50	0.64	0.8	1.00	1.26	1.26	1.60	2.00	2.52	3.20	4.00	4.99	6.39	7.99
1.25	0.21	0.26	0.33	0.41	0.51	0.66	0.82	1.03	1.30	1.30	1.65	2.06	2.6	3.30	4.12	5.15	6.59	8.24
1.6	0.21	0.26	0.33	0.41	0.52	0.66	0.83	1.03	1.30	1.30	1.65	2.07	2.61	3.31	4.14	5.17	6.62	8.27
2.0	0.19	0.24	0.31	0.39	0.48	0.62	0.77	0.97	1.22	1.22	1.55	1.94	2.44	3.10	3.87	4.84	6.19	7.74
2.5	0.17	0.21	0.27	0.34	0.42	0.54	0.68	0.84	1.06	1.06	1.35	1.69	2.13	2.70	3.38	4.22	5.41	6.76
3.15	0.14	0.18	0.23	0.29	0.36	0.46	0.57	0.72	0.90	0.90	1.15	1.44	1.81	2.30	2.87	3.59	4.59	5.74
4.0	0.13	0.16	0.20	0.25	0.32	0.41	0.51	0.63	0.80	0.80	1.01	1.27	1.60	2.03	2.53	3.17	4.06	5.07
5.0	0.12	0.15	0.19	0.24	0.30	0.39	0.48	0.60	0.76	0.76	0.96	1.20	1.52	1.93	2.41	3.01	3.85	4.81
6.3	0.12	0.15	0.19	0.24	0.30	0.39	0.48	0.61	0.76	0.76	0.97	1.21	1.53	1.94	2.42	3.03	3.88	4.85
8.0	0.13	0.16	0.21	0.26	0.32	0.41	0.51	0.64	0.81	0.81	1.03	1.28	1.62	2.05	2.56	3.21	4.10	5.13
10.0	0.14	0.18	0.22	0.28	0.35	0.45	0.56	0.70	0.88	0.88	1.12	1.40	1.76	2.24	2.80	3.50	4.48	5.59
12.5	0.16	0.20	0.25	0.31	0.39	0.50	0.63	0.78	0.99	0.99	1.25	1.57	1.97	2.51	3.13	3.92	5.02	6.27
16.0	0.18	0.23	0.29	0.37	0.46	0.59	0.73	0.92	1.15	1.15	1.47	1.83	2.31	2.93	3.66	4.58	5.86	7.33

For each subject, at each fundamental frequency of shock, the relation between the vibration dose value, φ, and the individual magnitude estimate of discomfort, Ψ, was determined using Stevens' Power law. Linear regression was performed at each frequency after logarithmic transformation of Equation (7.1) to:

$$\log_{10} \Psi = n.\log_{10} \varphi + \log_{10} k \quad (7.2)$$

The apparent masses of the subjects exposed to the same mechanical shocks are reported in Chapter 6. The association between subjective responses and biodynamic responses was investigated by calculating correlations between the ratio of the vertical apparent mass at two frequencies and the ratio of the subjective response at the same two frequencies. The ratios were calculated for all possible pairs of frequencies for all subjects when exposed to the middle magnitude of vibration in each of the three sessions.

7.3 Results

7.3.1 Rate of growth of discomfort

The medians and inter-quarter ranges of the exponent, *n*, at each frequency for all four sessions (i.e., low magnitude upward, low magnitude down, high magnitude upward, and high magnitude downward) are shown in Figure 7.3. For all four sessions, the exponent *n* varied with the fundamental frequency of the shocks ($p<0.001$; Friedman, Table 7.2). There was no significant difference in the exponent, *n*, between upward and downward shocks, or between low magnitude and high magnitude shocks, at any frequency ($p>0.05$, Wilcoxon).

The median and inter-quartile range of the exponent, *n*, for force at each frequency for both directions and both magnitudes are shown in Figure 7.4. For all four sessions, the force exponent, *n*, varied with the fundamental frequency of the shocks ($p<0.001$, Friedman; Table 7.2). Similar to the exponent for acceleration, at each frequency there was also no significant difference in the exponent between upward and downward shocks, or between low magnitude and high magnitude shocks ($p>0.05$, Wilcoxon).

There was no significant difference in the exponent, *n*, between acceleration and force with either direction of shock or either magnitude of shock, at any of the 13 frequencies ($p>0.05$ Wilcoxon).

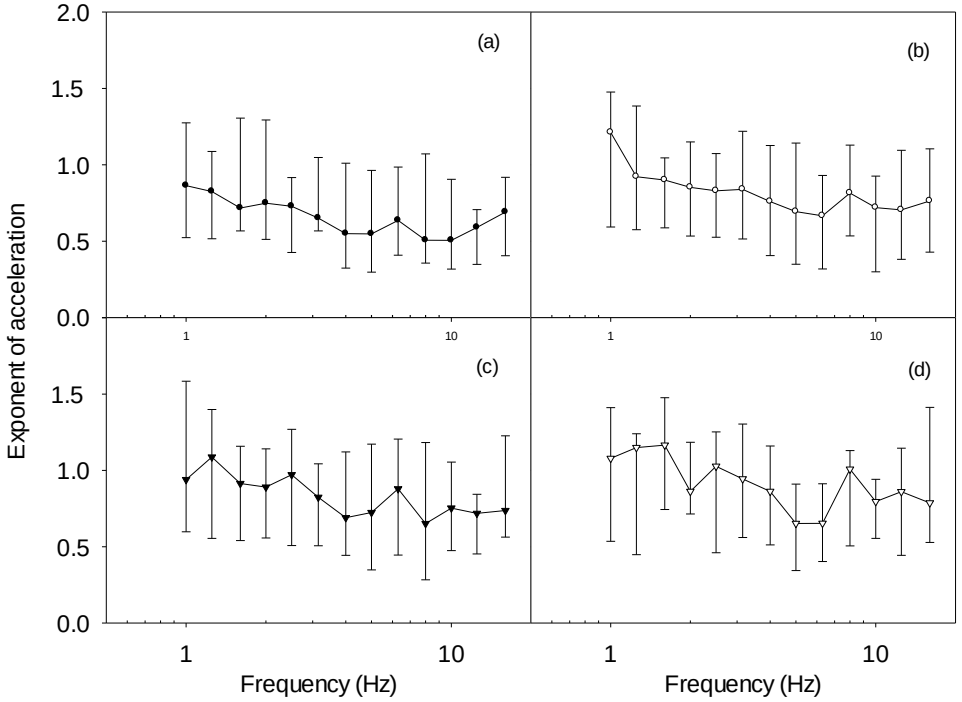

Figure 7.3. The rate of growth of discomfort, *n,* for vertical vibration acceleration : (a) higher magnitude upward shocks; (b) higher magnitude downward shocks; (c) lower magnitude upward shocks; (d) lower magnitude downward shocks. Medians and inter-quarter ranges from 20 subjects.

Table 7.2 Median exponents, *n*, for acceleration and force in each session.

Frequency	Exponent for acceleration				Exponent for force			
	Higher magnitude		Lower magnitude		Higher magnitude		Lower magnitude	
	upward	downward	upward	downward	upward	downward	upward	downward
1	0.79	0.76	0.94	0.89	0.76	0.77	0.96	0.89
1.25	0.79	0.82	0.95	1.01	0.77	0.81	1.02	1.02
1.6	0.68	0.84	0.91	1.05	0.66	0.85	0.86	1.05
2	0.75	0.85	0.89	0.88	0.71	0.86	0.90	0.89
2.5	0.68	0.76	0.95	0.87	0.66	0.76	0.87	0.83
3.15	0.63	0.82	0.82	0.64	0.64	0.82	0.78	0.65
4	0.52	0.69	0.73	0.70	0.56	0.69	0.76	0.62
5	0.49	0.69	0.72	0.66	0.52	0.71	0.68	0.61
6.3	0.57	0.64	0.77	0.56	0.65	0.68	0.70	0.59
8	0.50	0.78	0.70	0.77	0.48	0.83	0.63	0.79
10	0.39	0.70	0.69	0.61	0.44	0.76	0.51	0.53
12.5	0.55	0.65	0.75	0.89	0.63	0.75	0.78	0.86
16	0.68	0.52	0.61	0.73	0.73	0.59	0.65	0.77

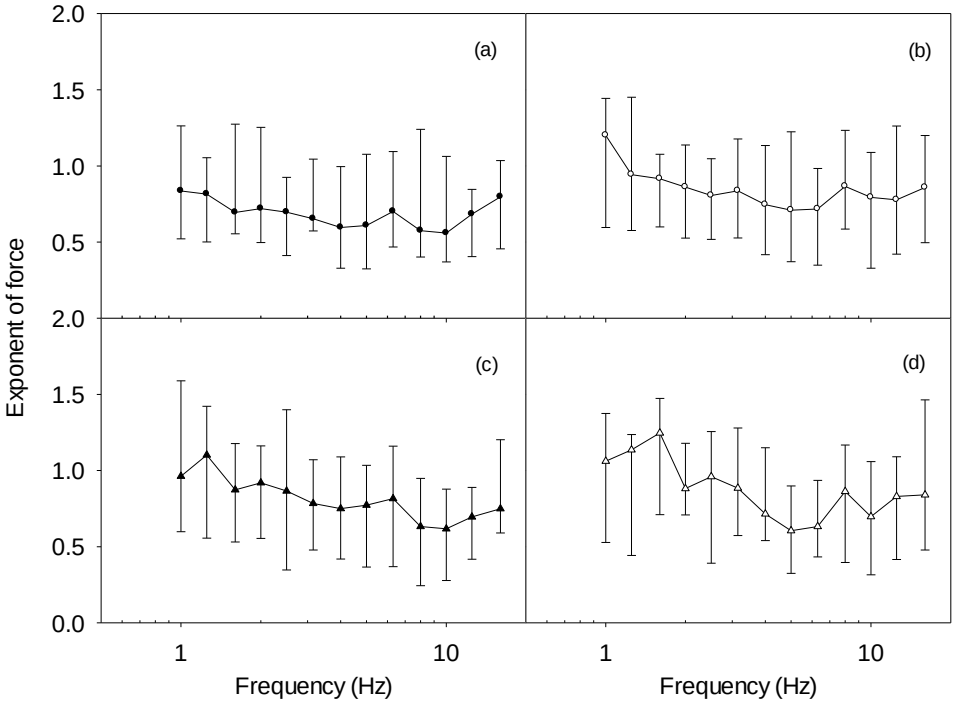

Figure 7.4 The rate of growth of discomfort, *n,* for vertical vibration force: (a) higher magnitude upward shocks; (b) higher magnitude downward shocks; (c) lower magnitude upward shocks; (d) lower magnitude downward shocks. Medians and inter-quarter ranges from 20 subjects.

7.3.2 Equivalent comfort contours

Equivalent comfort contours were determined for each subject by calculating the vibration magnitude, φ, corresponding to nine subjective magnitudes, ψ, from 40 to 250 at each vibration frequency (from 1 to 16 Hz) using equation (7.1). The magnitude of vibration (either acceleration or force) was expressed using the vibration dose value (with no frequency weighting). The equivalent comfort contours show the vibration magnitudes required to produce the same strength of sensation across the frequency range.

With both directions of shock and both magnitudes of shock, the acceleration equivalent comfort contours for all sensation magnitudes varied with the fundamental frequency of the shock (p<0.0001, Friedman; Figure 7.5). The acceleration equivalent comfort contours tended to reduce (i.e., the shocks became more uncomfortable) as the fundamental frequency increased from 1 to 5 Hz, and then remained roughly constant to 16 Hz.

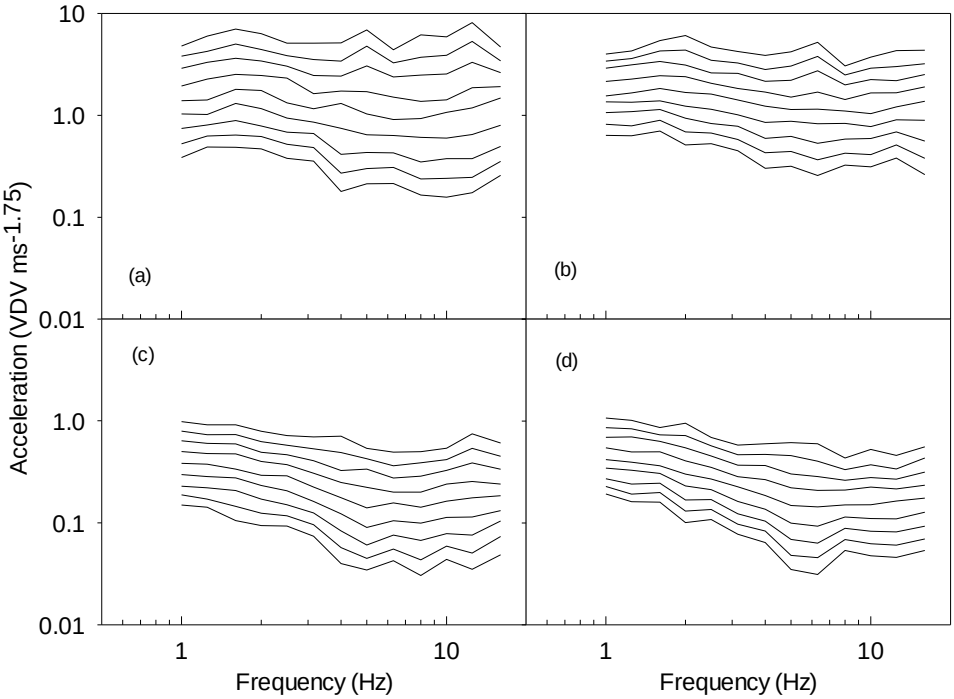

Figure 7.5 Acceleration equivalent comfort contours for shocks: (a) higher magnitude upward shocks; (b) higher magnitude downward shocks; (c) lower magnitude upward shocks; (d) lower magnitude downward shocks. Contours are for subjective magnitudes, ψ, of 40, 50, 63, 80, 100 125, 160, 200 and 250. Vibration dose values for acceleration without frequency weighting. Median values from 20 subjects.

Equivalent comfort contours for force also varied with the fundamental frequency of the shocks for both directions of shock and both magnitudes of shock (p<0.0001, Friedman; Figure 7.6).

Generally, the equivalent comfort contours for force reduce as the frequency increases from 1 to 16 Hz. Subjects showed greatest sensitivity to force at 16 Hz, except with the lowest magnitudes of vibration.

7.3.3 Effect of shock direction

Equivalent comfort contours for upward and downward shocks are compared for acceleration and force in Figure 7.7. There is no evidence of a consistent difference in the magnitude estimates for upward and downward shocks at either low or high magnitudes (p>0.05, Wilcoxon).

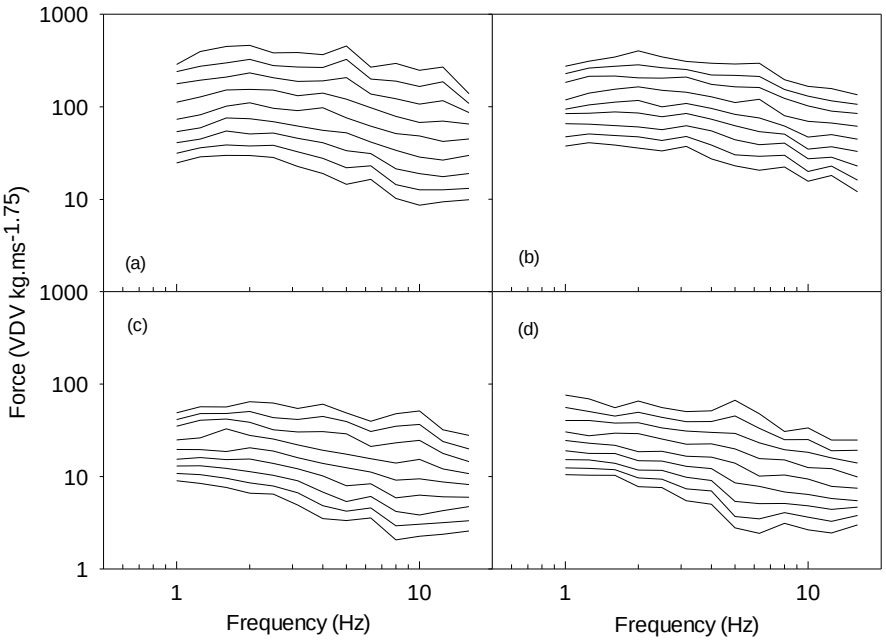

Figure 7.6 Force equivalent comfort contours for shcoks: (a) higher magnitude upward shocks; (b) higher magnitude downward shocks; (c) lower magnitude upward shocks; (d) lower magnitude downward shocks. Contours are for subjective magnitudes, ψ, of 40, 50, 63, 80, 100 125, 160, 200 and 250. Vibration dose values for force without frequency weighting.

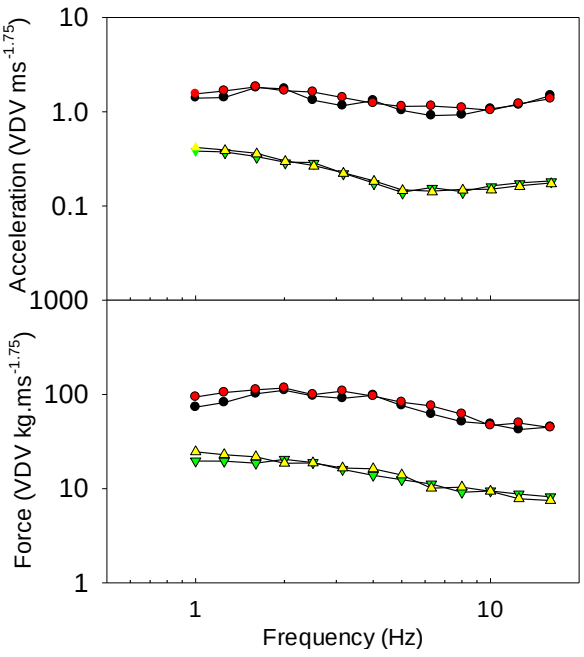

Figure 7.7 Comparison of equivalent comfort contours for upward and downward shocks: acceleration (upper figure) and force (lower figure); ●: higher magnitude upward shocks; ●: higher magnitude downward shocks; ▼: lower magnitude upward shocks; ▲: lower magnitude downward shocks. Median equivalent comfort contours from 20 subjects for ψ = 100.

7.3.4 Location of discomfort

Most discomfort was generally felt in either the buttocks or the thighs (Figure 7.8). As the shock magnitude increased, the location of most discomfort tended to move from the lower-body to the upper-body.

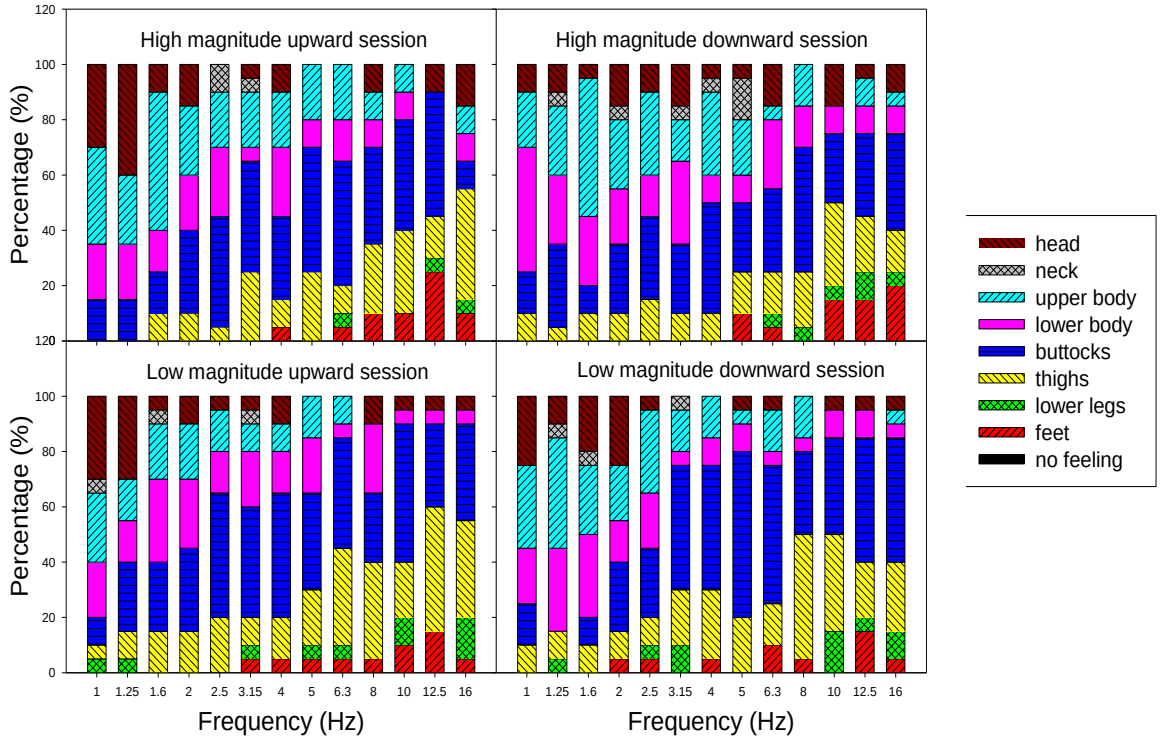

Figure 7.8 Locations of discomfort arising from exposure to vertical shocks: lower magnitude shocks (lower figures), higher magnitude shocks (upper figures); upward shocks (left figures); downward shocks (right figures).

7.3.5 Association between relative discomfort and normalised apparent mass

After adjustment for multiple comparisons, there was no clear pattern of statistically significant correlations between the relative apparent mass and the relative subjective response between any pair of frequencies for either upward or downward shocks of either low or high magnitude.

7.4 Discussion

7.4.1 Vibration discomfort for acceleration

The rate of growth of discomfort (the exponent *n* in Stevens' Power Law) varied with the fundamental frequency of the shocks, tending to reduce as the fundamental

frequency increased from 1 to 10 Hz (Figure 7.3). This is consistent with Ahn and Griffin (2008) who found the exponent reduced as the frequency increased from 0.5 to 8 Hz. In both studies there is a hint of an increase in the exponent as the frequency increases further to 16 Hz (Figure 7.9).

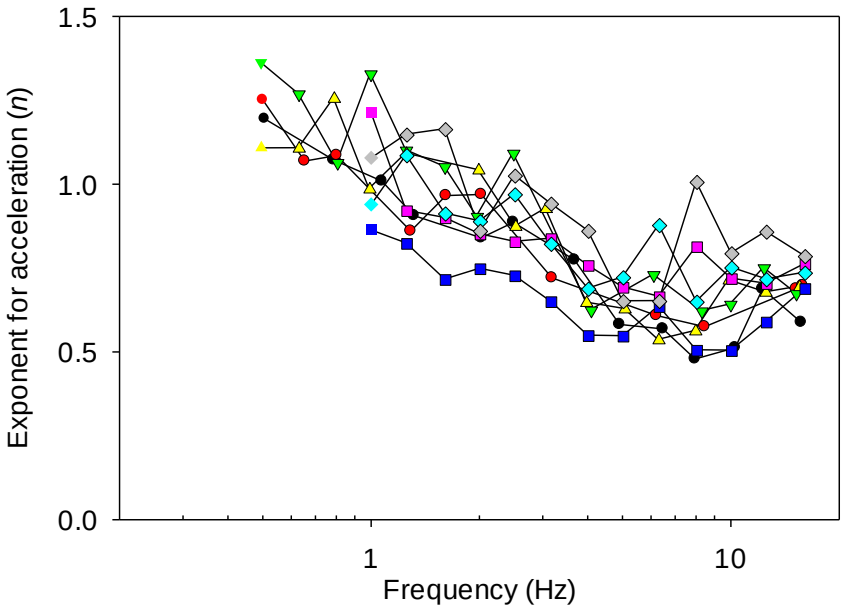

Figure 7.9 Comparison of rate of growth of discomfort, *n*, in two studies with shocks: present study and Ahn and Griffin (2008):●: Ahn and Griffin (2008) ζ=0.1; ●: Ahn and Griffin (2008) ζ=0.2; ▼: Ahn and Griffin (2008) ζ=0.4 ; ▲: Ahn and Griffin (2008) ζ=0.4(r); ■:Present study (higher magnitude upward shocks); ■:Present study (higher magnitude downward shocks); ♦: Present study (lower magnitude upward shocks); ♦:Present study (lower magnitude downward shocks).

The rates of growth of discomfort obtained with vertical shocks in this study are compared with those obtained previously using vertical sinusoidal vibration (Figure 7.10). It may be seen that the exponents are greater with sinusoidal vibration over the frequency range 2.5 to 5 Hz. All the factors influencing the rate of growth are not known, but the present finding suggest there is scope for greater understanding of how shock waveform influences the growth of discomfort with increasing shock magnitude.

Because the rate of growth of discomfort (i.e., the exponent *n*) for acceleration varied with the frequency of the vibration (Figure 7.3), the shapes of the equivalent comfort contours varied with the magnitude of the shocks (i.e., the acceleration equivalent comfort contours are not parallel, as seen in Figure 7.5).

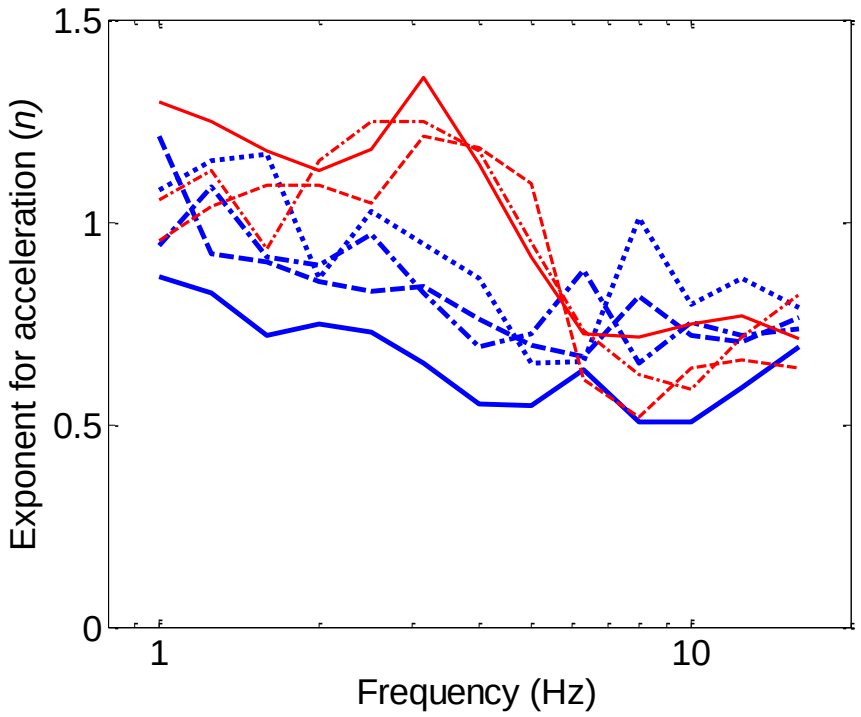

Figure 7.10 Comparison of rate of growth of discomfort, *n*, in present study with shocks and previous study with sinusoidal vibration (Chapter 5). Shocks: ——: higher magnitude upward shocks; — —: high magnitude downward shocks; —•—: lower magnitude upward shocks; • • • : lower magnitude downward shocks. Sinusoidal vibration: ——: higher magnitude sinusoidal vibration ; — —: medium magnitude sinusoidal vibration; —•—:lower magnitude sinusoidal vibration.

Expressed in terms of vibration dose values, the magnitudes of the shocks used by Ahn and Griffin (2008) are similar to those employed in the high magnitude session of the present study. Their equivalent comfort contours (obtained with various damping ratios and both upward and downward shocks) are compared with the equivalent comfort contours for the high magnitude upward and downward shocks in the present study in Figure 7.11. Although the shock waveforms (and therefore the frequency content of the shocks) differed, the equivalent comfort contours have similar characteristics, especially for shocks produced with a high damping ratio (i.e., ζ=0.4).

Equivalent comfort contours for shocks are compared with those previously obtained for sinusoidal vibration by normalising each contour to unity at 1 Hz (Figure 7.12). For both shocks and sinusoidal vibration, greater magnitudes are needed to produce vibration discomfort at the lower frequencies (less than about 4 Hz) than at the higher frequencies (i.e., greater than about 4 Hz). At the higher frequencies, greater magnitudes are required from shocks than from sinusoidal vibration to cause similar discomfort.

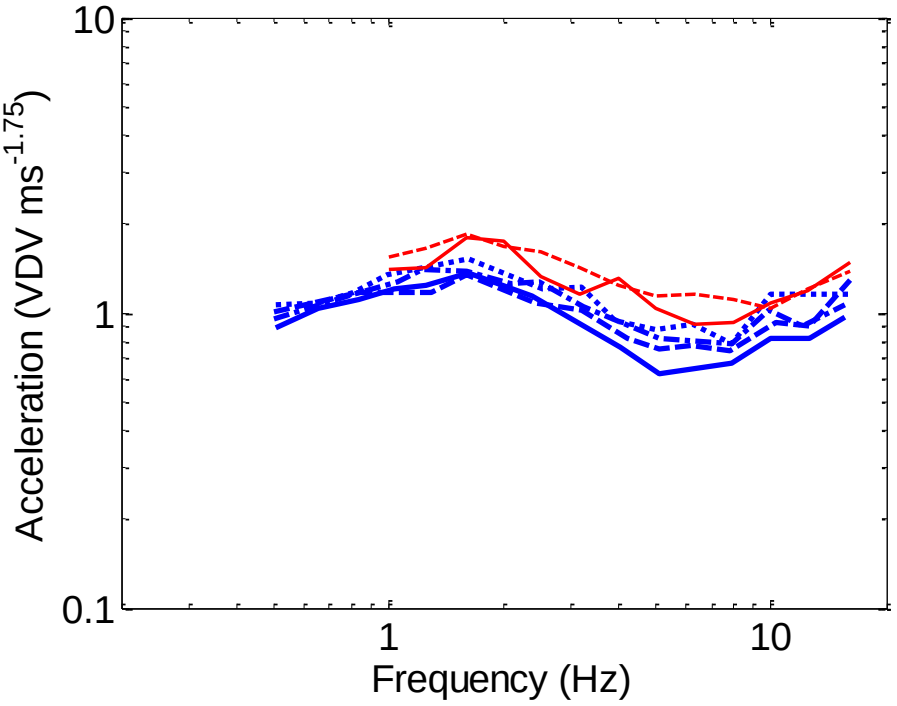

Figure 7.11 Frequency-dependence of equivalent comfort contours for acceleration: ——: Ahn and Griffin (2008) ζ=0.1; — —: Ahn and Griffin (2008) ζ=0.2; —•—: Ahn and Griffin (2008) ζ=0.4; • • •: Ahn and Griffin (2008) ζ=0.4(r); ——: Present study (high magnitude upward); — —: Present study (high magnitude downward). Vibration dose values for acceleration without frequency weighting.

There are several reasons why the equivalent comfort contours for shock differ from those for sinusoidal vibration. The sinusoidal contours were obtained with 6-s periods of motion and were expressed in terms of r.m.s. values, but because the duration was the same at all frequencies the ratio between r.m.s. values and vibration dose values does not depend on the frequency of the vibration. The shock contours were obtained using shocks whose duration reduced with increasing frequency and are expressed in terms of vibration dose values. If the time-dependency in the vibration dose value is appropriate, the effect of differing durations is nulled by comparing the contours in terms of vibration dose values, as in Figure 7.12. Whereas the sinusoidal vibrations were well-dominated by a single frequency, all the shocks contained energy at frequencies both greater than and less than their fundamental frequency. With shocks having fundamental frequencies less than about 4 Hz, the presence of the higher frequencies will have heightened sensitivity and reduced the equivalent comfort contours at the lower frequencies. With shocks having nominal frequencies greater than about 4 Hz, the presence of some energy at lower frequencies will have reduced sensitivity and so raised the equivalent comfort contours for shocks at these higher

frequencies. The four equivalent comfort contours for shocks in Figure 7.12 differ according to the shock magnitude: the nonlinearity in equivalent comfort contours for both shocks and sinusoidal vibration is another reason why the equivalent comfort contours for shock differ from those previously obtained for sinusoidal vibration.

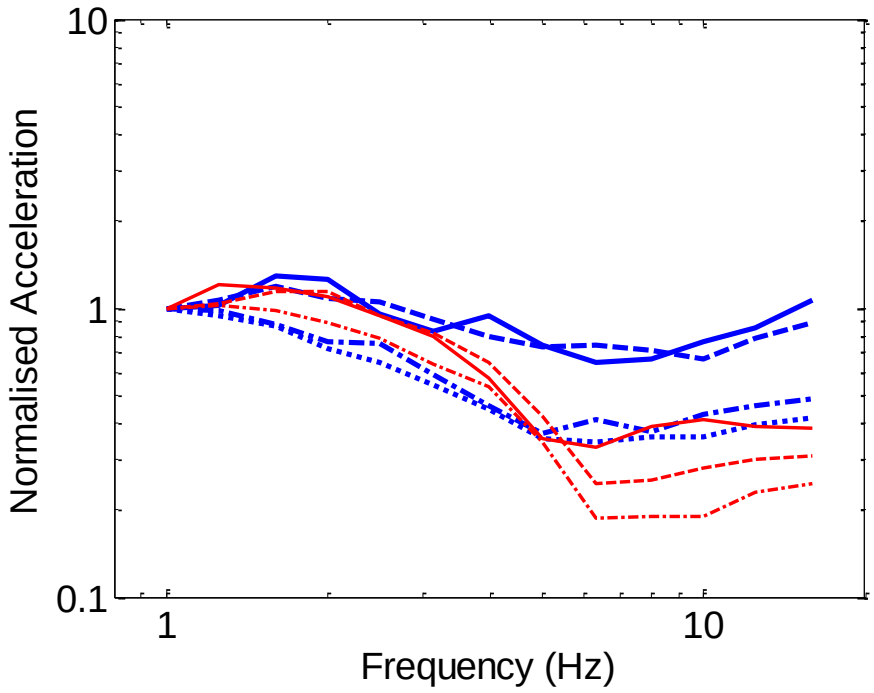

Figure 7.12 Comparison of acceleration equivalent comfort contours for shocks in the present study with equivalent comfort contours for sinusoidal vibration (from Chapter 5). Values are normalised to unity at 1 Hz (The shock equivalent comfort contours are based on VDV, and the sinusoidal equivalent comfort contours are based on r.m.s. values). Shocks: ——: higher magnitude upward shocks; — —: high magnitude downward shocks; —•—: lower magnitude upward shocks; • • • : lower magnitude downward shocks. Sinusoidal vibration: ——: higher magnitude sinusoidal vibration ; — —: medium magnitude sinusoidal vibration; —•—: lower magnitude sinusoidal vibration.

According to BS 6841:1987 and ISO 2631-1:1997, shocks with the same frequency-weighted VDV should produce similar discomfort. The median subjective responses obtained with shocks having the same W_b-weighted VDV over the full range of fundamental frequencies (1 to 16 Hz) and over the full range of shock magnitudes (0.05 to 2 $ms^{-1.75}$) are shown in Figure 7.13. Although some of the contours are flat (as expected if the frequency-weighted VDV provides a good prediction), some are not. The contours are consistent with the need for different frequency weightings at different magnitudes if shocks are to be evaluated over a wide range of magnitudes. Separate analysis (not shown) confirmed that the W_b-weighted VDV contours in Figure 7.12 were

more flat than equivalent contours obtained using unweighted VDV, r.m.s., or peak values.

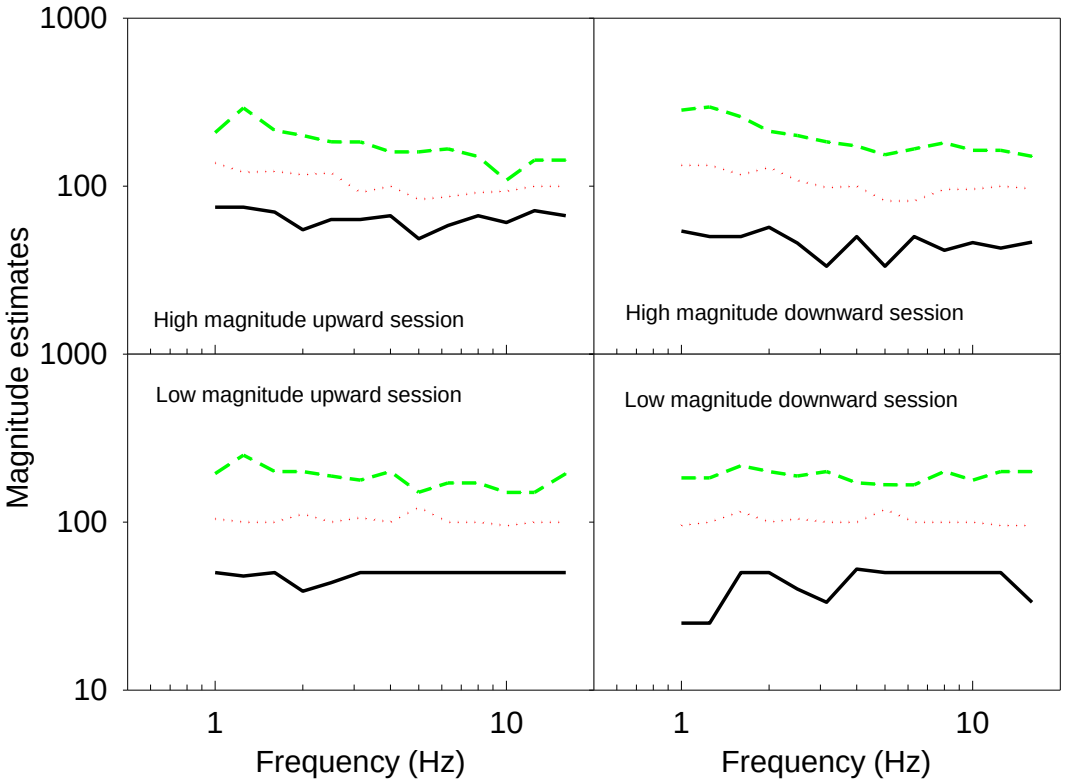

Figure 7.13 Magnitude estimates for shocks having the same frequency-weighted vibration dose values (using weighting W_b). Higher magnitude shocks: —— 0.315 $ms^{-1.75}$; ···: 0.8 $ms^{-1.75}$; – – –: 2.0 $ms^{-1.75}$; lower magnitude shocks: —— 0.05 $ms^{-1.75}$; ···: 0.125 $ms^{-1.75}$; – – –: 0.315 $ms^{-1.75}$. Median values from 20 subjects.

7.4.2 Vibration discomfort for force

Similar to the exponent for acceleration, the rate of growth of sensation for force varied with frequency (Figure 7.4). The minimum exponent tended to be around 10 Hz and so the force equivalent comfort contours show the greatest spread around 10 Hz (Figure 7.6).

With vertical sinusoidal whole-body vibration, force equivalent comfort contours have been found to be less nonlinear than acceleration equivalent comfort contours (Chapter 5). However, in the current study with mechanical shocks there were no differences in the exponent, *n*, between acceleration and force with either direction of shock or with any magnitude of shock at any of the 13 frequencies. This might be explained by the mechanical shocks having energy at all frequencies and not only at their nominal frequencies (Figure 7.14).

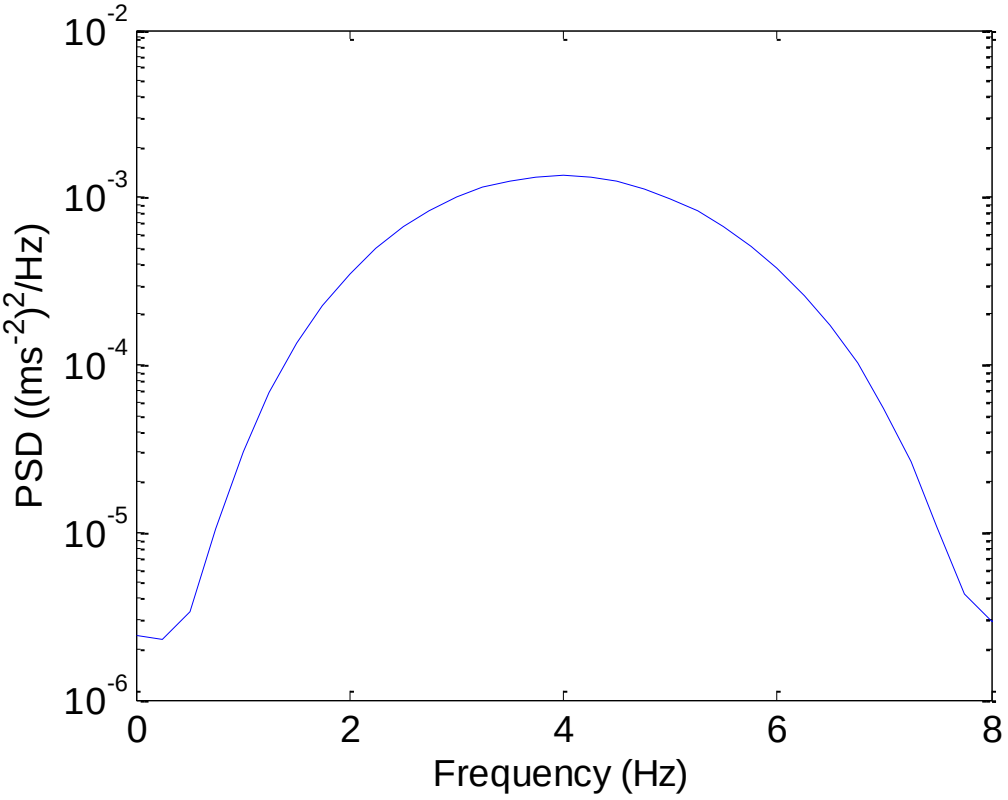

Figure 7. 14 Example of spectrum of a shock (with a fundamental frequency at 4 Hz).

Force equivalent comfort contours for shocks are compared with force equivalent comfort contours previously obtained for sinusoidal vibration (both normalised to unity at 1 Hz) in Figure 7.15. The comparison is broadly similar to that shown for acceleration in Figure 7.12. However, the contours differ less and the nonlinearity has resulted in the force contour for the lowest magnitude of shock being similar to force contours obtained with sinusoidal vibration.

7.4.3 Association between subjective and biodynamic response

An association between subjective responses and biodynamic responses might allow biodynamic measurements to be used to predict subjective responses. With sinusoidal vibration, distinct patterns of positive correlations have been found between the ratios of the apparent mass at pairs of frequencies and the ratios of subjective responses at these frequencies (Chapter 5). Such correlations were not found in the present study with mechanical shocks. This may be explained by the mechanical shocks having components at frequencies other than at the fundamental frequency of the shocks. The present findings do not allow any useful prediction of individual discomfort from the biodynamic responses of individuals.

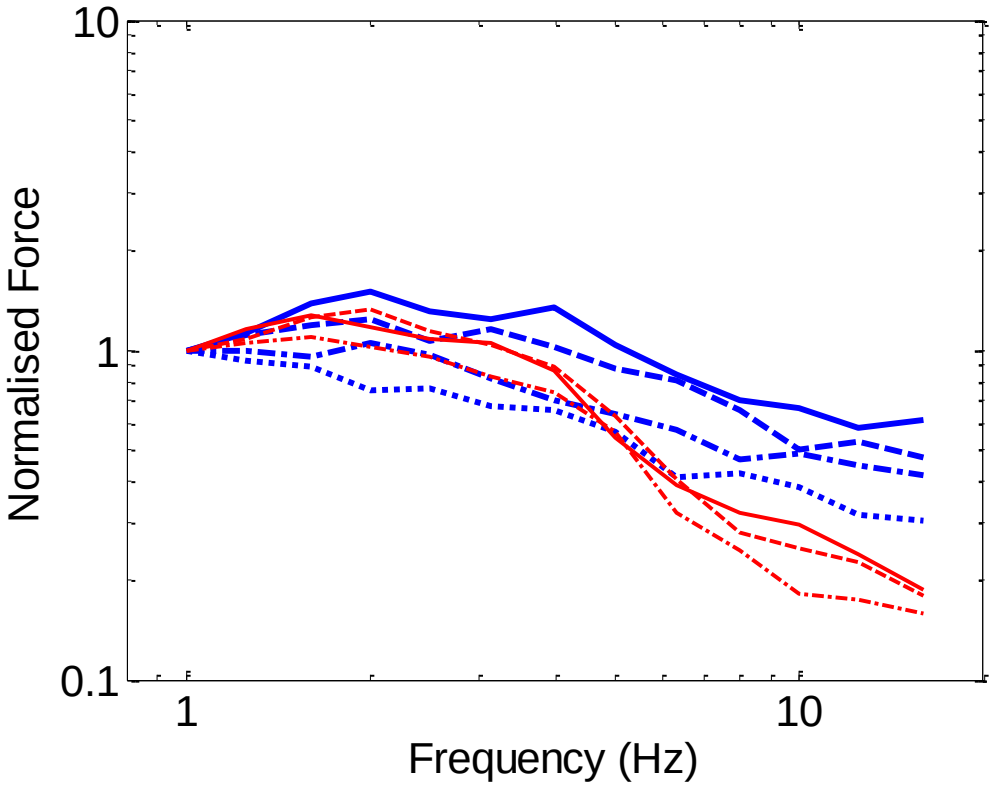

Figure 7. 15 Equivalent comfort contours for force from the present study with mechanical shocks compared with equivalent comfort contours for sinusoidal vibration (from Chapter 5). Values are normalised to unity at 1.0 Hz (The shock equivalent comfort contours are based on VDV, and the sinusoidal equivalent comfort contours are based on r.m.s. values). Shocks: ——: high magnitude upward session; — —: high magnitude downward session; —•—: low magnitude upward session; • • • : low magnitude downward session. Sinusoidal vibration: ——: high magnitude session ; — —: medium magnitude session ; —•—:low magnitude session.

7.5 Conclusions

For vertical whole-body mechanical shocks, the rate of growth in discomfort with increases in both acceleration and force depend on the frequency of vibration, but with no large difference in the rate of growth in discomfort between force and acceleration or between upward and downward shocks at the magnitudes investigated (peak unweighted accelerations at magnitudes up to about 8 ms^{-2} in the frequency range 1.0 to 16 Hz).

The frequency-dependence of the discomfort of seated people exposed to vertical shocks shows greatest sensitivity to acceleration at frequencies between about 5 and 12.5 Hz, but with a frequency-dependence that varies with shock magnitude and may

be expected to vary with shock waveform. No frequency weighting can accurately predict the discomfort caused by mechanical shocks over a large range of magnitudes, but frequency weighting W_b as defined in current standards provided a reasonable estimate of the relative discomfort caused by the shocks investigated in this study.

Chapter 8 Subjective responses to whole-body vertical vibration with rigid and soft seats

8.1 Introduction

When a person sits on a soft seat, the vibration acceleration they experience depends on the transmissibility of the seat, so most studies of equivalent comfort contours have used rigid seats that allow similar results to be obtained in other studies (e.g., Griffin *et al*., 1982; Oborne and Boarer, 1982; Morioka and Griffin, 2006; Chapter 5; Chapter 7). There has been little consideration of whether equivalent comfort contours on soft seats are similar to those on rigid seats, although one study suggested that the acceleration equivalent comfort contours measured between a simple block of foam and the body (measured with an accelerometer in an aluminium bar or a SIT-BAR) were similar to the acceleration equivalent comfort contours obtained when sitting on a rigid flat seat (Whitham and Griffin, 1977).

With a rigid seat, the acceleration at the seat-body interface is independent on the measurement location, but with a soft cushion the acceleration can vary over the area of the interface between the cushion and the human body. The non-uniform distribution of acceleration over the area of the cushion-body interface with a soft cushion could also result in acceleration equivalent comfort contours differing between a soft cushion and a rigid flat seat, especially if discomfort is localised to tissues close to the interface.

Unlike acceleration, the force transmitted to the body sitting on a soft cushion is not greatly affected by the dynamic properties of the cushion, if the cushion has little mass relative to the mass of the human body. Motions causing discomfort due to movements within the body (i.e., at locations away from the cushion-body interface) may be assumed to depend on the force acting on the body. The gross movement of the human body will be similar when the force at the interface supporting the body is the same, so it might be assumed that vibration discomfort will be more directly associated with the total force over this interface than the acceleration at any point on the interface.

This study was designed to compare the subjective responses to vertical whole-body vibration when sitting on rigid and soft seats. It was hypothesised that: (i) the same vertical acceleration at the interface supporting the human body would result different equivalent comfort contours when sitting on a rigid flat seat and a soft cushion; (ii) on both a rigid flat seat and on a soft cushion, equivalent comfort contours would be less

dependent on the magnitude of vibration when expressed in terms of dynamic force than when expressed in terms of acceleration.

8.2 Method

8.2.1 Experimental method

A 1-metre stroke electrohydraulic vibrator generated vertical vibration of a rigid flat seat with or without a polyurethane foam cushion resting on the seat. The experiment consisted of two sessions conducted on different days. In one session, subjects sat on the rigid seat (rigid seat session). In the other session, subjects sat on polyurethane foam supported on the same rigid seat (soft seat session). Figure 8.1 shows the experimental arrangement. In both sessions, subjects sat on the top surface of the seat without making contact with the backrest. They rested their feet on a footrest that was attached to the vibrator table and adjusted in height so that with and without the foam cushion the upper surfaces of the upper legs were approximately horizontal.

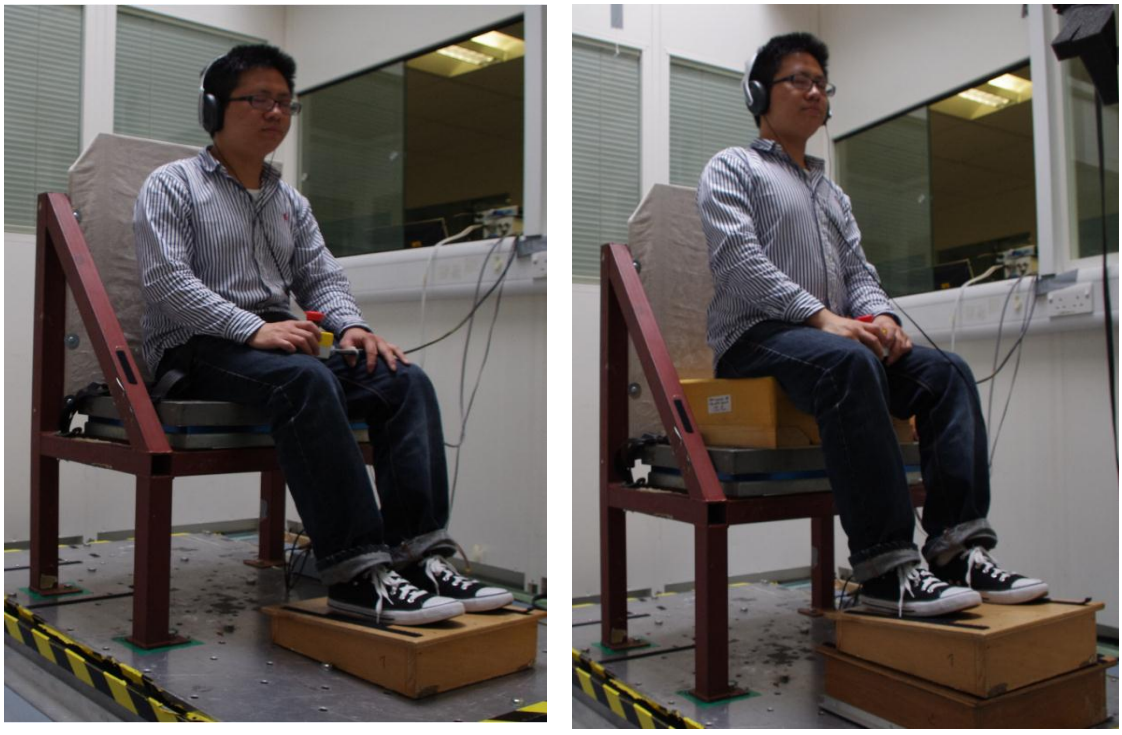

Figure 8.1 Experiment setup (left: rigid seat; right: foam cushion)

In both sessions, the vertical vibration excitation was measured using an accelerometer (Silicon Designs 2260-002) attached to the rigid seat and the vertical force at the upper surface of the rigid seat was measured using a force platform (Kistler 9281B). In the soft seat session, the vertical acceleration was also measured between the upper

surface of the foam and the ischial tuberosities of the subject using a SIT-pad containing an accelerometer (Willow Technologies KXD94-2808).

The polyurethane foam block suitable for automotive seats (composition: MDI; density: 75 kgm^{-3}; maximum thickness: 110 mm; weight: 1.35 kg) was used for the soft seat session. The upper surface of the foam block was 400 mm wide by 450 mm deep. The lower surfaces of the foam were flat, apart from a 40 mm reduction in thickness over 60 mm wide strips on both sides. The foam block was supported on a wooden base (weight: 2.1 kg) resting on the aluminium plate secured to the force platform.

8.2.2 Subjects

Twenty male subjects, students and staff at the University of Southampton, participated in the study. Their median age was 26.5 years (range 22 – 35), weight 70 kg (54 – 112), stature 175.5 cm (164 – 196), and sitting height 91 cm (80 – 96).

Subjects experienced white noise (65 dB(A) presented via a pair of headphones) and closed their eyes to prevent vision affecting their judgements of discomfort.

The experiment was approved by the Human Experimentation Safety and Ethics Committee of the Institute of Sound and Vibration Research at the University of Southampton. Informed consent to participate in the experiment was given by all subjects.

8.2.3 Experiment design

Subjects attended two sessions (i.e., the rigid seat session and the soft seat session) on two different days. In each session, subjects were exposed to a series of vertical sinusoidal vibrations. Each vibration had duration of 6 seconds, including a 1-second cosine taper at each end. In both sessions, sinusoidal vertical vibration was presented at each of the 13 preferred one-third octave centre frequencies from 1 to 16 Hz. At each frequency, the vibration was presented at nine magnitudes with the magnitudes adjusted so that the frequency-weighted accelerations were similar at each frequency (when using the W_b weighting as in BS 6841:1987). The magnitudes used in the rigid seat session are shown in Table 8.1.

The magnitudes used in the soft seat session differed from those used in the rigid seat session, so that the vertical accelerations experienced by each subject (as measured in the SIT-pad above the foam) were similar to the vertical accelerations they experienced in the rigid seat session. Because differing dynamic responses of different subjects are

associated with different seat transmissibilities, the vibration required at each frequency was calculated separately for each subject. Each subject was exposed to the middle magnitude at each of the 13 frequencies (the 5th column in Table 8.1) so that the acceleration above the foam could be compared with the acceleration beneath the foam. The stimulus was then adjusted so that accelerations above the foam were similar to those shown in Table 8.1 (assuming linear dynamic properties of both the foam and the human body). The median excitation magnitudes (i.e., the vibration magnitudes on the vibrator table beneath the foam) for the 20 subjects are shown in Table 8.2.

Table 8.1 Magnitudes of sinusoidal vibration employed at each frequency with the rigid seat.

Frequency	Magnitude of vibration (ms^{-2} r.m.s.)								
1	0.25	0.315	0.4	0.5	0.63	0.8	1	1.25	1.6
1.25	0.25	0.315	0.4	0.5	0.63	0.8	1	1.25	1.6
1.6	0.25	0.315	0.4	0.5	0.63	0.8	1	1.25	1.6
2	0.25	0.315	0.4	0.5	0.63	0.8	1	1.25	1.6
2.5	0.2	0.25	0.315	0.4	0.5	0.63	0.8	1	1.25
3.15	0.16	0.2	0.25	0.315	0.4	0.5	0.63	0.8	1
4	0.125	0.16	0.2	0.25	0.315	0.4	0.5	0.63	0.8
5	0.1	0.125	0.16	0.2	0.25	0.315	0.4	0.5	0.63
6.3	0.1	0.125	0.16	0.2	0.25	0.315	0.4	0.5	0.63
8	0.1	0.125	0.16	0.2	0.25	0.315	0.4	0.5	0.63
10	0.1	0.125	0.16	0.2	0.25	0.315	0.4	0.5	0.63
12.5	0.1	0.125	0.16	0.2	0.25	0.315	0.4	0.5	0.63
16	0.1	0.125	0.16	0.2	0.25	0.315	0.4	0.5	0.63

The method of absolute magnitude estimation was used. Subjects were asked to say the discomfort of each stimulus using any numerical value, but with greater values for greater discomfort. In each session, before the experiment commenced, the subjects practiced magnitude estimation by rating the lengths of lines drawn on paper and then practiced judging the discomfort caused by some of the motions included in the experiment so as to become familiar with the experimental procedure and the sensations produced by the range of stimuli used in the experiment.

Table 8. 2 Magnitudes of sinusoidal vibration beneath the foam employed at each frequency with the foam cushion. The magnitudes at the subject-seat interface above the foam were similar to those in Table 8.1. Medians over 20 subjects.

Frequency	Magnitude of vibration (ms^{-2} r.m.s.)								
1	0.24	0.31	0.40	0.50	0.64	0.82	1.02	1.28	1.64
1.25	0.24	0.31	0.40	0.50	0.64	0.82	1.01	1.27	1.63
1.6	0.23	0.29	0.37	0.46	0.59	0.76	0.95	1.18	1.51
2	0.21	0.27	0.35	0.43	0.55	0.70	0.87	1.09	1.39
2.5	0.15	0.19	0.23	0.30	0.37	0.47	0.60	0.75	0.93
3.15	0.09	0.12	0.15	0.19	0.25	0.31	0.39	0.48	0.60
4	0.06	0.09	0.11	0.14	0.19	0.23	0.29	0.38	0.48
5	0.08	0.10	0.15	0.19	0.24	0.31	0.38	0.48	0.61
6.3	0.13	0.17	0.23	0.29	0.36	0.45	0.58	0.71	0.89
8	0.15	0.20	0.26	0.33	0.41	0.52	0.66	0.84	1.04
10	0.13	0.17	0.23	0.29	0.36	0.46	0.60	0.74	0.93
12.5	0.14	0.19	0.24	0.31	0.39	0.49	0.64	0.79	1.00
16	0.16	0.22	0.29	0.37	0.48	0.59	0.73	0.93	1.18

At the end of each session, the lowest and highest magnitudes of vibration at each frequency (the 1st and 9th columns in Tables 1 and 2) were presented again in a randomised order. After experiencing each of these vibrations, the subjects were asked to indicate the location of most discomfort in their body according to a body map displayed in front of them.

8.2.4 Analysis

8.2.4.1 Vibration acceleration and force

With the rigid seat, the force at the interface with the human body was calculated after subtracting from the measured force time series data the mass of platform above the force cells multiplied the acceleration (i.e., mass cancellation in the time-domain, Figure 8.2(a)).

In the soft seat session, the force at the interface between foam and human body was calculated according to the model in Figure 8.2(b).

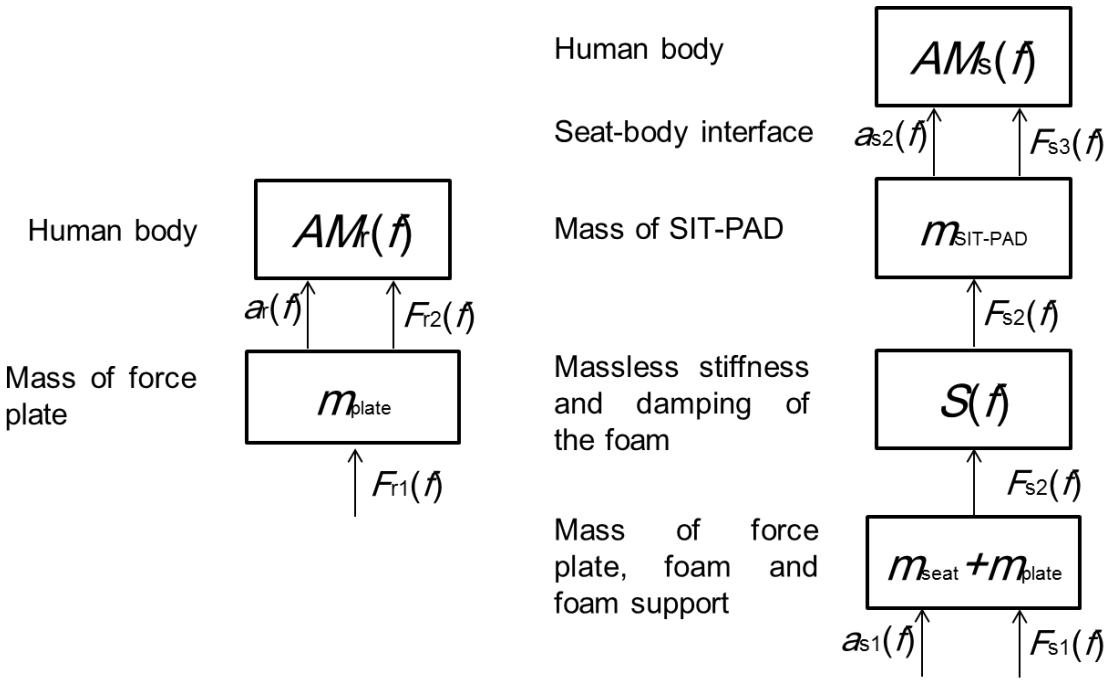

(a) (b)

Figure 8.2 Models for calculating apparent mass on rigid seat (a) and foam cushion (b)

The foam was assumed to be a pure complex stiffness element, with its mass, m_{seat}, (1.35 kg) added to the mass of the force plate, m_{plate}, for mass cancellation. It follows that:

$$F_{\text{s2}}(t) = F_{\text{s1}}(t) - (m_{\text{plate}} + m_{\text{seat}})a_{\text{s1}}(t) = F_{\text{s3}}(t) + m_{\text{SIT-pad}}a_{\text{s2}}(t) \tag{8.1}$$

So the force at the interface between the foam and the human body ($F_3(t)$) is obtained from:

$$F_{\text{s3}}(t) = F_{\text{s1}}(t) - (m_{\text{plate}} + m_{\text{seat}})a_{\text{s1}}(t) - m_{\text{SIT-pad}}a_{\text{s2}}(t) \tag{8.2}$$

8.2.4.2 Vibration discomfort

In each session, for all 117 stimuli (Table 8.1), the median value of the subjective responses of each subject was normalised to be 100, and the other values scaled so that the ratio between new value and 100 was the same as the ratio between original value and the original median value. The median value of the subjective responses of each subject can be different between the rigid seat and soft seat, the difference is ignored in this study when comparing the vibration discomfort on the rigid seat and soft seat.

For each frequency of vibration and for each subject, the relation between the vibration acceleration, φ, and the individual magnitude estimate of discomfort, Ψ, was determined using Stevens' Power law:

$$\Psi = k\,\varphi^{n} \tag{8.3}$$

Linear regression was performed at each frequency after logarithmic transformation of Equation (3) to:

$$\log_{10}\Psi = n.\log_{10}\varphi + \log_{10} k \tag{8.4}$$

8.3 Results

8.3.1 Rates of growth of vibration discomfort

The medians and inter-quarter ranges of the rates of growth of discomfort, *n*, from all 20 subjects with the rigid seat and the soft seat are compared in Figure 8.3. With both seating conditions, the exponents, n, for acceleration and force were highly dependent on the frequency of vibration ($p<0.001$, Friedman). After adjustment for multiple comparisons, the rates of growth of discomfort, *n*, for either acceleration or force did not differ between the two seating conditions (i.e., between the rigid seat and the soft seat) at any of the 13 frequencies ($p>0.05$, Wilcoxon).

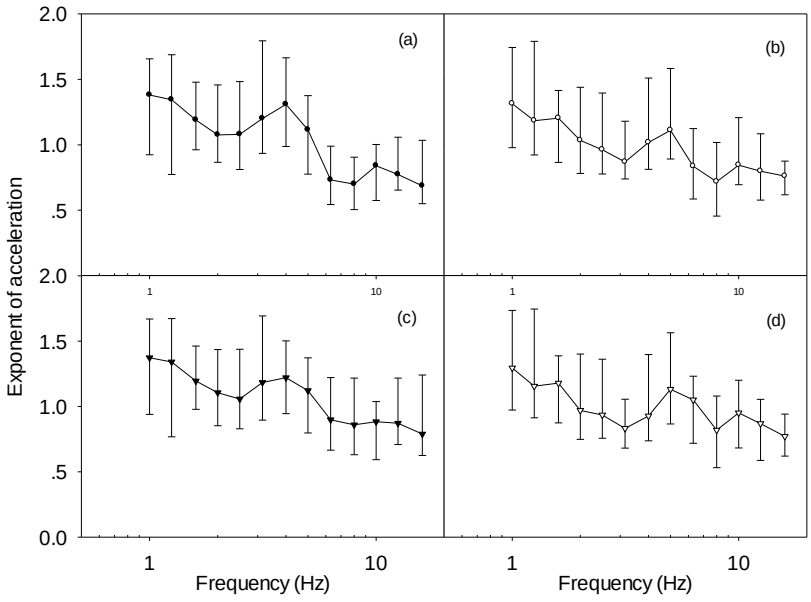

Figure 8.3 Rate of growth of discomfort with increasing magnitude of vibration (i.e., the exponent, *n*). For acceleration: a: rigid seat; b: foam cushion, and for force: c: rigid seat; d: foam cushion. Medians and inter-quarter ranges of 20 subjects.

There was no significant difference in the rate of growth of discomfort, *n*, between force and acceleration at any frequency with either the rigid seat or the soft seat (p>0.05, Wilcoxon matched-pairs signed ranks test, Figure 8.4).

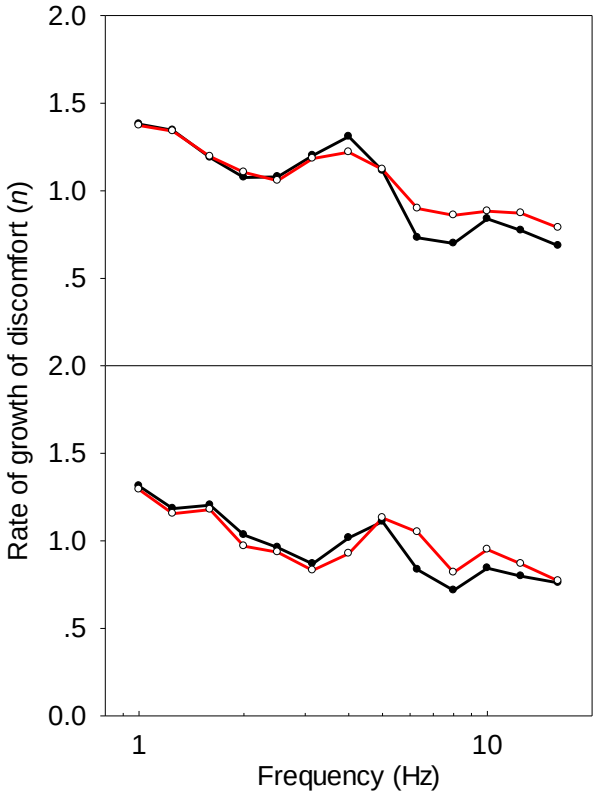

Figure 8.4 Rates of growth of discomfort for acceleration [—●—] and force [—○—] with two seat conditions. Upper graph: rigid seat; lower graph: foam cushion. Medians of 20 subjects.

Variation in the exponent over the frequency range indicates nonlinearity in the subjective response to vibration, with a greater variation suggesting greater nonlinearity. For each subject, over the 13 frequencies the difference between the maximum exponent and the minimum exponent was calculated. The differences in the exponent for acceleration, $\Delta_{acceleration}$, and the difference in the exponent for force, Δ_{force}, are compared in Table 8.3. With the rigid seat, the difference in acceleration exponent, $\Delta_{acceleration,}$ was significant greater than the difference in the exponent for force, Δ_{force} (p<0.05, Wilcoxon matched-pairs signed ranks test). Less variation in the exponent suggests more parallel in the equivalent comfort contours. With the soft seat, there was no significant difference in the difference in the exponent between acceleration and force (p>0.05, Wilcoxon matched-pairs signed ranks test).

Table 8.3 Differences between the maximum exponent and minimum exponent for acceleration and force over the frequency range 1.0 to 16 Hz within each subject.

Subject	rigid seat			foam cushion		
	$\Delta_{acceleration}$	Δ_{force}	Δ_{af}	$\Delta_{acceleration}$	Δ_{force}	Δ_{af}
1	0.81	0.63	0.18	0.53	0.52	0.01
2	0.85	0.75	0.10	0.47	0.51	-0.05
3	1.02	0.83	0.19	1.20	1.27	-0.06
4	0.32	0.30	0.02	0.28	0.31	-0.03
5	1.07	0.94	0.13	0.96	1.03	-0.06
6	2.07	2.10	-0.03	1.38	1.60	-0.22
7	0.64	0.70	-0.05	1.30	1.34	-0.04
8	0.67	0.68	-0.01	0.82	0.69	0.13
9	2.07	1.88	0.19	1.11	1.19	-0.08
10	1.51	1.22	0.29	1.20	1.02	0.18
11	1.03	0.93	0.10	0.76	0.66	0.10
12	1.00	0.81	0.19	0.76	0.70	0.06
13	1.12	0.80	0.33	0.53	1.44	-0.91
14	0.78	0.81	-0.03	0.92	0.81	0.11
15	0.62	0.68	-0.06	0.75	0.78	-0.03
16	1.13	1.08	0.04	1.69	1.74	-0.06
17	0.70	0.65	0.05	1.02	1.02	-0.01
18	1.44	1.45	0.00	1.00	0.89	0.11
19	0.87	0.83	0.05	0.88	0.86	0.02
20	0.38	0.42	-0.04	0.53	0.51	0.02

$\Delta_{acceleration}$: difference between the maximum and minimum exponent for acceleration

Δ_{force}: difference between the maximum and minimum exponent for force

Δ_{af}: $\Delta_{acceleration} - \Delta_{force}$

8.3.2 Equivalent comfort contours for acceleration

Acceleration equivalent comfort contours were calculated for the rigid seat and the soft seat for each subject by calculating the vibration acceleration, φ, corresponding to nine subjective magnitudes, ψ, from 40 to 250 at each vibration frequency using equation (8.3). The equivalent comfort contours illustrate the vibration magnitudes required to produce the same strength of sensation across the frequency range. With both seating conditions, the acceleration equivalent comfort contours for all sensation magnitudes varied with the frequency of vibration ($p<0.001$, Friedman; Figure 8.5).

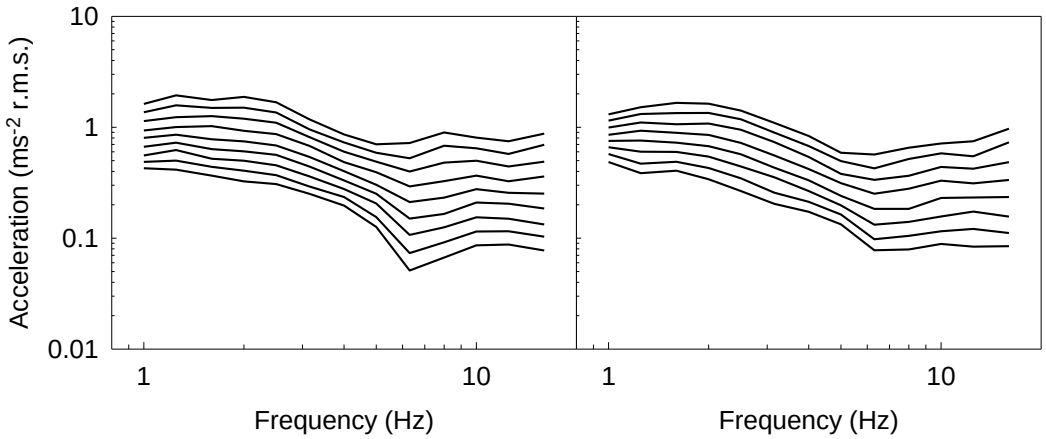

Figure 8.5 Acceleration equivalent comfort contours for subjective magnitudes, ψ, of 40, 50, 63, 80, 100 125, 160, 200 and 250 with rigid seat (left) and foam cushion (right). Medians of 20 subjects.

With both the rigid seat and the foam seat, the equivalent comfort contours have similar acceleration from 1 to 2 Hz and then show increased sensitivity to acceleration to around 6 Hz, for the lower sensation magnitudes, and to around 5 Hz for the higher sensation magnitudes.

The acceleration equivalent comfort contours (for ψ=50, 100 and 200) are compared between the rigid seat and the foam cushion in Figure 8.6. After adjustment for multiple comparisons, there was no significant different at any frequency except 1.6 Hz (when ψ=100, $p<0.001$; Wilcoxon).

8.3.3 Equivalent comfort contours for force

Equivalent comfort contours for force were constructed using the same method used to determine acceleration equivalent comfort contours (Figure 8.7). With both seating conditions, the force equivalent comfort contours at all sensation magnitudes varied with frequency ($p<0.001$, Friedman).

Comparing the force equivalent comfort contours (for ψ=50, 100 and 200) between the rigid seat and the foam cushion, after adjustment for multiple comparisons there was no significant difference at any frequency, except at 5 Hz (ψ=100 and 200, p<0.0025, Wilcoxon, Figure 8.8).

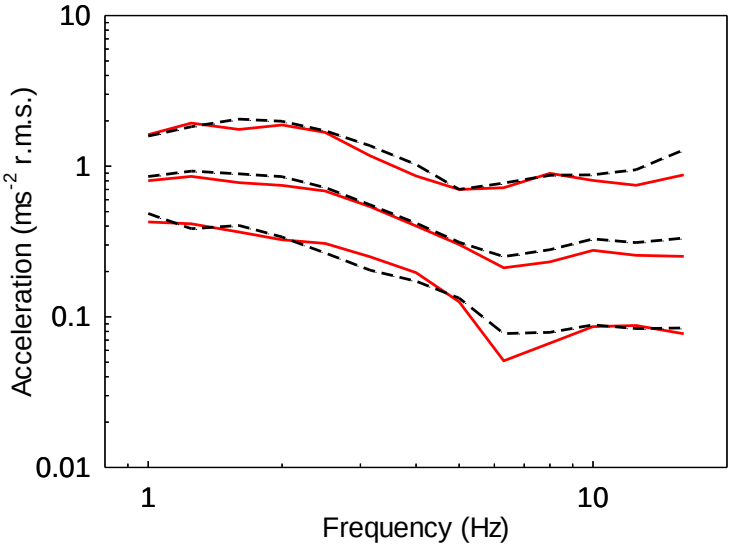

Figure 8.6 Acceleration equivalent comfort contours (for ψ =40, 100 and 250) for two seat conditions (—: rigid seat; — —: foam cushion). Medians of 20 subjects.

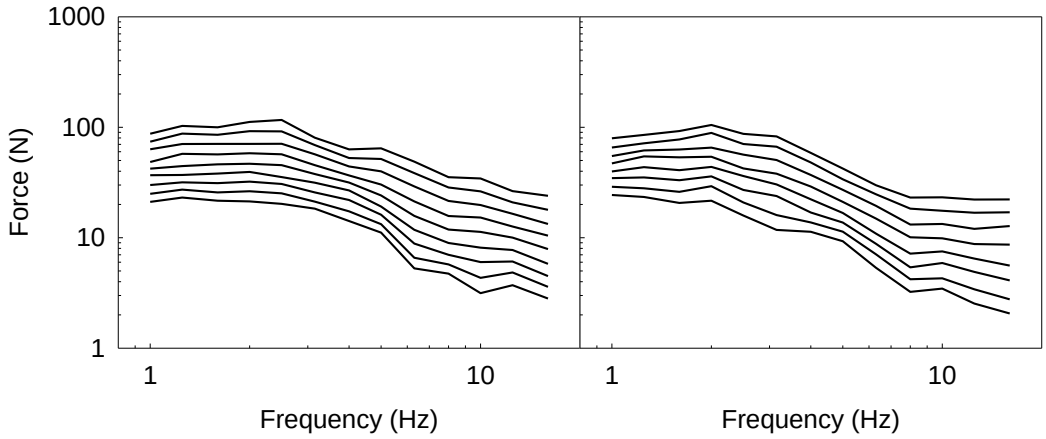

Figure 8.7 Force equivalent comfort contours for subjective magnitudes, ψ, of 40, 50, 63, 80, 100 125, 160, 200 and 250 with rigid seat (left) and foam cushion (right). Medians of 20 subjects.

8.3.4 Location of discomfort

The locations where subjects felt most discomfort were similar with the rigid seat and the soft seat for both low magnitude and high magnitude vibration (Figure 8.9). With the

greatest magnitude of vibration, most discomfort was generally felt in either the head or the upper-body with both the rigid seat and the foam cushion. With the lowest magnitude of vibration, most discomfort was generally felt in either the head or the thighs, with both the rigid seat and the foam. At the lowest frequencies, many subjects reported most discomfort at the head. With the soft seat, some subjects indicated the feet as the location of greatest discomfort caused by the higher frequencies.

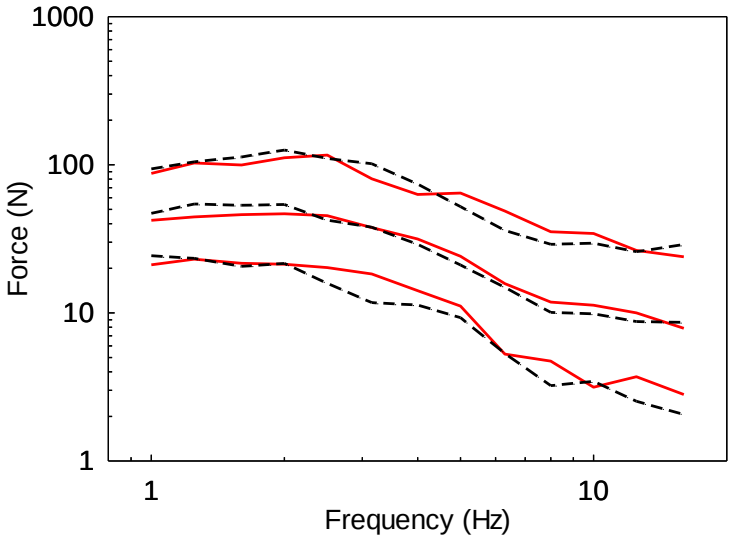

Figure 8.8 Force equivalent comfort contours (for ψ=40, 100 and 250) for two seat conditions (—: rigid seat; — —: foam cushion). Medians of 20 subjects.

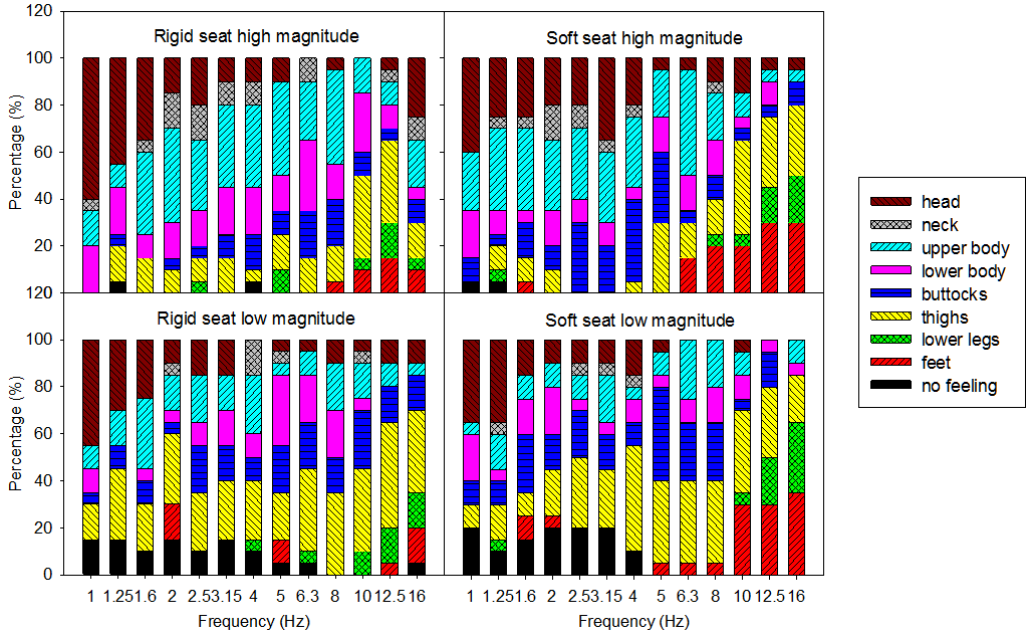

Figure 8.9 Locations of discomfort arising from exposure to low and high magnitudes of vertical vibration with rigid seat and foam cushion.

8.4 Discussion

There were no significant differences between the acceleration equivalent comfort contours obtained on the rigid seat and those obtained on the soft cushion (Figure 8.6). Whitham and Griffin (1977) also found that acceleration equivalent comfort contours obtained on rigid seat were a good approximation to equivalent comfort contours on a soft seat measured by inserting a SIT-BAR between the ischial tuberosities and a seat cushion.

The rate of growth of discomfort with increasing magnitude of vertical vibration (i.e., the exponent in Steven's power law) varied similarly with the frequency of vibration in the range 1 to 16 Hz for both the rigid seat and the soft cushion (Figure 8.4). Consequently, the acceleration equivalent comfort contours varied with the magnitude of the vibration in a similar way in both seating conditions. For example, with the rigid seat, at low magnitudes (φ=40) the equivalent comfort contour reduced with increasing frequency from 2.5 to 6.3 Hz, whereas with high magnitudes (φ=250) the equivalent comfort contour reduced with increasing frequency from 2 to 5 Hz (Figure 8.6). With the soft cushion, at low magnitudes (φ=40) the equivalent comfort contour reduced with increasing frequency from 1.6 to 6.3 Hz, whereas at high magnitudes (φ=250) the equivalent comfort contour reduced with increasing frequency from 2 to 5 Hz. British Standard 6841 (1987) uses the frequency weighting W_b for the evaluation of vertical whole-body vibration. The results in this study are consistent with previous studies questioning the applicability of a single frequency weighting for evaluating vibration over large range of vibration magnitudes (e.g., Morioka and Griffin, 2006; Chapter 5).

The rate of growth of discomfort with increasing vertical dynamic force also varied with the frequency of vibration from 1 to 16 Hz with both the rigid seat and the soft cushion (Figure 8.4). However, the general shapes of the force equivalent comfort contours are similar with the two seats. For example, with both seat conditions, the equivalent comfort contours at low magnitude (φ=40) and at high magnitude (φ=250) reduced with increasing frequency from 2 to 16 Hz (Figure 8.8). It seems that a frequency weighting derived from force equivalent comfort contours could be uniform over greater range of conditions that acceleration equivalent comfort contours: a greater range of vibration magnitudes and a range of different seating conditions.

8.5 Conclusions

In both rigid and soft seat conditions, the frequency-dependence of equivalent comfort contours, expressed in terms of either acceleration or force, vary with the magnitude of

vibration. However the force and acceleration equivalent comfort contours obtained on a rigid seat did not differ from those obtained on a foam cushion. The force equivalent comfort contours show less nonlinearity than the acceleration equivalent comfort contours, consistent with the biodynamic nonlinearity of the body, as reflected in the apparent mass, contributing to the nonlinearity in the acceleration equivalent comfort contours.

Chapter 9 General Discussion

9.1 Introduction

The overall objective of this study is to advance understanding of the combined influence of the magnitude and frequency of whole-body vertical vibration on subjective and biodynamic responses of the seated human body. Chapter 2 has reviewed the previous studies related to the subjective and biodynamic responses to whole-body vertical vibration, the relation between the subjective and biodynamic responses, and finally defined the key questions need to be answered in this study (Section 2.6). This chapter summaries the main findings of the all the experiments have been done in this study to answer those questions.

9.2 Biodynamic responses to vertical vibration

The biodynamic responses of the seated human body exposed to different magnitudes and different types of vertical whole-body vibration (e.g., random vibration, sinusoidal vibration, and mechanical shocks) have been studied systematically (e.g., Chapter 4 and Chapter 6). Nonlinearity was found in the biodynamic responses (i.e., the principal resonance frequency in the vertical apparent mass of the seated human body reduced as the magnitude of vibration increased) with all types of vibration when subjects sat on the rigid seat.

The first experiment investigated nonlinearity in the vertical apparent mass and the fore-and-aft cross-axis apparent mass with both random vibration and sinusoidal vibration. Over the frequency range 1.0 to 16 Hz, the modulus and the phase of the vertical apparent mass and the fore-and-aft cross-axis apparent mass obtained with random vibration were similar to those obtained with sinusoidal vibration of the same overall acceleration magnitude (Chapter 4). The passive thixotropy of soft tissues, rather than geometric nonlinearity or voluntary or involuntary muscular, has been suggested as the most likely primary cause of the nonlinearity in the biodynamic response of the human body to whole-body vibration (Huang and Griffin, 2008; Huang and Griffin, 2009). The similarity in the nonlinearity with sinusoidal and random vibration also suggests it is unlikely that changes in muscle activity are the principal cause of the nonlinearity. Some other mechanisms have been suggested to be responsible for the nonlinearity in the vertical apparent mass and the fore-and-aft cross-axis apparent mass (see Section 2.3.4). In present study, the primary resonance

frequencies in the fore-and-aft cross-axis apparent mass were highly correlated with the primary resonance frequencies in the vertical apparent mass, consistent with the finding of Qiu and Griffin (2010). This suggests the mechanism causing the nonlinearity evident in the fore-and-aft cross-axis apparent mass might be the same as that causing nonlinearity in the vertical apparent mass.

The similarity in the nonlinearity with sinusoidal and random vibration shows that the nonlinearity in the vertical apparent mass of the seated human body is more dependent on the magnitude and the frequency of the vibration excitation than the waveform of excitation. This is consistent with the finding from Nawayseh and Griffin (2005). By comparing the apparent mass obtained with cross-spectral density (CSD) method and power-spectral density (PSD) method, Nawayseh and Griffin (2005) has suggested that although the human body was nonlinear, the body behaved linearly at a vibration magnitude but differently at another magnitude. Partly because of the above reason, most of current human body models are linear and modelled in frequency domain, which is easier to identify model parameters and also show the ability to capture the key biodynamic characteristic of human body. However, for further understanding the biodynamic of human body, more detailed and complex models are required. Some models have been developed to represent particular nonlinear behaviour of the body by using nonlinear components or nonlinear geometric arrangements (Section 2.4.2). In this study, two lumped parameter models are developed to present the seated human body response to vertical mechanical shocks in the time-domain (Chapter 6). The optimum stiffness and damping of both models reduced with increasing shock magnitude with all except the lowest frequencies of shock. The reduction in stiffness with increasing magnitudes of shock is consistent with the passive thixotropy of soft tissues which has been suggested as the primary cause of the nonlinearity in biodynamic responses to whole-body vibration (e.g., Huang and Griffin, 2008; Huang and Griffin, 2009). Similar to the reduction in optimum damping of the frequency domain model with random and sinusoidal vibration (Chapter 4), the optimum damping of both time domain models also reduced with increasing magnitude of shocks. No previous study has reported a significant reduction in the optimum damping.

Overall, this study suggests the biodynamic response of the human body may vary with the stimuli, but the human body is inherently a ‘softening’ nonlinear system.

9.3 Subjective response to vertical vibration

The nonlinearity in subjective response to vibration has been noticed previously (e.g., Morioka and Griffin, 2006), the rate of growth of discomfort (i.e., the exponent *n* in Steven's power law) varied with the frequency of vibration, so the acceleration equivalent comfort contours vary with the magnitude of vibration. However, no previous study has systematically investigated this nonlinearity at low frequencies, which has restricted the application of current frequency weightings to predict vibration discomfort over large range of magnitudes at low frequencies. Besides the nonlinear biodynamic study, this thesis was designed to further investigate the nonlinearity in vibration discomfort and also seek a better predictor for vibration discomfort.

Because the acceleration is only one of several possible ways of describing a vibration (i.e., the vibration can also been described by velocity or displacement), and the driving force is the cause of the vibration, the driving force is considered a more fundamental reason for vibration discomfort, in present study, the driving force was also considered as a predictor of vibration discomfort.

A psychophysical law (i.e., Stevens' power law, $\Psi=k\varphi^{n}$) was applied to find the relation between the psychological response (i.e., subjective response to vibration) and the physical measurements (i.e., acceleration or dynamic force measured during vibration). Because the coefficient *k* varies with number scale or unit of the measured data, and the exponent *n* is independent of the way of presenting experimental data, the exponent *n* was considered the main parameter to investigate the relation between subjective responses and biodynamic measurements. The exponents from all three experiments subjective are summarized in Figures 9.1 and 9.2. The frequency-dependence of the exponent indicated that to obtain the same increment in vibration discomfort at different frequencies, different increments in vibration magnitude are needed. The reason can be explained by a different mechanism being involved in vibration discomfort at different vibration frequencies, as indicated by the body map of discomfort (Figures 5.7, 7.8 and 8.9). The variation in the exponent results in both the force and the acceleration equivalent comfort contours at different magnitudes not being parallel (Figures 5.5, 5.6, 7.5, 7.6, 8.5 and 8.7). The equivalent comfort contours were less dependent on the magnitude of vibration when expressed by force than by acceleration. Although the nonlinearity in force equivalent comfort contours still exists, the reduction in nonlinearity is an important finding.

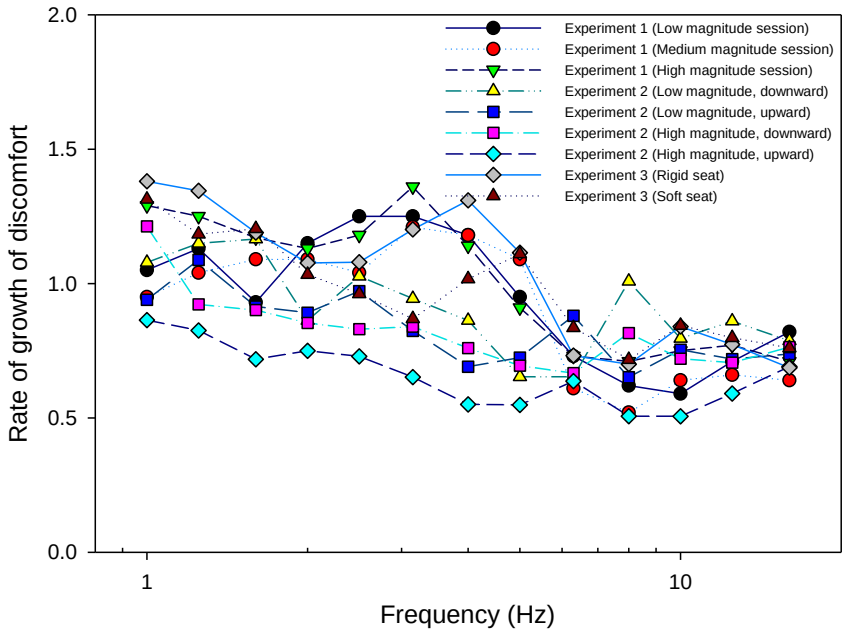

Figure 9.1 Median rate of growth of discomfort with increasing acceleration from all three experiments.

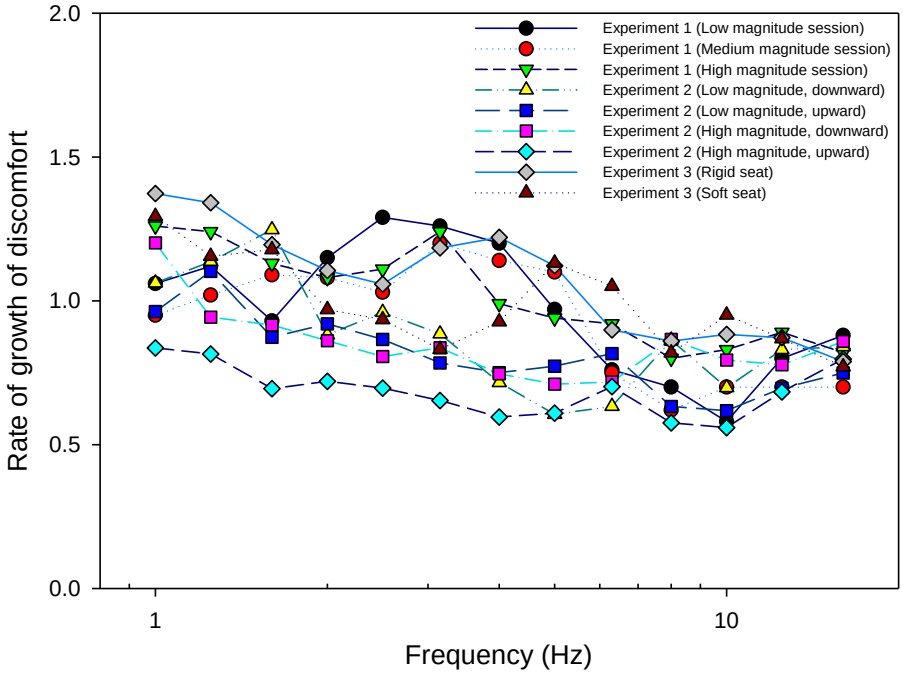

Figure 9.2 Median rate of growth of discomfort with increasing dynamic force from all three experiments.

9.4 Methodology assessment

Vibration discomfort was evaluated using the method of magnitude estimation with a reference (i.e., RME method) in Experiment 1 but without a reference in Experiment 2

and Experiment 3 (i.e., AME method). Zwislocki and Goodman (1980) investigated the magnitude estimation method without a reference (i.e., AME) and suggested subjects were more likely to give 'real' subjective magnitudes to stimuli when using AME because they have difficulty in judging low magnitude vibration stimuli that produce sensations that are different from those produced by the reference stimulus. Previous studies have shown that the magnitude estimates were not significantly different between RME and AME (Huang and Griffin, 2014). The AME and RME method can also been compared using the data from this study (i.e., comparing Experiment 1 judgements with medium magnitude vibration with Experiment 3 judgements). Table 9.1 compares the statistics of the subjective magnitude estimates from Experiment 1 (medium magnitude session with 20 male subjects, RME) and Experiment 3 (rigid seat with 20 male subjects, AME), with other experimental conditions unchanged. For RME, the reference vibration was chosen so that it could produce nearly the mean discomfort over all the stimuli, and assumed to be 100 during the experiment. For AME, the median subjective response data was normalised to be 100, and the other values scaled to that the ratio between new values and 100 was the same as the ratio between original value and the original value. With both methods, the mean magnitude estimates are greater than 100. The range of subjective responses obtained by RME is slightly narrower than with AME. There is no significant difference in the mean of magnitude estimates obtained with RME and AME (p>0.05, Mann-Whitney U test). Considering AME takes only half the time required for RME, the AME is recommended in further study.

Table 9.1 Distribution of magnitude estimates using relative magnitude estimation and absolute magnitude estimation methods

	RME	AME
Number of magnitude estimates	2340	2340
Mean of magnitude estimates	129.47	117.98
Standard deviation	82.58	89.2
Minimum of magnitude estimates	0*	0*
Maximum of magnitude estimates	600	714

*: 0 indicates the subject could not feel the vibration

9.5 Associations between subjective and biodynamic responses

Considering the similarity of nonlinearity in the biodynamic response and subjective response of the human body exposed to vertical vibration (i.e., as the magnitude of vibration increased, the resonance frequency of apparent mass shifts to lower frequency, and the subjects also show more sensitive to lower frequencies), it is reasonable to expect there may be some relation between the subjective and biodynamic responses.

Various vibration modes of the human body have been found at frequencies less than 10 Hz (e.g., Kitazaki and Griffin, 1997), which is in the most sensitive range for provoking subjective responses. This suggests there may be some associations between the subjective and biodynamic responses to vibration, as found by Matsumoto and Griffin (2005) and Subashi *et al.* (2009). The present study continued the investigation of the association between subjective and biodynamic responses by calculating correlations between the ratios of the apparent masses at two frequencies and the ratios of the subjective responses between the same two frequencies (Chapter 5, Chapter 7). Distinct patterns of statistically significant positive correlations were found between the relative apparent mass and the relative subjective response when subjects were exposed to sinusoidal vibration at frequencies in the range 1 to 16 Hz. The associations show that biodynamic differences between subjects (reflected in differences in the forces at the seat when the acceleration is the same) influence the frequency-dependence of discomfort caused by vertical vibration at frequencies over the range 1 to 16 Hz. The finding has potential benefit to the use of biodynamic measures to help predict subjective responses. However, these associations were not clear when subjects were exposed to vertical shocks.

Chapter 10 Conclusions and recommendations

10.1 Conclusions

As the magnitude of the excitation increased, the resonance frequency of the apparent mass of the human body decreased in subjects exposed to sinusoidal and random vibration (Chapter 4) and mechanical shocks (Chapter 6).

Male and female subjects had similar vertical and fore-and-aft cross-axis apparent mass (after adjusting for subject weight) and a similar principal resonance frequency with both random and sinusoidal vibration (Chapter 4). The change in the biodynamic response with changing vibration magnitude depends on the frequency of the vibration excitation, but is similar with sinusoidal and random excitation. With sinusoidal vibration and random vibration, the optimum stiffness and optimum damping of a single degree-of-freedom lumped parameter model of the body reduced with increasing magnitude of vibration.

The biodynamic responses of human body exposed to vertical mechanical shocks can be well presented by lumped parameter models in which the optimum stiffness and optimum damping vary with the magnitude and the nominal frequency of the shock (Chapter 6). There are correlations between the optimum stiffness and optimum damping obtained with models optimised in the time-domain and the optimum stiffness and optimum damping obtained with models optimised in the frequency-domain.

When the seated human body is exposed to vertical whole-body vibration, the frequency-dependence of equivalent comfort contours depends on the magnitude of the vibration, but is less dependent on the magnitude of the dynamic force than the magnitude of acceleration, consistent with the biodynamic nonlinearity of the body causing some of the magnitude-dependence of equivalent comfort contours (Chapter 5). There are significant associations between the biodynamic responses and subjective responses at all frequencies in the range 1 to 16 Hz.

When seated people are exposed to vertical mechanical shocks, they show greatest sensitivity to acceleration at frequencies between about 5 and 12.5 Hz, but with a frequency-dependence that varies with shock magnitude and shock waveform (Chapter 7). There is no large difference in the rate of growth of discomfort between dynamic force and acceleration, or between upward and downward shocks. Unlike subjects

exposed to sinusoidal vibration, there were no significant associations between relative apparent mass and relative subjective responses during exposure to shocks.

When sitting on a rigid seat and soft seat, there were no statistically significant differences in either force equivalent comfort contours or acceleration equivalent comfort contours (Chapter 8). Similar to the findings on a rigid seat, the force equivalent comfort contours on the soft seat also showed less nonlinearity than the acceleration equivalent comfort contours.

10.2 Recommendation for future work

The biodynamic nonlinearity of the human body has been studied for decades, and although many studies have measured the nonlinearity during exposure to vibration, only a few have investigated the mechanism responsible for the nonlinearity (e.g., Huang and Griffin, 2006, 2008). Lumped parameter models have been developed to present the biodynamic response of the human body in the frequency domain, and the models have been applied to study the dynamic response of combined seat-body systems. Because of the complexity of the body, most models are linear and only represent the biodynamic response of the human body at particular magnitudes. In the present study, a time-domain model has been developed. Although the model developed in this thesis is linear, it has potential to be developed to a nonlinear model that could predict the biodynamic response of the human body over a wide range of magnitudes. To achieve this objective, further understanding the mechanisms controlling the nonlinearity of the human body are needed. A model is required with the capability to predict the nonlinear in the biodynamic responses of the human body in a general way but without excessive complexity.

Because of the complex dynamic behaviour of both soft seats and the human body, understanding of subjective and biodynamic responses of the human body sitting on soft seats is far from complete. Measuring the forces between seat cushions and the human body is still challenging, so better techniques are required to get more accurate force data which will allow better predictions of both biodynamic and subjective responses of the human body sitting on soft seats.

Sinusoidal vibration has been used in most studies of subjective responses to vibration. Because of the nonlinearity in the subjective response, equivalent comfort contours derived from studies using sinusoidal vibration, and frequency weightings based on such contours, may have limited applicability to other waveforms and over the wide

range of magnitudes that occurs in real life. Further studies are needed to investigate the subjective and biodynamic responses to other types of stimuli (e.g., mechanical shocks, random vibration etc.). It is also appropriate to further investigate what predictors of vibration discomfort may be useful alternatives to acceleration, so as to reduce the nonlinearity in subjective responses and have the capability to predict subjective responses to different types of stimuli over wide range of magnitudes.

The present study has shown that there is an association between biodynamic responses and subjective responses when subjects are exposed to sinusoidal vibration, but the association was less clear in subjects exposed to mechanical shocks. Considering the similarity in the nonlinearity between the subjective responses and the biodynamic responses, it is appropriate to investigate further the correlation between subjective and biodynamic responses of the human body exposed to different types of stimuli. In such a study, the ratios of the apparent masses at two frequencies and the ratios of the subjective responses between the same two frequencies may be compared. It is also worth investigating the relation between the subjective responses and other biodynamic quantities (e.g., transmissibility, impedance etc.).

Appendices

Appendix A Instructions to subjects

A.1 Instructions to subjects in the first experiment reported in Chapter 4 and 5

Thank you for participating in this research project.

The experiment has been approved by the ISVR Human Experimentation Safety and Ethics Committee.

There are three sessions to be conducted on three different days. In the first two sessions, two tests will be conducted: **Test 1**: equivalent comfort, **Test 2**: location of discomfort. In the last session, three tests will be conducted: **Test 1**: equivalent comfort, **Test 2**: location of discomfort, **Test 3**: biodynamic measurements.

Please read carefully and follow the instructions below.

Before the experiment (on your first day)

Complete the questionnaires.

Your standing height, sitting height, shoulder height, buttock-to-popliteal length, knee height, shoulder breadth, hip breadth, and weight will be measured (or taken during your last session).

You will undergo short training to familiarise you with the test.

To begin the experiment

Sit comfortably on the rigid seat as guided by the experimenter.

Fasten the seat belt loosely, but securely, by adjusting the ‘tightness’ of the belt

Put on the headphones and the blindfold (or close your eyes).

Hold the emergency stop button (to be used to stop the vibration if you are concerned).

Lay your hands on your lap and rest your feet on the footrest.

Do not lean against the backrest

In each session, you will undergo a few practice trials before the actual test commences

During the experiment

Test 1 (about 35 minutes)

You will be presented with pairs of motions: a ‘reference’ stimulus followed by a ‘test’ stimulus. The reference stimulus and the test stimulus each have durations of 6 seconds. There will be a 1-second interval with no motion between the reference stimulus and the test stimulus.

Appendix 2

Rate the DISCOMFORT caused by each ‘test’ stimulus relative to the DISCOMFORT caused by the preceding ‘reference’ stimulus. Assume the discomfort caused by the reference stimulus is 100.

Test 2 (about 3 minutes)

You will resume sitting as for Test 1. A series of 6-second test stimuli will be presented to you.

After each stimulus, use the body map to indicate to the experimenter the location in your body where you felt the MOST DISCOMFORT.

Test 3 (for the last session, about 6 minutes)

You will resume sitting as for Test 1. Five 60-second stimuli (random vibrations) will be presented to you with short intervals between the stimuli. You will be asked to maintain your posture while the transmission of vibration from the seat is measured. No judgement is required.

Break

There will a break in the middle of Test 1 and at the end of Test 1.

Thank you very much for your cooperation.

In order to let you know understand the method of magnitude estimation, please estimate the rate of the right bar compared with the left.

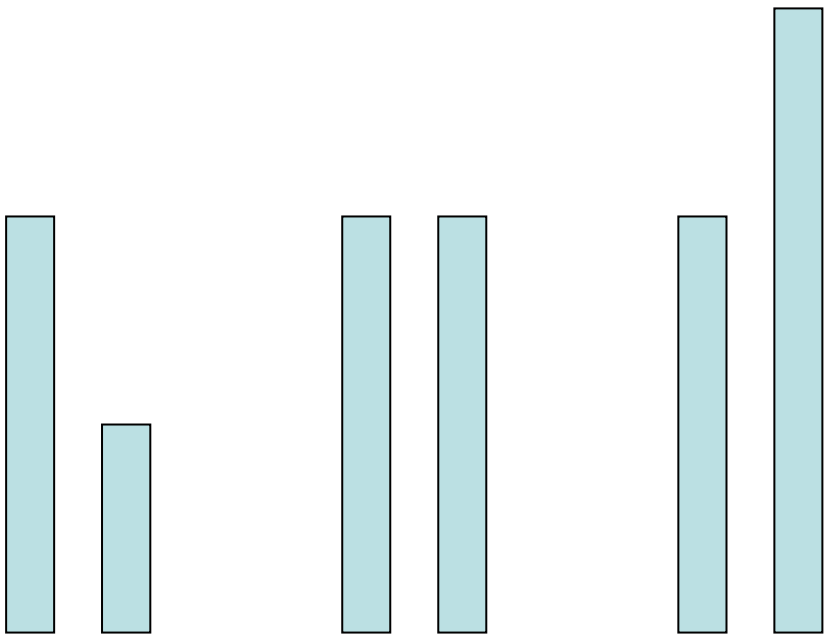

A.2 Instructions to subjects in the second experiment reported in Chapter 6 and 7

Thank you for participating in this research project.

The experiment has been approved by the ISVR Human Experimentation Safety and Ethics Committee.

There are two sessions to be conducted on two different days. In the first session, two tests will be conducted: **Test 1**: equivalent comfort, **Test 2**: location of discomfort. In the second session, three tests will be conducted: **Test 1**: equivalent comfort, **Test 2**: location of discomfort, **Test 3**: biodynamic measurements.

Please read carefully and follow the instructions below.

Before the experiment (on your first day)

Complete the questionnaires.

Your standing height, sitting height, shoulder height, buttock-to-popliteal length, knee height, shoulder breadth, hip breadth, and weight will be measured (or taken during your last session).

You will undergo short training to familiarise you with the test.

To begin the experiment

Sit comfortably on the rigid seat as guided by the experimenter.

Fasten the seat belt loosely, but securely, by adjusting the ‘tightness’ of the belt

Put on the headphones and the blindfold (or close your eyes).

Hold the emergency stop button (to be used to stop the vibration if you are concerned).

Lay your hands on your lap and rest your feet on the footrest.

Do not lean against the backrest

In each session, you will undergo a few practice trials before the actual test commences

During the experiment

Test 1 (about 40 minutes)

You will be presented with motions in two directions (upward and downward)

Your task is to say the discomfort of motion using any numerical value.

A sensible median value might be ‘100’.

Test 2 (about 3 minutes)

You will resume sitting as for Test 1. A series test stimuli will be presented to you.

After each stimulus, use the body map to indicate to the experimenter the location in your body where you felt the MOST DISCOMFORT.

Test 3 (for the second session, about 6 minutes)

You will resume sitting as for Test 1. Five 60-second stimuli (random vibrations) will be presented to you with short intervals between the stimuli. You will be asked to maintain your posture while the transmission of vibration from the seat is measured. No judgement is required.

Break

There will a few breaks during test.

Thank you very much for your cooperation.

A.3 Instructions to subjects in the third experiment reported in Chapter 6 and 7

Thank you for participating in this research project.

The experiment has been approved by the Ethics Committee of the Faculty of Engineering and the Environment at the University of Southampton.

There are two sessions to be conducted on two different days. In each session, there will be conducted: **Test 1**: vibration discomfort, **Test 2**: location of discomfort, **Test 3**: biodynamic measurements.

Please read carefully and follow the instructions below.

Before the experiment (on your first day)

Complete the questionnaires.

Your standing height, sitting height, knee height, and weight will be measured.

You will undergo short training to familiarise you with the test.

To begin the experiment

Sit comfortably on the seat (one session uses a rigid seat, the other session uses a soft seat) as guided by the experimenter.

Fasten the seat belt loosely, but securely, by adjusting the ‘tightness’ of the belt

Put on the headphones and the blindfold (or close your eyes).

Hold the emergency stop button (to be used to stop the vibration if you are concerned).

Lay your hands on your lap and rest your feet on the footrest.

Do not lean against the backrest.

In each session, you will undergo a few practice trials before the actual test commences.

During the experiment

Test 1 (about 20 minutes)

You will be exposed to vibration stimuli, each lasting 6 s.

Appendix 2

Your task is to say the discomfort caused by each motion using an appropriate numerical value.

A sensible median value might be ‘100’.

Please rate the discomfort caused by each subsequent stimulus using the same scale.

If you are not sure of your rating, please say ‘repeat’.

Test 2 (about 3 minutes)

You will resume sitting as for Test 1. A series of 6-second test stimuli will be presented to you.

After each stimulus, use the body map to indicate to the experimenter the location in your body where you felt the MOST DISCOMFORT.

Close your eyes during each stimulus, and open your eyes to indicate the location.

Test 3 (about 6 minutes)

You will resume sitting as for Test 1. Five 60-second stimuli (random vibrations) will be presented to you with short intervals between the stimuli. You will be asked to maintain your posture while the transmission of vibration from the seat is measured. No judgement is required.

Break

There will a break in the middle of Test 1 and at the end of Test 1.

Thank you very much for your cooperation.

Appendix B Individual equivalent comfort contours in Chapter 5

Appendix B.1 Individual, median, and inter-quarter ranges of equivalent comfort contours (for ψ=100) for acceleration: (a) 0.8 ms^{-2} r.m.s. 4-Hz reference; (b) 0.315 ms^{-2} r.m.s. 4-Hz reference; (c) 0.125 ms^{-2} r.m.s. 4-Hz reference

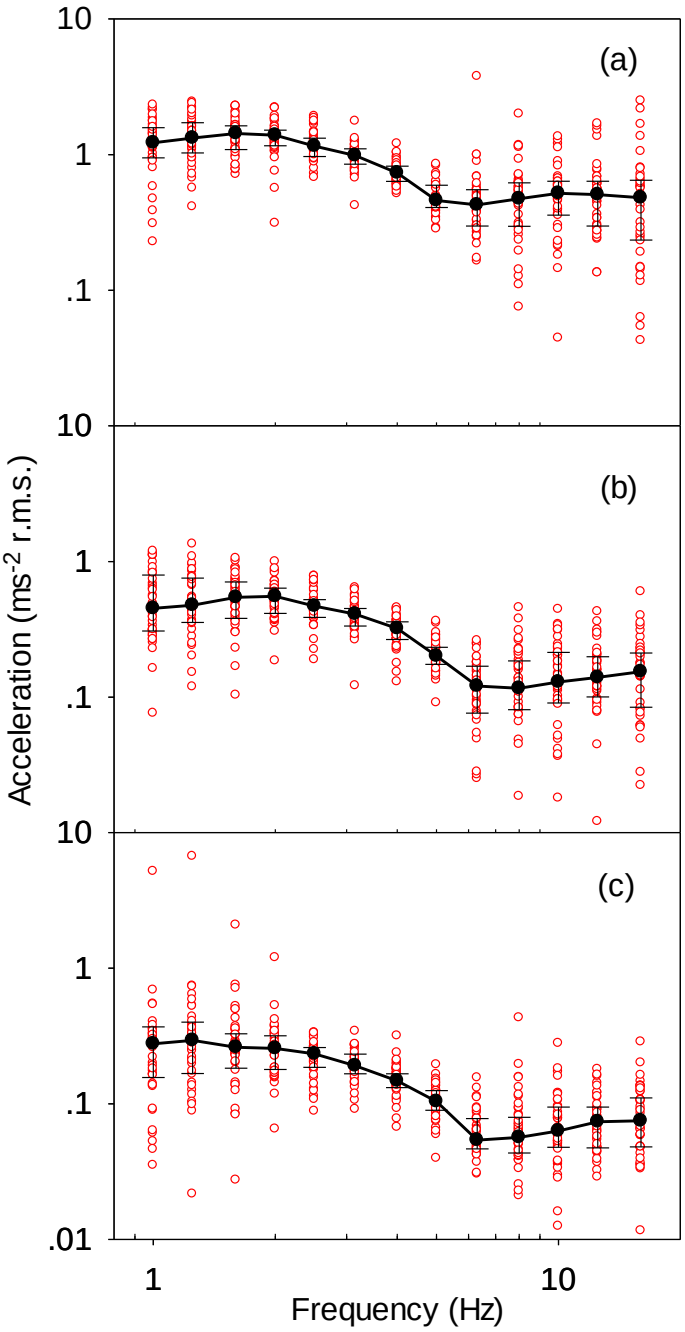

Appendix B.2 Individual, median, and inter-quarter ranges of equivalent comfort contours (for ψ=100) for force (a) 0.8 ms^{-2} r.m.s. 4-Hz reference; (b) 0.315 ms^{-2} r.m.s. 4-Hz reference; (c) 0.125 ms^{-2} r.m.s. 4-Hz reference.

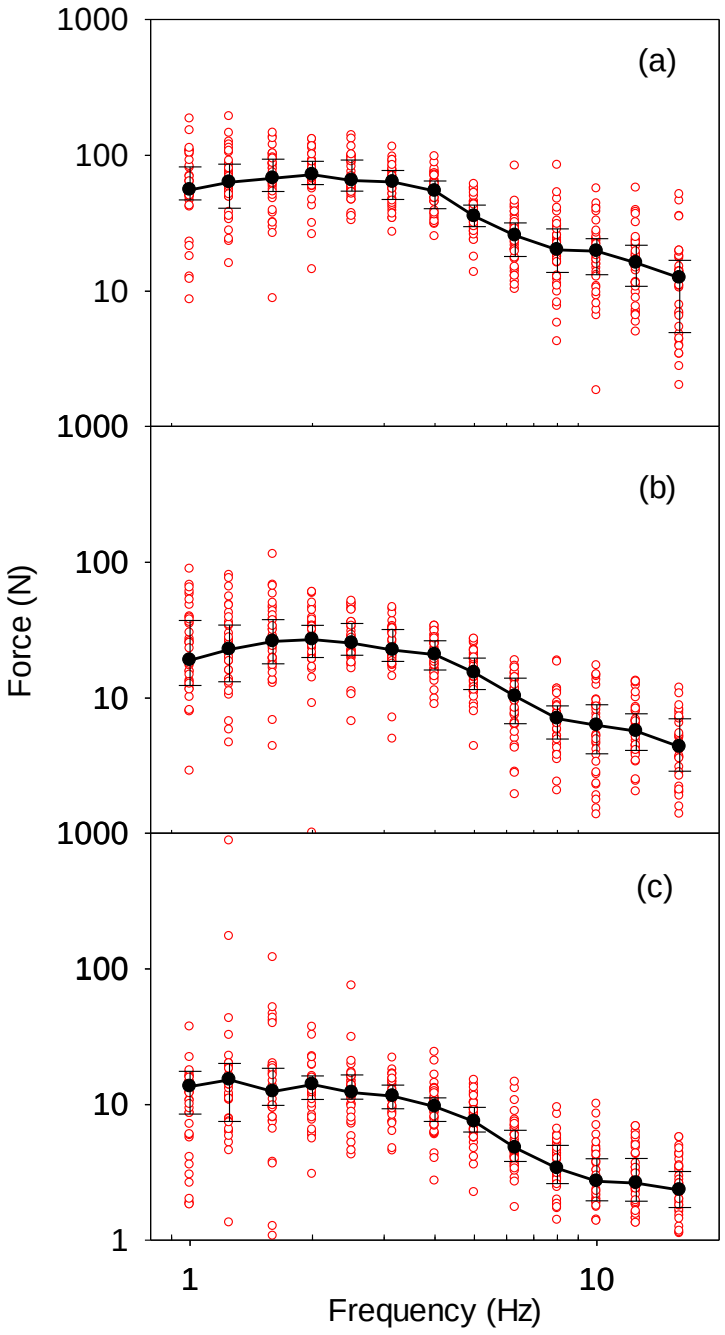

List of References

Ahn, S J, & Griffin, M J. (2008). Effects of frequency, magnitude, damping and direction on the discomfort of vertical whole-body mechanical shocks. Journal of Sound and Vibration, 311(1-2), 485-497.

Boileau, P.E., Wu, X., & Rakhe, S. (1998). Definition of a range of idealized values to characterize seated body biodynamic response under vertical vibration. Journal of Sound and Vibration, 215(4), 841-862.

British Standards Institution. (1987). BS6841. Guide to Measurement and Evaluation of Human Exposure to Whole-body Mechanical Vibration and Repeated Shock.

Clarke, M J, & Oborne, D J. (1975). Reaction of passengers to public service vehicle ride. National Aeronautics and Space Administration, 437-470.

Corbridge, C, & Griffin, M J. (1986). Vibration and comfort: vertical and lateral motion in the range 0.5–5.0 Hz. Ergonomics, 29, 249-272.

Donati, P, Grosjean, A, Mistrot, P, & Roure, L. (1983). The subjective equivalence of sinusoidal and random whole-body vibration in the sitting position (an experimental study using the 'floating reference vibration ' method). Ergonomics, 26(251-273).

Dupuis, H, Hartung, E, & Louda, L (a). (1972). The effect of random vibrations of a limited frequency band compared with sinusoidal vibrations, on human beings.

Dupuis, H, Hartung, E, & Louda, L (b). (1972). Random vibration of a limited frequency range compared with sinusoidal vibration with regards to its effect on man.

Fairley, T E , & Griffin, M J. (1989). The apparent mass of the seated human body: vertical vibration. Journal of Biomechanics, 22(2), 81-94.

Fothergill, L C, & Griffin, M J. (1977). The Subjective Magnitude of Whole-body Vibration. Ergonomics, 20(5), 521-533.

Fothergill, L C, & Griffin, M J. (1977). The use of an intensity matching technique to evaluate human response to whole-body vibration. Ergonomics, 20(3), 249-261.

Fothergill, L C , & Griffin, M J. (1977a). The evaluation of discomfort produced by multiple frequency whole-body vibration. Ergonomics, 20(3), 263-276.

Griffin, M J. (1976). Subjective equivalence of sinusoidal and random whole-body vibration. Journal of Acoustic Society of America, 60(5), 1140-1145.

List of References

Griffin, M J. (1990). Handbook of human vibration. New York: Academic Press.

Griffin, M J, & Whitham, E M. (1978). Individual variability and its effect on subjective and biodynamic response to whole-body vibration. Journal of Sound and Vibration, 58, 239-250.

Griffin, M J, & Whitham, E M. (1980). Discomfort produced by impulsive whole-body vibration. Journal of Acoustic Society of America, 68(5), 1277-1284.

Griffin, M. J., Whitham, E.M., & Parsons, K.C. (1982). Vibration and comfort. I: translational seat vibration. Ergonomics, 25, 603-630.

Hanes, R M. (1970). Human sensitivity to whole-body vibration in urban transportation systems: a literature review. Transportation Programs Report. Applied Physics Laboratory, The Johns Hopkins University, Maryland.

Hinz, B., Bluthner, R., Menzel, G. , Rutzel, S., Seidel, H., & Wolfel, H.P. (2006). Apparent mass of seated men—Determination with single- and multi-axis excitation at different magnitudes. Journal of Sound and Vibration, 298(3), 788-809.

Hinz, B., & Seidel, H. (1987). The nonlinearity of the human body's dynamic response during sinusoidal whole body vibration. Industrial Health, 25, 169-181.

Hoddinott, J C. (1986). Investigation of the effect of duration on alternative methods of assessing human response to implusive motion. Paper presented at the UK Informal Group Meeting on Human Response to Vibration, University of Technology, Loughborough.

Holmlund, P., Lundstrom, R., & Lindberg, L. (2000). Mechanical impedance of the human body in vertical direction. Applied Ergonomics, 31(1), 415-422.

Howarth, H V C, & Griffin, M J. (1988). The frequency dependence of subjective reaction to vertical and horizontal whole-body vibration at low magnitudes. Journal of Acoustic Society of America, 83, 1406-1413.

Howarth, H V C, & Griffin, M J. (1991). Subjective reaction to vertical mechanical shocks of various waveforms. Journal of Sound and Vibration, 147(3), 395-408.

Huang, Y. & Griffin, M. J. (2014). Comparison of absolute magnitude estimation and relative magnitude estimation for judging the subjective intensity of noise and vibration. Applied Acoustics 77, 82-88.

Huang, Y., & Griffin, M.J. (2006). Effect of voluntary periodic muscular activity on nonlinearity in the apparent mass of the seated human body during vertical random whole-body vibration. Journal of Sound and Vibration, 298(3), 824-840.

Huang, Y., & Griffin, M.J. (2008). Nonlinear dual-axis biodynamic response of the semi-supine human body during vertical whole-body vibration. Journal of Sound and Vibration, 312(1-2), 296-315.

Huang, Y., & Griffin, M.J. (2009). Nonlinearity in apparent mass and transmissibility of the supine human body during vertical whole-body vibration. Journal of Sound and Vibration, 324(1-2), 429-452.

International Organization for Standardization (1997). ISO 2631. Mechanical vibration and shock - evaluation of human exposure to whole-body vibration - Part 1: General requirement. International Organization for Standardization, Geneva.

Jang, H-K, & Griffin, M.J. (1999). The Effect of Phase of Differential Vertical Vibration at the Seat and Feet on Discomfort. Journal of Sound and Vibration, 223(5), 785-794.

Jang, H-K, & Griffin, M.J. (2000). Effect Of Phase, Frequency, Magnitude And Posture On Discomfort Associated With Differential Vertical Vibration At The Seat And Feet. Journal of Sound and Vibration, 229(2), 273-286.

Jones, A.J, & Saunders, D.J. (1972). Equal comfort contours for whole body vertical, pulsed sinusoidal vibration. Journal of Sound and Vibration, 23(1), 1-14.

Jones, A J, & Saunders, D J. (1974). A scale of human reaction to whole body, vertical, sinusoidal vibration. journal of Sound and Vibration, 35, 503-520.

Kitazaki, S., & Griffin, M.J. (1997). A modal analysis of whole-body vertical vibration, using a finite element model of the human body. Journal of Sound and Vibration, 200(1), 83-103.

Kitazaki, S., & Griffin, M.J. (1998). Resonance behaviour of the seated human body and effects of posture. Journal of biomechanics, 31, 143-149.

Leatherwood J D., & Dempsey, T K. (1976). Psychophysical relationships characterising human response to whole-body sinusoidal vertical vibration. National Aeroautics and Space Administration, NASN TN D-8188.

Mansfield, N.J., & Griffin, M.J. (1998). Effect of magnitude of vertical whole-body vibration on absorbed power for the seated human body. Journal of Sound and Vibration, 215(4), 813-825.

Mansfield, N J, & Griffin, M J. (2000). Non-linearities in apparent mass and transmissibility during expoure to whole-body vertical vibration. Journal of Biomechanics, 33(8), 933-941.

Mansfield, N J, & Griffin, M J. (2002). Effects of posture and vibration magnitude on apparent mass and pelvis rotation during exposure to whole-body vertical vibration. Journal of Sound and Vibration, 253(1), 93-107.

Mansfield, N J, Holmlund, P, Lundström, R, Lenzuni, P, & Nataletti, P. (2006). Effect of vibration magnitude, vibration spectrum and muscle tension on apparent mass and cross axis transfer functions during whole-body vibration exposure. Journal of Biomechanics, 39, 3062-3070.

Mansfield, N J, & Maeda, S. (2005). Equal sensation curves for whole-body vibration expressed as a function of driving force. Journal of Acoustic Society of America, 117(6), 3853-3859.

Matsumoto, Y., & Griffin, M.J. (1998). Dynamic responses of the standing human body exposed to vertical vibration: influence of posture and vibration magnitude. Journal of Sound and Vibration, 212(1), 85-107.

Matsumoto, Y, & Griffin, M J. (2001). Modelling the dynamic mechanisms associated with the principal resonance of the seated human body. Clinical Biomechanics, 16 (Sup.1), S31-S44.

Matsumoto, Y., & Griffin, M.J. (2002a). Non-linear Characteristics in the Dynamic Responses of seated Subjects Exposed to Vertical Whole-body Vibration. Journal of Biomechanical Engineering, 124(5), 527-532.

Matsumoto, Y., & Griffin, M.J. (2002b). Effect of muscle tension on non-linearities in the apparent masses of seated subjects exposed to vertical whole-body vibration. Journal of Sound and Vibration, 253(1), 77-92.

Matsumoto, Y, & Griffin, M J. (2005). Nonlinear subjective and biodynamic responses to continuous and transient whole-body vibration in the vertical direction. Journal of Sound and Vibration, 287, 919-937.

Miwa, T. (1967). Evaluation methods for vibration effect. Part1: measurements of threshold and equal sensation contours of whole body for vertical and horizontal vibrations. Industrial Health, 5, 183-205.

Miwa, T. (1967). Evaluation methods for vibration effects. Part 2. Measurement of equal sensation contours of whole body between vertical and horizontal sinusoidal vibrations. Industrial Health, 5, 206-212.

Miwa, T. (1968). Evaluation methods for vibration effect. Part 4. Measurements of vibration greatness for whole body and hand in vertical and horizontal vibrations. Industrial Health, 6, 1-10.

Miwa, T. (1968). Evaluation methods for vibration effect. Part 7. The vibration greatness of the pluses. Industrial Health, 6, 143-164.

Miwa, T (b). (1968). Evaluation methods for vibration effect. Part 5. Calculation method of vibration greatness level on compound vibrations. Industrial Health, 6, 11-17.

Morioka, M, & Griffin, M J. (2006a). Magnitude-dependence of equivalent comfort contours for fore-and-aft, lateral and vertical whole-body vibration. Journal of Sound and Vibration, 298(3), 755-772.

Morioka, M, & Griffin, M J. (2006b). Magnitude dependence of equivalent comfort contours for fore and aft, lateral and vertical hand-transmitted vibration. Journal of Sound and Vibration, 295, 633-648.

Muksian, Robert, & Nash, C D. (1974). A model for the response of seated humans to sinusoidal displacement of the seat. Journal of Biomechanics, 7(3), 209-215.

Muksian, Robert, & Nash, C D. (1976). On frequency-dependent damping coefficients in lumped-parameter models of human beings. Journal of Biomechanics, 9(5), 339-342.

Nawayseh, N., & Griffin, M J. (2003). Non-linear dual-axis biodynamic response to vertical whole-body vibration. Journal of Sound and Vibration, 268(3), 503-523.

Nawayseh, N., & Griffin, M.J. (2005). Non-linear dual-axis biodynamic response to fore-and-aft whole-body vibration. Journal of Sound and Vibration, 282, 831-862.

Nawayseh, N, & Griffin, M J. (2009). A model of the vertical apparent mass and the fore-and-aft cross-axis apparent mass of the human body during vertical whole-body vibration. Journal of Sound and Vibration, 319(1-2), 719-730.

List of References

Oborne, D J. (1978). The stability of equal sensation contours for whole-body vibration. Ergonomics, 21, 651-658.

Oborne, D.J., & Boarer, P.A. (1982). Subjective response to whole-body vibration The effects of posture. Ergonomics, 25(7), 673-681.

Paddan, G.S., & Griffin, M.J. (1998). A review of the transmission of translation seat vibration to the head. Journal of Sound and Vibration, 215(4), 863-882.

Pankoke, S, Buck, B, & Woelfel, H.P. (1998). Dynamic FE model of sitting man adjustable to body height, body mass and posture used for calculating internal forces in the lumbar vertebral disks. Journal of Sound and Vibration, 215(4), 827-839.

Qiu, Y., & Griffin, M.J. (2010). Biodynamic responses of the seated human body to single-axis and dual-axis vibration. Industrial Health, 48, 615-627.

Shoenberger, R W. (1975). Subjective response to very low-frequency vibration. Aviation, Space and Environmental Medicine, 46, 785-790.

Shoenberger, R W, & Harris, C S. (1971). Psychophysical assessment of Whole-body vibration. Human Factors, 13(1), 41-50.

Spang, K, Arnberg, P W, Bennerhult, O, & Kloow, T. (1984). The influence of transient vibrations on perception experimental study. Part I. IFM Akustikyran.

Stevens, S S. (1957). On the psychophysical law. Psychological Review, 64(3), 153-181.

Stevens, S S. (1975). Psychophysics, Introduction to its Perceptual, Neural and Social Prospects. New York: Wiley.

Subashi, G.H.M.J., Matsumoto, Y., & Griffin, M.J. (2006). Apparent mass and cross-axis apparent mass of standing subjects during exposure to vertical whole-body vibration. Journal of Sound and Vibration, 293, 78-95.

Subashi, G H M J, Nawayseh, N, Matsumoto, Y, & Griffin, M J. (2009). Nonlinear subjective and dynamic responses of seated subjects exposed to horizontal whole-body vibration. Journal of Sound and Vibration, 321(1-2), 416-434.

Thuong, O. (2011). Predicting the vibration discomfort of standing passengers in transport. (Doctor of Philosophy), University of Southampton.

Toward, M. G. R. (2002). Apparent mass of the human body in the vertical direction: effect of input spectra. Paper presented at the 37th United Kingdom Conference on Human Response to Vibration, Department of Human Sciences, Loughborough University.

Toward, M. G.R.T., & Griffin, M J. (2011). Apparent mass of the human body in the vertical direction: Inter-subject variability. Journal of Sound and Vibration, 330, 827-841.

Toward, M.G.R.T, & Griffin, M.J. (2011). The transmission of vertical vibration through seats: influence of the characteristics of the human body. Journal of Sound and Vibration, 330(26), 6526-6543.

Wang, W., Rakheja, S., & Boileau, P.E. (2004). Effect of sitting postures on biodynamic response of seated occupants under vertical vibration. International Journal of Industrial Ergonomics, 34(4), 289-306.

Wei, L., & Griffin, M.J. (1998). Mathematical models for the apparent mass of the seated human body exposed to vertical vibration. Journal of Sound and Vibration, 212(5), 855-874.

Worden, Keith, & Tomlinson, G.R. (2000). Nonlinearity in Structural Dynamics: Detection, Identification and Modelling: Taylor & Francis.

Wyllie, I.H., & Griffin, M.J. (2007). Discomfort from sinusoidal oscillation in the roll and lateral axes at frequencies between 0.2 and 1.6 Hz. Journal of Acoustic Society of America, 121(5), 2644-2654.

Wyllie, I.H., & Griffin, M.J. (2009). Discomfort from sinusoidal oscillation in the pitch and fore-and-aft axes at frequencies between 0.2 and 1.6 Hz. Journal of Sound and Vibration, 324(1-2), 453-467.

Yonekawa Yoshiharu, & Miwa, T. (1972). Sensational responses of sinusoidal whole body vibrations with ultra-low frequencies. Industrial Health, 10(63-76).

Zwislocki, J J, & Goodman, D A. (1980). Absolute scaling of sensory magnitudes: a validation Perception & Psychophysics, 28(1), 28-38.